Martin P. Bendsøe

Optimization of Structural Topology, Shape, and Material

Springer-Verlag Berlin Heidelberg GmbH

Martin P. Bendsøe

Optimization of Structural Topology, Shape, and Material

With 85 Figures

Springer

Dr. Martin P. Bendsøe
Technical University of Denmark
Mathematical Institute
Building 303
DK-2800 Lyngby

ISBN 978-3-662-03117-9 ISBN 978-3-662-03115-5 (eBook)
DOI 10.1007/978-3-662-03115-5

CIP-data applied for

This work is subject to copyright. All rights are reserved, whether the whole or part of the material is concerned, specifically the rights of translation, reprinting, reuse of illustrations, recitation, broadcasting, reproduction on microfilm or in other ways, and storage in data banks. Duplication of this publication or parts thereof is permitted only under the provisions of the German Copyright Law of September 9, 1965, in its current version, and permission for use must always be obtained from Springer-Verlag Berlin Heidelberg GmbH.
Violations are liable for prosecution act under German Copyright Law.

© Springer-Verlag Berlin Heidelberg 1995
Originally published by Springer-Verlag Berlin Heidelberg New York in 1995
Softcover reprint of the hardcover 1st edition 1995
The use of general descriptive names, registered names, trademarks, etc. in this publication does not imply, even in the absence of a specific statement, that such names are exempt from the relevant protective laws and regulations and therefore free for general use.

Production: PRODUserv Springer Produktions-Gesellschaft, Berlin
Typesetting: Camera-ready copy by author
Cover-layout: Struve & Partner, Heidelberg

SPIN 10489882 61/3020- 5 4 3 2 1 0 Printed on acid-free paper

To

Susanne
Charlotte
Anne

Preface

This work is an attempt to provide a unified presentation of methods for the optimal design of topology, shape and material for continuum and discrete structures. The emphasis is on recently matured techniques for the topology design of continuum structures. As the first designs using this methodology are now being produced, it seems timely to collect and describe research results from the last decade in one publication.

The field of structural optimization combines mechanics, variational calculus and mathematical programming to obtain better designs of structures. This places any author in a somewhat problematic position on how to present the material at hand. Here we take an operational approach, with strict mathematical formalism reserved for situations where this is crucial for a precise statement of results.

The findings and methods presented in this monograph are very much the result of an international research effort and I wish to thank W. Achtziger, A. Ben-Tal, A.R. Díaz, R.B. Haber, R.T. Haftka, J.M. Guedes, C. Jog, N. Kikuchi, R. Lipton, N. Olhoff, P. Pedersen, S. Plaxton, J. Rasmussen, H.C. Rodrigues, G.I.N. Rozvany, J. Sokolowski, J.E. Taylor, N. Triantafyllidis and J. Zowe for the research collaboration which has provided the bulk of the material described in this book. Also, I would like to acknowledge G. Allaire, G. Buttazzo, L. Trabucho de Campos, A.V. Cherkaev, G. Francfort, R.V. Kohn, K. Lurie, P. Papalambros, U. Raitums, U. Ringertz, O. Sigmund, O. Smith and D. Tortorelli for many very fruitful discussions on the subjects of this book. On another note, I thank Vagn Lundsgaard Hansen and Niels Olhoff for luring me into and guiding me through my initial stages of scientific endeavour. Finally, I am indebted to my colleagues at the Mathematical Institute, Technical University of Denmark, for providing scientifically and socially inspiring work conditions.

Lyngby, February, 1995

Martin Philip Bendsøe

Contents

Introduction

The efficient use of materials is important in many different settings. The aerospace industry and the automotive industry, for example, apply sizing and shape optimization to the design of structures and mechanical elements. Shape optimization is also used in the design of electromagnetic, electrochemical and acoustic devices. The subject of non-linear, finite-dimensional optimization for this type of problem is now relatively mature. It has produced a number of successful algorithms that are widely used for structural optimization, including some that have been incorporated in commercial finite element codes. However, these methods are unable to cope with the problem of topology optimization, for either discrete or continuum structures.

The optimization of the geometry and topology of structural lay-out has great impact on the performance of structures, and the last decade has seen a revived interest in this important area of structural optimization [3], [8]* . This has been spurred in part by the success of the recently developed so-called 'homogenization method' for generating optimal topologies of structural elements [10]. This method employs a composite material as a basis for defining shape in terms of material density and the method unifies two subjects, each of intrinsic interests and previously considered distinct. One is structural optimization at the level of macroscopic design, using a macroscopic definition of geometry given by for example thicknesses or boundaries [1]. The other subject is micromechanics, the study of the relation between microstructure and the macroscopic behaviour of a composite material [23].

Materials with microstructure enter naturally in problems of optimal structural design, be it shape or sizing problems. This was for example clearly demonstrated in the papers by Cheng and Olhoff, 1981, 1982, on optimal thickness distribution for elastic plates. Their work led to a series of works on optimal design problems introducing microstructures in the formulation of the problem [23], [31]. The homogenization method for topology design can be seen as a natural continuation of these studies and has lead to the capability to predict computationally the optimal topologies of continuum structures. Moreover, the introduction of composite materials in the shape design context leads naturally to the design of

---

* This is a reference to the bibliographical notes (chapter 6). To avoid long lists of references in the text, use is made of bibliographical notes for a survey of the literature.

materials themselves, opening up a totally new field of applications of structural design techniques [24], [25].

For thin structures, that is, structures with a low fraction of available material compared to the spatial dimension of the structure, the homogenization method predicts grid- and truss-like structures. Thus the homogenization method supplements classical analytical methods for the study of fundamental properties of grid like continua, as first treated by Michell, 1904 [16]. Applications of numerical methods to truss problems and other discrete models were first described in the early sixties [26] but only recently have these challenging large-scale problems attracted renewed interest, especially for producing specialized algorithms [27].

In its most general setting shape optimization of continuum structures should consist of a determination for every point in space if there is material in that point or not. Alternatively, for a FEM discretization every element is a potential void or structural member. In this setting the topology of the structure is not fixed a priori, and the general formulation should allow for the prediction of the layout of a structure. Similarly, the lay-out of a truss structure can be found by allowing all connections between a fixed set of nodal points as potential structural or vanishing members. Topology design problems formulated this way are inherently discrete optimization problems. For truss problem it is natural to avoid this by using the continuously varying cross-sectional bar areas as design variables, allowing for zero bar areas. For shape optimization a necessary relaxation of the problem introduces composites such as layered periodic media, leading to a description of shape by a density of material. This density can take on all values between zero and one and intermediate density values make physical sense.

The approach to topology design outlined above is known as the ground structure approach. This means that for an initially chosen layout of nodal points in the truss structure or in the finite element mesh, the optimum structure connecting the imposed boundary conditions and external loads is found as a subset of all the elements of the initially chosen set of connections between the truss nodal points or the initially chosen set of finite elements. The positions of nodal points are not used as design variables, so a high number of nodal points should be used in the ground structure to obtain efficient topologies. Figure 1 show example ground structures for a planar truss and for a plane stress problem. Also, the number of nodal points is not used as design variables, so the approach appears as a standard sizing problem and for continuum structures, the shape design problem has been cast as a problem of finding the optimal density distribution of material in a fixed domain, modelled with a fixed FEM mesh. This is of major importance for the implementation of topology optimization methods.

The material in this monograph is divided into six chapters. Chapter 1 contains an exposition of the fundamental ingredients of the homogenization method for topology design, ranging over basic modelling and existence issues, derivation of effective moduli of periodic composites, derivation of optimality criteria and computational as well as implementation issues. Chapter 1 is also concerned with

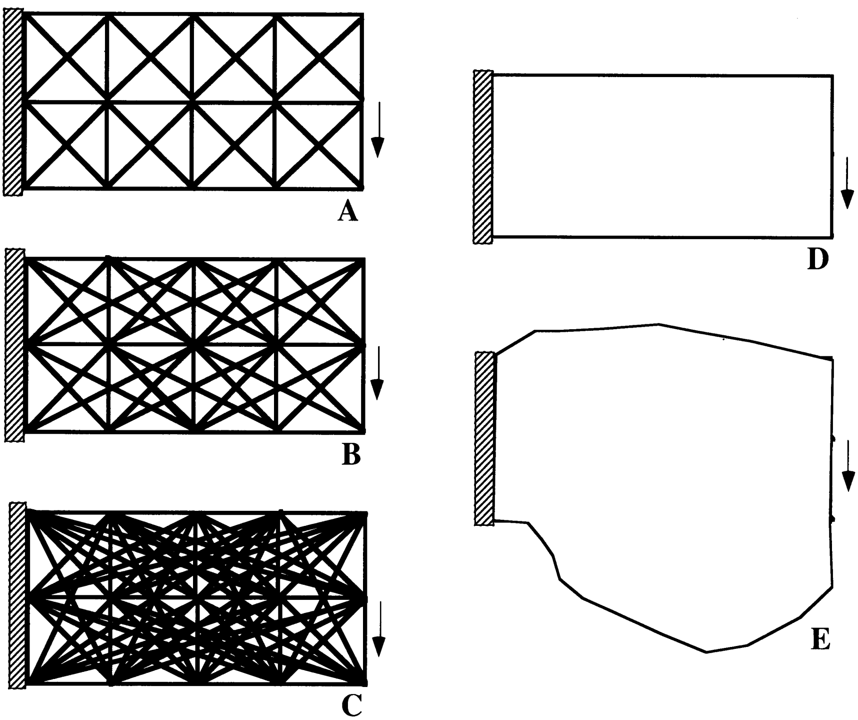

Fig. 1. Ground structures for transmitting a vertical force to a vertical line of supports. *(A), (B), (C)*: Truss ground structures of variable complexity in a rectangular domain. *(D), (E)*: Continuum model design domains, for the bending of a short cantilever.

the use of a topology design methodology in an integration with boundary shape design, and we illustrate the importance of topology for the performance of a structure.

Chapter 2 serves to underline the close connection between materials science and generalized optimal shape design and shows how the fundamental extremal energy principles of mechanics constitute a convenient framework for analytical studies as well as for alternative computational strategies. Specifically we show in chapter 2 how the potential and complementary energies of a structure can be optimized with respect to microstructure and how this calculation leads to considering auxiliary non-linear elasticity problems with a reduced set of design parameters.

Working with design optimized energy potentials constitutes the basic unifying idea of the remainder of the book. In chapter 3 we take the developments one step further to formulate the structural optimization problem in a form that encompasses the free design of structural material, within the usual limitations for physical materials. Material properties are represented in the most general form possible for a linear elastic continuum: the unrestricted set of elements of positive semi-definite constitutive tensors. Employing this description of the material we are able to demonstrate in analytical form the local properties associated with materials that are optimal with respect to the global compliance objective. Also, it is seen how topologies associated with the optimum structural distribution of the optimized materials are in effect predicted out of the same treatment of the structural optimization problem.

The optimization of the free choice of material parameters described in chapter 3 results in auxiliary problems that are almost identical to truss topology design problems. This leads us naturally to chapter 4, where the topology design of trusses is analyzed with the purpose of devising efficient numerical algorithms. As in chapter 2 and 3, the fundamental approach revolves around the derivation of optimal energy functionals and we are in this process able to derive a whole series of equivalent problem statements, relating recent developments to classical truss topology design formulations.

Finally, in chapter 5 various extensions of topology and material design are described, albeit rather briefly. Reversing the historical developments, the plate design problem is treated in this last part of the main text of the book. Of other subjects covered are design for vibration and stability problems, hierarchical design of topology and geometry of the ground structure and design for thermo-elastic problems.

Chapter 6 contains bibliographical notes covering the main subjects of this exposition as well as related background material the reader may want to consult.

It is the aim of this monograph to demonstrate the importance of topology and material design for structural optimization and that effective means for handling such design problems do exist. Structural optimization enforces rather than removes the creative aspect of designing and the final design must be a product of creativity rather than availability or lack of analysis facilities. A topology and material design methodology is an important brick in providing such facilities.

We close this brief introduction by remarking that the homogenization method for topology design has demonstrated its potential in a large number of case studies at universities and in industry. Also, commercial design software is now available for structural design of two and three dimensional structures, plates and shells, and the first products developed with the help of this technology are now being produced. Irrespective of this success it should, however, be made clear that the methodology is still in its infancy and that only fairly simple design formulations can be handled. Among other things, this is caused by limited computational optimization capability. Also, the mathematics of more general design formulations becomes immensely complicated and the right framework for treating these problems may still have to be devised. There is thus plenty of work to be done.

1 The homogenization approach to topology design

In this chapter we present an overview of the basic ingredients of the so-called homogenization method for finding the optimum layout of a linearly elastic structure. In this context the "layout" of the structure includes information on the topology, shape and sizing of the structure and the homogenization method allows for addressing all three problems simultaneously.

Sizing, shape, and topology optimization problems address different aspects of the structural design problem. In a typical *sizing* problem the goal may be to find the optimal thickness distribution of a linearly elastic plate. The optimal thickness distribution minimizes (or maximizes) a physical quantity such as the mean compliance (external work), peak stress, deflection, etc., while equilibrium and other constraints on the state and design variables are satisfied. The design variable is the thickness of the plate and the state variable may be its deflection. The main feature of the sizing problem is that the domain of the design model and state variables is known *a priori* and is fixed throughout the optimization process. On the other hand, in a *shape* optimization problem the goal is to find the optimum shape of this domain, that is, the shape problem is defined on a domain which is now the design variable. *Topology* optimization of solid structures involves the determination of features such as the number and location of holes and the connectivity of the domain.

In order to simplify as well as clarify the presentation we choose in the following to describe the basic ideas and techniques for the case of space dimension two (planar systems). The basic approach described carries over directly to three dimensional structures, but certain results have not yet been completely clarified for dimension three. In these cases this is indicated in the text.

1.1 Problem formulation and parametrization of design

The layout problem that shall be defined in the following combines several features of the traditional problems in structural design optimization. The purpose of layout optimization is to find the optimal layout of a structure within a specified region. The only known quantities in the problem are the applied loads, the possible support conditions, the volume of the structure to be constructed and possibly some additional design restrictions such as the location and size of prescribed holes. In this problem the physical size and the shape and connectivity of the structure are unknown. The topology, shape, and size of the structure are not represented by standard parametric functions but by a set of distributed functions defined on a *fixed design domain.* These functions in turn represent a parametrization of the rigidity tensor of the continuum and it is the suitable choice of this parametrization which leads to the proper design formulation for layout optimization.

1.1.1 Minimum compliance design formulations

In the following the general set-up for optimal shape design formulated as a material distribution problem is described. The set-up is analogous to well known formulations for sizing problems for discrete and continuum structures [1], and to truss topology design formulations that are described in chapter 4. It is important to note that the problem type we will consider is from a computational point of view inherently large scale both in state and in the design variables. For this reason we choose to consider only the simplest type of design problem formulation in terms of objective and constraint, designing for minimum compliance (maximum global stiffness) under simple resource constraints.

Consider a mechanical element as a body occupying a domain Ω^m which is part of a larger reference domain Ω in $\mathbf{R}^2$. The reference domain Ω is chosen so as to allow for a definition of the applied loads and boundary conditions and the reference domain is sometimes called the ground structure, in parallel with terminology used in truss topology design (cf. Chap. 4). Referring to the reference domain Ω we can define the optimal shape design problem as the problem of finding the optimal choice of elasticity tensor $E_{ijkl}(x)$* which is a variable over the domain. Introducing the energy bilinear form (i.e. the internal virtual work of an elastic body at the equilibrium u and for an arbitrary virtual displacement v):

$$a(u,v) = \int_{\Omega} E_{ijkl}(x)\varepsilon_{ij}(u)\varepsilon_{kl}(v)\,\mathrm{d}\Omega$$

with linearized strains $\varepsilon_{ij}(u) = \frac{1}{2}\left(\frac{\partial u_i}{\partial x_j} + \frac{\partial u_j}{\partial x_i}\right)$ and the load linear form

$$l(u) = \int_{\Omega} pu\,\mathrm{d}\Omega + \int_{\Gamma_T} tu\,\mathrm{d}s\ ,$$

* In what follows we use a standard tensor notation consistent with a Cartesian reference frame; this does not imply a loss of generality.

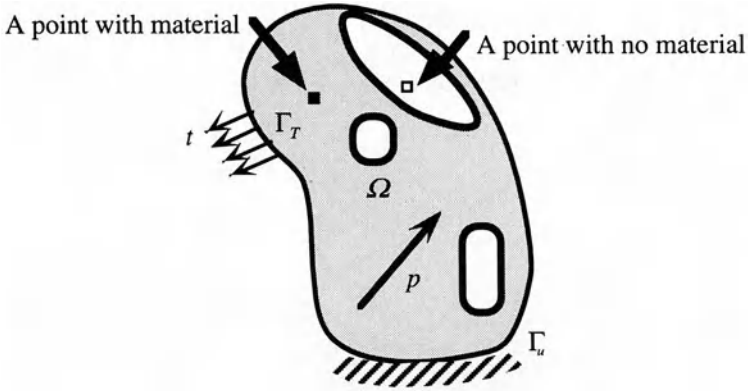

Fig. 1.1. The generalized shape design problem of finding the optimal material distribution.

the minimum compliance (maximum global stiffness) problem takes the form

$$\begin{aligned} &\underset{u \in U,\, E}{\text{minimize}} \quad l(u) \\ &\text{subject to :} \\ &\quad a_E(u,v) = l(v), \quad \text{for all } v \in U, \\ &\quad E \in \mathrm{E}_{ad} \end{aligned} \tag{1.1}$$

Here the equilibrium equation is written in its weak, variational form, with U denoting the space of kinematically admissible displacement fields, p are the body forces and t the boundary tractions on the traction part $\Gamma_T \subset \Gamma \equiv \partial\Omega$ of the boundary. Note that we use the index E to indicate that the bilinear form a_E depends on the design variables.

In problem (1.1), E_{ad} denotes the set of admissible rigidity tensors for our design problem. In the case of topology design, E_{ad} could, for example, consist of all rigidity tensors that attain the material properties of a given isotropic material in the (unknown) set Ω^m and zero properties elsewhere, the limit of resource being expressed as $\int_{\Omega^m} 1 \,\mathrm{d}\Omega \le V$. The various possible definitions of E_{ad} is the subject of the following section.

For the developments in the following it is important to note that problem (1.1) can be given in a number of equivalent formulations which are extremely useful for analysis and the development of computational procedures. For this purpose we note that the equilibrium condition of problem (1.1) can be expressed in terms of the principle of minimum potential energy. That is, the displacement field u^* is a minimizer of the functional $F(u) = \frac{1}{2} a_E(u,u) - l(u)$ on U (the total potential energy) . Then note that the value $F(u^*)$ of the potential energy at equilibrium equals $-\frac{1}{2} l(u^*) < 0$. Thus problem (1.1) can be written as

$$\max_{E \in \mathrm{E}_{ad}} \min_{u \in U} \left\{ \tfrac{1}{2} a_E(u,u) - l(u) \right\} \tag{1.2}$$

Problem (1.2) can also be formulated in terms of stresses. Expressing the inner equilibrium problem of (1.2) in terms of the (dual) principle of minimum complementary energy, we have the formulation

$$\min_{E \in \mathrm{E}_{ad}} \min_{\sigma \in S} \left\{ \tfrac{1}{2} \int_{\Omega} C_{ijkl} \sigma_{ij} \sigma_{kl} \, \mathrm{d}\Omega \right\} \tag{1.3}$$

of the minimum compliance design problem. Here $C_{ijkl} = \left[E^{-1} \right]_{ijkl}$ is the compliance tensor, and the minimization with respect to the stresses σ is taken over the set S of statically admissible stress fields, i.e.

$$S = \left\{ \sigma \mid \operatorname{div} \sigma + p = 0 \ \text{ in } \Omega, \ \ \sigma \cdot n = t \ \text{ on } \Gamma_T \right\}$$

In the following we will also consider cases of design for multiple load conditions and in order to simplify computations we will consider the case of minimizing a weighted average of the compliances for each of the load cases. We thus obtain a simple multiple load formulation as:

$$\begin{aligned} &\underset{u^k \in U,\, E}{\text{minimize}} \quad \sum_{k=1}^{M} w^k l^k\left(u^k\right) \\ &\text{subject to :} \\ &\quad a_E(u^k, v) = l^k(v), \quad \text{for all } v \in U, \ k = 1, \ldots, M, \\ &\quad E \in \mathrm{E}_{ad} \end{aligned} \tag{1.4}$$

for a set $w^k, p^k, t^k, \ \ k = 1, \ldots, M$, of weighting factors, loads and tractions, and corresponding load linear forms given as

$$l^k(u) = \int_{\Omega} p^k u \, \mathrm{d}\Omega + \int_{\Gamma_T^k} t^k u \, \mathrm{d}s,$$

for the M load cases we consider.

In this formulation the displacement fields for each individual load case are independent, thus implying that the multiple load formulation has the equivalent forms:

$$\max_{E \in \mathrm{E}_{ad}} \ \min_{\substack{\boldsymbol{u} = \left\{u^1, \ldots, u^M\right\} \\ u^k \in U, \ k = 1, \ldots, M}} \left\{ \int_{\Omega} W(E, \boldsymbol{u}) \, \mathrm{d}\Omega - l\,(\boldsymbol{u}) \right\} \tag{1.5a}$$

where

$$W\left(E, \boldsymbol{u}=\left\{u^1,\ldots,u^M\right\}\right)=\tfrac{1}{2}\sum_{k=1}^{M} w^k E_{ijpq}(x)\varepsilon_{ij}(u^k)\varepsilon_{pq}(u^k)$$
$$l\left(\boldsymbol{u}=\left\{u^1,\ldots,u^M\right\}\right)=\sum_{k=1}^{M} w^k l^k(u^k) \tag{1.5b}$$

for the displacement based formulation, and

$$\min_{E\in \mathrm{E}_{ad}} \min_{\substack{\operatorname{div}\sigma^k+p^k=0 \text{ in } \Omega,\\ \sigma^k\cdot n=t^k \text{ on } \Gamma_T^k\\ k=1,\ldots,M}} \left\{ \tfrac{1}{2}\int_\Omega \sum_{k=1}^{M} w^k\, C_{ijpq}\sigma_{ij}^k\sigma_{pq}^k \, d\Omega \right\} \tag{1.6}$$

for the stress based formulation.

Note that the topology optimization problem in the formulations above has been cast as a problem in a *fixed* reference domain. Actually, the problems seem to be in the form of simple sizing problems, but this belies the complications hidden in the choice of the set E_{ad} of admissible rigidity tensors.

1.1.2 Parametrization of design by homogenized media

In the design of the topology of a structure we are interested in the determination of the optimal placement of a given isotropic material in space, i.e., we should determine which points of space should be material points and which points should remain void (no material)*. Restricting our spatial extension to the reference domain Ω, we shall determine the optimal subset Ω^m of material points. For the optimization problems defined above, this approach implies that the set E_{ad} of admissible rigidity tensors consists of those tensors for which:

$$E_{ijkl}\in L^\infty(\Omega)$$
$$E_{ijkl}=1_{\Omega^m}E_{ijkl}^0,\quad 1_{\Omega^m}=\begin{cases}1 & \text{if } x\in\Omega^m\\ 0 & \text{if } x\in\Omega\setminus\Omega^m\end{cases} \tag{1.7}$$
$$\int_\Omega 1_{\Omega^m}\, d\Omega=\mathrm{Vol}(\Omega^m)\le V$$

Here the last inequality expresses a limit on the amount of material at our disposal, so that the minimum compliance design is for limited (fixed) volume. The tensor E_{ijkl}^0 is the rigidity tensor for the given *isotropic* material. Note that this definition of E_{ad} means that we have formulated a distributed, discrete valued design

---

* We consider isotropic materials only, as for anisotropic materials the placement of the principal directions of the material should also be considered as a design variable.

problem (a 0-1 problem). For any finite element discretization that is reasonable for analysis, this 0-1 problem will be large scale and out of reach for standard discrete optimization methods. Moreover every function evaluation will involve a very costly finite element analysis, so using methods like simulated annealing or genetic algorithms is computationally prohibitive, but for small scale test examples. Examples of the direct discrete approach can be found in Anagnostou, Rönnquist and Patera, 1992.

Another and in a sense more serious problem associated with the 0-1 problem statement is the now well established lack of existence of solutions to the distributed problem [20], [23]. This is not only a serious theoretical drawback. It also has the effect of making the computational results sensitive to finite element mesh discretization, thus making the very expensive computational solution procedures for the discretized problem unreliable. Theoretical studies have shown that the key to assuring the existence of solutions to our basic shape optimization problem with unknown topology is the introduction of composite materials constructed from the given isotropic material (as defined by E^0_{ijkl}) [20]-[23]. The design variable is then the continuous density of the base material in these composites. It is interesting to note that the required relaxation of the problem thus also makes the problem more tractable for computations, and it is this operational perspective that will be underlined in this chapter. Further discussion on the issue of relaxation and the use of extremal composites and the history of these subjects will be covered in chapter 2 (see also the bibliographical notes, chapter 6).

The main purpose in the following is thus to use the insight gained from theoretical studies on existence of solutions in order to obtain an operational framework for treating the topology problem in a setting with continuous design variables. Introducing a material density ρ by constructing a composite material consisting of an infinite number of infinitely small holes periodically distributed through the base material, we can transform the topology problem to the form of a sizing problem. The on-off nature of the problem is avoided through the introduction of this density, with $\rho=0$ corresponding to a void, $\rho=1$ to material and $0 < \rho < 1$ to the porous composite with voids at a micro level. We thus have a set of admissible rigidity tensors given in the form:

$$\begin{gathered}
\text{Geometric variables } \mu, \gamma, \ldots \in L^\infty(\Omega), \text{ angle } \theta \in L^\infty(\Omega) \\
E_{ijkl}(x) = \tilde{E}_{ijkl}(\mu(x), \gamma(x), \ldots, \theta(x)), \\
\text{density of material } \rho(x) = \rho(\mu(x), \gamma(x), \ldots) \\
\int_\Omega \rho(x)\, \mathrm{d}\Omega \le V; \qquad 0 \le \rho(x) \le 1,\ x \in \Omega
\end{gathered} \tag{1.8}$$

where $\tilde{E}_{ijkl}(x)$ are the effective material parameters for the composite. These quantities can be obtained analytically or numerically through a suitable micro mechanical modelling (see Sect. 1.1.3 on homogenization). The composite material will, in general, be anisotropic (or orthotropic) so the angle of rotation of the directions of orthotropy enters as a design variable, via well-known transformation formulas for frame rotations. Observe that the density of material ρ is, in itself, a function of a number of design variables which describe the geometry of the holes at the micro level and it is these variables that should be optimized. Note that for any material consisting of a given linearly elastic material with microscopic inclusions of void, intermediate values of the density of the base material will provide the structure with strictly less than proportional rigidity (see Figs. 1.7 and 1.8). In an optimal structure one should then expect to find ρ-values of 0 and 1 in most elements. However, this turns out to be dependent on the choice of microstructure, as the use of optimal microstructures (see later) usually results in a very efficient use of intermediate densities of material.

Figure 1.2 shows a two-dimensional continuum structure made of a material with microstructure and figures 1.3, 1.5, 1.6 and 1.9 show the typical types of microstructures that are used for optimal design. The figures show the unit cells for a material with a periodically distributed microstructure, so the cells in the structure are considered as being infinitely small, but infinitely many. We should emphasize at this point that of the illustrated cells it is only the layered material which assure existence of solutions, but we consider them all here as these composite possess various features that are convenient for implementation (see later).

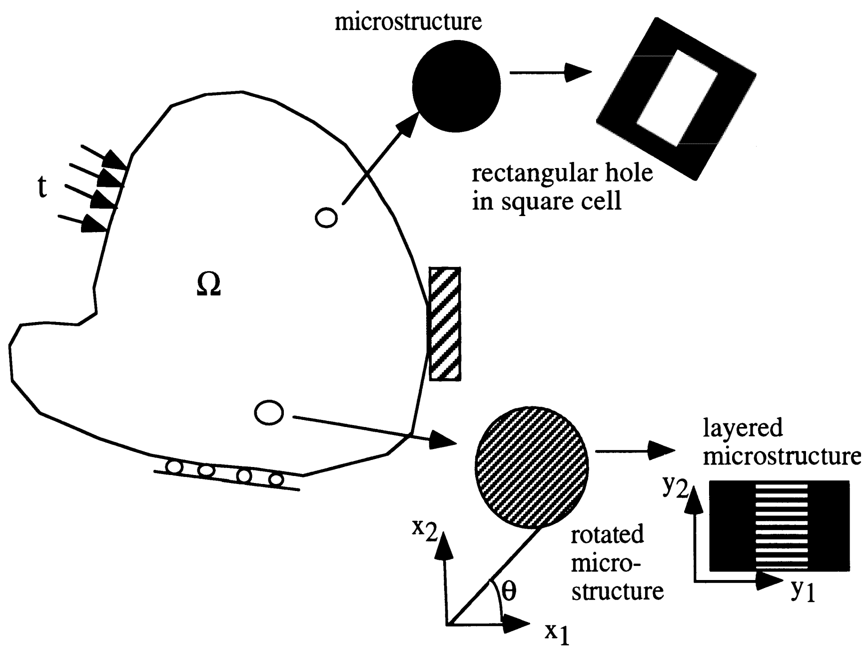

Fig. 1.2. A structure made of materials with micro structure.

Figure 1.4 illustrates how the rotation of the unit *cells* influences a microscopic view of the material and figure 1.7 shows the non-linear density-rigidity relation for a composite with square holes aligned with the axes of reference. Also shown in this figure is the dependence of the effective properties on the angle of rotation of the cells.

Finally, figure 1.8 shows the relation between the effective material properties and the design variables characterizing the unit cells in a microstructure consisting of a so-called rank-2 layering* (cf., Figs. 1.3 and 1.5).

We remark here that it is possible to regularize the minimum compliance problem formulated as an 0-1 problem by restricting the possible range of material sets to measurable sets of bounded perimeter (i.e. the total length of the boundaries of the structure is constrained) (Ambrosio and Buttazzo, 1993). This means that the definition (1.7) of the set of domains of material is augmented by the restriction that

$$\mathrm{per}(\Omega^m,\Omega) = \sup\left\{ \int_{\Omega^m} \mathrm{div}\varphi \; d\Omega \;\middle|\; \varphi \in C_c^1(\Omega,\mathbf{R}^n),\ |\varphi| \le 1 \right\} \le M \tag{1.9}$$

This constraint does not remove the discrete valued nature of the problem. For computational implementations this regularization does not seem to improve on the inherent complications, but the perimeter constraint as such has proven useful as a postiori penalization in the homogenization modelling (see Chap. 2). The perimeter penalization removes the possible generation of microstructures with rapid variation of density of material, and the existence results also holds for a variable thickness sheet model, where the admissible rigidity tensors are given as

$$\begin{gathered}
\text{"Thickness" of material } \rho(x) \in L^\infty(\Omega) \\
E_{ijkl}(x) = \rho(x) E^0_{ijkl} \\
\int_\Omega \rho(x)\, d\Omega \le V \\
0 < \rho_{\min} \le \rho(x) \le 1, \quad x \in \Omega \\
\sup\left\{ \int_\Omega \rho\, \mathrm{div}\varphi \; d\Omega \;\middle|\; \varphi \in C_c^1(\Omega,\mathbf{R}^n),\ |\varphi| \le 1 \right\} \le M
\end{gathered} \tag{1.10}$$

Here one can actually prove existence of solutions for compliance minimization even without the perimeter penalization, cf., Sect. 1.5.1.

---

* It is common in the theoretical materials science literature to see these structures denoted as laminates. However, to avoid confusion with the use of this word in a structures context we call these structures 'layerings'.

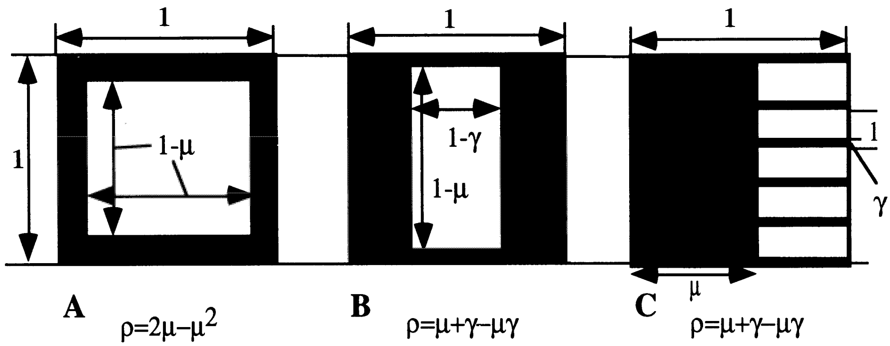

Fig. 1.3. Typical unit cells used in the homogenization method for topology design of continuum structures. The variables μ, γ, and ρ are the design variables and the bulk density, respectively. *(A):* A square cell with a square hole. *(B):* A square cell with a rectangular hole. *(C)*: A rank-2 layered material of layerings at two scales.

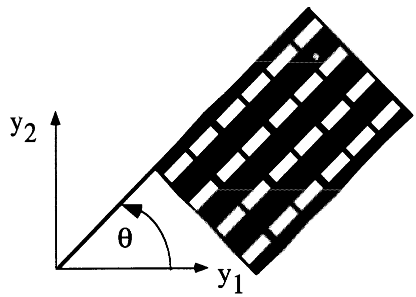

Fig. 1.4. Rotation of a micro structure by rotation of the unit cells. Θ is the angle of cell rotation.

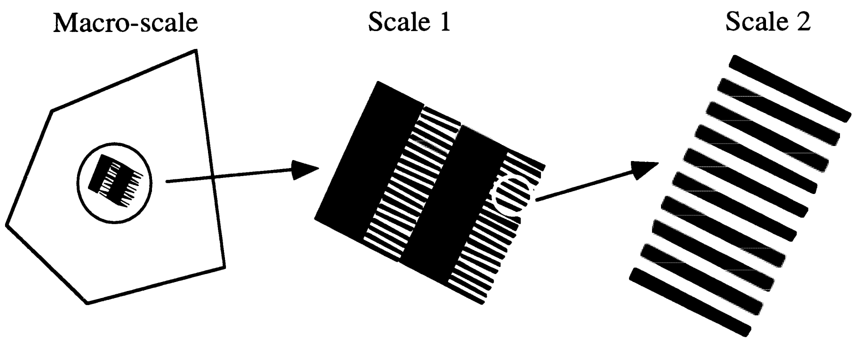

Fig. 1.5. Layered materials for single load cases in dimension 2. The build-up of a second rank layered material, by successive layering of mutual orthogonal layers, resulting in an orthotropic material.

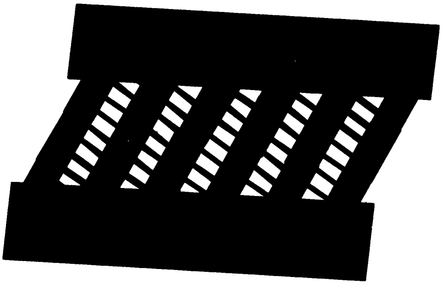

Fig. 1.6. Layered materials for multiple load cases in dimension 2. The build-up of a rank-3 layered material, by successive layering at three different scales. Here the layers are not orthogonal, possibly resulting in a generally anisotropic material.

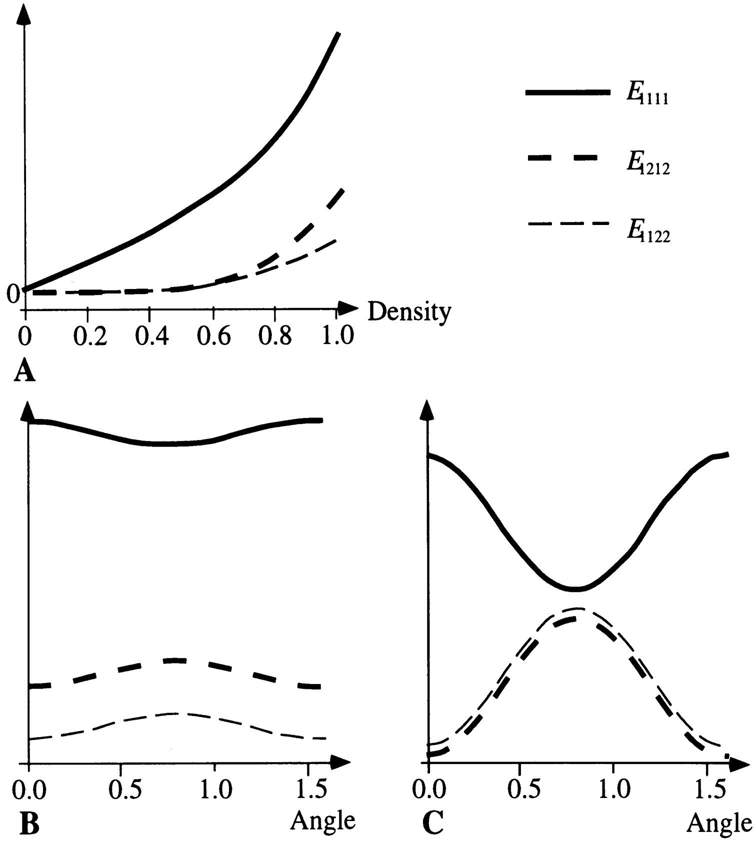

Fig. 1.7. The dependence of the effective material properties of a periodic composite with square holes in square cells on the size of hole and the angle of rotation of the cell. *(A)*: The effective properties in a frame aligned with the directions of the sides of the cell. Dependence on material density $\rho = 1 - x^2$ for an x by x hole in a 1 by 1 cell. *(B)*, *(C)*: The dependence on cell rotation (seen from a fixed frame), for a small sized hole with density of material in cell 0.91 *(B)* and for a large sized hole with density of material in cell 0.36 *(C)*.

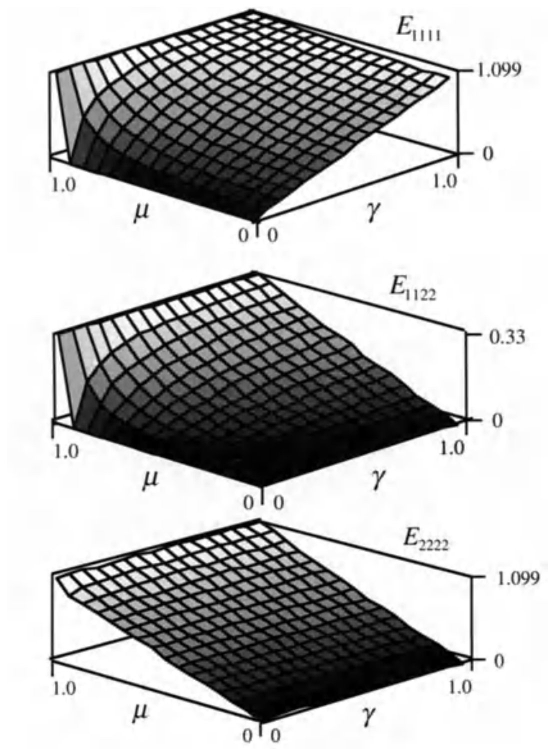

Fig. 1.8. The effective moduli for a microstructure consisting of a (orthogonal) rank-2 layerings. For layerings the element E_{1212} of the stiffness tensor is zero (the weak material is void).

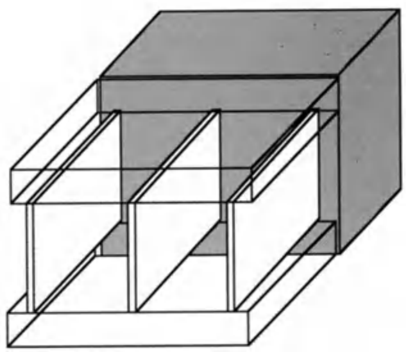

Fig. 1.9. A 3-dimensional cell of a rank-3 layering, with orthogonal layerings at three different scales. This microstructure is useful for single load problems in 3 dimensions.

1.1.3 The homogenization formulas

The material distribution approach to topology design of continuum structures as described above relies on the ability to model a material with microstructure and thus allowing for the description of a structure by a density of material. Here we take an approach where the porous material with microstructure is constructed from a basic unit cell, consisting at a macroscopic level of material and void. The composite, porous medium then consists of infinitely many of such cells, now infinitely small, and repeated periodically through the medium. At this limit, we can also have continuously varying density of material through the medium, as required for topology optimization (cf., Fig. 1.2). The resulting medium can be described by effective, macroscopic material properties which depend on the geometry of the basic cell, and these properties can be computed by invoking the formulas of homogenization theory.

The computation of these effective properties play a key role for the topology optimization, so for this reason and for the sake of completeness of the presentation, the formulas of homogenization will be briefly presented for the case of dimension 2. For details, the reader is referred to the references quoted in the bibliographical notes (chapter 6) [4], [9], [12], [13]. Suppose that a periodic micro structure is assumed in the neighbourhood of an arbitrary point x of a given linearly elastic structure (cf., Fig. 1.2). The periodicity is represented by a parameter δ which is very small and the elasticity tensor E^{δ}_{ijkl} is given in the form

$$E^{\delta}_{ijkl}(x) = E_{ijkl}(x, \frac{x}{\delta})$$

where $y \rightarrow E_{ijkl}(x,y)$ is Y-periodic, with cell $\mathrm{Y} = [\mathrm{Y}_{1\mathrm{R}}, Y_{1L}] \times [\mathrm{Y}_{2\mathrm{R}}, Y_{2L}]$ of periodicity. Here x is the macroscopic variation of material parameters, while x/δ gives the microscopic, periodic variations. Now, suppose that the structure is subjected to a macroscopic body force and a macroscopic surface traction. The resulting displacement field $u^{\delta}(x)$ can then be expanded as

$$u^{\delta}(x) = u_0(x) + \delta\, u_1(x, \frac{x}{\delta}) + \;\ldots\ldots\ldots$$

where the leading term $u_0(x)$ is a macroscopic deformation field that is independent of the microscopic variable y. It turns out that this effective displacement field is the macroscopic deformation field that arises due to the applied forces when the rigidity of the structure is assumed given by the effective rigidity tensor

$$E^{\mathrm{H}}_{ijkl}(x) = \frac{1}{|Y|} \int_{Y} \left[E_{ijkl}(x,y) - E_{ijpq}(x,y) \frac{\partial \chi^{kl}_{p}}{\partial y_q} \right] \mathrm{d}y \qquad (1.11)$$

Here χ^{kl} is a microscopic displacement field that is given as the Y-periodic solution of the cell-problem (in weak form):

$$\int_Y \left[E_{ijpq}(x,y)\frac{\partial \chi_p^{kl}}{\partial y_q} \right] \frac{\partial \varphi_i}{\partial y_j} \mathrm{d}y = \int_Y E_{ijkl}(x,y)\frac{\partial \varphi_i}{\partial y_j} \mathrm{d}y \quad \text{for all } \varphi \in U_Y \tag{1.12}$$

where U_Y denotes the set of all Y-periodic virtual displacement fields. With $y^{11} = (y_1, 0)$, $y^{12} = (y_2, 0)$, $y^{21} = (0, y_1)$ and $y^{22} = (0, y_2)$, the variational form of equations (1.11) and (1.12) reads:

$$E_{ijkl}^{\mathbf{H}}(x) = \min_{\varphi \in U_Y} \frac{1}{|Y|} a_Y(y^{ij} - \varphi, y^{kl} - \varphi) \tag{1.13a}$$

while the form of these equations in compact notation is

$$E_{ijkl}^{\mathbf{H}}(x) = \frac{1}{|Y|} a_Y(y^{ij} - \chi^{ij}, y^{kl} - \chi^{kl}) \tag{1.13b}$$

$$a_Y(y^{ij} - \chi^{ij}, \varphi) = 0 \quad \text{for all } \varphi \in U_Y \tag{1.14}$$

From Equations (1.11) and (1.12) we see that the effective moduli for plane problems can be computed by solving three analysis problems for the unit cell Y. For most geometries this has to be done numerically using finite element methods, [13], or, as can be advantageous, by use of boundary element methods or spectral methods. For use in a design context the homogenization process should be implemented as an easy-to-use pre-processor (Guedes and Kikuchi, 1990). Equations (1.11) and (1.12) hold for mixtures of linearly, elastic materials and for materials with voids (Cioranescu and St. Jean Paulin, 1986). Figures 1.7 and 1.8 show the variation of the effective moduli for some typical microstructures, as illustrated in Fig. 1.3.

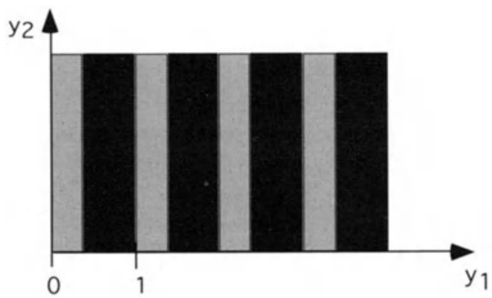

Fig. 1.10. A rank-1 layered material.

Now, consider a layered material, as illustrated in Fig. 1.10 with layers directed along the y_2- direction and repeated periodically along the y_1-axis. The unit cell is $[0,1]\times\mathbf{R}$, and it is clear that the unit cell fields χ^{kl} are independent of the variable y_2. Also note that in Equation (1.11), the term involving the cell deformation field χ^{kl} is of the form $E_{ijpq}(x,y)\dfrac{\partial\chi_p^{kl}}{\partial y_q}$, so an explicit expression for χ^{kl} is not needed.

Using periodicity and appropriate test functions and assuming that the direction of the layering coalesces with the directions of orthotropy of the materials involved, the only non-zero elements E_{1111}, E_{2222}, E_{1212} $(=E_{1221}=E_{2121}=E_{2112})$, E_{1122} $(=E_{2211})$ of the tensor E_{ijkl} can be calculated as (see Sect. 1.6):

$$E_{1111}^{\mathbf{H}}=\left[M\left(\frac{1}{E_{1111}}\right)\right]^{-1}$$

$$E_{2222}^{\mathbf{H}}=M(E_{2222})-\left[M\left(\frac{E_{2211}^{\;2}}{E_{1111}}\right)\right]+\left[M\left(\frac{E_{2211}}{E_{1111}}\right)\right]^{2}\left[M\left(\frac{1}{E_{1111}}\right)\right]^{-1}$$

$$E_{1122}^{\mathbf{H}}=\left[M\left(\frac{E_{1122}}{E_{1111}}\right)\right]\left[M\left(\frac{1}{E_{1111}}\right)\right]^{-1}$$

$$E_{1212}^{\mathbf{H}}=\left[M\left(\frac{1}{E_{1212}}\right)\right]^{-1}$$

where $M(\ )$ denotes the average over the unit cell.

For a layering of two isotropic materials with the same Poisson ratio ν, with different Young's moduli E^+ and E^- and with layer thicknesses γ and (1- γ), respectively, the layering formulas (in plane stress) reduce to the following simple expressions :

$$\begin{aligned}
&E_{1111}^{\mathbf{H}}=I_1, \qquad E_{2222}^{\mathbf{H}}=I_2+\nu^2 I_1\\
&E_{1212}^{\mathbf{H}}=\frac{1-\nu}{2}I_1, \quad E_{1122}^{\mathbf{H}}=\nu I_1\\
&I_1=\frac{1}{1-\nu^2}\frac{E^+E^-}{\gamma E^-+(1-\gamma)E^+}\\
&I_2=\gamma E^+ +(1-\gamma)E^-
\end{aligned} \tag{1.15}$$

For a rank-2 layering of material and void with primary layerings of density μ in the 2-direction and the secondary layer of density γ in direction 1, the effective material properties of the resulting material can be computed by recursive use of

(1.15). The moduli are computed as the material is constructed, bottom up and the resulting material properties are:

$$
\begin{gathered}
E_{1111} = \frac{\gamma E}{\mu\gamma(1-\nu^2)+(1-\mu)}\,, \quad E_{1122} = \mu\nu E_{1111}\,, \\
E_{2222} = \mu E + \mu^2\nu^2 E_{1111}\,, \qquad E_{1212} = 0
\end{gathered}
\tag{1.16}
$$

where E is Young's modulus and ν is Poisson's ratio of the base material.

We see from (1.16) that for layered materials consisting of material and *void*, the effective rank-2 material in dimension two does not possess any shear stiffness ($E_{1212} = 0$). Thus, for a computational topology design scheme that is based on equilibrium analyses with these materials, voids should be represented by a very weak material in order to avoid singular stiffness matrices. On the other hand, layered materials have analytical expressions for the effective moduli which is a distinct advantage for optimization. For other types of micro voids the effective moduli have to be computed numerically for a number of dimensions of the voids in the unit cell, and for other values of densities the effective moduli can be interpolated using for example Legendre polynomials or splines; this gives an easy method for computing design derivatives as well. Note that the interpolation only needs to be carried out for different values of Poisson's ratio, as Young's modulus enters as a scaling factor. The plot in figure 1.7 was generated this way. A detailed derivation of the layer formulas is described in section 1.6, where the relation of the homogenization theory to traditional engineering smear-out techniques is also outlined.

It is important here to underline that the use of homogenized material coefficients is consistent with a basic property of the minimum compliance problem as formulated in (1.1). To this end, consider a minimizing sequence of designs in the set of 0-1 designs defined in (1.7) and assume that this sequence of designs consists of microcells given by a scaling parameter $\delta > 0$. In the limit of $\delta \to 0$, the sequence of designs has a response governed by the homogenized coefficients. It is a fundamental property of the homogenization process that the displacements $u^{\delta}(x)$ of the sequence of designs will converge *weakly* to the displacement $u_0(x)$ of the homogenized design (cf., [4]). As the compliance functional is a weakly continuous functional of the displacements this implies the convergence of the compliance values. We can thus conclude that inclusion of homogenized materials in the design formulation does not provide for a jump in performance, but rather provides (some) closure of the design space. However, at the same time we achieve a design description by continuous variables.

1.1.4 Alternative design parametrizations

The design problem for a fixed domain can also be formulated as a sizing problem by modifying the stiffness matrix so that it depends continuously on an artificial density-like function [14]. This function is then the design variable. The

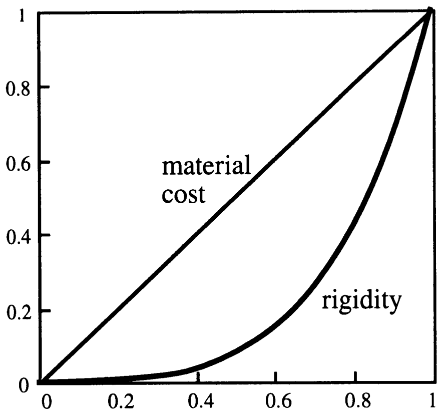

Fig. 1.11. The cost and stiffness of an artificial material, with cost proportional to the 'density' η and with rigidity proportional to η^4.

requirement is that the optimization results in designs consisting almost entirely of regions of material or no material. This means that intermediate values of this artificial density function should be penalized in a manner analogous to other continuous optimization approximations of 0-1 problems. One possibility which seems to be very popular is to use a relation:

$$\begin{gathered} \eta \in L^\infty(\Omega) \\ E_{ijkl}(x) = \eta(x)^q E^0_{ijkl}, \ q > 1 \\ \int_\Omega \eta(x) \, d\Omega \le V; \ 0 \le \eta(x) \le 1, \quad x \in \Omega \end{gathered} \tag{1.17}$$

where $\eta(x)$ is the design function and E^0_{ijkl} represents the material properties of a given isotropic material. We choose here $q > 1$ so that intermediate densities are unfavourable in the sense that the rigidity obtained is small compared to the cost of the material. Another related type of design parametrization is the attempt to achieve a continuous transition from material to no material by approximating the indicator functions of the basic parametrization (1.7) by a smooth function (a mollifier function approach) [14].

The idea behind the penalized density approaches is to think of the physical reality as the design of a variable thickness sheet, for which intermediate thicknesses are penalized. This makes sense for planar problems, where the extra dimension in 3-space makes it possible to make a physical interpretation of an eventual resultant intermediate density. However, for fully three dimensional problems this interpretation is not possible, and there is no direct way to physically interpret intermediate densities, and such will appear, albeit often in small regions, in the optimized solution. These more direct approaches work reasonably well numerically and give a good prediction of topology, but the methods suffer from the non-existence of solutions as a distributed parameter problem, as for the general discrete valued 0-1 case (the problem is now completely analogous to the variable thickness plate problem for which the lack of existence is well-known, see Sect. 5.3). This may not cause problems for concrete discretizations, but will make the results prone to mesh dependence for fine meshes. Thus, refining the finite element mesh for the ground structure (reference domain) will ultimately lead to the generation of the fine composite structures which the relaxation predicts for the optimum structure.

It should be noted that for planar problems, the penalized approach given by the relations (1.17) reduces to the setting of the well-known variable thickness sheet design problem if we set $q = 1$; in this case the density function η is precisely the thickness of the sheet. The variable thickness sheet design problem corresponds directly to a truss design problem in the sense that the stiffness of the structure as well as the volume of the structure depend linearly on the design variable. This implies that a finite element approximation of the problem can be solved using some very efficient algorithms that have been developed for truss topology design (cf. Chap. 4). The linear dependence on the design function η has, however, a more fundamental implication for the continuum problem, as one can prove existence of solutions (see Sect. 1.5.1), thus avoiding the need for relaxation and the introduction of materials with micro structure. It is also possible to obtain existence of solutions to the general penalized density function approach (1.17) by restricting further the variations of the density function:

$$
\begin{gathered}
\eta \in H^1(\Omega) \\
E_{ijkl}(x) = \eta(x)^q E^0_{ijkl}, \; q > 1 \\
\int_\Omega \eta(x)\,\mathrm{d}\Omega \le V\,; \;\; 0 \le \eta(x) \le 1, \quad x \in \Omega \\
\| \eta \|_{H^1} = \left[\int_\Omega (\eta^2 + (\nabla \eta)^2)\,\mathrm{d}\Omega \right]^{1/2} \le M
\end{gathered}
\tag{1.18}
$$

Here we assume that η as well as its gradient has bounded variation, and the existence then follows from the Sobolev embedding theorem (see Sect. 1.5.2). Note here that for three dimensional problems we have to enforce $q < 3$ as well. The definition (1.18) of E_{ad} implies a certain measure of penalization on the average variation of the density. Note that we for any finite element discretization of the ground structure Ω can choose a large enough bound M on the norm of η so that the norm constraint remains inactive, thus seemingly returning to the formulation (1.17) for this discretization. Thus implementation of (1.18) requires utmost care and should involve experimenting with a range of values of the bound M.

It should be recognized that the variable thickness design problem (i.e., (1.17) with $q = 1$) can also be interpreted as a design formulation where we seek the optimum design over all isotropic materials with given Poisson ratio and continuous varying Young's modulus [14]. The volume constraint is in this case somewhat artificial. The advantage of this setting is that we maintain the existence of solutions arising from the linear design-rigidity relation. Also, this problem is computationally simple. However, the setting is somewhat restrictive as we do not approximate the 0-1 type solution as in the case of the penalized density formulation. Also, from the relaxation of the 0-1 problem we know that composites should be used if really optimal structures should be predicted, and this possibility is excluded by this design parametrization. It turns out, though, that the introduction of composites and the linear design-rigidity relation can be combined in one formulation by considering a completely free parametrization of the rigidity tensors over all positive definite tensors. This will be discussed in detail in chapter 3.

In order to complete the discussion on shape design parametrization, we shall briefly outline the standard boundary variations parametrization of shape. To this end, we refer all admissible domains to a reference domain Ω through differentiable one-to-one maps (C^1-diffeomorfisms) $\Phi:\Omega \to \Phi(\Omega) \subseteq \mathbf{R}^2$. Thus all domains are of the form $\Phi(\Omega)$, with the volume constraint being expressed as

$$\mathrm{Vol}(\Phi(\Omega)) = \int_{\mathbf{R}^2} 1_{\Phi(\Omega)}\, dx \le V = \int_{\mathbf{R}^2} 1_\Omega \, dx = \mathrm{Vol}(\Omega)$$

This parametrization means that the topology of *all* admissible domains is given by the choice of reference domain Ω and no change in lay-out is possible. Also, note that in this the setting the state variables and the integrals in the problem statements (1.1), (1.2) and (1.3) are all defined on varying domains. For analysis it is crucial to have a formulation on a common domain of reference. The standard technique to obtain this is to use a transformation of coordinates in order to express the equilibrium conditions for the domains $\Phi(\Omega)$ on the reference domain Ω. This results in a formulation (1.1) for which

$$l(u) = \int_\Omega pu \left|\det \nabla\varphi^{-1}\right| d\Omega + \int_{\Gamma_T} tu \left|\mathrm{adj}\nabla\varphi^{-1}\right| d\Gamma$$

and the rigidity tensors are of the form

$$E_{ijkl} = E^0_{ipkq}(\nabla\varphi^{-1})_{jp}(\nabla\varphi^{-1})_{lq}\left|\det\nabla\varphi^{-1}\right|$$

The problem is still basically of the form of (1.1), but now the loads are also design dependent. Also, the rigidity tensor depends in an intricate way on the design parametrization. Note that for existence of solutions one can often refer to compactness arguments by restricting the admissible diffeomorfisms to have bounded first and second derivatives [2].

The variation of shape is in implementations of the boundary variations method often controlled via a discrete parametrization of the boundary for example through the control points of splines. The solution of the shape optimization problem using a finite element method for the analysis has to be able to handle the changes in shape introduced after each optimization iteration. These changes often require the construction of a new discrete model of the structure after each optimization step. The new mesh should be generated automatically and directly from the design variables used to parametrize the shape. The complications in the boundary shape variations method thus lies almost entirely in the analysis and design sensitivity, while the optimization in itself is simplified by the small number of design variables typically used for these problems. The methodology is, however, very well established and there exist several commercially available software systems for boundary shape design of structures ([2], [7], [15]).

1.2 Conditions of optimality

In the following we shall derive the necessary conditions of optimality for the minimum compliance design problem that employs composite materials in the parametrization of design. For this design formulation there are two distinct types of design variables. First, the composite material is an anisotropic (normally orthotropic) material for which the angle of rotation of the unit cell is an important unconstrained design variable, and second, the sizes describing the unit cells constitutes a different type of variables which are globally constrained through the volume constraint.

1.2.1 Optimal rotation of orthotropic materials

The formulation of the material distribution method for generating optimal continuum structures involves the introduction of a composite consisting of the base material with periodically repeated micro-voids. The composites with cell symmetry described in the preceding sections are orthotropic, and the angle of rotation of the material axes of this material will influence the value of the compliance of the structure. It turns out that the optimal rotation can be found analytically and this is of great importance for computations and it is interesting in its own right.

The optimal rotation of an orthotropic material is not only of importance for the present setting of topology design, but is equally significant in the design of composite structures, laminates, etc. For this reason we will here derive the conditions of optimality for material rotations in plane stress/strain problems (i.e. 2-D) [17].

Assume an orthotropic material as given. Then in the frame of reference given by the material axes of this material we have a stress-strain relation

$$\sigma_{ij} = E_{ijkl}\varepsilon_{kl}$$

with E_{1111}, E_{2222}, E_{1122}, E_{1212}, being the only non-zero components of the rigidity tensor E_{ijkl} . We assume that $E_{1111} \geq E_{2222}$, and assume that a given set $\varepsilon_{ij}^k,\ k=1,...,M$ of strain fields for a number of load cases are given. With compliance design in mind, we see from the formulations (1.2) and (1.5) of the minimum compliance problem that our interest is to maximize the weighted sum of a number of strain energy densities:

$$W = \sum_{k=1}^{M} w^k \left[\frac{1}{2} E_{1111}\, {\varepsilon_{11}^{k}}^2 + \frac{1}{2} E_{2222}\, {\varepsilon_{22}^{k}}^2 + E_{1122}\, \varepsilon_{11}^{k}\varepsilon_{22}^{k} + 2E_{1212}\, {\varepsilon_{12}^{k}}^2 \right]$$

We now express the strains in terms of the principal strains ε_I^k, ε_{II}^k , where we choose $|\varepsilon_I^k| \geq |\varepsilon_{II}^k|$ for convenience:

$$\varepsilon_{11}^k = \frac{1}{2}\left[(\varepsilon_I^k + \varepsilon_{II}^k) + (\varepsilon_I^k - \varepsilon_{II}^k)\cos 2\psi^k\right]$$

$$\varepsilon_{22}^k = \frac{1}{2}\left[(\varepsilon_I^k + \varepsilon_{II}^k) - (\varepsilon_I^k - \varepsilon_{II}^k)\cos 2\psi^k\right]$$

$$\varepsilon_{12}^k = -\frac{1}{2}(\varepsilon_I^k - \varepsilon_{II}^k)\sin 2\psi^k$$

Here ψ^k is the angle of rotation of the material frame relative to the frame of the k'th principal strains. We are interested in the angle Θ of rotation of the material relative to a chosen frame of reference which maximizes the function W . Each angle ψ^k is thus written as $\psi^k = \Theta - \alpha^k$, where α^k is the angle of rotation of the k'th strain field (see figure 1.12).

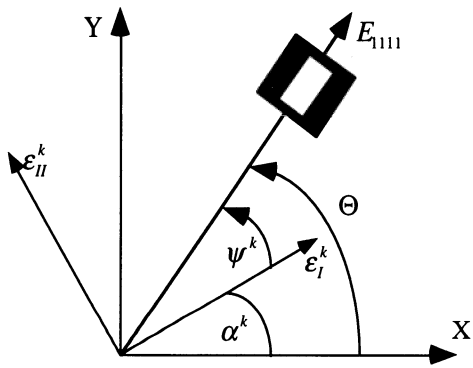

Fig. 1.12. The definition of angles of rotation of material and principal strain axes.

Inserting the expressions for the strains expressed in terms of the reference principal strains into the equation for W and differentiating, we get the condition of stationarity as:

$$\sum_{k=1}^{M} w^k \left[A^k \sin 2(\Theta - \alpha^k) + B^k \sin 2(\Theta - \alpha^k) \cos 2(\Theta - \alpha^k) \right] = 0$$

with

$$A^k = (\varepsilon_I^{k2} - \varepsilon_{II}^{k\,2})(E_{1111} - E_{2222}), \quad B^k = (\varepsilon_I^k - \varepsilon_{II}^k)^2 (E_{2222} + E_{1111} - 2E_{1122} - 4E_{1212})$$

Stationarity is thus achieved if the following fourth order polynomial in $\sin 2\Theta$ is zero:

$$P(\sin 2\Theta) = a_4 \sin^4 2\Theta + a_3 \sin^3 2\Theta + a_2 \sin^2 2\Theta + a_1 \sin 2\Theta + a_0$$

where

$$a_4 = z_3^2 + z_4^2, \quad a_3 = 2z_1 z_4 - 2z_3 z_2,$$
$$a_2 = z_1^2 + z_2^2 - z_3^2 - z_4^2,$$
$$a_1 = z_2 z_3 - 2z_1 z_4, \quad a_0 = \frac{z_3^2}{4} - z_1^2$$

$$z_1 = \sum_{k=1}^{M} w^k A^k \sin 2\alpha^k, \quad z_2 = \sum_{k=1}^{M} w^k A^k \cos 2\alpha^k$$
$$z_3 = 2\sum_{k=1}^{M} w^k B^k \sin 4\alpha^k, \quad z_2 = 2\sum_{k=1}^{M} w^k B^k \cos 4\alpha^k$$

W is periodic so there exist at least two real roots of P. Also, as the order of P is four, the roots of P can be given analytically. The actual minimizer of the compliance is found by evaluating W for the four or eight stationary rotations. This feature is of great importance for the numerical implementation of the homogenization method for optimal topology design, as the iterative optimization of a periodic function with several local minima and maxima is very likely to give the wrong result. Also, the analytical derivation of the optimal angles saves considerably in computational time.

For the single load case we can express directly the stationary angle ψ by (using the principal strain axes as the reference system)

$$\sin 2\psi = 0 \ \text{ or } \ \cos 2\psi = -\gamma, \text{ with } \gamma = \frac{\alpha}{\beta} \frac{\varepsilon_I + \varepsilon_{II}}{\varepsilon_I - \varepsilon_{II}}, \quad \text{and}$$
$$\alpha = (E_{1111} - E_{2222}) \geq 0, \quad \beta = (E_{2222} + E_{1111} - 2E_{1122} - 4E_{1212})$$

Inserting these values in the second variation of W with respect to ψ (see Pedersen, 1989), it can be seen that the maximizing ψ (i.e. the compliance minimizer) depends on the sign of the parameter β . The parameter β is a measure of the shear stiffness of the orthotropic material. For low shear stiffness, that is, $\beta \geq 0$, the globally minimal compliance is achieved for $\psi = 0$, i.e. the intuitive result that the numerically largest principal strain is aligned with the strongest material axis; also, from the stress-strain relation, we see that in this case these axes are aligned with the axes of principal stresses, also. The materials used in topology design (as described in Sect. 1.1.2) are weak in shear , i.e. $\beta \geq 0$. For certain (engineering) laminates with ply-angle $\pm\phi$, $22.5^\circ \leq \phi \leq 45^\circ$, we can have the situation of high shear stiffness, i.e. $\beta \leq 0$ (Pedersen, 1989). In this case, $\cos 2\psi = -\gamma$ is the global minimum for compliance as long as $-1 < \gamma < 0$ (γ has the sign of β), and for $\gamma \leq -1$, $\psi = 0$ is again the global minimum.

Note that a similar analysis holds for stresses. For a single field of stress/strains, the principal strains, the principal stresses and the material axes should all be aligned at the optimum for materials that are weak in shear.

For three dimensional elasticity we have three angles of rotations possible for the axes of orthotropy (e.g. using Euler angles) and the expressions above for first variations with respect to angles become infinitely more complicated. For the materials used for design, it is possible to show stationarity of the alignment of material axes, principal strain axes and principal stress axes. The full answer to the 3-D cases is still open [17].

For the materials involving multi-layered media (the rank-n laminates/layerings) the result on the optimal rotation follows by alternative means from the studies on optimal bounds on effective moduli of materials [21]. For these materials it is thus proven that for the single load case, the optimal rotation of the material is consistent with an alignment of the layerings with the principal stresses/strains and this holds in dimension two *and* three.

We remark here that the problem of optimal design of the spatially varying angle of rotation of a fixed orthotropic material is not well-posed in general. Relaxation is needed for this case also, as the introduction of for example layered materials consisting of the orthotropic material at various rotations extends the range of available materials. This is discussed in Fedorov and Cherkaev, 1983.

1.2.2 Optimality conditions for density

Following standard optimality criteria methods used in structural optimization [18], the simple structure of the continuum, multiple load problem (1.5) can be utilized to generate extremely efficient computational update schemes for solving the problems we address here. The key is to devise iterative methods which update the design variables at each point (or rather at each element of a finite element discretization) independently from the updates at other points, based on the necessary conditions of optimality.

For the problems at hand we note that E_{ijkl} depends on geometric quantities which define the microstructure. For a square, 1 by 1, micro cell with a rectangular hole of dimension $(1-\mu)$ times $(1-\gamma)$ the density of material is given as $\rho = \mu + \gamma - \mu\gamma$ (cf., figure 1.3) and the constraints on the design variables μ, γ are

$$\int_\Omega (\mu(x) + \gamma(x) - \mu(x)\gamma(x))\, d\Omega = V,$$
$$0 \le \mu(x) \le 1 \;, 0 \le \gamma(x) \le 1 \;, \quad \text{for all } x \in \Omega,$$

This relation also holds for the rank-2 layered material, cf., figure 1.3.

With Lagrange multipliers $\Lambda, z_\mu^-(x), z_\mu^+(x), z_\gamma^-(x), z_\gamma^+(x)$ for these constraints, the necessary conditions for optimality for the sizing variables μ, γ are a subset of the stationarity conditions for the Lagrange function

$$\begin{aligned} L = \sum_{k=1}^{M} w^k l^k(u^k) - \left\{ \sum_{k=1}^{M} a_E(u^k, \bar{u}^k) - l^k(\bar{u}^k) \right\} + \\ \Lambda\left(\int_\Omega [\mu(x) + \gamma(x) - \mu(x)\gamma(x)]\, d\Omega - V\right) + \\ \int_\Omega z_\mu^+(x)(\mu(x) - 1)\, d\Omega - \int_\Omega z_\mu^-(x)\mu(x)\, d\Omega + \\ \int_\Omega z_\gamma^+(x)(\gamma(x) - 1)\, d\Omega - \int_\Omega z_\gamma^-(x)\gamma(x)\, d\Omega \end{aligned}$$

where $\bar{u}^k$, $k=1,\ldots,M$, are Lagrange multipliers for the equilibrium constraints. Note that $\bar{u}^k$ belongs to the set U of kinematically admissible displacement fields. Under the assumption of uniform ellipticity of the forms a_E, the necessary condition for optimality give that $\bar{u}^k = w^k u^k$ and the conditions for μ, γ become:

$$\begin{aligned} \sum_{k=1}^{M} w^k \frac{\partial E_{ijpq}}{\partial \mu} \varepsilon_{ij}(u^k)\varepsilon_{pq}(u^k) = \Lambda(1-\gamma) + z_\mu^+ - z_\mu^- \\ \sum_{k=1}^{M} w^k \frac{\partial E_{ijpq}}{\partial \gamma} \varepsilon_{ij}(u^k)\varepsilon_{pq}(u^k) = \Lambda(1-\mu) + z_\gamma^+ - z_\gamma^- \end{aligned} \tag{1.19}$$

with the switching conditions

$$z_\mu^- \ge 0, \quad z_\mu^+ \ge 0, \quad z_\mu^- \mu = 0, \quad z_\mu^+(\mu - 1) = 0$$
$$z_\gamma^- \ge 0, \quad z_\gamma^+ \ge 0, \quad z_\gamma^- \gamma = 0, \quad z_\gamma^+(\gamma - 1) = 0$$

For intermediate densities $(0 < \mu < 1 \,, 0 < \gamma < 1)$ the conditions (1.19) can be written as

$$
\begin{aligned}
&\frac{1}{\Lambda(1-\gamma)}\sum_{k=1}^{M} w^k \frac{\partial E_{ijpq}}{\partial \mu}\varepsilon_{ij}(u^k)\varepsilon_{pq}(u^k)=1\\
&\frac{1}{\Lambda(1-\mu)}\sum_{k=1}^{M} w^k \frac{\partial E_{ijpq}}{\partial \gamma}\varepsilon_{ij}(u^k)\varepsilon_{pq}(u^k)=1
\end{aligned}
\tag{1.20}
$$

which can be interpreted as a statement that expresses that the energy-like left-hand side terms are constant equal to 1 for all intermediate densities. This is thus a condition that reminds us of the fully stressed design condition in plastic design. As we expect areas with high energy to be too low on rigidity, we devise the following fix-point type update scheme for the densities [18]:

$$
\mu_{K+1}=\begin{cases}
\max\{(1-\varsigma)\mu_K,0\} \ \text{ if } \ \mu_K \mathrm{B}_K^{\eta}\le \max\{(1-\varsigma)\mu_K,0\}\\
\mu_K \mathrm{B}_K^{\eta} \ \text{ if } \ \max\{(1-\varsigma)\mu_K,0\}\le \mu_K \mathrm{B}_K^{\eta}\le \min\{(1+\varsigma)\mu_K,1\}\\
\min\{(1+\varsigma)\mu_K,1\} \ \text{ if } \ \min\{(1+\varsigma)\mu_K,1\}\le \mu_K \mathrm{B}_K^{\eta}
\end{cases}
$$

$$
\gamma_{K+1}=\begin{cases}
\max\{(1-\varsigma)\gamma_K,0\} \ \text{ if } \ \gamma_K \mathrm{E}_K^{\eta}\le \max\{(1-\varsigma)\gamma_K,0\}\\
\gamma_K \mathrm{E}_K^{\eta} \ \text{ if } \ \max\{(1-\varsigma)\gamma_K,0\}\le \gamma_K \mathrm{E}_K^{\eta}\le \min\{(1+\varsigma)\gamma_K,1\}\\
\min\{(1+\varsigma)\gamma_K,1\} \ \text{ if } \ \min\{(1+\varsigma)\gamma_K,1\}\le \gamma_K \mathrm{E}_K^{\eta}
\end{cases}
$$

Here μ_K, γ_K denotes the variables at iteration step K, and B, E are

$$
\mathrm{B}_K=[\Lambda_K(1-\gamma_K)]^{-1}\sum_{k=1}^{M} w^k \frac{\partial E_{ijpq}}{\partial \mu}(\mu_K,\gamma_K)\ \varepsilon_{ij}(u_K^k)\varepsilon_{pq}(u_K^k)
$$

$$
\mathrm{E}_K=[\Lambda_K(1-\mu_K)]^{-1}\sum_{k=1}^{M} w^k \frac{\partial E_{ijpq}}{\partial \gamma}(\mu_K,\gamma_K)\ \varepsilon_{ij}(u_K^k)\varepsilon_{pq}(u_K^k)
$$

η is a tuning parameter and ζ a move limit, which can be made adjustable for efficiency of the method. Note that the updates μ_{K+1} and γ_{K+1} depend on the present value of the Lagrange multiplier Λ, and thus Λ should be adjusted in an inner iteration loop in order to satisfy the active volume constraint. It is readily seen that the volume of the updated values of the densities is a continuous and decreasing function of the multiplier Λ. Moreover, the volume is strictly decreasing in the interesting intervals, where the bounds on the densities are not active in all points (elements of a FEM discretization). This means that we can uniquely determine the value of Λ, using a bisection method or a Newton method. The values of η and ζ are chosen by experiment, in order to obtain a suitable rapid and stable convergence of the iteration scheme. Typical useful values of η and ζ are 0.8 and 0.5, respectively. If the density is given through a number of other design variables describing the micro geometry of voids, update schemes like the above should be generated for these variables. Finally, the angle of rotation of the orthotropic material with voids should also be updated, using that the axes of orthotropy are given by the axes of principal strains or principal stresses, as described above.

It is interesting to note that many models used in bio-mechanics for bone adaptation have a form which is similar to the optimality criteria algorithm described above [18]. These models are usually based on energy arguments and are not derived from an optimization principle. The similarity in approach to material redistribution updates has now lead to bone adaptation models being proposed as topology redesign methods, see for example Reiter, Rammerstorfer and Böhm, 1993.

1.3 Implementation of the homogenization approach

In sections 1.1 and 1.2 we have outlined the basic ingredients of the direct method for implementing the homogenization procedure for topology design. These consist of the basic parametrization of design through the geometric quantities defining a microstructure, the design-rigidity relation given through the formulas of homogenization and the update scheme based on the optimality conditions. Finally, these update schemes are based on the ability to solve the equilibrium equations, and here we presume this to be performed by the finite element method.

1.3.1 Computational procedure

The direct method of layout design using the homogenization modelling is based on the numerical calculation of the globally optimal distribution of the design variables that define the microstructures in use. This in turn, then, determines the distribution of the density of material, the primary target of our scheme. We will in chapter 2 consider implementation methods that are based on the analytical derivation of the optimized *local* material properties.

The direct method for finding the optimal topology of a structure constructed from a single isotropic material consists of the following steps:

Pre-processing of material properties:

- Choose a composite, constructed by periodic repetition of a unit cell consisting of the given material with one or more holes or a layered material. Compute the effective material properties of the composite, using homogenization theory. This gives a functional relationship between the density of material in the composite (i.e. sizes of holes or layerings) and the effective material properties of the resulting orthotropic material.

- Generate a database of material properties as functions of the design variables with one set of data for each allowed value of Poisson ratio. For layered materials no database is required, only a suitable subroutine.

Pre-processing of geometry and loading:
- Choose a suitable reference domain (the ground structure) that allows for the definition of surface tractions, fixed boundaries, etc. (see Fig. 1.13).
- Choose the parts of the reference domain that should be designed, and what parts of the ground structure that should be left as solid domains or voids (see Fig. 1.13).
- Construct a FEM mesh for the ground structure. This mesh should be fine enough in order to describe the structure in what would seem a bit-map representation and should make it possible to define the a priori given areas of the structure by assigning fixed design variables to such areas. The mesh is unchanged through-out the design process.
- Construct finite element spaces for the independent fields of displacements and the design variables.

Optimization:
Compute the optimal distribution over the reference domain of the design variables. These variables describe the properties of the composite material. The optimization uses a displacement based analysis and the optimality update criteria schemes for the densities and the result on optimal angles of rotation for the cell rotation. The structure of the algorithm is:
- Make initial design, e.g., homogeneous distribution of material.

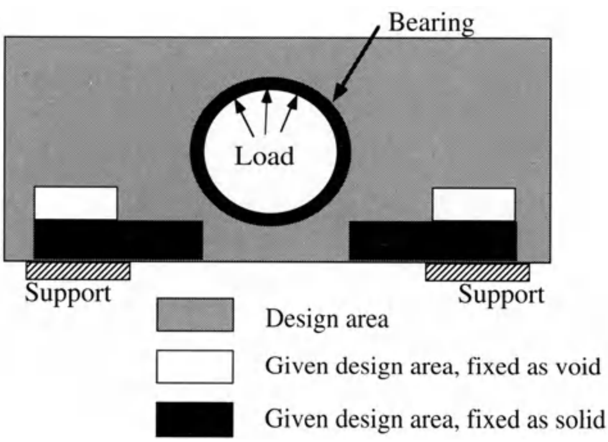

Fig. 1.13. The possibility of letting the design area be a sub-area of the reference domain.

The iterative part of the algorithm is then:

- For present design defined by density (geometry) variables and angle of rotation of cell, compute the rigidity tensor throughout the structure, based on the database/subroutine mentioned above and the well-known frame-rotation formulas.
- For this distribution of rigidity, compute by the finite element method the resulting displacements and associated principal strains and stresses, for each load case.
- Compute the compliance of this design. If only marginal improvement (in compliance) over last design, stop the iterations. Else, continue. For detailed studies stop when necessary conditions of optimality are satisfied (cf. section 1.2)
- Update angle of cell rotations based on the optimality criteria described in section 1.2.1. For stability of scheme, base this on the principal stresses.
- Independently of the update of the angles, compute the update of the density variables, based on the scheme shown in section 1.2.2. The energy expressions B, E are most conveniently computed from the principal strains. This step also consists of an inner iteration loop for finding the value of the Lagrange multiplier Λ for the volume constraint.
- Repeat the iteration loop.

For a case where there are parts of the structure which are fixed (as solid and/or void) the updating of the design variables should only be invoked for the areas of the ground structure which are being redesigned (reinforced).

Post-processing of results:

- Interpret the optimal distribution of material as defining a shape, in the sense of the traditional boundary shape formulations.

For the method above one should at an initial stage decide on a choice of a basic unit cell as the basis for the computation of effective moduli. The important quantity for the shape design aspect of the homogenization method is the density of material and the underlying geometric quantities defining this density are in a sense of less interest.

Employing for 2-D problems micro voids which are square holes in square unit cells the density is described by just one geometric variable, namely the length of the sides of the square. Also the density can take on all values between 0 and 1, a feature that is not satisfied for, e.g. circular holes in square cells, for which zero density is impossible.

Using rectangular micro voids in square cells gives a slightly more complicated microstructure, doubling the number of geometric design variables. Several experiments have shown that the use of rectangular holes usually gives a more stable iteration history for the optimality criteria update scheme and also results in slightly better compliance values. For 3-D problems, box-like holes in cubic cells is a simple choice of micro structure.

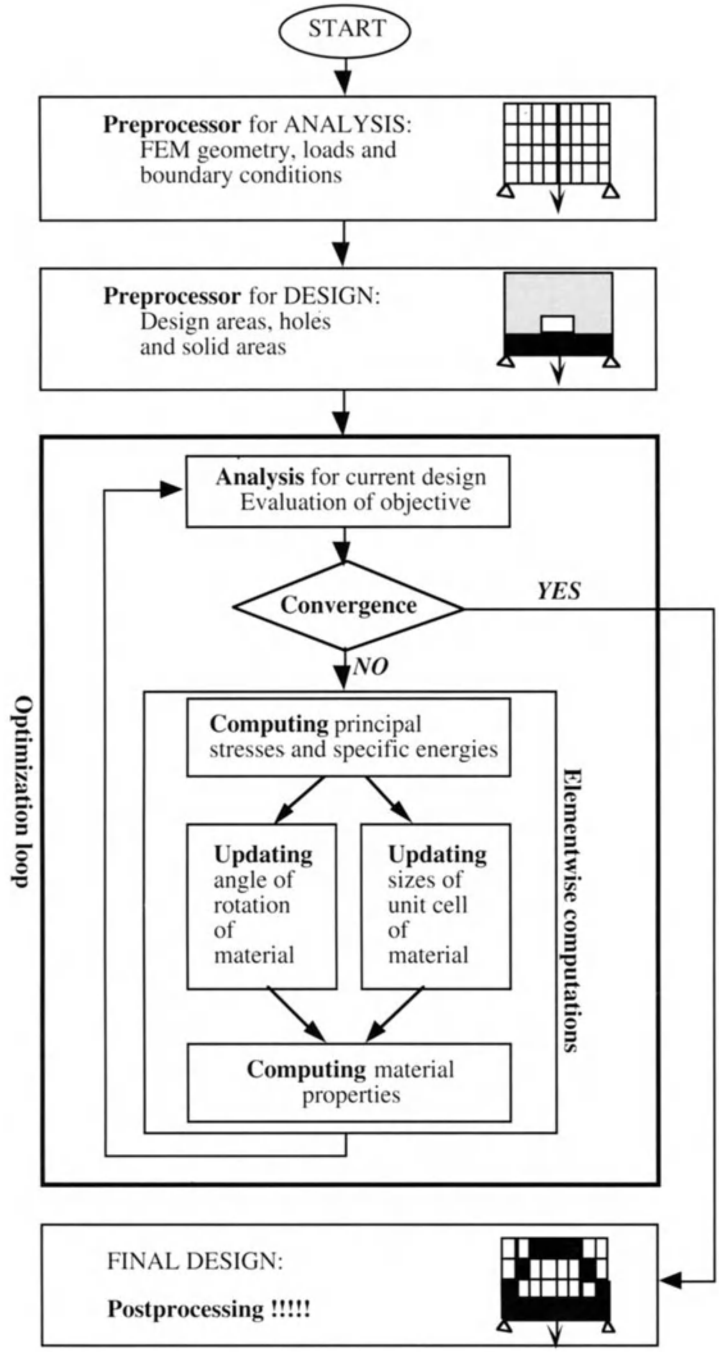
START
Preprocessor for ANALYSIS:
FEM geometry, loads and boundary conditions
Preprocessor for DESIGN:
Design areas, holes and solid areas
Optimization loop
Analysis for current design
Evaluation of objective
Convergence
YES
NO
Elementwise computations
Computing principal stresses and specific energies
Updating angle of rotation of material
Updating sizes of unit cell of material
Computing material properties
FINAL DESIGN:
Postprocessing !!!!!

We should at this point emphasize that the use of the single inclusion cells as outlined above is not justified from a mathematical point of view, as these composites do not assure existence of solutions to the optimization problem at hand. Thus these composites should be seen only as a simple type of composites which are useful for removing the 0-1 nature of the generalized shape design problem. For existence, the layered materials provide the answer, as these materials can be shown to be able generate the strongest microstructure constructed from our given material (this will be discussed in more detail in chapter 2). Also, the effective rigidity tensors for these materials are given analytically, thus simplifying the pre-processing for finding the effective material properties.

In case layered materials are used, it is important to note that different refinements of the unit cells are required. This depends on the spatial dimension and on whether the problem is a single load problem or a multiple load problem [21]. This is indicated in table 1.1 below.

From an engineering point of view the use of the non-optimal single inclusion, single scale microstructures seems more natural. Also, it is interesting to note that topology optimization using for example the square holes in square cells gives rise to very well defined designs consisting almost entirely of areas with material or no material and very little area with intermediate density of material, i.e. very little composite material. The use of layered materials usually gives less well defined shapes, with larger areas of intermediate densities. These designs tend to be slightly more efficient than the designs obtained using single inclusion cells. This is consistent with the optimality of the layered materials and indicates that the use of square or rectangular holes in square cells at a single level of micro geometry is sub-optimal. However, as mentioned before, the well defined shapes obtained using square holes in square cells as well as its simplicity tend to favour the use of this micro geometry and the success of the homogenization method in applications would probably never have come about if such sub-optimal microstructures had not been used in the initial numerical studies of the method (this was before the optimality of the layered materials had been proven).

TABLE 1.1. Optimal microstructures	Dimension of space is 2	Dimension of space is 3
Single load	Rank-2 materials with orthogonal layers along directions of principal stresses/strains. See Figs. 1.3 and 1.5.	Rank-3 materials with orthogonal layers along directions of principal stresses/strains. See Fig. 1.9.
Multiple loads	Rank-3 materials with non-orthogonal layers. See Fig. 1.6.	Rank-6 materials with non-orthogonal layers.

The way the updating of the angle of cell rotation is carried out in the optimality criterion update scheme also has some influence on the resulting designs. Thus the layered materials tend to give sub-optimal designs if the rotation angle is updated in single Newton steps, instead of using the alignment of material and stress/strain axes at each iteration step.

We should underline that the optimality criteria method described above formally requires that the assembled stiffness matrix of the problem is positive definite. For this reason, the inequalities like $\mu \geq 0$, $\gamma \geq 0$ for densities should be exchanged by inequalities $\mu \geq \mu_{\min} > 0$, $\gamma \geq \gamma_{\min} > 0$ where $\mu_{\min}, \gamma_{\min}$ are suitable small lower bounds ($\mu_{\min}, \gamma_{\min} \sim 0.0$).

The type of algorithm described above has been used to great effect in a large number of structural topology design studies and is well established as an effective (albeit heuristic) method for solving large scale problems [10], [18]. The effectiveness of the algorithm comes from the fact that each design variable is updated independently of the update of the other design variables, except for the rescaling that has to take place for satisfying the volume constraint.

1.3.2 The checkerboard problem.

Patches of checkerboard patterns appear often in solutions obtained by the homogenization method that use the displacement based finite element method, cf., figures 1.15, 1.17 and 1.18. Within a checkerboard patch of the structure the density of the material assigned to contiguous finite elements varies in a periodic fashion similar to a checkerboard. The origin of the checkerboard patterns is related to features of the finite element approximation and are of the same nature as patterns observed in the spatial distribution of the pressure in some finite element analyses of Stokes flows [11]. This hypothesis is supported by the fact that the remedies that control these patterns for the Stokes flow problem also works for the homogenization problem and it suggests a number of strategies to prevent the formation of checkerboards in layout optimization problems.

The displacement based numerical implementation for the homogenization method is concerned with the solution of a problem of the form

$$\max_{E \in \mathrm{E}_{ad}} \; \min_{v \in U} \left\{ \tfrac{1}{2} \int_{\Omega} E_{ijkl} \, \varepsilon_{ij}(v) \varepsilon_{kl}(v) \, d\Omega - l(v) \right\}$$

that is, a min-max type problem for a functional of two variables. It is well-known that the finite element analysis of such problems can cause problems, and for saddle point problems for concave-convex quadratic functionals on reflexive function spaces the so-called Babuska-Brezzi condition for the finite element discretization will guarantee a stable numerical scheme, see Brezzi and Fortin, 1991.

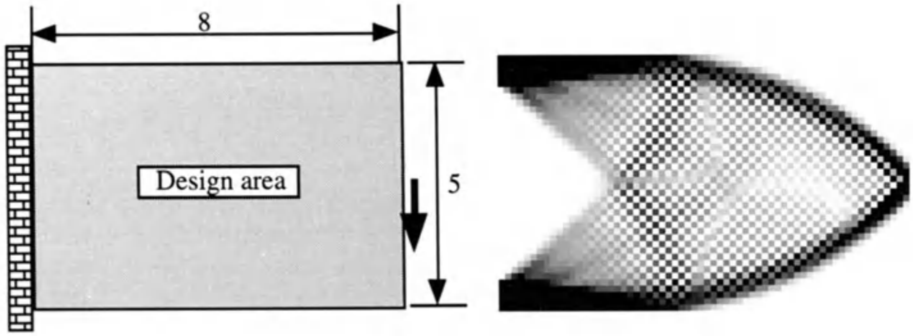

Fig. 1.15. Optimal design of a short cantilever. The design domain is a 8 by 5 rectangular domain, loaded at the mid-point of the right-hand border. All of the left-hand side of the rectangle is a possible support. The right-hand picture shows the results of topology design with a rank-2 layered material. Notice the appearance of checkerboard patterns. Bendsøe, Díaz and Kikuchi, 1993.

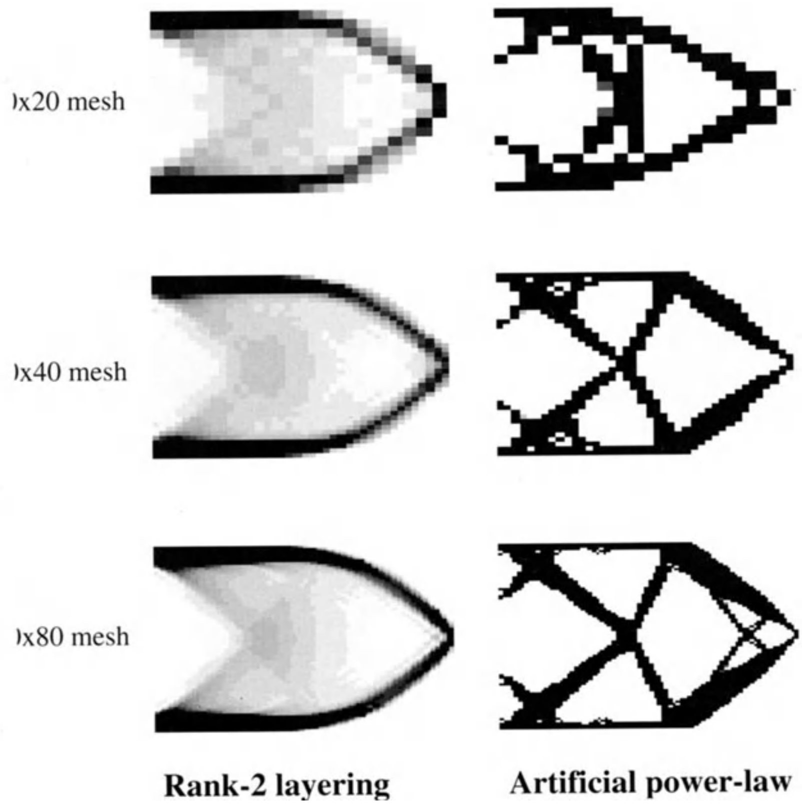

Fig. 1.16. A comparison of optimal designs computed using different design parametrizations. Left-hand column is for optimal rank-2 layering and right-hand column is for the artificial density-rigidity power-law relation given in formula (1.17). Bendsøe, Díaz and Kikuchi, 1993.

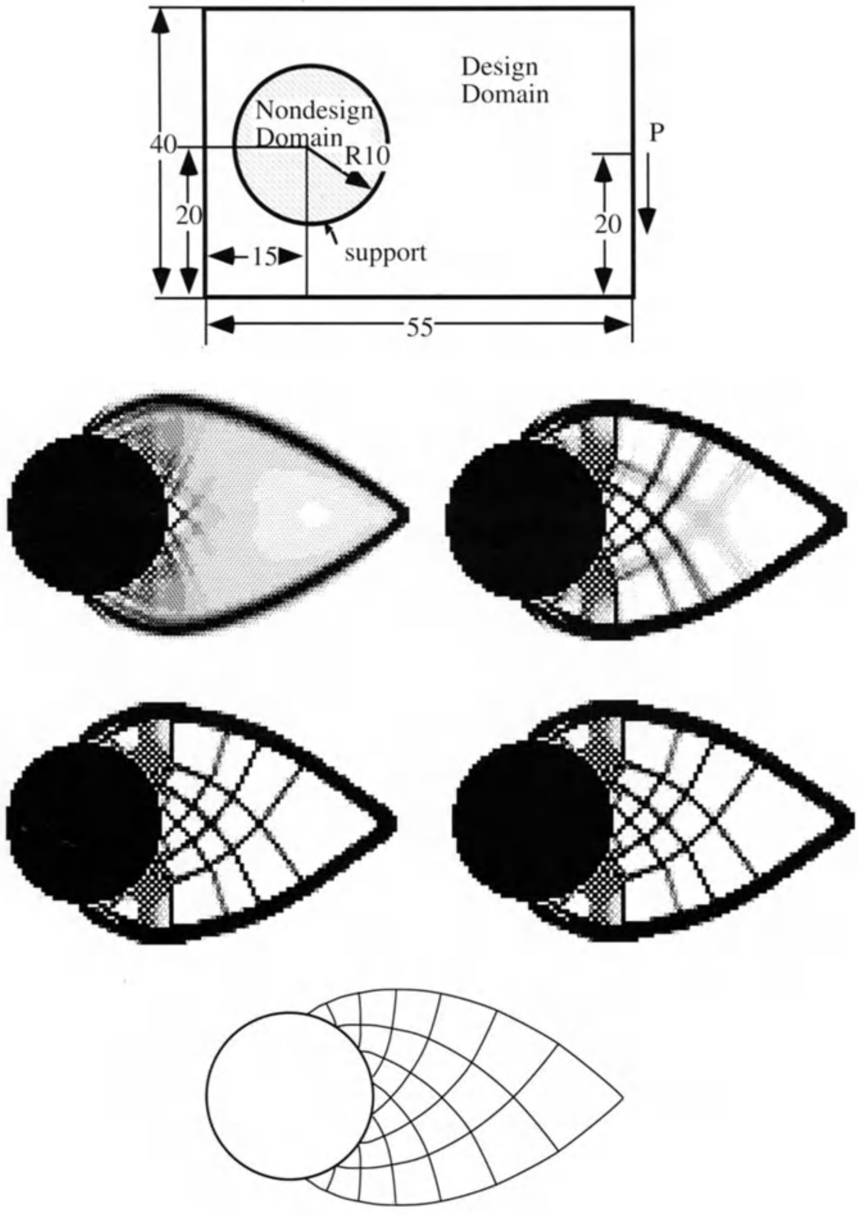

Fig. 1.17. A layout design problem that yields a Michell truss like structure. Results obtained by the homogenization method with square cells with rectangular holes and a finite element discrete model of 110 x 80 uniform rectangular elements. The amount of available volume for design is 13% of the reference domain volume. Figure shows the iteration history of the topology for 10, 20, 40 and 50 iterations of the optimality criteria method. A classical analytical solution to this problem with Mitchell-like truss members is shown at the bottom of the figure. Bendsøe, Díaz and Kikuchi, 1993.

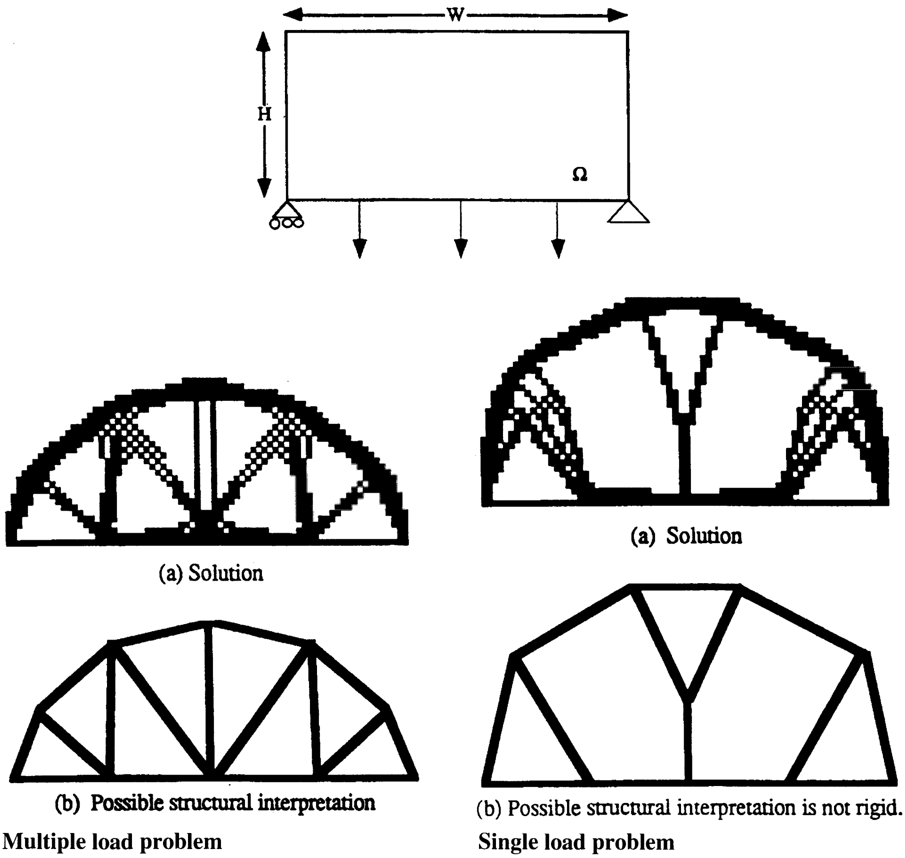

Fig. 1.18. Optimal design for multiple loads. Three load cases apply, with equal weights on each of the compliances. Design obtained using a microstructure of square cells with rectangular holes. For multiple load solution as well as the single load solution possible truss interpretations are shown. Díaz and Bendsøe, 1992.

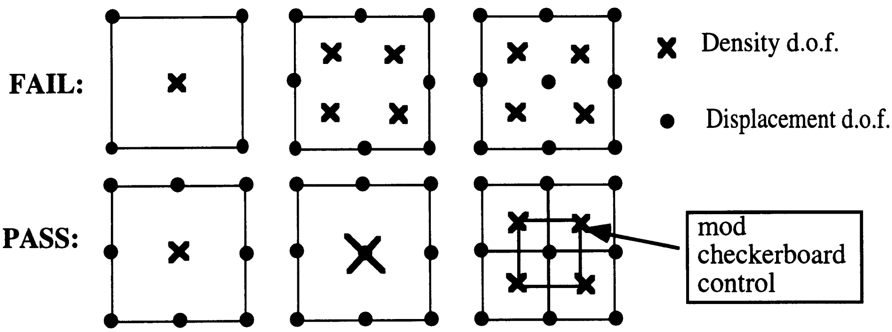

Fig. 1.19. Stability of various mixed finite element models with discontinuous pressure fields for the topology design problem. The checkerboard controlled element consisting of 4 Q4 elements is described in the text below.

For the topology problem at hand, the functional is neither concave-convex nor quadratic, and the design variables typically belong to a non-reflexive space (L^∞), so we are not in a situation covered by standard saddle point theory and the related application of the Babuska-Brezzi condition.. However, these problem aside, taking a direct analogy to the similar problem in Stokes flow indicates none the less that certain combinations of finite element discretizations will be unstable and some stable, as indicated in figure 1.19. This has been confirmed by numerical experiments for both the use of layered materials as well as in the case where the single inclusion cells are used [11]; a recent analysis based on a patch test of the finite element models substantiates this finding (Jog and Haber, 1994). As stable combinations of elements we note that the use of Q8 or Q9 quadrilaterals for the displacements in combination with an element wise constant discretization of density provides for stable solutions.

An alternative to the matching of the finite element approximations as just described, is to implement a strategy which controls the formation of checkerboards in meshes of 4-node quadrilateral elements and constant material properties within each element (motivated by the work of Kikuchi, Oden and Song, 1984). Thus one can maintain the use of low order elements. However, as in the methods described above, the end result is still the introduction of some type of element with a higher number of nodes, as the method in effect results in a "super-element" for the density and displacement functions in 4 neighbouring elements..

In what follows we will assume that the design domain Ω is rectangular and it is discretized using square, 4-node iso-parametric elements. An element K in the mesh is identified by

$$\mathrm{K}_{ij} = \{(x,y) \in \mathbf{R}^2 \mid (j-1)h \le x \le jh,\ (i-1)h \le y \le ih\}, i = 1,\dots,M \text{ and } j = 1,\dots,N$$

where M and N are the number of elements per side and h is the element size. We will assume that M and N are even numbers. We restrict the discussion to the standard minimum compliance problem in plane elasticity but the results can be easily extended to other problems, as well as meshes made up by four-node quadrilateral elements.

We will temporarily consider material density as the design variable, rather than the usual cell size parameters. In the standard, minimum compliance problem the conditions for optimality of the density distribution $\rho(x)$ at $x \in \Omega$ under a constraint on the total amount of available material are (in weak form)

$$-\int_\Omega \left[\frac{\partial E_{ijkl}}{\partial \rho} \varepsilon_{ij} \varepsilon_{kl} \right] \delta\rho \, \mathrm{d}\Omega + \int_\Omega \left[\Lambda + (\lambda_{\rho 1} - \lambda_{\rho 0}) \right] \delta\rho \, \mathrm{d}\Omega = 0$$

for all admissible variations $\delta\rho$ and non negative multipliers Λ, $\lambda_{\rho 0}$, $\lambda_{\rho 1}$ with $\lambda_{\rho 0}\,\rho = \lambda_{\rho 1}(1-\rho) = 0$. Here $\rho(x)$ and $\delta\rho(x)$ are restricted to the space of piece wise constant functions on Ω, i.e. the space

$$V = \left\{ v \in L^{\infty}(\Omega) \mid v(x) = v_K, \text{constant within element } \mathrm{K} \subset \Omega, \text{whenever } x \in \mathrm{K} \right\}$$

If $\rho \in V$, $\delta\rho \in V$ and the energy density term $\dfrac{\partial E_{ijkl}}{\partial \rho}\varepsilon_{ij}\varepsilon_{kl}$ is evaluated only at the element centroid, the optimality conditions reduce to the more familiar form (as we have seen earlier)

$$-\frac{\partial E_{ijkl}}{\partial \rho}\varepsilon_{ij}\varepsilon_{kl}\bigg|_{\mathrm{K}} + \Lambda + (\lambda_{\rho 1} - \lambda_{\rho 0})\big|_{\mathrm{K}} = 0 \text{ for all elements } \mathrm{K} \subset \Omega$$

Consider now a patch $\mathrm{P}_{i\,j}$ of four contiguous elements $\mathrm{K}_{i\,j}$, $\mathrm{K}_{i+1\,j}$, $\mathrm{K}_{i\,j+1}$ and $\mathrm{K}_{i+1\,j+1}$, as shown in Fig. 1.20, i.e.,

$$\mathrm{P}_{i\,j} = \mathrm{K}_{i\,j} \cup \mathrm{K}_{i+1\,j} \cup \mathrm{K}_{i\,j+1} \cup \mathrm{K}_{i+1\,j+1}$$

Associated with $\mathrm{P}_{i\,j}$ we introduce basis functions ϕ^1_{ij}, ϕ^2_{ij}, ϕ^3_{ij} and ϕ^4_{ij} which take the values ± 1 in $\mathrm{P}_{i\,j}$ according to the pattern shown in figure 1.20 and are zero outside $\mathrm{P}_{i\,j}$. Here we note that:

1. The functions $\{ \phi^k_{ij} \}$ are an orthogonal basis for V.
2. A "pure" checkerboard pattern is of the form $u = \sum_{\mathrm{P}_{i\,j}} u_{ij}\phi^4_{ij}$

This suggests that, even if we wish to retain one density design variable per finite element, in order to avoid the formation of checkerboard patterns we need to restrict ρ and $\delta\rho$ to lie within the more restricted, checkerboard-free space

$$\overline{V} = \{\ v \in \mathrm{R}\text{: } v(x) = \sum_{\mathrm{P}_{ij}} (v^1_{ij}\phi^1_{ij} + v^2_{ij}\phi^2_{ij} + v^3_{ij}\phi^3_{ij}),\ (v^1_{ij}, v^2_{ij}, v^3_{ij}) \in \mathbf{R}^3,\ x \in \Omega\ \}$$

This approach is consistent with a similar method to avoid the formation of checkerboard patterns and achieve *O(h)* convergence in the pressure variable of the Stokes problem, see Johnson and Pitkränta, 1982.

One way to implement the restrictions on ρ and $\delta\rho$ (or on the more standard design variables, the cell size parameters and associated variations) is to rewrite the optimality conditions as

$$\sum_{\substack{i=1,2,\ldots\\ j=1,2,\ldots}} \int_{\mathrm{P}_{i\,j}} \left\{ \left[-\frac{\partial E_{ijkl}}{\partial \rho}\varepsilon_{ij}\varepsilon_{kl} \right] + \left[\Lambda + (\lambda_{\rho 1} - \lambda_{\rho 0}) \right] \right\} \delta\rho \; d\Omega = 0$$

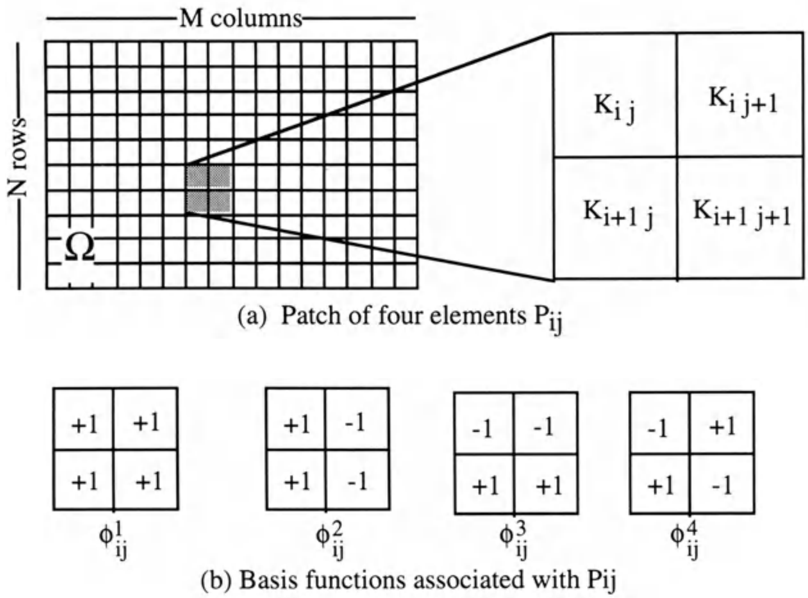

Fig. 1.20. Patches and basis functions used for checkerboard control

---

and use the discretization $\delta\rho = \delta\rho^1_{ij}\phi^1_{ij} + \delta\rho^2_{ij}\phi^2_{ij} + \delta\rho^3_{ij}\phi^3_{ij}$ within each patch P_{ij} to reach the optimality conditions

$$\int_{\mathrm{P}_{ij}} \left\{ \left[-\frac{\partial E_{ijkl}}{\partial \rho} \varepsilon_{ij}\varepsilon_{kl} \right] + \left[\Lambda + (\lambda_{\rho 1} - \lambda_{\rho 0}) \right] \right\} \phi^k_{ij} \, \mathrm{d}\Omega = 0, \quad k = 1,2,3$$

These conditions hold for each patch P_{ij}, linking the four elements in the patch in a way that makes it difficult to apply the usual iterative optimality condition method. Instead, the following simpler procedure can be employed:

1. At each iteration of the optimization algorithm the cell size parameters within each element K are updated using the usual optimality criterion approach.

2. For each patch P_{ij} let $\{\rho_1, \rho_2, \rho_3, \rho_4\}$ be the be the updated densities in the four quadrants of the patch associated with the updated cell sizes. Write the (piece-wise constant) density as

$$\rho(x) = r_1\phi^1 + r_2\phi^2 + r_3\phi^3 + r_4\phi^4\,, \quad x \in \mathrm{P}_{ij}$$

using known constant coefficients r_k that depend on ρ_1, ρ_2, ρ_3 and ρ_4 (for convenience the subscripts "ij" have been dropped from the basis functions ϕ_{ij}^k). We seek a new piece-wise constant density distribution within the patch, say $\bar{\rho}$, of the form

$$\bar{\rho}(x) = \bar{r}_1 \phi^1 + \bar{r}_2 \phi^2 + \bar{r}_3 \phi^3 + \bar{r}_4 \phi^4 \,, \quad x \in \mathrm{P}_{ij}$$

such that

(i) $\bar{\rho}$ is free of checkerboard patterns , i.e., $\bar{r}_4 = 0$

(ii) $\bar{\rho}$ preserves the amount of material within the patch, i.e.,

$$\int_{\mathrm{P}_{ij}} \bar{\rho} \, \mathrm{d}\Omega = \int_{\mathrm{P}_{ij}} \rho \, \mathrm{d}\Omega$$

We select $\bar{\rho}$ as the best L^2 approximation to ρ in P_{ij} under the constraints imposed by (i) and (ii). This $\bar{\rho}$ is such that the updated densities within each element in the patch become

$$\bar{\rho}_1 = \bar{\rho}\big|_{\text{quadrant 1}} = \frac{1}{4}(3\rho_1 + \rho_2 + \rho_3 - \rho_4)$$

$$\bar{\rho}_2 = \bar{\rho}\big|_{\text{quadrant 2}} = \frac{1}{4}(\rho_1 + 3\rho_2 - \rho_3 + \rho_4)$$

$$\bar{\rho}_3 = \bar{\rho}\big|_{\text{quadrant 3}} = \frac{1}{4}(\rho_1 - \rho_2 + 3\rho_3 + \rho_4)$$

$$\bar{\rho}_4 = \bar{\rho}\big|_{\text{quadrant 4}} = \frac{1}{4}(-\rho_1 + \rho_2 + \rho_3 + 3\rho_4)$$

3. The final step is to retrieve the cell size parameters from the new densities. A simple approach is to update by a proportionality factor, such that the resized cell size parameters gives a density equal to the new densities $\bar{\rho}_k$ just computed.

Notice that since the basis functions ϕ_{ij}^k are orthogonal, if ρ is free from checkerboard patterns then $\bar{\rho} = \rho$, which indicates that the method does not disturb areas of the domain where no checkerboard control is needed. This simple strategy has been proven to be effective in a variety of problems. Note again that the method corresponds to introducing a "super-element" of four Q4 elements with a total of 9 displacements nodal points and with 3 degrees of freedom for the density approximation. Thus the method maintains more resolution in densities, as compared to, say, the approach of using Q9 elements for displacements and element-wise constant density ρ .

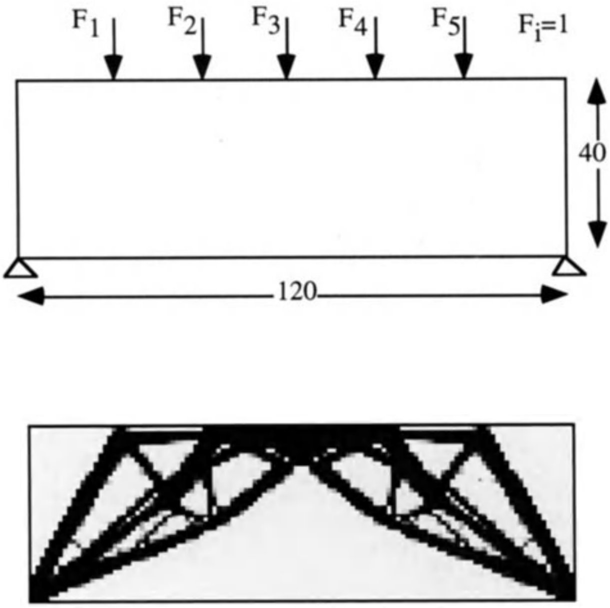

Fig. 1.21. Optimal design for multiple loads, with checkerboard control implemented. Five load cases apply, with equal weights on each of the compliances. Volume constraint corresponds to 35% of the total volume of the design area. Bendsøe, Díaz and Kikuchi, 1993.

1.4 Topology optimization as a design tool

In the following we will try to illustrate some basic features of the homogenization method when used for design. Also, we shall emphasize the use of the topology design method as a pre-processor in an integrated design process where boundary variation techniques are employed for refining a design created by the homogenization based topology design method.

It should be emphasized that the practical use of topology design to date often has been on the level of a creative sparring partner in the initial phase of a design process. Thus the output of the homogenization method has been used to identify potential good designs, the completion of the design being based entirely on traditional skills of the design office. One effect of the topology method that cannot be underestimated is the efficient testing of the appropriateness of the model of loads and supports. As the *topology* is very sensitive to a proper modelling of the load environment, one can immediately discover discrepancies or inaccuracies in this modelling.

1.4.1 Examples of topology design

The homogenization method for topology design has been tested on a large number of examples, a few being illustrated in this and the preceding sections. The method allows for an efficient prediction of the optimal topology, the optimal shape and the optimal use of the prescribed possible support conditions. Also, it has proven to be a flexible and reliable design tool. The methodology has over the last couple of years seen its first industrial applications, especially among some major car manufacturers.

For an efficient use the problem should be formulated on a reference domain that is chosen as simple as possible to reduce the size of the analysis problem. The domain should, as described section 1.3.1, allow for definition of loads and tractions and of boundary condition. The use of an automatic mesh generator will, of course, simplify the treatment of problems with complicated geometry such as non-simply connected reference domains. Complicated reference domains are needed for cases where design requirements imply the exclusion of certain parts of space as parts of the structure. If the precise shapes of inner holes in a non-simply connected reference domain are unimportant, it is advisable to cater for such holes by fixing the density of material to be zero for the elements defining the hole (or parts of it). These considerations have led to most examples being treated in rectangular reference domains, but the use of the method is of course not restricted to such domains.

For very low volume fractions, very fine discretization meshes are required for the case of sub-optimal unit cells as the structures break up if coarse meshes are used. However, for high volume fractions, even coarse meshes give a very good indication of shape and topology and a good estimate of the optimal compliance. Note that for comparatively small volume fractions, the method predicts the lay-out of truss like structures and Michell frames, thus supplementing lay-out theory and truss topology methods (see Chapt. 4) for cases with a large, dense set of nodes; the homogenization method not only predicts the optimal connectivities, but also the optimal location of nodal points.

The results of using the homogenization method for optimal topology design tend to favour the use of the sub-optimal microstructures, as these from a practical point of view results in more classically useful structures. This is certainly not so pleasing from a theoretically point of view. One may argue that with present day technology for producing advanced composite materials one should certainly *not* remain limited by a wish to predict black and white designs only. Also, it will probably in the future be viable to work with the optimized materials and to implement for example production requirements as constraints that will limit the final design. Such limitations could be the use of a small number of composites or restricting the structure to having a finite set of voids of certain minimum size and maximum boundary curvature. One attempt in this direction will be described in section 2.3.2.

Here and in the following sections we show only a restricted number of examples of optimal topologies. Further examples of topology designs obtained through the use of the homogenization modelling of microstructure can be found in the literature [10], [11]. We remark here that the fundamental idea of the material design formulation for topology design extends readily to a whole range of problem settings. We include here some examples of plate and shell problems, and will return to such problems in chapter 5.

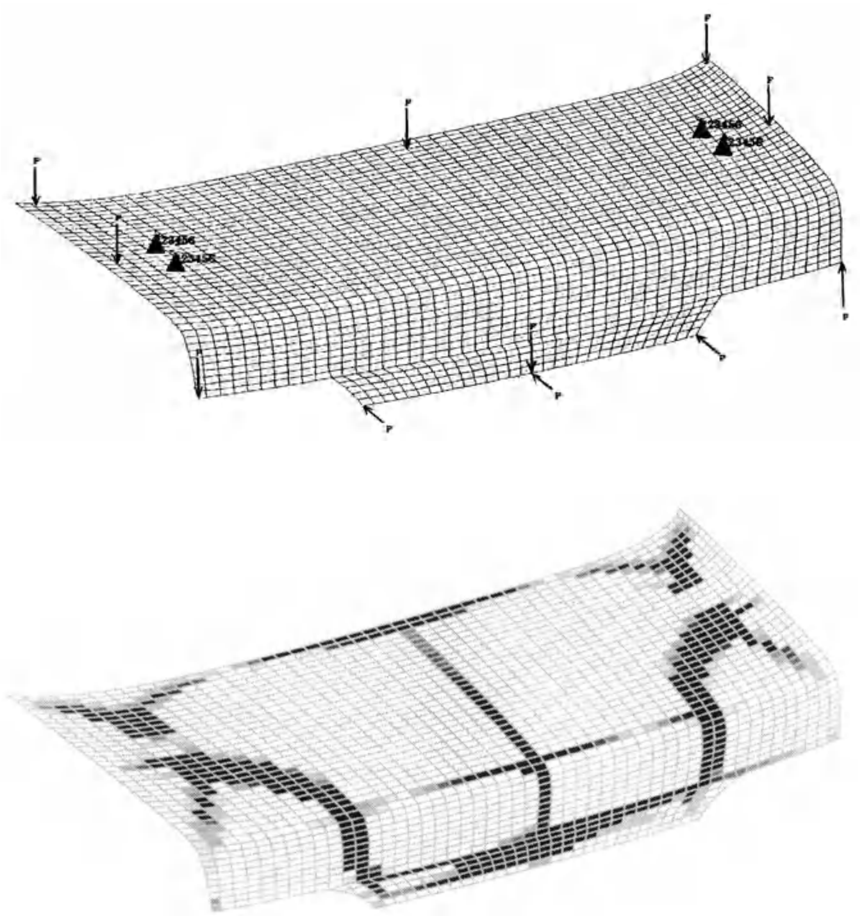

Fig. 1.22. Optimal design of a car-hood. Multiple load, minimum compliance design for reinforcement, using a laminate shell model. By courtesy of Altair Computing, via A. Díaz.

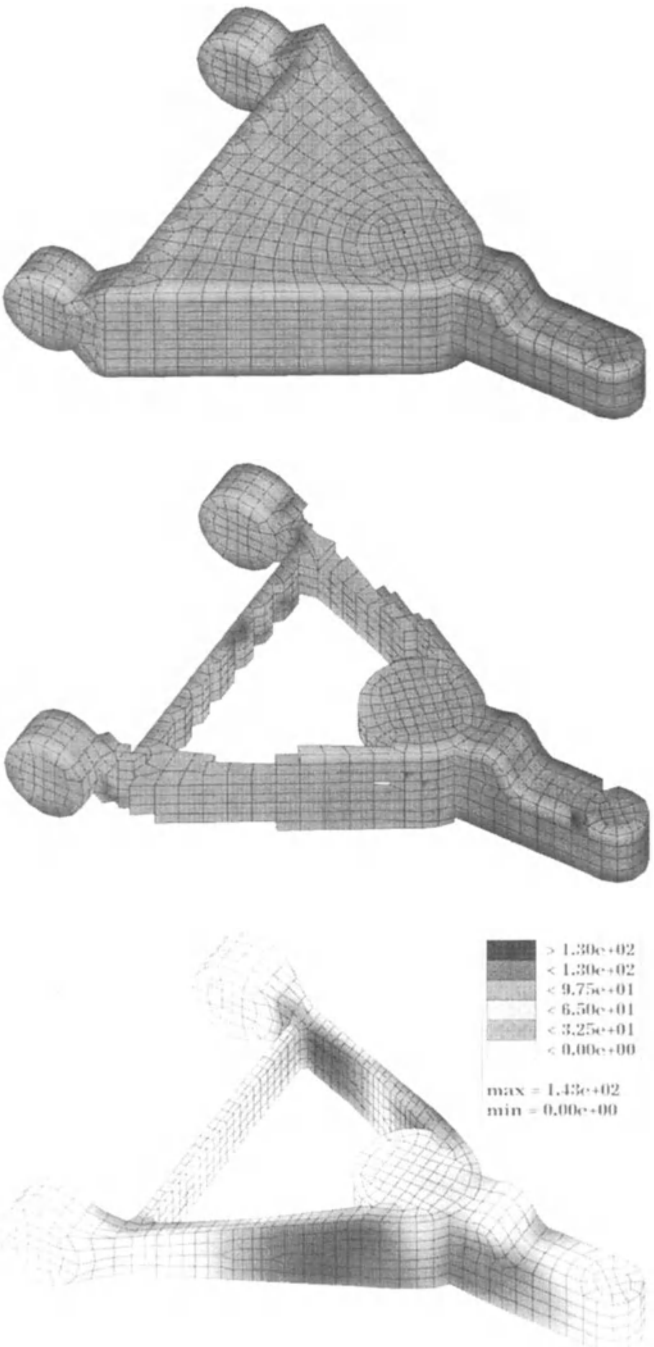

Fig. 1.23. Optimal design of a wishbone. Multiple load design using a 3-D model. The lower picture shows the stress levels in a postprocessed design. By courtesy of Altair Computing, via A. Díaz.

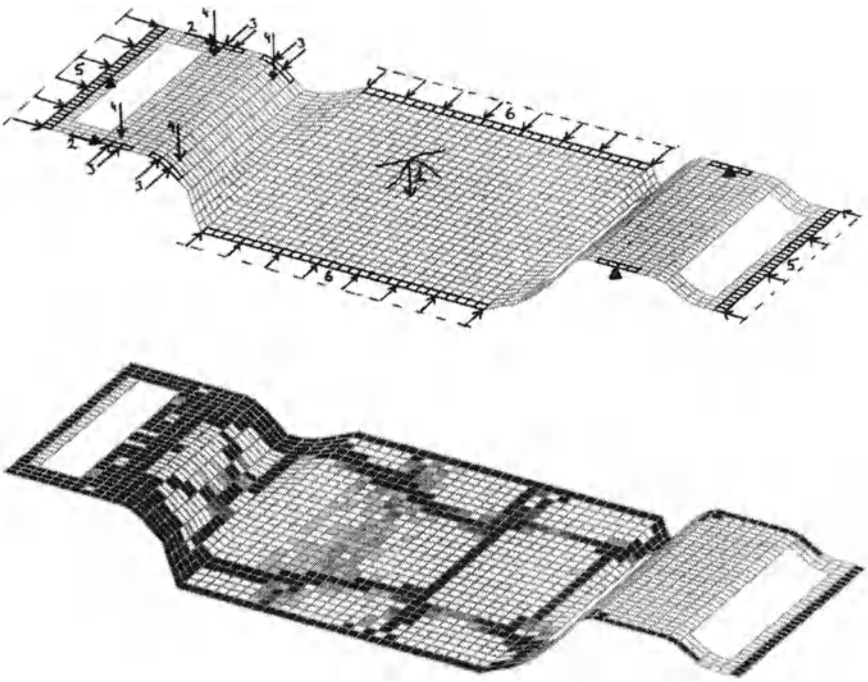

Fig. 1.24. Example of the optimal design of a car floor. Multiple load design for optimal reinforcement using a laminate shell model. There are 6 independent loading conditions and the problem is treated in the weighted average formulation. By courtesy of Altair Computing, via A. Díaz.

1.4.2 Integrated approach to shape design

Traditionally, in shape design of mechanical bodies, a shape is defined by the oriented boundary curves of the body and in shape optimization the optimal form of these boundary curves is computed. This approach is very well established and the literature is extensive [2], [7], [15]. On the other hand, we have just seen how the material distribution formulation can give a (rough) estimate of the boundary curves of a structure, but here a reasonable prediction of the finer details of the boundaries requires very large FEM models. Also, the inherent large scale nature of the topology optimization method is such that the objectives used for the optimization should be global criteria, e.g. compliance, volume, average stress, etc. The focal point in this presentation is the minimization of the compliance of a structure subject to a constraint on the volume of the structure. On the other hand, the description of the body by boundary curves allows the finer details of the body to be controlled and this can be applied for studying problems such as the minimization of the maximum value of the displacements or of the Von Mises equivalent stress in the body, subject to an isoperimetric constraint on the volume of the body.

It is thus natural to integrate the material distribution method and the boundary variations approach into one design tool, employing the topology optimization techniques as a pre-processor for boundary shape optimization. The possibility of generating the optimal topology for a body can be used by the designer to select the shape of the initial proposed form of the body for the boundary variations technique. This is usually left entirely to the designer, but the material distribution method gives the designer a rational basis for his choice of initial form. As to be expected, the topology is of great importance for the performance of the structure, and it has turned out that the compliance optimized topologies generated using the homogenization method are very good starting points for optimization concerning several other criteria such as maximum stress, maximum deflection, etc.

The integration of topology optimization methods as carried out using the homogenization method is complicated by the fact that the description of a structure by a density function is fundamentally different from a description by boundary curves, as used in boundary variations shape optimization methods. In a CAD integrated shape optimization system for two dimensional structures, it is natural that the integration is based on the designer drawing the initial shape for the boundary variations technique directly on the top of a picture of the topology optimized structure, allowing for designer interaction [19]. Thus we propose a design situation where the ingenuity of the designer is put to use for generating a 'good' initial form from the topology optimization results.

The term 'good' in this context covers considerations such as ease of production, aesthetics, etc. that may not have a quantified form. A reduction of the number of holes proposed by the topology optimization by ignoring relatively small holes exemplifies design decisions that could be taken before proceeding with the boundary variations technique.

Automatic interfacing between the topology optimization method and other structural optimization methods can be based on image processing, taking advantage of the ability of such techniques to identify patterns (e.g. truss nodal points, etc.) and to generate boundary curves from grey level pictures [19]. Such techniques will prove important for an effective integration of topology design methodology in general purpose 3-D Computer Aided Optimal Design systems.

We note that any integration of the two design methods is simplified by the fact that the integration can be based on a common FEM mesh generator and analysis module and a common CAD input-output facility. The requirements on the mesh generator are mainly governed by the boundary variations technique, as mesh distortions and mesh nonuniformities for that problem can become critical because of the shape changes.

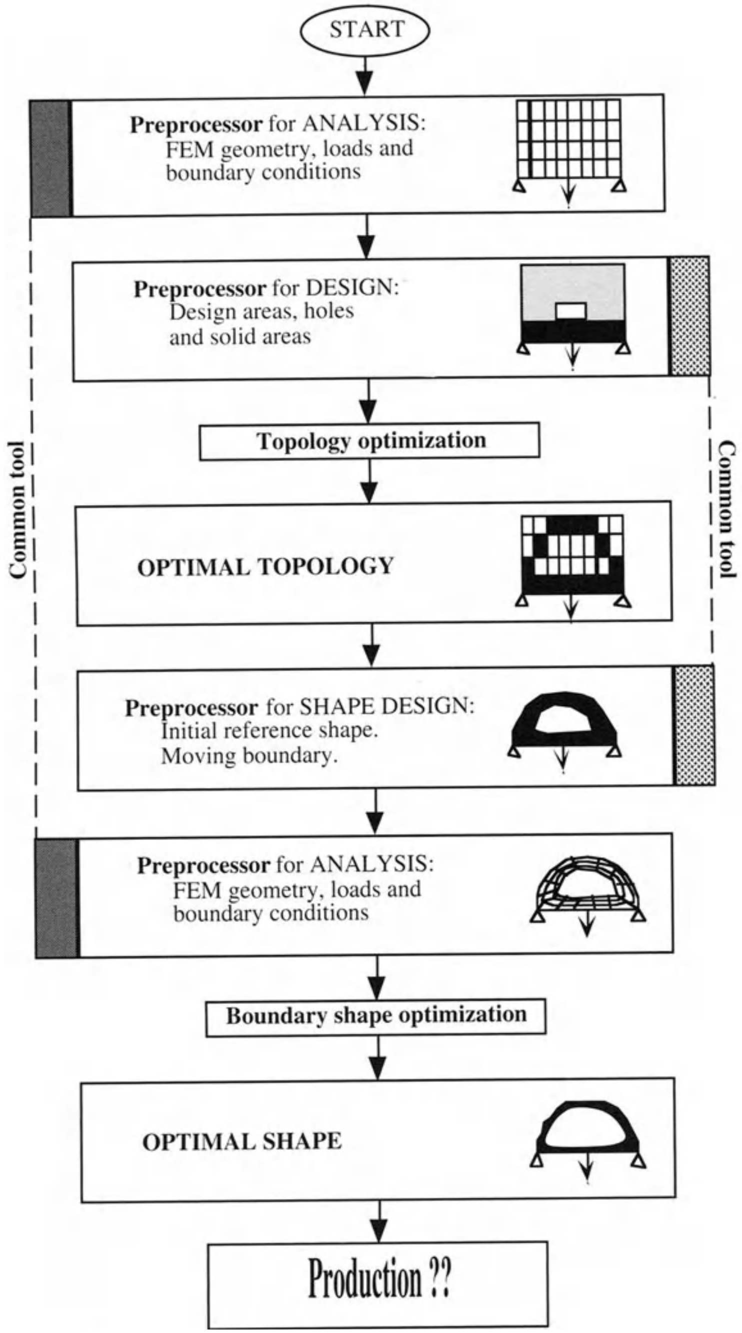

Fig. 1.25. Flow of an integrated design system with topology design and boundary shape design modules.

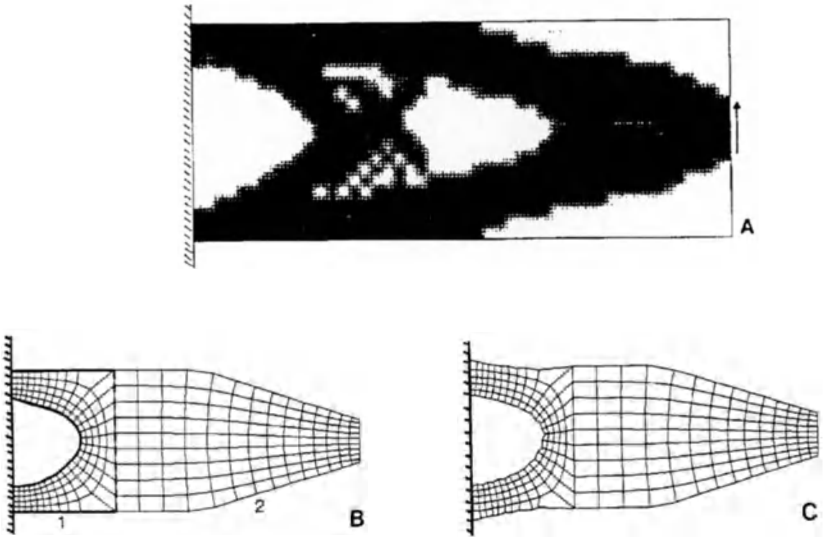

Fig. 1.26. Optimal design of a beam with the objective of minimizing the maximum von Mises stress, and with a constraint on compliance and volume. *(A)*: Optimal topology with outline showing reference domain. *(B)* and *(C)*: Initial and final design using the boundary variations method. Two blocks are used for an elliptic mesh generator. Only the boundaries of block 1 can move. The maximum stress is reduced by 55.7% and the compliance by 7.3%. Design boundaries are shown as bold solid lines. Bendsøe and Rodrigues, 1991.

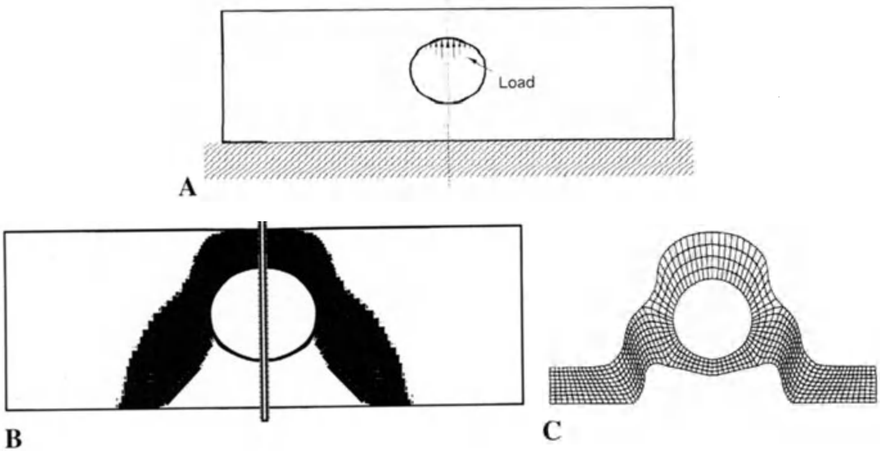

Fig 1.27. The optimal design of a bearing pedestal, using the homogenization method integrated with the boundary shape design system CAOS (see Rasmussen, Lund, Birker and Olhoff, 1993). *(A)*: The reference domain, with loading. The rim of the inner hole was kept as a solid in the homogenization method (c.f. figure 1.13). *(B)*: The result of the homogenization method. *(C)*: The final design, after boundary shape design for minimum maximal Von Mises stress and after adding outer parts to the structure for fastening. Utilizing symmetry only one half of the structure was analysed, as indicated in *(A)* and *(B)*. Olhoff, Bendsøe and Rasmussen, 1992.

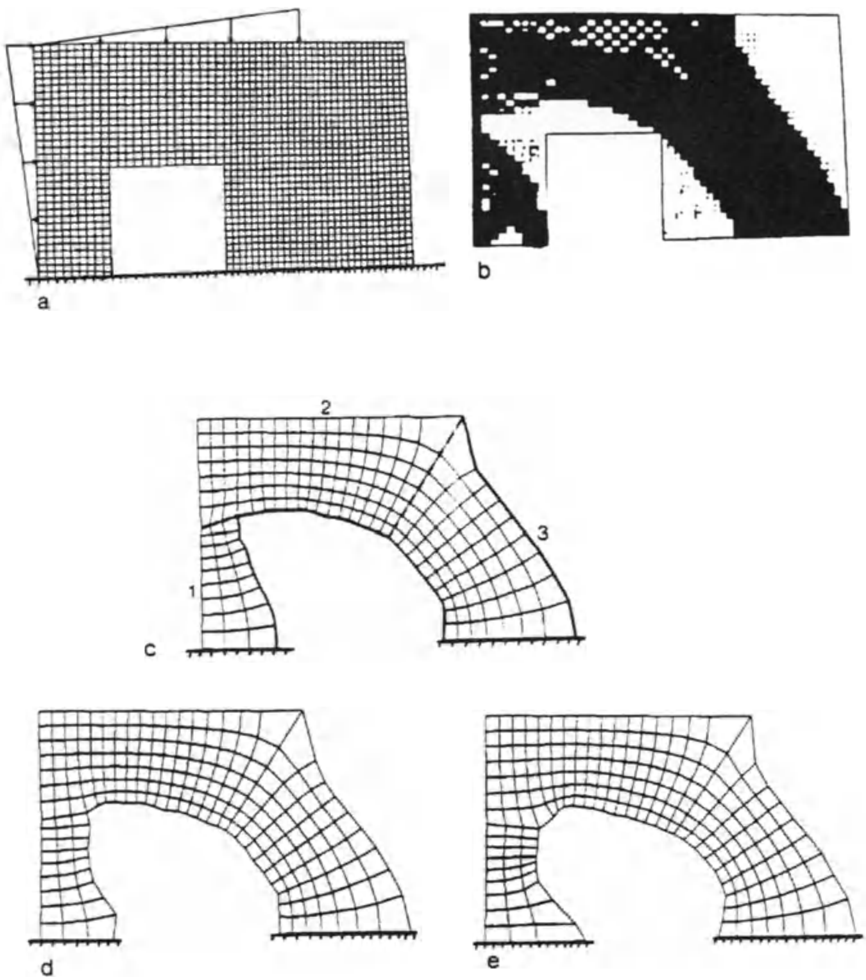

Fig.1.28. The design of a portal using the homogenization method with rectangular holes in square cells and a boundary variations method based on a mixed finite elements method. *(A)*: The reference domain with FEM mesh and loads. *(B)*: The result of the homogenization method, using a microstrcuture of square cells with square holes. *(C)*: The initial design for the boundary variations method. FEM mesh generated with an elliptic mesh generator for each of the blocks 1, 2 and 3. The boundaries that are designed are shown as thick, solid curves. *(D)*, *(E)*: Optimal designs for minimizing the maximal von Mises equivalent stress, subject to the constraint that the volume and compliance does not exceed the values of the starting design. *(D)* shows the result where the area of support is kept fixed and *(E)* the result where the support area can be enlarged. In *(D)* the reduction of the von Mises stress level is 14.5% and the reduction of the compliance is 9.1%, as compared to the initial design *(C)*. The values for *(E)* are 23.8% and 17.8%, respectively. Bendsøe and Rodrigues, 1991.

	Fig.	Volume	Deflection	Max. stress
Initial, infeasible design	*(A)*	1.07	10.1	292
Optimal circular holes		1.10	9.4	248
Optimal boundary of holes	*(B)*	1.02	9.4	372
Optimal topology	*(C)*	1.10	6.0	227
Final design	*(D)*	0.62	9.4	305

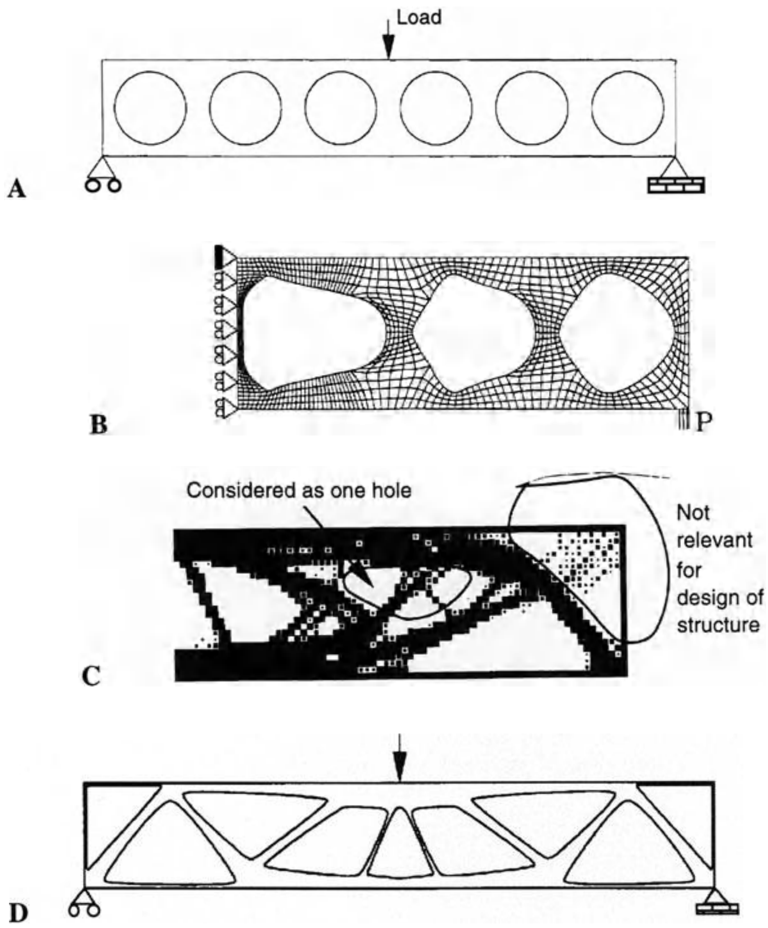

Fig. 1.29. Optimal design of an aircraft support beam. Design requirements are: upper and lower surfaces must be planar and the beam of constant depth: there must be a number of holes in the structure to allow for running wires, pipes etc. through the beam. The optimal design problem is to minimize weight so that the maximum deflection does not exceed 9.4 (mm), and the maximum von Mises stress should not exceed 385 (N/mm}). Only half of the beam needs to be analyzed. The final design is 64% better than the design with optimally shaped boundaries of initial holes. See table for values of objective etc. and figure references. Olhoff, Bendsøe and Rasmussen, 1992.

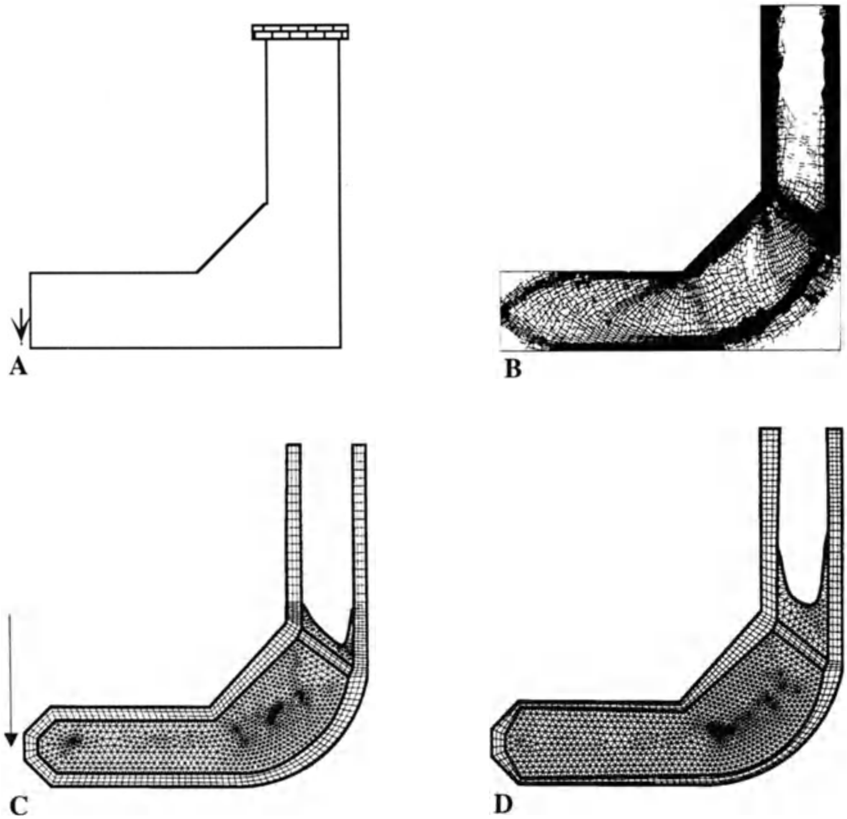

Fig. 1.30. Optimal design of a structure made of two materials, resulting in a sandwich structure for the problem described in *(A)*. In *(B)* we see the optimal two-material topology computed using rank-3 layered materials. *(C)* shows the initial design for a refinement using boundary shape optimization. All boundaries between skin and core are restricted to be piece wise straight lines. For the boundary design the weight is minimized without increasing the compliance relative to the optimal topology. *(D)* shows the final structure. By courtesy of Rasmussen, Thomsen and Olhoff.

1.4.3 The basics of a boundary shape design method

For the sake of completeness of presentation and to compare with the homogenization approach to shape design, a method of boundary shape design will be briefly described. The method is based on standard shape sensitivity analysis and boundary shape variations, with the required precision of local data being obtained with a mixed finite element method. In order to be able to handle moderately large shape variations, a remeshing scheme is also used, in the form of an elliptic mesh generator. For further literature on boundary shape design and boundary shape design sensitivity analysis, the reader is referred to the now vast literature on the subject [2], [7], [15]. For details on the specific method described here, we refer to Rodrigues, 1988, and Bendsøe and Rodrigues, 1991.

Problem Formulation. We see here the boundary shape optimization as a methodology for post-processing of results from the topology design method. That is, the optimal topology and initial boundary shape are defined and the objective is to refine this initial shape, in this case so that the Von Mises equivalent stress in the body is minimized.

For a two dimensional linear elastic body the objective is to find, by means of the boundary variation, the shape of the domain $\Omega \subseteq \mathbf{R}^2$ such that the maximum value of the Von Mises equivalent stress is minimized subject a resource constraint and a compliance constraint. We formulate the problem by a bound formulation in order to remove the non-smoothness of the max-stress function (see for example Taylor and Bendsøe, 1984, Olhoff, 1989 for other structural optimization applications of this idea). The problem is then

$$
\begin{aligned}
&\min_{\substack{\Omega \subseteq \mathbf{D} \\ \gamma, \sigma, u}} \beta \\
&\text{subject to:} \\
&\int_\Omega E_{ijkl}\gamma_{ij}\kappa_{kl}\,\mathrm{d}\Omega - \int_\Omega \gamma_{ij}\tau_{ij}\,\mathrm{d}\Omega - \int_\Omega \kappa_{ij}\sigma_{ij}\,\mathrm{d}\Omega \\
&\qquad + \int_\Omega \sigma_{ij}\,\varepsilon_{ij}(v)\mathrm{d}\Omega + \int_\Omega \tau_{ij}\,\varepsilon_{ij}(u)\mathrm{d}\Omega - l(v) = 0 \quad \text{for all } \kappa, \tau, v \qquad (1.21) \\
&\bar{\sigma}_{eq}(x) \le \beta \quad \text{for all } x \in \Omega \\
&l(u) \le \Phi, \qquad \int_\Omega \mathrm{d}\Omega \le V
\end{aligned}
$$

Here **D** denotes the set of admissible shapes, defined through local geometric constraints. The equilibrium is defined via the stationarity condition in weak form for the Hu Washizu variational principle (Washizu, 1983), using independent fields γ, σ, u of strains, stresses and displacements. The computational scheme will make use of a mixed finite element method to provide for accurate computation of stresses and strains at the element nodes.

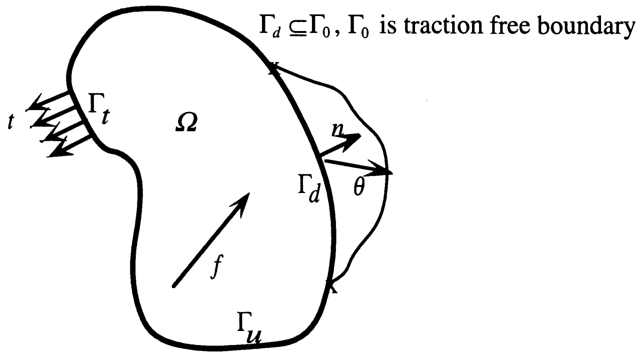

Fig. 1.31. The setting of a boundary shape design problem, indicating a shape perturbation.

The methods which can be used to obtain the set of necessary conditions, to be satisfied at the optimal domain, Ω^*, are well documented in the literature, so we restrict our presentation to the statement of the results obtained [2].

The derivation of the necessary conditions employ the speed method for boundary shape variations. This is an infinitesimal version of the mapping method for shape parametrization, as outlined in section 1.1.4. We thus define a perturbation of the optimal domain as

$$\Omega^t = (I + t\theta)(\Omega^*)$$

where θ is the domain perturbation vector field (see figure 1.31). The set $\mathbf{D}_\theta$ of admissible perturbation fields is defined via,

$$\mathbf{D}_\theta = \left\{\theta \,\middle|\, \Omega^t = (I + t\theta)(\Omega^*) \in \mathbf{D}, \text{ for } t \text{ small enough}\right\}$$

The optimality condition associated with this variation of the domain can be stated as a boundary integral condition

$$\int_{\Gamma_d} \left[\sigma_{ij}\bar{\gamma}_{ij} - u \cdot f + \Lambda_1 + \Lambda_2 \sigma_{ij}\gamma_{ij}\right](\theta \cdot n)\, \mathrm{d}\Gamma = 0 \tag{1.22}$$

where $\Lambda_1 \geq 0$, $\Lambda_2 \geq 0$ are Lagrange multipliers for the volume and compliance constraints, respectively. Also, in this equation $\bar{\gamma}_{ij}$ is the adjoint strain field, that is, it is the solution of the adjoint equation, written in mixed variational form as,

$$\int_\Omega E_{ijkl}\bar{\gamma}_{ij}\kappa_{kl}\, \mathrm{d}\Omega - \int_\Omega \bar{\gamma}_{ij}\tau_{ij}\, \mathrm{d}\Omega - \int_\Omega \kappa_{ij}\bar{\sigma}_{ij}\, \mathrm{d}\Omega$$
$$+ \int_\Omega \bar{\sigma}_{ij}\, \varepsilon_{ij}(v)\mathrm{d}\Omega + \int_\Omega \tau_{ij}\, \varepsilon_{ij}(\bar{u})\mathrm{d}\Omega + \int_\Omega \eta\left(\frac{\partial \bar{\sigma}_{eq}}{\partial \gamma_{ij}}\kappa_{ij}\right)\mathrm{d}\Omega = 0 \quad \text{for all } \kappa, \tau, v$$

Here $\eta \geq 0$ is the Lagrange multiplier associated with the bound constraint in (1.21) on the Von Mises stress (η satisfies $\int_\Omega \eta\, \mathrm{d}\Omega = 1$).

For the case without local geometric constraints on the design domains and without the compliance constraint, the optimality condition becomes

$$\int_{\Gamma_d} \left[\sigma_{ij}\bar{\gamma}_{ij} + \Lambda_1\right](\theta \cdot n)\, \mathrm{d}\Gamma = 0 \quad \text{for all } \theta$$

According to this result, the mutual energy $\sigma_{ij}\bar{\gamma}_{ij}$ has constant value along the design boundary Γ_d.

We remark here that it may not be convenient to use (1.22) in its boundary integral form, but instead a domain integral should be used. This will depend on the quality of the prediction of the stress at the boundary. Note also that in concrete discretizations, (1.22) should be used in a form that is consistent with the discretization. These aspect are discussed in detail in the literature ([2], [7], [15]).

Numerical model. For the example problem at hand (given in (1.21)), the discrete version of the mixed variational formulation of problem (1.21) can be achieved through a discretization of stress, strain and displacement fields using for example four node isoparametric finite elements. The mixed variational form leads to an indefinite system of equation in the nodal values of the stress, strain and displacement fields. Once this system is solved, the adjoint displacement field can be found from the adjoint equation, discretized using the same finite element interpolation fields as defined for the primal problem. Note that we need the solution of the primal problem to define the force term of the adjoint problem. The Lagrange multiplier $\eta \geq 0$ is interpolated using bilinear shape functions within each element where stresses are at the maximum level.

The discretization of the design perturbation field θ can be obtained through a range of different approaches. In order to maintain smoothness of the design interpolation using splines or global design functions are commonly employed ([2], [7], [15]). The shape of the body is then given through a discrete set of design variables $\{d_i\}$, which for example are the lengths of the position vectors of the respective spline interpolation nodes, expressed with respect to a pre-defined origin. The design perturbation field is expressed through the perturbations $\{\Delta_i\}$ of the lengths of the position vectors.

With the discretizations described above, the discrete design variables for the optimal boundary shape can be computed iteratively, either based on a direct solution of the discrete optimality condition or by employing well-known gradient type algorithms.

In order to solve numerically the shape optimal design problem, there is for large design changes a need for an automatic grid generator for the finite element

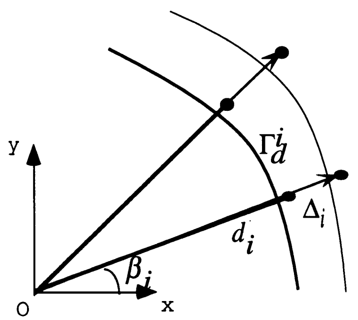

Fig. 1.32. A possible discretization of a shape perturbation.

model. Note that estimates for stress and adjoint strains fields are determining for the evaluation of the cost function and the design sensitivity leading to the optimal domain. If grid adaptation and optimization is used, then additional finite element analyses are needed to define the new adapted (optimized) grid. A less computationally costly approach is to recalculate the grid through the shape variation iterations. We are in other words interested in maintaining 'good' mesh properties that might otherwise be destroyed during the shape modification in the design iteration. Those properties that affect the shape redesign process are the main concern.

The choice of an automatic grid generator should not be arbitrary and it should relate sensibly to the problem type to be solved. In the case of shape optimal design the solution of the optimality condition requires accurate stress and adjoint strain estimates along the design boundary. Also, to minimize the interpolation error of the finite element solution there is a need for grid smoothness and orthogonality. Also, during the domain shape variation, geometric singularities can develop along the design boundaries. The grid generator should minimize the propagation into the domain of mesh non-uniformities, due to these singularities. Finally, we note that the initial shapes can be quite arbitrary. The grid generator should be able to operate on quite general shapes and permit interior boundaries. To cater for these requirements a number of various grid generation techniques for shape design have been used for shape design [15], and for the methods that have been integrated with topology design, free-mesh (Thomsen, Rasmussen and Olhoff, 1993), design-element (Olhoff, Bendsøe and Rasmussen, 1992) and elliptical (Bendsøe and Rodrigues, 1991) mesh generators have been used with good results. The latter method is based on a subdivision of the domain by blocks. For each block a mesh is obtained via the solution of a system of elliptical partial differential equations. Defining appropriate boundary conditions, mesh orthogonality can be obtained along the domain boundary.

It is quite evident from the description above that the boundary shape variations methods in essence is computationally more involved than the topology design method described earlier. On the other hand, the homogenization method is a large scale optimization problem requiring special algorithms such as the optimality criteria method. Describing boundaries by for example spline control points requires a much lower number of design variables, meaning that standard mathematical programming techniques can be used. The main complication in the boundary shape variations methods is the derivation and computation of shape sensitivities, as required for algorithms using gradient information. Note also that the basic approach to topology design generalizes ad verbatim to three dimensional structures (ignoring the use of optimal microstructures), but that the description of geometry for boundary shape design is much more complicated in dimension three. One recent approach to this is to use basic elements of solid modelling in a parametric modelling technique, combined with a free-mesh FEM mesh generator (Rasmussen, Lund og Olhoff, 1993a,b).

1.5 The existence issue

1.5.1 Variable thickness sheet design: Existence

The variable thickness sheet problem reads:

$$
\begin{aligned}
&\underset{u,\,\eta}{\text{minimize}} \quad l(u) \\
&\text{subject to :} \\
&\quad a_\eta(u,v) \equiv \int_\Omega \eta(x) E^0_{ijkl}\,\varepsilon_{ij}(u)\varepsilon_{kl}(v)\,\mathrm{d}\Omega = l(v), \quad \text{for all } v \in U, \\
&\quad \eta \in L^\infty(\Omega), \\
&\quad \int_\Omega \eta(x)\,\mathrm{d}\Omega \le V\,; \\
&\quad 0 < \eta_{\min} \le \eta \le \eta_{\max} < \infty
\end{aligned}
$$

Here E^0_{ijkl} is the fixed rigidity tensor for a given linearly elastic material and η is the thickness distribution of the sheet. It is a classical result in the field of distributed optimal control that there exists a solution to this problem (Cea and Malanowski, 1970). This follows from the fact that the admissible thickness function η belongs to a closed and bounded and thus weak* compact set in $L^\infty(\Omega)$ and the fact that the compliance, as a function of η given through the equilibrium equation is a lower weak*-semi-continuous function. The latter property is seen by considering the following calculation for a set of feasible thickness functions η_n, $n \in \mathbf{N} \cup \{0\}$ and corresponding displacements u_n, $n \in \mathbf{N} \cup \{0\}$:

$$
\begin{aligned}
l(u_n) - l(u_0) &= l(u_n) - 2l(u_0) + l(u_0) \\
&= a_{\eta_n}(u_n, u_n) - 2a_{\eta_n}(u_n, u_0) + a_{\eta_0}(u_0, u_0) \\
&= a_{\eta_n}(u_n - u_0, u_n - u_0) + a_{\eta_0 - \eta_n}(u_0, u_0)
\end{aligned}
$$

As the bilinear forms $a_\eta(\ ,\ )$ are uniformly elliptic on our set of admissible designs it follows that:

$$
\begin{aligned}
&\lim\inf \left[l(u_n) - l(u_0) \right] \ge 0 \quad \text{whenever} \\
&\lim_{n\to\infty} \int_\Omega \left[\eta_n - \eta_0 \right] \varphi\,\mathrm{d}\Omega = 0 \quad \text{for all } \varphi \in L^1(\Omega)
\end{aligned}
$$

so the compliance is a lower weak*-semi-continuous function of η.

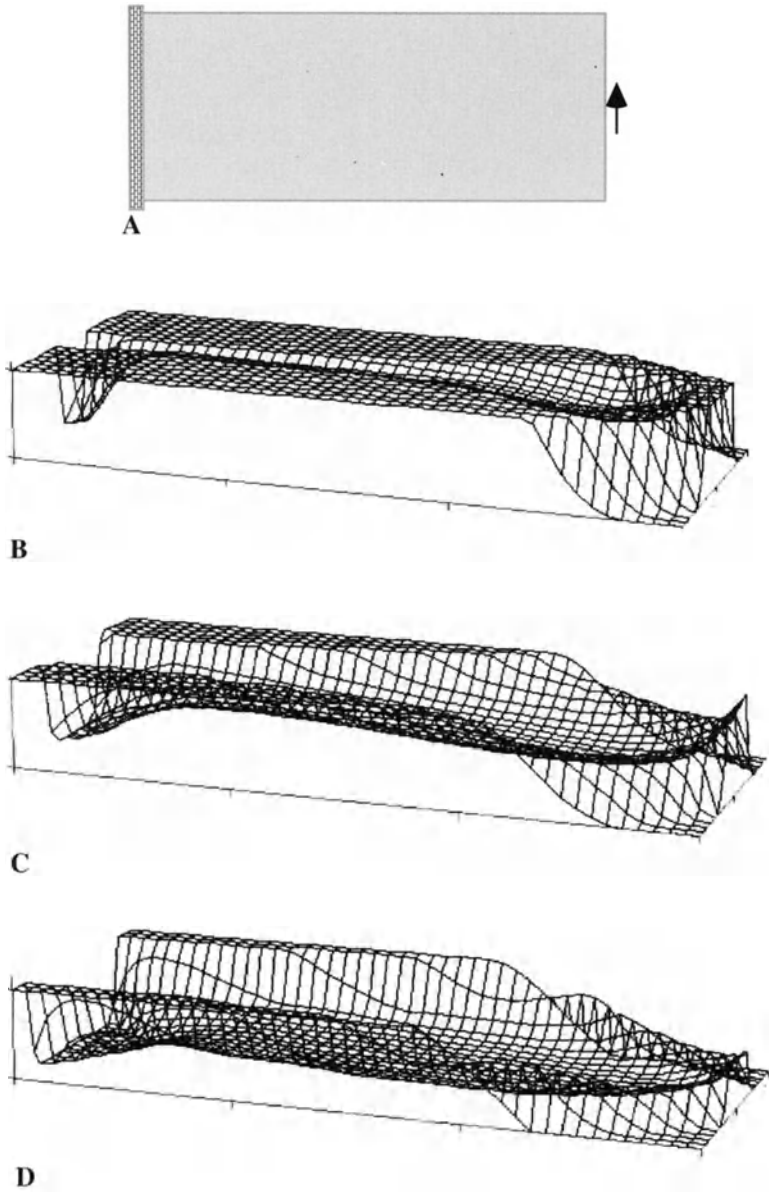

Fig. 1.33. The design of a variable thickness sheet for a cantilever-like ground structure and associated load. *(A)*: The ground structure, load and supports. *(B)*, *(C)*, *(D)*: The optimal designs for a volume constraint which is 91%, 64% and 36%, respectively, of the volume of a design with uniform thickness $\eta_{\max}$ (cf. constraints on thickness). Notice that the areas of intermediate thickness is considerable, especially for low amounts of available material. Thus the variable thickness design does not predict the topology of the structure as a true 2-dimensional object, but utilizes that the structure is in effect a 3-dimensional object. Bendsøe and Kikuchi, 1988.

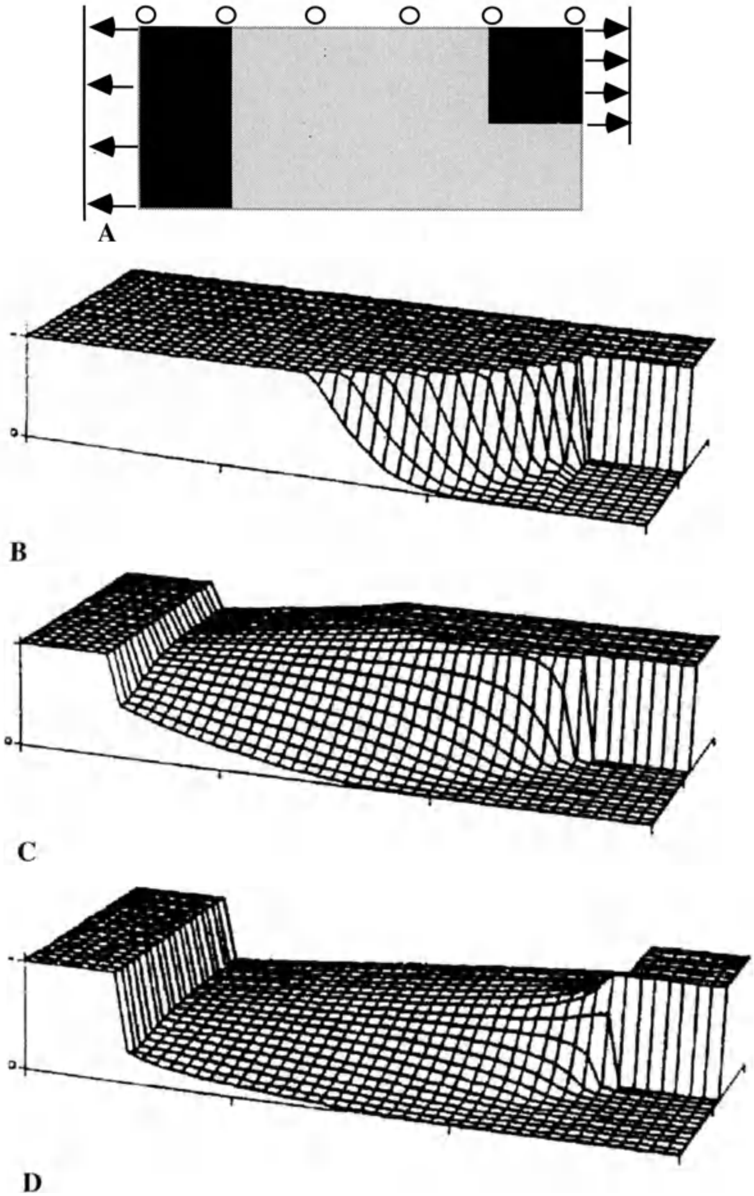

Fig. 1.34. The design of a variable thickness sheet for a well-known fillet problem. *(A)*: The ground structure, load and supports. Grey areas are areas of design, black areas are fixed at unit thickness. *(B)*, *(C)*, *(D)*: The optimal designs for a volume constraint which is 91%, 64% and 36%, respectively, of the volume of a design with uniform thickness $\eta_{\max}$ (cf. constraints on thickness). Bendsøe and Kikuchi, 1988.

The existence of solutions is easily extended to any problem for which the volume constraint is of the form $\int_\Omega f(\eta)\,\mathrm{d}\Omega \le V$, with a convex function $f:\mathbf{R}\to\mathbf{R}$ (such constraints are lower weak*-semi-continuous). Unfortunately, the penalties needed to generate solid-void designs require the use of *concave* functions f.

We shall see later that certain material design problem have reduced equivalent problem statements that falls under the category of variable thickness sheet problems. This underlines the importance of this very special case.

Note that the existence of solutions could also be proved by considering the equivalent formulation (cf. problem (1.2))

$$\max_{\substack{\eta\in L^\infty(\Omega),\\ 0\le\eta_{\min}\le\eta\le\eta_{\max}<\infty\\ \int_\Omega \eta(x)\,\mathrm{d}\Omega\le Vol}} \quad \min_{v\in U} \left\{ \Psi(\eta,v) = \tfrac{1}{2}\int_\Omega \eta(x) E^0_{ijkl}\,\varepsilon_{ij}(v)\varepsilon_{kl}(v)\,\mathrm{d}\Omega - l(v) \right\}$$

This problem is a max-min problem for a concave-convex functional $\Psi(\eta,v)$. The functional and the constraint sets satisfies conditions for the existence of a saddle point, thus proving the existence of solutions to the variable thickness sheet problem. The topologies we invoke on the spaces are here the weak-* topology on $L^\infty(\Omega)$ and the standard norm topology on U (i.e., on $H^1(\Omega)$). Then the following conditions for the existence of a saddle point are satisfied:

- The set $G=\left\{\eta\in L^\infty(\Omega)\,\middle|\, 0\le\eta_{\min}\le\eta\le\eta_{\max}<\infty,\ \int_\Omega \eta(x)\,\mathrm{d}\Omega\le V\right\}$ is convex and compact in $L^\infty(\Omega)$-weak-*.
- $\Psi(\bullet,v)$ is concave and continuous on $L^\infty(\Omega)$-weak-*, for all $v\in U$.
- $\Psi(\eta,\bullet)$ is convex and continuous on U, for all $\eta\in G$.
- There exists an element $\eta^0\in G$, so that $\Psi(\eta^0,v)\to\infty$ for $\|v\|_{H^1}\to\infty$, that is, there exists an admissible thickness distribution for which the potential energy is coercive.

Compared to the proof above we can here accept thickness distributions with vanishing thickness (the uniform coercivity is not required). Also, remark that the saddle point problem considered here is somewhat different from such problems encountered in analysis (in, e.g., mixed finite elements). First, the function $\Psi(\eta,v)$ in not quadratic and second, we are not working on reflexive spaces. This means that we have to invoke a general minimax theorem (e.g., Sion, 1958)).

Note that if we do impose the constraint $\eta\ge\eta_{\min}>0$ we have uniqueness of the displacement of the optimal solution (the thickness may not be unique). If

$\eta \geq \eta_{\min} > 0$, the functions $\Psi(\eta, \bullet)$ are strictly convex for all η, implying that $\min_{v \in U} \max_{\eta \in G} \Psi(\eta, v)$ is a strictly convex problem in the displacements.

We shall at several points in the following use this result on existence for the variable thickness sheet problem.

1.5.2 Penalized density design with a gradient constraint: Existence

The penalized density design problem with a gradient constraint on the allowable density variations reads:

$$
\begin{aligned}
&\underset{u,\,\eta}{\text{minimize}} \quad l(u) \\
&\text{subject to :} \\
&\quad a_\eta(u,v) = l(v), \quad \text{for all } v \in U \subseteq H^1(\Omega), \\
&\quad \eta \in H^1(\Omega) \\
&\quad \int_\Omega \eta(x)\, \mathrm{d}\Omega \leq V \; ; \; 0 < \eta_{\min} \leq \eta(x) \leq 1, \quad x \in \Omega \\
&\quad \| \eta \|_{H^1} = \left[\int_\Omega (\eta^2 + (\nabla \eta)^2)\, \mathrm{d}\Omega \right]^{1/2} \leq M
\end{aligned}
$$

where

$$a_\eta(u,v) = \int_\Omega \eta^q(x) E^0_{ijkl}\, \varepsilon_{ij}(u) \varepsilon_{kl}(v)\, \mathrm{d}\Omega$$

with

$$1 < q < n/(n-2) \quad \left(\Omega \subseteq \mathbf{R}^n,\, n = 2,3\right)$$

Now consider this problem in the following setting. As the problem objective function does not depend explicitly on the design variable, the problem can be considered as a minimization of a function over a set U^* of displacements arising from each of the admissible designs:

$$U^* = \left\{ u \in U \,\middle|\, \exists \eta \in G_P\!: \; a_\eta(u,v) = l(v), \text{ for all } v \in U \right\}$$

Here the set of admissible designs is

$$G_P = \left\{ \eta \in H^1(\Omega) \,\middle|\, \| \eta \|_{H^1} \leq M; \; \int_\Omega \eta(x)\, \mathrm{d}\Omega \leq V \; ; \; 0 < \eta_{\min} \leq \eta(x) \leq 1, \quad x \in \Omega \right\}$$

From the fact that $0 < \eta_{\min} \le \eta(x)$, it follows that the family $\{a_\eta(\bullet,\bullet) \mid \eta \in G_P\}$ of forms is uniformly elliptic, that is, there exists a $c>0$, so

$$a_\eta(u,u) \ge c \,\|u\|_{H^1}^2, \quad \text{for all} \quad \eta \in G_P$$

Equilibrium then gives that

$$c\,\|u\|_{H^1}^2 \le a_\eta(u,u) = l(u) \le \|p\|_2 \|u\|_2$$
$$\text{so} \quad \|u\|_{H^1} \le c^{-1}\|p\|_2, \quad \text{for} \quad u \in U^*$$

Thus the set U^* is bounded and thus weakly pre-compact in the reflexive space U. Since the objective function is weakly continuous in the displacements, existence of solutions to the problem would be assured if the set U^* was weakly closed as well. This is the case here.

That the set U^* is weakly closed follows from the Sobolev imbedding theorem, which implies that the bounded set G_P is imbedded as a compact set in $L^{2q}(\Omega)$. As U^* is bounded in U, we thus for any sequence (u_n) of displacements in U^* with corresponding designs (η_n) have a subsequence (for convenience denoted by (u_n), (η_n) as well), for which

$$\eta_n^q \to \eta_0^q, \text{ in } L^2(\Omega), \text{ strongly as } n \to \infty$$
$$u_n \to u_0, \text{ in } U, \text{ weakly as } n \to \infty$$

where η_0 is in G_P. From this it follows that

$$a_{\eta_n}(u_n,\varphi) \to a_{\eta_0}(u_0,\varphi) \text{ as } n \to \infty, \text{ for all } \varphi \in C_c^\infty(\Omega)$$

and thus

$$a_{\eta_0}(u_0,\varphi) = l(\varphi), \text{ for all } \varphi \in C_c^\infty(\Omega)$$

Thus, u_0 is in U^*, and we have proved that U^* is weakly closed.

We note that the properties of G_P shown here not only implies existence of solutions for the minimum compliance problem. Existence of solutions holds for a whole range of problems, encompassing minimizing the average deflection, minimizing the average stresses, minimizing the maximum displacement, maximizing the minimum eigenfrequency of free vibrations as well as maximizing the minimum in-planar buckling load (see, e.g., Bendsøe, 1983, 1984).

We remark here that we have obtained existence of solutions by restricting the set of admissible designs. For the 0-1 formulation of shape design, with admissible designs given as

$$
\begin{gathered}
E_{ijkl} \in L^\infty(\Omega) \\
E_{ijkl} = 1_{\Omega^m} E^0_{ijkl} = \begin{cases} E^0_{ijkl} & \text{if } x \in \Omega^m \\ 0 & \text{if } x \in \Omega \setminus \Omega^m \end{cases} \\
\int_\Omega 1_{\Omega^m} \, d\Omega = \mathrm{Vol}(\Omega^m) \le V
\end{gathered}
\tag{1.7}
$$

the corresponding set of displacements is not closed under weak convergence. This can be seen from taking a sequence of increasingly rapidly varying layered designs, for which the corresponding displacements do converge weakly (follows from homogenization), but where the limiting design is an orthotropic material not covered by the set of admissible designs. As layered designs may be stronger than a macroscopic variation of material and void then means that the existence of solutions is not assured.

Note that we above actually have proved that the set G_P is **G**-closed (or closed under H-convergence) [5], [22]. Here the **G**-topology is the topology on designs induced by the weak convergence of solutions to the corresponding equilibrium equations. We thus say that (η_n) **G**-converges to η_0 if, for all load linear forms, the solutions

$$
\begin{aligned}
a_{\eta_n}(u_n, v) &= l(v)\,, \quad \text{for all } v \in U \\
a_{\eta_0}(u_0, v) &= l(v)\,, \quad \text{for all } v \in U
\end{aligned}
$$

satisfy $u_n \rightarrow u_0$, in U, weakly, as $n \rightarrow \infty$. The set of designs (1.7) is not **G**-closed, and the full description of its **G**-closure is still not known for elasticity. The existence of solutions for the minimum compliance problem that is obtained through the introduction of finite rank layerings is achieved by extending the set of designs with designs that contains the **G**-limits of the minimizing sequences for the *specific* design problem at hand, thus generating only *part of the* **G**-closure. We mention that the finite rank layerings in the case of the scalar problem of conduction provides a complete description of the **G**-closure for 0-1 designs [23]. For a complete coverage of the problem of existence of solutions, the relation to **G**-converge, H-convergence, homogenization and Γ-convergence, we refer the reader to the vast literature on this subject [5], [9], [20], [22], [23], [34].

1.6 Layered materials

We shall here discuss various derivations of the effective moduli of layered materials, mainly to draw a parallel between the homogenization method and the traditional engineering smear-out techniques. Also, we shall see how a specific algebraic form of the formulas of effective moduli leads to a design parametrization that does not involve angles of rotation. These latter formulas were originally derived in the materials science literature as a tool for showing the optimality of bounds on the effective properties of composite materials, but they are also extremely useful for topology design. The reader is referred to [21], [23], [24] for a list of literature on the subject of layering formulas and the relationship to optimal bounds.

1.6.1 The homogenization formulas

In the following we consider a (single-layer) layered material constructed from two different orthotropic materials with rigidity tensors E^+, E^-, respectively. The layers are in the unit direction t, with the unit normal to the layering direction being denoted by n (see figure 1.2), and the thickness of material E^+ is μ, while the thickness of material E^- is $(1-\mu)$. For the local frame of reference given by (n,t) we choose coordinates (y_1, y_2), and the unit cell we consider is $[0,1] \times \mathbf{R}$. We assume that the axes of orthotropy of the materials are aligned with the layer directions, so that the only non-zero elements of the rigidity tensors for the materials (and the homogenized material) in the chosen frame are the elements with indices 1111, 2222, 1212 (1221, 2121, 2112) and 1122 (2211).

We will first work directly on the homogenization formulas, using suitable test fields. The homogenization formulas reads

$$
\begin{aligned}
E^{\mathrm{H}}_{ijkl}(x) &= \min_{\varphi \in U_Y} \frac{1}{|Y|} a_Y(y^{ij} - \varphi, y^{kl} - \varphi) = \frac{1}{|Y|} a_Y(y^{ij} - \chi^{ij}, y^{kl} - \chi^{kl}) \\
&= \frac{1}{|Y|} \int_Y \left[E_{ijkl}(x,y) - E_{ijpq}(x,y) \frac{\partial \chi_p^{kl}}{\partial y_q} \right] \mathrm{d}y
\end{aligned}
\tag{1.11}
$$

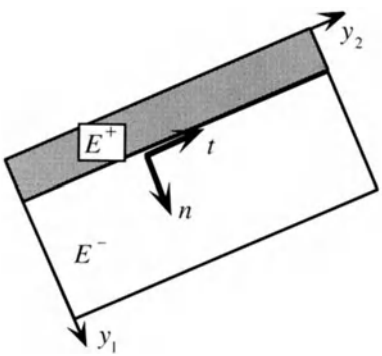

Fig. 1.35. The layered material.

with cell problem

$$\left.\begin{aligned}&a_Y\,(y^{ij}-\chi^{ij},\,\varphi)=0\ \text{ or}\\&\int_Y\left[E_{ijpq}(x,y)\frac{\partial\chi_p^{kl}}{\partial y_q}\right]\frac{\partial\varphi_i}{\partial y_j}\mathrm{d}y=\int_Y E_{ijkl}(x,y)\frac{\partial\varphi_i}{\partial y_j}\mathrm{d}y\end{aligned}\right\}\ \text{for all } \varphi\in U_Y \qquad (1.12)$$

where $y^{11}=(y_1,0)$, $y^{12}=(y_2,0)$, $y^{21}=(0,y_1)$ and $y^{22}=(0,y_2)$.

Let us now derive the expression for $E^{\mathbf{H}}_{ijkl}(x)$ for the layered material we consider. It is clear that the unit cell fields χ^{kl} are independent of the variable y_2. Also note that in equation (1.11), the term involving the cell deformation field χ^{kl} is of the form $E_{ijpq}(x,y)\dfrac{\partial\chi_p^{kl}}{\partial y_q}$, so an explicit expression for χ^{kl} is not needed.

Using orthotropy, the homogenization formula for $E^{\mathbf{H}}_{ijkl}(x)$ reads

$$\begin{aligned}E^{\mathbf{H}}_{1111}(x)&=\int_0^1\left[E_{1111}-E_{1111}\frac{\partial\chi_1^{11}(y_1)}{\partial y_1}\right]\mathrm{d}y_1\\E^{\mathbf{H}}_{2222}(x)&=\int_0^1\left[E_{2222}-E_{1122}\frac{\partial\chi_1^{22}(y_1)}{\partial y_1}\right]\mathrm{d}y_1\end{aligned}\qquad (1.23a)$$

$$\begin{aligned}E^{\mathbf{H}}_{1212}(x)&=\int_0^1\left[E_{1212}-E_{1212}\frac{\partial\chi_2^{12}(y_1)}{\partial y_1}\right]\mathrm{d}y_1\\E^{\mathbf{H}}_{1122}(x)&=\int_0^1\left[E_{1122}-E_{1111}\frac{\partial\chi_1^{22}(y_1)}{\partial y_1}\right]\mathrm{d}y_1\end{aligned}\qquad (1.23b)$$

and the corresponding cell problems written with test functions of the form $(\varphi(\mathrm{y}_1),0)$ for χ^{11},χ^{22} and test functions of the form $(0,\psi(\mathrm{y}_1))$ for χ^{kl}, have the form:

$$\begin{aligned}&\int_0^1 E_{1111}\frac{\partial\chi_1^{11}(y_1)}{\partial y_1}\frac{\partial\varphi(y_1)}{\partial y_1}\mathrm{d}y_1=\int_0^1 E_{1111}\frac{\partial\varphi(y_1)}{\partial y_1}\mathrm{d}y_1,\ \text{all }\varphi\\&\int_0^1 E_{1111}\frac{\partial\chi_1^{22}(y_1)}{\partial y_1}\frac{\partial\varphi(y_1)}{\partial y_1}\mathrm{d}y_1=\int_0^1 E_{1122}\frac{\partial\varphi(y_1)}{\partial y_1}\mathrm{d}y_1,\ \text{all }\varphi\\&\int_0^1 E_{1212}\frac{\partial\chi_2^{12}(y_1)}{\partial y_1}\frac{\partial\psi(y_1)}{\partial y_1}\mathrm{d}y_1=\int_0^1 E_{1212}\frac{\partial\psi(y_1)}{\partial y_1}\mathrm{d}y_1,\ \text{all }\psi\end{aligned}$$

This means that

$$E_{1111}\frac{\partial \chi_1^{11}(y_1)}{\partial y_1}=E_{1111}+c_{11}$$

$$E_{1111}\frac{\partial \chi_1^{22}(y_1)}{\partial y_1}=E_{1122}+c_{22}$$

$$E_{1212}\frac{\partial \chi_2^{12}(y_1)}{\partial y_1}=E_{1212}+c_{12}$$

and the periodicity condition restricts the constants c_{11}, c_{22}, c_{12} to satisfy:

$$c_{11} = -\left[M\left(\frac{1}{E_{1111}}\right)\right]^{-1}$$

$$c_{22} = -\left[M\left(\frac{E_{2211}}{E_{1111}}\right)\right]\left[M\left(\frac{1}{E_{1111}}\right)\right]^{-1}$$

$$c_{12} = -\left[M\left(\frac{1}{E_{1212}}\right)\right]^{-1}$$

where $M(\;)$ denotes the average over the unit cell.

Inserting these expression in the formulas in (1.23) and using that

$$E_{1122}\frac{\partial \chi_1^{22}(y_1)}{\partial y_1}=\frac{E_{1122}}{E_{1111}}\left[E_{1111}\frac{\partial \chi_1^{22}(y_1)}{\partial y_1}\right]=\frac{E_{1122}}{E_{1111}}\left[E_{1122}+c_{22}\right]$$

we obtain the result for $E^{\mathbf{H}}$:

$$E^{\mathbf{H}}_{1111}=\left[M\left(\frac{1}{E_{1111}}\right)\right]^{-1}=\left[\frac{\mu}{E^{+}_{1111}}+\frac{(1-\mu)}{E^{-}_{1111}}\right]^{-1}=\frac{E^{+}_{1111}E^{-}_{1111}}{\mu E^{-}_{1111}+(1-\mu)E^{+}_{1111}}$$

$$E^{\mathbf{H}}_{2222}=M(E_{2222})-\left[M\left(\frac{E_{1122}{}^{2}}{E_{1111}}\right)\right]+\left[M\left(\frac{E_{1122}}{E_{1111}}\right)\right]^{2}\left[M\left(\frac{1}{E_{1111}}\right)\right]^{-1}$$

$$=\mu E^{+}_{2222}+(1-\mu)E^{-}_{2222}-\left[\frac{\mu\,(E^{+}_{1122})^{2}}{E^{+}_{1111}}+\frac{(1-\mu)\,(E^{-}_{1122})^{2}}{E^{-}_{1111}}\right]+$$

$$+\left[\frac{\mu\,E^{+}_{1122}}{E^{+}_{1111}}+\frac{(1-\mu)\,E^{-}_{1122}}{E^{-}_{1111}}\right]^{2}\frac{E^{+}_{1111}E^{-}_{1111}}{\mu E^{-}_{1111}+(1-\mu)E^{+}_{1111}}$$

$$E_{1122}^{\mathbf{H}} = \left[M\left(\frac{E_{1122}}{E_{1111}} \right) \right] \left[M\left(\frac{1}{E_{1111}} \right) \right]^{-1}$$

$$= \left[\frac{\mu\, E_{1122}^{+}}{E_{1111}^{+}} + \frac{(1-\mu)\, E_{1122}^{-}}{E_{1111}^{-}} \right] \frac{E_{1111}^{+} E_{1111}^{-}}{\mu\, E_{1111}^{-} + (1-\mu) E_{1111}^{+}}$$

$$E_{1212}^{\mathbf{H}} = \left[M\left(\frac{1}{E_{1212}} \right) \right]^{-1} = \frac{E_{1212}^{+} E_{1212}^{-}}{\mu\, E_{1212}^{-} + (1-\mu) E_{1212}^{+}}$$

For a layering of two isotropic materials with the same Poisson ratio ν, with different Young's moduli E^{+} and E^{-}, respectively, we have that $E_{1212} = \frac{1}{2}(1-\nu)E_{1111}$ and $E_{1122} = \nu\, E_{1111}$ in both materials, so the layering formulas (in plane stress) reduce to the following simple expressions :

$$E_{1111}^{\mathbf{H}} = I_1, \qquad E_{2222}^{\mathbf{H}} = I_2 + \nu^2 I_1$$

$$E_{1212}^{\mathbf{H}} = \frac{1-\nu}{2} I_1, \quad E_{1122}^{\mathbf{H}} = \nu\, I_1$$

$$I_1 = \frac{1}{1-\nu^2} \frac{E^{+}E^{-}}{\gamma E^{-} + (1-\gamma) E^{+}}$$

$$I_2 = \gamma E^{+} + (1-\gamma) E^{-}$$

1.6.2 The smear-out process

We will now consider a different method for solving the homogenization formulas for the layered case by means that relates directly to more traditional ways of computing effective moduli for such materials. To this end we interpret the homogenization formulas in the following way. Let $\bar{\varepsilon}$ be any macroscopic strain. Then the homogenized material coefficients are defined by the energy relation (with no macroscopically varying parameters)

$$E_{ijkl}^{\mathbf{H}}\, \bar{\varepsilon}_{ij}\, \bar{\varepsilon}_{kl} = \min_{\varphi \in U_Y} \frac{1}{|Y|} \int_Y E_{ijkl}(y) \left(\bar{\varepsilon}_{ij} - \varepsilon_{ij}(\varphi) \right) \left(\bar{\varepsilon}_{kl} - \varepsilon_{kl}(\varphi) \right) \mathrm{d}y\,, \text{ for all } \bar{\varepsilon} \quad (1.24)$$

For the minimization over the periodic test fields φ, we have the minimizer φ^{*} given as a solution to the cell problem

$$\frac{1}{|Y|} \int_Y E_{ijkl}(y) \left(\bar{\varepsilon}_{ij} - \varepsilon_{ij}(\varphi^{*}) \right) \varepsilon_{kl}(\zeta)\, \mathrm{d}y = 0 \quad \text{for all } \zeta \in U_Y \qquad (1.25)$$

From this it follows, that

$$E^{\mathrm{H}}_{ijkl}\,\bar{\varepsilon}_{ij}\,\bar{\varepsilon}_{kl} = \frac{1}{|Y|}\int_Y E_{ijkl}(y)\left(\bar{\varepsilon}_{ij} - \varepsilon_{ij}(\varphi^*)\right)\bar{\varepsilon}_{kl}\,\mathrm{d}y \quad \text{for all } \bar{\varepsilon} \tag{1.26}$$

so that the macroscopic stress field defined as $\bar{\sigma}_{ij} = E^{\mathrm{H}}_{ijkl}\,\bar{\varepsilon}_{kl}$ satisfies

$$\bar{\sigma}_{ij} = E^{\mathrm{H}}_{ijkl}\,\bar{\varepsilon}_{kl} = \frac{1}{|Y|}\int_Y E_{ijkl}(y)\left(\bar{\varepsilon}_{kl} - \varepsilon_{kl}(\varphi^*)\right)\mathrm{d}y \tag{1.27}$$

We will now show that (1.25) for the layered case is solved by a field φ^*, for which $\left(\bar{\varepsilon}_{ij} - \varepsilon_{ij}(\varphi^*)\right)$ is constant in each material region, that is

$$\left(\bar{\varepsilon}_{ij} - \varepsilon_{ij}(\varphi^*)\right)(y) = \begin{cases} \varepsilon^+ & \text{in material } + \\ \varepsilon^- & \text{in material } - \end{cases} \tag{1.28}$$

where $\varepsilon^+, \varepsilon^-$ are constant fields. Remembering now that we have that

$$E_{ijkl}(y) = \begin{cases} E^+_{ijkl} & \text{in material } + \\ E^-_{ijkl} & \text{in material } - \end{cases} \tag{1.29}$$

together with (1.28) implies that the cell problem is solved for such a field φ^*, provided the interface conditions along the layer interface are satisfied. The natural boundary condition is that the normal component of stress along the interface is continuous. This follows directly from the variational statement (1.25). Moreover, because of regularity of the solution (see, e.g., Escauriaza and Seo, 1993), the tangential component of strain must be continuous (this latter property could also be posed as an ansatz, which is then proven to be true after we have shown that such a condition gives a solution). The continuity conditions are thus:

$$\begin{gathered} \sigma^+_{ij}n_in_j = E^+_{ijkl}\,\varepsilon^+_{kl}n_in_j = E^-_{ijkl}\,\varepsilon^-_{kl}n_in_j = \sigma^-_{ij}n_in_j \\ \sigma^+_{ij}n_it_j = E^+_{ijkl}\,\varepsilon^+_{kl}n_it_j = E^-_{ijkl}\,\varepsilon^-_{kl}n_it_j = \sigma^-_{ij}n_it_j \\ \varepsilon^+_{ij}\,t_it_j = \varepsilon^-_{ij}\,t_it_j \end{gathered} \tag{1.30}$$

Also, remark that from (1.28), (1.29) and (1.27) and from periodicity, it follows that

$$\begin{aligned} \bar{\varepsilon}_{ij} &= \frac{1}{|Y|}\int_Y \left(\bar{\varepsilon}_{ij} - \varepsilon_{ij}(\varphi^*)\right)\mathrm{d}y = \mu\,\varepsilon^+_{ij} + (1-\mu)\,\varepsilon^-_{ij} \\ \bar{\sigma}_{ij} = E^{\mathrm{H}}_{ijkl}\,\bar{\varepsilon}_{kl} &= \frac{1}{|Y|}\int_Y E_{ijkl}(y)\left(\bar{\varepsilon}_{kl} - \varepsilon_{kl}(\varphi^*)\right)\mathrm{d}y = \mu E^+_{ijkl}\,\varepsilon^+_{kl} + (1-\mu)\,E^-_{ijkl}\varepsilon^-_{kl} \end{aligned} \tag{1.31}$$

Here (1.31) expresses that the homogenized coefficients describe the linear stress-strain relation between the average strain and the average stress, and (1.30) expresses continuity conditions for the stresses and strains in the individual constituents. The equations (1.31) and (1.30) are precisely the equations used in standard smear-out calculations, and it is from these equations that we will calculate $\varepsilon^+, \varepsilon^-$ (i.e. prove that we have a solution) and in the process we will also derive the homogenized rigidity tensor E^{H}_{ijkl}. We can now write the constant tensors $\varepsilon^+, \varepsilon^-$ in terms of the average strain $\bar{\varepsilon}$ and the basis vectors n, t:

$$\varepsilon^+_{ij} = \bar{\varepsilon}_{ij} + a_1 n_i n_j + \frac{a_2}{2}\left[n_i t_j + t_i n_j\right] + a_3 t_i t_j$$

$$\varepsilon^-_{ij} = \bar{\varepsilon}_{ij} + b_1 n_i n_j + \frac{b_2}{2}\left[n_i t_j + t_i n_j\right] + b_3 t_i t_j$$

In this expression a_i, b_i, $i = 1,2,3$ are constants to be determined; when determined, we have the solution ε^+, ε^-. To this end, note that (1.31) and (1.30) constitutes nine dependent, linear equations, from which we can find a_i, b_i, $i = 1,2,3$.

First, the continuity of the tangential component of strains imply that $a_3 = b_3 = 0$. Then, from the average strain expression in (1.31) we get

$$\mu\, a_1 + (1-\mu)\, b_1 = 0 \quad \text{or} \quad b_1 = -\frac{\mu}{1-\mu} a_1$$

and

$$\mu\, a_2 + (1-\mu) b_2 = 0 \quad \text{or} \quad b_2 = -\frac{\mu}{1-\mu} a_2$$

Inserting this in the conditions of continuity of the normal stress, we get the following two expressions for determining a_1, a_2 (here and in the following we use the symmetry properties of the rigidity tensors):

$$E^+_{ijkl}\, \bar{\varepsilon}_{kl} n_i n_j + a_1 E^+_{ijkl}\, n_k n_l n_i n_j + a_2 E^+_{ijkl} n_k t_l\, n_i n_j =$$
$$E^-_{ijkl}\, \bar{\varepsilon}_{kl} n_i n_j - \frac{\mu}{1-\mu} a_1 E^-_{ijkl}\, n_k n_l n_i n_j - \frac{\mu}{1-\mu} a_2 E^-_{ijkl}\, n_k t_l\, n_i n_j$$

$$E^+_{ijkl}\, \bar{\varepsilon}_{kl} n_i t_j + a_1 E^+_{ijkl}\, n_k n_l n_i t_j + a_2 E^+_{ijkl}\, n_k t_l\, n_i t_j =$$
$$E^-_{ijkl}\, \bar{\varepsilon}_{kl} n_i t_j - \frac{\mu}{1-\mu} a_1 E^-_{ijkl}\, n_k n_l n_i t_j - \frac{\mu}{1-\mu} a_2 E^-_{ijkl}\, n_k t_l\, n_i t_j$$

It is now convenient to introduce the following notation:

$$M(f) = \mu f^{+} + (1-\mu) f^{-}, \quad N(f) = (1-\mu) f^{+} + \mu f^{-}$$
$$\text{when} \quad f(y) = \begin{cases} f^{+} & \text{in material } + \\ f^{-} & \text{in material } - \end{cases}$$

Then our linear equations in a_1, a_2 can be written as:

$$a_1 N(E_{ijkl} n_i n_j n_k n_l) + a_2 N(E_{ijkl} n_i n_j n_k t_l) = (1-\mu)\left[E^{-}_{ijkl} - E^{+}_{ijkl}\right] n_i n_j \bar{\varepsilon}_{kl}$$
$$a_1 N(E_{ijkl} n_i n_j n_k t_l) + a_2 N(E_{ijkl} n_i t_j n_k t_l) = (1-\mu)\left[E^{-}_{ijkl} - E^{+}_{ijkl}\right] n_i t_j \bar{\varepsilon}_{kl}$$

and we see that a_1, a_2 and thus the fields ε^{+}, ε^{-} can be written linearly in terms of $\bar{\varepsilon}$, and in terms of geometric data. To write a_1, a_2 explicitly, we use the notation

$$D = N(E_{ijkl} n_i n_j n_k n_l) N(E_{ijkl} n_i t_j n_k t_l) - N(E_{ijkl} n_i n_j n_k t_l)^2$$

so that

$$a_1 = \frac{(1-\mu)}{D}\left[E^{-}_{ijkl} - E^{+}_{ijkl}\right]\left[N(E_{rstu} n_r t_s n_t t_u) n_i n_j - N(E_{rstu} n_r n_s n_t t_u) n_i t_j\right] \bar{\varepsilon}_{kl}$$
$$a_2 = \frac{(1-\mu)}{D}\left[E^{-}_{ijkl} - E^{+}_{ijkl}\right]\left[N(E_{rstu} n_r n_s n_t n_u) n_i t_j - N(E_{rstu} n_r n_s n_t t_u) n_i n_j\right] \bar{\varepsilon}_{kl}$$

Now write the average stress in terms of ε^{+}, ε^{-} and a_1, a_2 (using symmetry)

$$\begin{aligned}
\bar{\sigma}_{ij} &= \mu E^{+}_{ijkl} \varepsilon^{+}_{kl} + (1-\mu) E^{-}_{ijkl} \varepsilon^{-}_{kl} \\
&= \mu E^{+}_{ijkl}\left[\bar{\varepsilon}_{kl} + a_1 n_k n_l + a_2 n_k t_l\right] + (1-\mu) E^{-}_{ijkl}\left[\bar{\varepsilon}_{kl} + b_1 n_k n_l + b_2 n_k t_l\right] \\
&= M(E_{ijkl})\bar{\varepsilon}_{kl} + \mu\left[E^{+}_{ijpq} - E^{-}_{ijpq}\right]\left[a_1 n_p n_q + a_2 n_p t_q\right] \\
&= \left(M(E_{ijkl}) - \frac{\mu(1-\mu)}{D}\left[E^{+}_{ijpq} - E^{-}_{ijpq}\right]\left[E^{+}_{mnkl} - E^{-}_{mnkl}\right] \Xi_{mnpq}\right) \bar{\varepsilon}_{kl}
\end{aligned}$$

where to achieve symmetry of the homogenized tensor we have set

$$\begin{aligned}
\Xi_{mnpq} &= N(E_{rstu} n_r t_s n_t t_u) n_m n_n n_p n_q \\
&\quad + \frac{1}{4} N(E_{rstu} n_r n_s n_t n_u)\left(n_m t_n n_p t_q + t_m n_n n_p t_q + n_m t_n t_p n_q + t_m n_n t_p n_q\right) \\
&\quad - \frac{1}{4} N(E_{rstu} n_r n_s n_t t_u)\left(t_m n_n n_p n_q + n_m t_n n_p n_q + n_m n_n t_p n_q + n_m n_n n_p t_q\right)
\end{aligned}$$

From these equations it follows that the homogenized rigidity matrix is given as

$$E^{\mathbf{H}}_{ijkl} = M(E_{ijkl}) - \frac{\mu(1-\mu)}{D}\left[E^{+}_{ijpq} - E^{-}_{ijpq}\right]\left[E^{+}_{mnkl} - E^{-}_{mnkl}\right]\Xi_{mnpq} \tag{1.32}$$

and holds for anisotropic constituents as well. (1.32) expresses that the effective tensor is given as the average of the rigidities of the constituents *plus* some correction terms. For the case of orthotropic constituents which have their axes of orthotropy along the directions n, t, terms of the form $E_{ijkl}n_i n_j n_k t_l$ are all zero, and the effective material parameters can be written as

$$\begin{aligned} E^{\mathbf{H}}_{ijkl} &= M(E_{ijkl}) - \mu(1-\mu)\left[E^{+}_{ijpq} - E^{-}_{ijpq}\right]\left[E^{+}_{mnkl} - E^{-}_{mnkl}\right]\Xi^{\text{ortho}}_{mnpq} \\ \Xi^{\text{ortho}}_{mnpq} &= \frac{n_m n_n n_p n_q}{N(E_{rstu}n_r n_s n_t n_u)} + \frac{\left(n_m t_n n_p t_q + t_m n_n n_p t_q + n_m t_n t_p n_q + t_m n_n t_p n_q\right)}{4N(E_{rstu}n_r t_s n_t t_u)} \end{aligned} \tag{1.33}$$

It can be verified by inspection that (1.33) are equal to the formulas shown earlier.

Let us now perform the same type of operations for the compliance tensor, i.e.

$$\varepsilon^{+}_{kl} = C^{+}_{ijkl}\,\sigma^{+}_{ij}, \quad \varepsilon^{-}_{kl} = C^{-}_{ijkl}\,\sigma^{-}_{ij}, \quad \bar{\varepsilon}_{kl} = C^{\mathbf{H}}_{ijkl}\,\bar{\sigma}_{ij}$$

Here the continuity conditions are, as before

$$\begin{aligned} \sigma^{+}_{ij}n_i n_j &= \sigma^{-}_{ij}n_i n_j \\ \sigma^{+}_{ij}n_i t_j &= \sigma^{-}_{ij}n_i t_j \\ \varepsilon^{+}_{ij}\,t_i t_j = C^{+}_{ijkl}\,\sigma^{+}_{kl}t_i t_j &= C^{-}_{ijkl}\,\sigma^{-}_{kl}t_i t_j = \varepsilon^{-}_{ij}\,t_i t_j \end{aligned}$$

From this we see that we can write the constant tensors σ^{+}, σ^{-} in terms of the average stress $\bar{\sigma}$ and the basis vectors n, t:

$$\begin{aligned} \sigma^{+}_{ij} &= \bar{\sigma}_{ij} + c_3\,t_i t_j \\ \sigma^{-}_{ij} &= \bar{\sigma}_{ij} - \frac{\mu}{1-\mu}c_3\,t_i t_j \end{aligned}$$

where we have used the continuity of the normal component of stress and the average stress expression. Inserting this in the conditions of continuity of the tangential strain, we get the following expression for determining c_3

$$c_3\,N(C_{rstu}t_r t_s t_t t_u) = (1-\mu)\left[C^{-}_{ijkl} - C^{+}_{ijkl}\right]t_i t_j\,\bar{\sigma}_{kl}$$

Now write the average strain in terms of σ^{+}, σ^{-} and c_3

$$\begin{aligned}\bar{\varepsilon}_{ij} &= \mu C^+_{ijkl}\sigma^+_{kl} + (1-\mu)C^-_{ijkl}\sigma^-_{kl}\\ &= M(C_{ijkl})\bar{\sigma}_{kl} + \mu\left[C^+_{ijpq} - C^-_{ijpq}\right]c_3 t_p t_q\\ &= \left(M(C_{ijkl}) - \frac{\mu(1-\mu)}{N(C_{rstu}t_r t_s t_t t_u)}\left[C^+_{ijpq} - C^-_{ijpq}\right]\left[C^+_{mnkl} - C^-_{mnkl}\right]t_m t_n t_p t_q\right)\bar{\sigma}_{kl}\end{aligned}$$

so

$$C^{\mathbf{H}}_{ijkl} = M(C_{ijkl}) - \frac{\mu(1-\mu)}{N(C_{rstu}t_r t_s t_t t_u)}\left[C^+_{ijpq} - C^-_{ijpq}\right]\left[C^+_{mnkl} - C^-_{mnkl}\right]t_m t_n t_p t_q \tag{1.34}$$

This is the inverse of the tensor given in (1.32). For the case of orthotropic constituents, the different elements of $C^{\mathbf{H}}_{ijkl}$ are given as

$$C^{\mathbf{H}}_{1111} = M(C_{1111}) - \left[M\left(\frac{C_{1122}^{\ 2}}{C_{2222}}\right)\right] + \left[M\left(\frac{C_{1122}}{C_{2222}}\right)\right]^2\left[M\left(\frac{1}{C_{2222}}\right)\right]^{-1}$$

$$C^{\mathbf{H}}_{2222} = \left[M\left(\frac{1}{C_{2222}}\right)\right]^{-1}, \quad C^{\mathbf{H}}_{1122} = \left[M\left(\frac{C_{1122}}{C_{2222}}\right)\right]\left[M\left(\frac{1}{C_{2222}}\right)\right]^{-1}$$

$$C^{\mathbf{H}}_{1212} = M\left(C_{1212}\right)$$

Note the similarity with the rigidity case, except for the 1212 term. We shall see later in chapter 5 that this plays a role for using plane elasticity results for plate problems.

1.6.3 The moment formulation

Let us now write the effective compliance tensor in a different form, which is suitable for iterated homogenization. These formulas have played an important role in the theoretical materials science [21], and were for the elasticity case derived by Murat and Francfort, 1986. Here we derive the formulas in the spirit of the smear-out process just carried out. We do, however, proceed in a somewhat different manner.

With the notation of above we have from the average of stresses that

$$\sigma^+_{ij} = \frac{1}{\mu}\left(\bar{\sigma}_{ij} - (1-\mu)\sigma^-_{ij}\right)$$

Now insert this expression in the average over strains, to achieve

$$C^{\mathbf{H}}_{ijkl}\bar{\sigma}_{ij} = \mu C^{+}_{ijkl}\sigma^{+}_{ij} + (1-\mu)C^{-}_{ijkl}\sigma^{-}_{ij} = C^{+}_{ijkl}\bar{\sigma}_{ij} - (1-\mu)C^{+}_{ijkl}\sigma^{-}_{ij} + (1-\mu)C^{-}_{ijkl}\sigma^{-}_{ij}$$

Rearranging, we get the equation

$$\left[C^{\mathbf{H}}_{ijkl} - C^{+}_{ijkl}\right]\bar{\sigma}_{ij} = (1-\mu)\left[C^{-}_{ijkl} - C^{+}_{ijkl}\right]\sigma^{-}_{ij}$$

If $\left[C^{-}_{ijkl} - C^{+}_{ijkl}\right]$ is invertible (this is the case if the materials are well-ordered, i.e. if $\left[C^{-}_{ijkl} - C^{+}_{ijkl}\right]$ is positive or negative definite), we can write this as

$$\sigma^{-}_{ij} = \frac{1}{(1-\mu)}\left[C^{-} - C^{+}\right]^{-1}_{ijpq}\left[C^{\mathbf{H}}_{pqkl} - C^{+}_{pqkl}\right]\bar{\sigma}_{kl} \tag{1.35}$$

From the conditions of continuity, we have that

$$\sigma^{+}_{ij} = \sigma^{-}_{ij} + \lambda t_i t_j$$

$$C^{+}_{ijkl}\sigma^{+}_{ij}t_k t_l = C^{+}_{ijkl}\left(\sigma^{-}_{ij} + \lambda t_i t_j\right)t_k t_l = C^{-}_{ijkl}\sigma^{-}_{ij}t_k t_l$$

where the constant λ then must be given as

$$\lambda = \frac{1}{C^{+}_{rstu}t_r t_s t_t t_u}\left[C^{-}_{ijkl} - C^{+}_{ijkl}\right]\sigma^{-}_{ij}t_k t_l$$

Now using again the average of stresses we can express $\bar{\sigma}$ as

$$\bar{\sigma}_{ij} = \mu\sigma^{+}_{ij} + (1-\mu)\sigma^{-}_{ij} = \sigma^{-}_{ij} + \mu\frac{1}{C^{+}_{rstu}t_r t_s t_t t_u}\left[C^{-}_{pqkl} - C^{+}_{pqkl}\right]t_k t_l \sigma^{-}_{pq}t_i t_j$$

Inserting in (1.35) we get that

$$\sigma^{-}_{ij} = \frac{1}{(1-\mu)}\left[C^{-} - C^{+}\right]^{-1}_{ijkl}\left[C^{\mathbf{H}}_{klmn} - C^{+}_{klmn}\right]\left[\sigma^{-}_{mn} + \frac{\mu}{C^{+}_{tuvz}t_t t_u t_v t_z}\left[C^{-}_{pqrs} - C^{+}_{pqrs}\right]t_r t_s \sigma^{-}_{pq}t_m t_n\right]$$

As this must hold for all stresses σ^{-} we get after a little rearranging and using index-free notation

$$\left[C^{\mathbf{H}} - C^{+}\right]^{-1} = \frac{1}{(1-\mu)}\left[\left[C^{-} - C^{+}\right]^{-1} + \mu\,\Gamma^{C}(t)\right] \tag{1.36}$$

where the tensor $\Gamma^{C}(t)$ is defined as $\Gamma^{C}_{ijkl} = \dfrac{1}{C^{+}_{rstu}t_r t_s t_t t_u}t_i t_j t_k t_l$. Equation (1.36) can also be written as

$$C^{\mathrm{H}} = C^{+} + (1-\mu)\left[\left[C^{-} - C^{+}\right]^{-1} + \mu\,\Gamma^{C}(t)\right]^{-1} \tag{1.37}$$

We remark here that the form (1.36) is particularly suited for computing effective moduli for multiple layered materials. To this end let the material indexed by C^{-} in itself consist of a layering in a direction $\bar{t}$ of the material C^{+} and the material C^{0}, in proportion γ , $(1-\gamma)$. Then from (1.36)

$$\left[C^{-} - C^{+}\right]^{-1} = \frac{1}{(1-\gamma)}\left[\left[C^{0} - C^{+}\right]^{-1} + \gamma\,\Gamma^{C}(\bar{t})\right]$$

Now insert this in the formula for C^{H} to obtain

$$\begin{aligned}\left[C^{\mathrm{H}} - C^{+}\right]^{-1} &= \frac{1}{(1-\mu)}\left[\frac{1}{(1-\gamma)}\left[\left[C^{0} - C^{+}\right]^{-1} + \gamma\,\Gamma^{C}(\bar{t})\right] + \mu\,\Gamma^{C}(t)\right] \\ &= \frac{1}{(1-\mu)(1-\gamma)}\left[\left[C^{0} - C^{+}\right]^{-1} + \gamma\,\Gamma^{C}(\bar{t}) + (1-\gamma)\mu\,\Gamma^{C}(t)\right]\end{aligned}$$

This is similar to the expression (1.36), and we note that $\vartheta^{0} = (1-\mu)(1-\gamma)$ is the amount of material C^{0}, while $\vartheta^{+} = 1-\vartheta^{0} = 1-(1-\mu)(1-\gamma) = \gamma + (1-\mu)\gamma$ is the amount of material C^{+}. Repeating this process, we see that for any multiple layering constructed from an initial layering of C^{0} and C^{+}, which is then layered consecutively with C^{+}, the effective parameters can be written as

$$\left[C^{\mathrm{H}} - C^{+}\right]^{-1} = \frac{1}{(1-\vartheta^{+})}\left[\left[C^{0} - C^{+}\right]^{-1} + \vartheta^{+}\sum_{r=1}^{m}\mu_{r}\,\Gamma^{C}(t^{r})\right], \quad \sum_{r=1}^{m}\mu_{r} = 1 \tag{1.38}$$

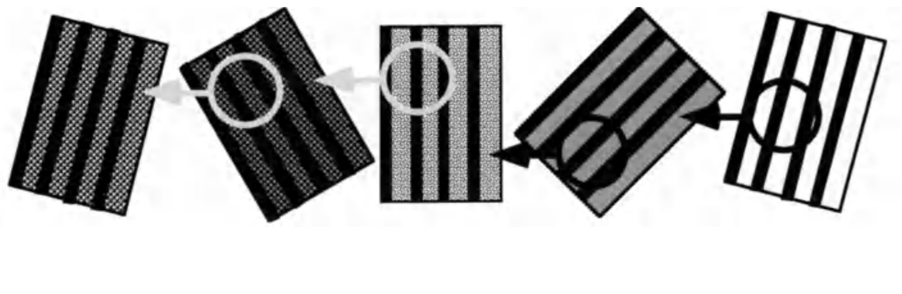

Fig. 1.36. Construction of a rank-5 layered material. The layers of the black C^{+} material are the same for each layering in this case.

for a total density ϑ^+ of C^+ placed in m layers in directions t^r; these layers need not be perpendicular.

Now let us very briefly show how a similar formula is achieved for the rigidity tensors, assuming that the material E^+ is *isotropic*, so that any term of the form $E^+_{rstu}n_r n_s n_t t_u$ is zero. As above, we get

$$\left[E^{\mathbf{H}}_{ijkl} - E^+_{ijkl}\right]\bar{\varepsilon}_{ij} = (1-\mu)\left[E^-_{ijkl} - E^+_{ijkl}\right]\varepsilon^-_{ij}$$

while we from the conditions of continuity have (using isotropy of E^+)

$$\varepsilon^+_{ij} = \varepsilon^-_{ij} + \lambda_1 n_i n_j + \frac{1}{2}\lambda_2(n_i t_j + t_i n_j)$$

$$E^+_{ijkl}\varepsilon^+_{ij} n_k n_l = E^+_{ijkl}\left(\varepsilon^-_{ij} + \lambda_1 n_i n_j\right)n_k n_l = C^-_{ijkl}\varepsilon^-_{ij} n_k n_l$$

$$E^+_{ijkl}\varepsilon^+_{ij} n_k t_l = E^+_{ijkl}\left(\varepsilon^-_{ij} + \lambda_2 n_i t_j\right)n_k t_l = C^-_{ijkl}\varepsilon^-_{ij} n_k t_l$$

giving constants λ_1, λ_2 as

$$\lambda_1 = \frac{1}{E^+_{rstu}n_r n_s n_t n_u}\left[E^-_{ijkl} - E^+_{ijkl}\right]\varepsilon^-_{ij} n_k n_l, \quad \lambda_2 = \frac{1}{E^+_{rstu}n_r t_s n_t t_u}\left[E^-_{ijkl} - E^+_{ijkl}\right]\varepsilon^-_{ij} n_k t_l$$

Repeating the calculations as above, we finally get for the rank-m layering (cf., eq. (1.38)), that

$$\left[E^{\mathbf{H}} - E^+\right]^{-1} = \frac{1}{(1-\vartheta^+)}\left[\left[E^0 - E^+\right]^{-1} + \vartheta^+\sum_{r=1}^{m}\mu_r \Gamma^E(t^r)\right], \quad \sum_{r=1}^{m}\mu_r = 1 \quad (1.39)$$

where now the tensor $\Gamma^E(t)$ for symmetry reasons is defined as

$$\Gamma^E_{ijkl} = \frac{1}{E^+_{1111}}n_i n_j n_k n_l + \frac{1}{4E^+_{1212}}\left(n_i t_j n_k t_l + n_i t_j t_k n_l + t_i n_j n_k t_l + t_i n_j t_k n_l\right)$$

(as E^+ is assumed isotropic)

From (1.39) one now have the effective material properties of any rank-m layering given in terms of $2m$ parameters, namely the bulk density ϑ^+ of C^+ material, the m relative layer thicknesses μ_r (of which (m-1) are independent) and the m layer directions given by the angle of rotations of the layers, $n^r = (\cos\theta^r, \sin\theta^r)$, $t^r = (-\sin\theta^r, \cos\theta^r)$. Notice, that the tensor $\Gamma^E(t)$ consists entirely of terms of the form $\cos^2\theta\sin^2\theta$, $\cos\theta\sin^3\theta$, $\cos^3\theta\sin\theta$, $\cos^4\theta$ and $\sin^4\theta$. For topology design, it is known that the optimal microstructures for the single load case is a rank-2 layering and for multiple loads is a rank-3 layering. Thus for topology design we need only consider (1.39) for m equal to two or three.

Note however, that for a numerical optimization the parametrization of rigidity in the form of angles is probably not suitable, instead one should consider writing the layer directions as $n = (a, \sqrt{1-a^2}), t^r = (-\sqrt{1-a^2}, a), |a| \leq 1$. For analytical studies, however, the unconstrained parametrization in terms of angles is preferable. We shall now describe a reduction in the number of describing parameters, in terms of the convex set of *moments*.

We regard the bulk density ϑ^+, $0 \leq \vartheta^+ \leq 1$, of the C^+ material as a suitable design variable, as the volume constraint of the minimum compliance problem is the simple expression $\int_\Omega \vartheta^+(x)\, d\Omega \leq V$. However, we would exchange the angles of the material tensors with a different type of variables. To this end we notice that every element of the tensors

$$\hat{\Gamma}^E = \sum_{r=1}^{m} \mu_r \Gamma^E(t^r), \quad \hat{\Gamma}^C = \sum_{r=1}^{m} \mu_r \Gamma^C(t^r)$$

are simple affine combinations of parameters of the form

$$\left.\begin{aligned} m_1 &= \sum_{r=1}^{m} \mu_r \cos(2\theta^r), & m_2 &= \sum_{r=1}^{m} \mu_r \cos(4\theta^r) \\ m_3 &= \sum_{r=1}^{m} \mu_r \sin(2\theta^r), & m_4 &= \sum_{r=1}^{m} \mu_r \sin(4\theta^r) \end{aligned}\right\} \text{with} \quad \sum_{r=1}^{m} \mu_r = 1$$

Moreover, if we consider design over all possible layer combinations as well as layer directions, the tensors $\Gamma^E(t), \Gamma^C(t)$ will be parametrized by $(m_1, m_2, m_3, m_4) \in \mathbf{R}^4$ belonging to the convex hull M of the curve $(\cos 2\theta, \cos 4\theta, \sin 2\theta, \sin 4\theta)$, $\theta \in \mathbf{R}$, in 4-space. This convex hull will also encompass the material tensors of rank-2 and rank-3 layerings. However, compared to a rank-3 layering described by 2 relative densities and 3 directions of layerings, by introduction of the *moments* (m_1, m_2, m_3, m_4) we have one less variable to worry about. This would not help us much if it was not for the solution of the trigonometric moment problem (Krein and Nudelman, 1977) from which it can be concluded that the convex set M is given as (Avellaneda and Milton, 1989)

$$M = \left\{ (m_1, m_2, m_3, m_4) \in \mathbf{R}^4 \;\middle|\; \begin{aligned} & m_1^2 + m_3^2 \leq 1, \; -1 \leq m_2 \leq 1, \\ & 2m_1^2(1 - m_2) + 2m_3^2(1 + m_2) + \\ & + (m_2^2 + m_4^2) - 4m_1 m_3 m_4 \leq 1 \end{aligned} \right\}$$

For the solution of the of the topology optimization problem using the homogenization modelling, we could thus consider the following set E_{ad} of admissible rigidity tensors

$$
\begin{gathered}
E(x) = E^{+} + (1 - \vartheta^{+}(x))\left[\left[E^{0} - E^{+}\right]^{-1} + \vartheta^{+}(x)\hat{\Gamma}^{E}(\boldsymbol{m}(x))\right]^{-1} \\
\boldsymbol{m}(x) = (m_1, m_2, m_3, m_4) \\
m_1^2 + m_3^2 \leq 1 \\
-1 \leq m_2 \leq 1 \\
2m_1^2(1 - m_2) + 2m_3^2(1 + m_2) + (m_2^2 + m_4^2) - 4m_1 m_3 m_4 \leq 1 \\
0 \leq \vartheta^{+}(x) \leq 1 \\
\int_{\Omega} \vartheta^{+}(x)\, \mathrm{d}\Omega \leq V
\end{gathered}
\tag{1.40}
$$

as a design parametrization.

The moment description used above was first used by Avellaneda and Milton, 1989, for studying bounds on effective moduli. In their presentation as well as other similar works [21], [31], one of the moduli above are often removed by introducing the overall rotation of the composite as a variable. As we here seek to avoid periodic functions in the description, all moments are kept throughout, as also suggested in Díaz, Lipton and Soto, 1994, and Lipton, 1994d. A method of constructing a layered material which achieves a certain moment combination can be found in for example Avellaneda and Milton, 1989, and Díaz, Lipton and Soto, 1994.

The parametrization (1.40) is not directly suited for the optimality criterion method described in section 1.2.2. However, as the the effective tensor is concave in the moments (Lipton, 1993a, 1994b) this parametrization is perfectly suited for a hierarchical approach where locally optimal material properties are found (numerically) as solutions to a set of inner optimization problems. Such an approach will described in chapter 2.

2 Optimized energy functionals for the design of topology and shape

In the homogenization method described in chapter 1 the main goal of the optimization is to determine the spatial distribution of material. In order to parameterize material distribution by a continuum density variable and in order to avoid ill-posedness of the problem statement, an extra set of variables were introduced namely the variables defining local microstructure. These variables can be thought of as auxiliary variables, which of course should be chosen optimally as well. However, as we allow the material variables to vary from point to point it seems reasonable to distinguish between the optimization of the spatial distribution of material and the local optimal choice of microstructure. This perspective gives the inspiration for some alternative approaches to solving the homogenization topology problem.

2.1 Combining local optimization of material properties and spatial optimization of material distribution

2.1.1 Problem separation

In the following, we will consider the homogenization model with any geometry of basic cell for the base composite material. The design problem is thus defined through the pointwise varying cell rotation $\theta(x)$ as well as a set of geometric variables $\mu(x), \gamma(x), \ldots$ which define the geometry of the basic cell. In turn these variables also determine the pointwise density ρ of material (the bulk density), so the density is a function of the geometry variables.

Using the bulk density ρ as an additional variable we can then write the minimum compliance design problems (1.2) and (1.3) as

$$\max_{\substack{\text{density} \\ \rho(x),\, x\in\Omega, \\ \int_\Omega \rho \,\mathrm{d}\Omega \le V}} \; \max_{\substack{E \text{ for} \\ \text{microstructure} \\ \text{of density } \rho(x).}} \; \min_{u \in U} \left\{ \tfrac{1}{2} \int_\Omega E_{ijkl}\big(\rho(x), \theta(x), \mu(x), \gamma(x), \ldots\big) \varepsilon_{ij}(u) \varepsilon_{kl}(u) \,\mathrm{d}\Omega - l(u) \right\} \tag{2.1}$$

$$\min_{\substack{\text{density}\\ \rho(x),\,x\in\Omega,\\ \int_\Omega \rho\, d\Omega\le V}} \quad \min_{\substack{E \text{ for}\\ \text{microstructure}\\ \text{of density } \rho(x).}} \quad \min_{\substack{\sigma\\ \operatorname{div}\sigma+p=0\\ \sigma\cdot n=t}} \left\{ \tfrac{1}{2}\int_\Omega C_{ijkl}\big(\rho(x),\theta(x),\mu(x),\gamma(x),\ldots\big)\sigma_{ij}\sigma_{kl}\, d\Omega \right\} \tag{2.2}$$

The basic idea is then to interchange the optimization over the design of the microstructure and the optimization over stresses or displacement. This interchange provides us with a basis for constructing some alternative computational procedures for solving the design problem.

The interchange of min-min in the stress formulation (2.2) results in an equivalent problem as the constraint sets for the two operators in the inf-inf problem are given entirely in terms of the variable over which each individual infimum is sought. Introduction of, for example, stress constraints at the outer design level of problem (2.2) would destroy this feature.

For the displacement formulation (2.1) the interchange will in general not result in an equivalent problem. As

$$\sup_x \inf_y \varphi(x,y) \le \inf_y \sup_x \varphi(x,y)$$

holds for any function of two parameters, the interchange will provide us with an upper bound on the optimal objective in (1.2) and thus a lower bound the compliance of the optimal structure. Moreover, *if* the problem satisfies conditions for the existence of a saddle value (saddle point), the interchange will result in an equivalent problem also for the strain case. For layered materials, the effective material tensor is concave in the data defining the local microstructure (the geometric moments, cf., section 1.6.3) and for this important class of microstructures the interchange results in an equivalent problem (Lipton, 1993a, 1994b). As also the optimal microstructures can be realized with layered materials these microstructures plays a central role for design. The situation for single load problems in dimension 2 will be considered in more detail in section 2.2.

The interchange of equilibrium analysis and optimization of local material properties results in the problems

$$\max_{\substack{\text{density}\\ \rho(x),\,x\in\Omega,\\ \int_\Omega \rho\, d\Omega\le V}} \quad \min_{u\in U} \quad \max_{\substack{E \text{ for}\\ \text{microstructure}\\ \text{of density } \rho(x).}} \left\{ \tfrac{1}{2}\int_\Omega E_{ijkl}\big(\rho(x),\theta(x),\mu(x),\gamma(x),\ldots\big)\varepsilon_{ij}(u)\varepsilon_{kl}(u)\, d\Omega - l(u) \right\} \tag{2.3}$$

$$\min_{\substack{\text{density}\\ \rho(x),\,x\in\Omega,\\ \int_\Omega \rho\, d\Omega\le V}} \quad \min_{\substack{\sigma\\ \operatorname{div}\sigma+p=0\\ \sigma\cdot n=t}} \quad \min_{\substack{E \text{ for}\\ \text{microstructure}\\ \text{of density } \rho(x).}} \left\{ \tfrac{1}{2}\int_\Omega C_{ijkl}\big(\rho(x),\theta(x),\mu(x),\gamma(x),\ldots\big)\sigma_{ij}\sigma_{kl}\, d\Omega \right\} \tag{2.4}$$

for the displacement based and stress based formulation, respectively.

Here we can, as the optimization of microstructure is pointwise, move the inner extremization under the integration over the domain. The final reformulation is then in the displacement based formulation

$$\max_{\substack{\text{density} \\ \rho(x),\, x\in\Omega, \\ \int_\Omega \rho\, d\Omega \le V}} \min_{u \in U} \left\{ \int_\Omega \overline{W}(\rho,\, \varepsilon_{ij}(u))\, d\Omega - l(u) \right\} \tag{2.5}$$

where $\overline{W}(\rho, \varepsilon)$ denotes the pointwise optimal strain energy density expression given by

$$\overline{W}(\rho, \varepsilon) = \max_{\substack{E \text{ for} \\ \text{microstructure} \\ \text{of density } \rho(x).}} \left\{ \tfrac{1}{2} E_{ijkl}(\rho(x), \theta(x), \mu(x), \gamma(x), \ldots)\, \varepsilon_{ij}\varepsilon_{kl} \right\} \tag{2.6}$$

In the stress based case we have

$$\min_{\substack{\text{density} \\ \rho(x),\, x\in\Omega, \\ \int_\Omega \rho\, d\Omega \le V}} \min_{\substack{\sigma \\ \operatorname{div}\sigma + p = 0 \\ \sigma \cdot n = t}} \left\{ \int_\Omega \overline{\Pi}(\rho, \sigma_{ij})\, d\Omega \right\} \tag{2.7}$$

with an optimized complementary energy density

$$\overline{\Pi}(\rho, \sigma_{ij}) = \min_{\substack{E \text{ for} \\ \text{microstructure} \\ \text{of density } \rho(x).}} \left\{ \tfrac{1}{2} C_{ijkl}(\rho(x), \theta(x), \mu(x), \gamma(x), \ldots)\, \sigma_{ij}\sigma_{kl} \right\} \tag{2.8}$$

For the optimization problems consisting of (2.5)-(2.6) and (2.7)-(2.8) we can identify three coupled optimization sub problems, which we label the *local anisotropy*, the *equilibrium*, and the *material distribution* optimization problems, respectively. The equilibrium problems are the inner problems of (2.5), (2.7) and the material distribution problems are the outer problems of (2.5), (2.7). Finally the local anisotropy problems are the problems (2.6) and (2.8).

The local anisotropy problems (2.6) and (2.8) correspond to finding the pointwise strongest material for a given fixed strain or fixed stress field and a given density of material. This is a standard problem setting in the theory of variational bounds on effective moduli of anisotropic materials. It is of great importance in its own right and has been the subject of intense studies in the materials science [4], [21], [23], [31], [34]. We are thus in a position to utilize, for the purpose of optimum compliance design, the great amount of work that has been done on bounding theorems in materials science. The main feature of the results we will employ is the (recent) identification of the microstructures which solve the problems (2.6) and (2.8). We can then from this parametrization solve these sub-problems by analytical or numerical means.

The specific choice of a parametrization of the effective material parameters of the optimal microstructures should depend on the solution strategy for solving the problems (2.6) and (2.8). Thus for an analytical derivation, unconstrained rotation angles of the microstructure are easier to handle than constrained parameters, while the many stationary points expected from such a parametrization makes such variables unsuited for a purely numerical procedure. For such methods the parametrization of effective properties by the geometric moment description shown in section 1.6.3 is to be recommended, even though it does not give a direct physical interpretation. It is possible, however, to construct from any moment combination a layered material which realizes this combination (see, e.g., Avellaneda and Milton, 1989, and Díaz, Lipton and Soto, 1994).

The equilibrium problem in (2.5) seeks kinematically admissible equilibrium displacements for the locally optimum energy functional, for a given distribution of resource ρ, while the equilibrium problem in (2.7) seeks statically admissible equilibrium stress fields which minimize the locally optimum energy functional, again for a given distribution of resource ρ . It should be noted that, since the locally optimum energies depend on the displacement and stress fields in a complex fashion via the optimization problems (2.6) and (2.8), the inner equilibrium statements of the problems (2.5) and (2.7) are in fact constitutively non-linear and non-smooth elasticity problems, except in very special cases. However, as we shall see in the coming section and in chapter 3, there are important cases of material modelling where this equilibrium problem becomes a problem in linear elasticity or where the non-smoothness is isolated to unimportant strain/stress values. For the strain based problem, it is worth remarking that the equilibrium problem remains a convex problem after the optimization over local material properties. The optimal strain energy density $\overline{W}(\rho, \varepsilon)$ is derived as a maximization of convex functions in the strains and is thus in itself convex in these variables.

Note finally, that the local anisotropy and equilibrium problems are solved for a fixed but arbitrary spatial distribution of the resource function ρ. The optimum material distribution problem then seeks the resource distribution that minimizes compliance.

Earlier in the presentation of the homogenization method for topology design, the introduction of composites into the generalized shape design problem has been viewed mainly as a practical tool for solving the discrete valued material distribution problem using continuous variables. However, as we have indicated, the generalized optimal shape design problem formulated as a material or no material problem requires regularization. This regularization can be achieved for example by the introduction of materials with microstructure. Regularization can also be obtained by working directly on the original problem statement, using methods such as for example quasi-convexification, Γ-convergence and H-convergence from the theory of variations (see remarks at the end of section 1.5.2). In section 2.2 we take the approach of using the results from the materials science on optimal micro structures directly to solve the problems (2.6) and (2.8).

2.1.2 A hierarchical solution procedure: Basic concept and implementation

The problem separation described above naturally leads one to consider a different computational implementation of the homogenization method for topology design, as compared to the procedure described in the section 1.3. We concentrate our discussion of possible computational schemes to the displacements based formulation which is compatible with the popular finite element stiffness method.

The implementation will work with problem (2.5) in the displacements and density only. We will accordingly consider the solution to (2.6) as given, either through an analytical or computational procedure. In the latter case, an element wise computation of the solution to (2.6) is required, but as this problem typically will be of small size it is viable to perform this numerically. The computational flow of this procedure is shown in figure 2.1, where the optimization loop is an optimality criterion algorithm of the form:

k - th iteration step:

1. For ρ_k fixed, solve the equilibrium problem

$$\min_{u \in U} \left\{ \int_{\Omega} \overline{W}(\rho_k, \varepsilon(u))\, d\Omega - l(u) \right\},$$

with solution u_k

2. Update density by

$$\rho_{k+1} = \max\left\{ \rho_{\min}, \min\left\{ \left[\frac{1}{\Lambda_k} \frac{\partial \overline{W}}{\partial \rho}(\rho_k, \varepsilon(u_k)) \right]^{\eta} \rho_k \, , 1 \right\} \right\} \tag{2.9}$$

with Λ_k determined by the constraint

$$\int_{\Omega} \rho_{k+1}\, d\Omega = V$$

This update scheme is completely analogous to the procedure described in section 1.3. The design update in step 2. of (2.9) is an optimality criteria based update where the scalar Lagrange multiplier for the volume constraint has to be determined in an inner iteration loop. This multiplier is determined by the volume constraint and its value should be determined by a Golden Section method or a Newton procedure. As for the procedure described earlier a tuning parameter η is introduced. This should be adjusted in order to obtain convergence and stability of the algorithm. Note that we for the density update have to compute the derivative of the optimized strain energy with respect to the density. For the analytically derived optimal strain energy functionals this derivative is straightforward to obtain, while for computationally derived optimal strain energy functionals this derivative is given simply as the Lagrange multiplier for the volume constraint of problem (2.6), i.e., the derivative is given directly from the computation of the optimal energy.

The equilibrium problem in (2.9) is in general a non-linear problem, so the equilibrium problem requires an inner iteration loop at this point, but computational experience has shown that, as the optimization over the bulk density is in itself iterative, only one (or a few) equilibrium iterations need to be used for each design update.

One of the advantages of the computational program described is that the main flow of the procedure is *independent* of the modelling of the material used for the description of design. This latter information is added as an external module (the solution of (2.6)). This feature makes it possible to more easily generate flexible procedures, where the material model can be changed easily. It is especially convenient that when and if algebraic solutions to the local anisotropy problem are found, only minor changes to the general data flow and programme structure needs to be implemented. The approach has been successfully implemented for both the homogenization modelling (Jog, Haber and Bendsøe, 1993, 1994a), see sections 2.2 and 2.3, and for a free material design modelling (Bendsøe, Díaz, Lipton and Taylor, 1994), see chapter 3.

The main objection to the procedure outlined here is, of course, the need for non-linear analysis iterations. This does complicate implementation. On the other hand, we shall see here and in chapter 3 that in many cases it is possible to manage this part by iterative use of even simple FEM systems based on linear, isotropic material models. Also, in certain cases it even turns out that the optimization of energy actually results in a *linear* equivalent problem, thus removing the need for analysis iterations.

However, if the non-linearity is a major concern, one can in certain cases use a short-cut by implementing a method which mixes the philosophy of the method of chapter 1 and the method proposed here. The flow of computations is shown in figure 2.2, and shows that the optimization problem (2.6) is now used to generate the parameters of the optimal rigidity tensor for each displacement iteration. The direct coupling between the material parameters and the displacements is then ignored in the implementation of the *linear* equilibrium analysis. This approach has been tested and proved operational for the homogenization modelling, both with a geometric parametrization of microstructure for a single load problem as well as with a parametrization using the moment formulation described in section 1.6.3. The computation of the optimal local material parameters were here performed numerically by a sequential quadratic optimization algorithm (NLPQL, Schittkowski, 1985). The computational procedure outlined in figure 2.2 is especially attractive for multiple load problems where (2.6) in principle also introduces a coupling between the displacements for the different loads. However, this is ignored in this method. The multiple load problem for plates has been treated recently by this approach in Díaz, Lipton and Soto, 1994, using the moment description of the effective properties of layered materials.

In the development above we could have performed one further interchange, namely the interchange of the optimization over density and the extremum form of the equilibrium problem. Such an interchange would result in the problems

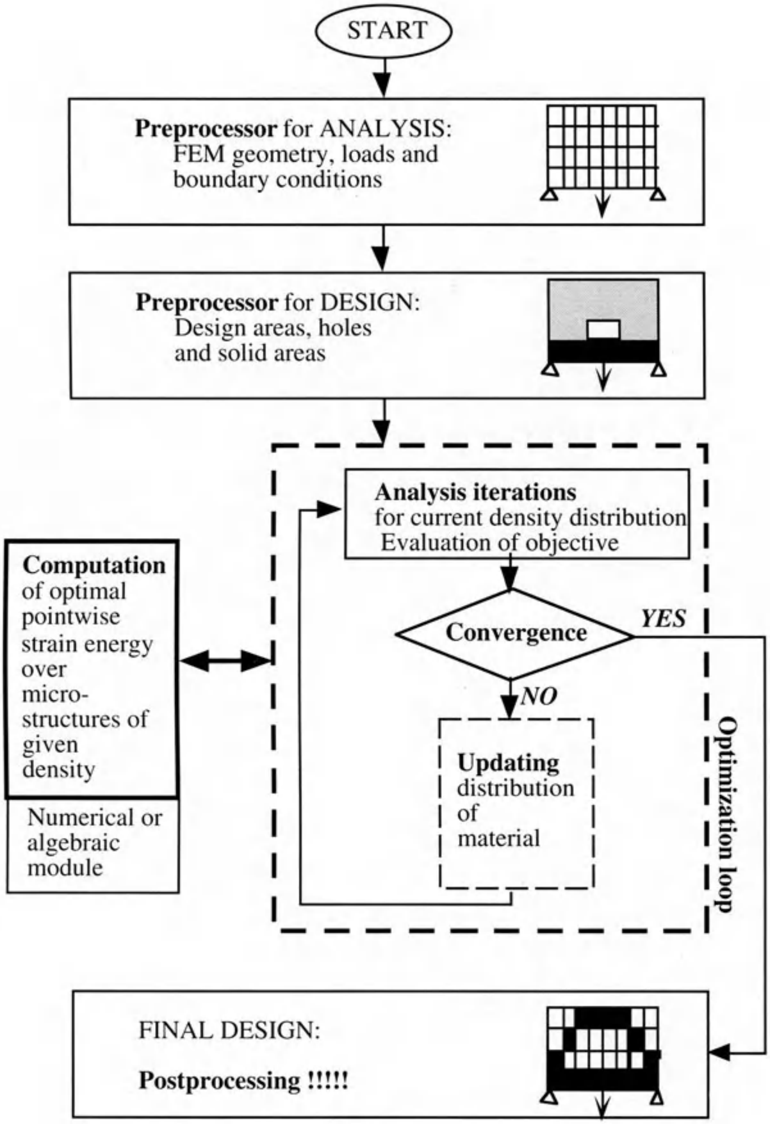

Fig. 2.1. Topology design using explicitly optimized energy functionals.

$$\min_{u \in U} \left\{ \hat{W}(u) - l(u) \right\}, \quad \hat{W}(u) = \max_{\substack{\text{density} \\ \rho(x),\, x \in \Omega, \\ \int_\Omega \rho \, d\Omega \le V}} \int_\Omega \overline{W}(\rho, \varepsilon_{ij}(u)) \, d\Omega \tag{2.10}$$

in the strain based case, while we for the stress formulation have

$$\min_{\substack{\sigma \\ \operatorname{div}\sigma+p=0 \\ \sigma\cdot n=t}} \left\{\hat{\Pi}(\sigma)\right\}, \quad \hat{\Pi}(\sigma)=\min_{\substack{\text{density} \\ \rho(x),x\in\Omega, \\ \int_\Omega \rho\, d\Omega\le V}} \left[\int_\Omega \overline{\Pi}(\rho,\sigma_{ij})\, d\Omega\right] \tag{2.11}$$

Here, problem (2.11) is equivalent to the original problem (2.2), as this problem is a pure min-min problem. However, it is known that for the layered materials case (see below) problem (2.10) and problem (2.5) are *not* equivalent. However, for the case of free material design as we shall consider in chapter 3, problems (2.1), (2.5) and (2.10) are all equivalent.

We have written problems (2.10) and (2.11) in a form which underlines that these reduced problems should be interpreted as equilibrium *only* problems for globally optimized potential and complementary energy expressions, respectively. The optimized energies are non-smooth and couples all degrees of freedom through the volume constraint. This latter complication can be circumvented by considering the volume constraint of the original problems (2.1) and (2.2) in the form of a penalization and not a constraint (Allaire and Kohn, 1993d, and Allaire and Francfort, 1993). With this interpretation problem (2.11), for example, becomes

$$\min_{\substack{\sigma \\ \operatorname{div}\sigma+p=0 \\ \sigma\cdot n=t}} \left\{\hat{\Pi}_\Lambda(\sigma)\right\},$$

$$\hat{\Pi}_\Lambda(\sigma)=\min_{\substack{\text{density} \\ \rho(x),x\in\Omega}} \left[\int_\Omega \left(\overline{\Pi}(\rho,\sigma_{ij})+\Lambda\rho\right) d\Omega\right]=\int_\Omega \min_{\substack{\text{density} \\ \rho(x),x\in\Omega}} \left[\overline{\Pi}(\rho,\sigma_{ij})+\Lambda\rho\right] d\Omega \tag{2.12}$$

where Λ is a fixed penalty factor (or fixed Lagrange multiplier).

For a computational procedure for problem (2.12) one could then solve the inner problem by analytical or computational means and implement a non-smooth optimization method for solving the equilibrium problem. Such a procedure for layered microstructures is described in Allaire and Kohn, 1993d, while Allaire and Francfort, 1993, have implemented a method as illustrated in figure 2.2, but with both the material properties *and* density being given (algebraically) by the solution of the optimization of the complementary energy (see section 2.2 for the derivation of these expressions).

As mentioned above, it does not make sense, in general, to consider computational schemes for solving problem (2.10), as this problem may have no reasonable relation to the original problem (2.1) (except providing a lower bound on the optimum compliance). As mentioned above, however, for certain problems is does make sense to work with problem (2.10), and we shall see in chapter 4 how special algorithms developed for trusses may be used for solving problem (2.10) in these cases.

We close this section by noting that the problems (2.5) and (2.7) are design problems in the distribution of material, as described by the density function ρ. This implies that in many cases it may be convenient to keep these basic problem

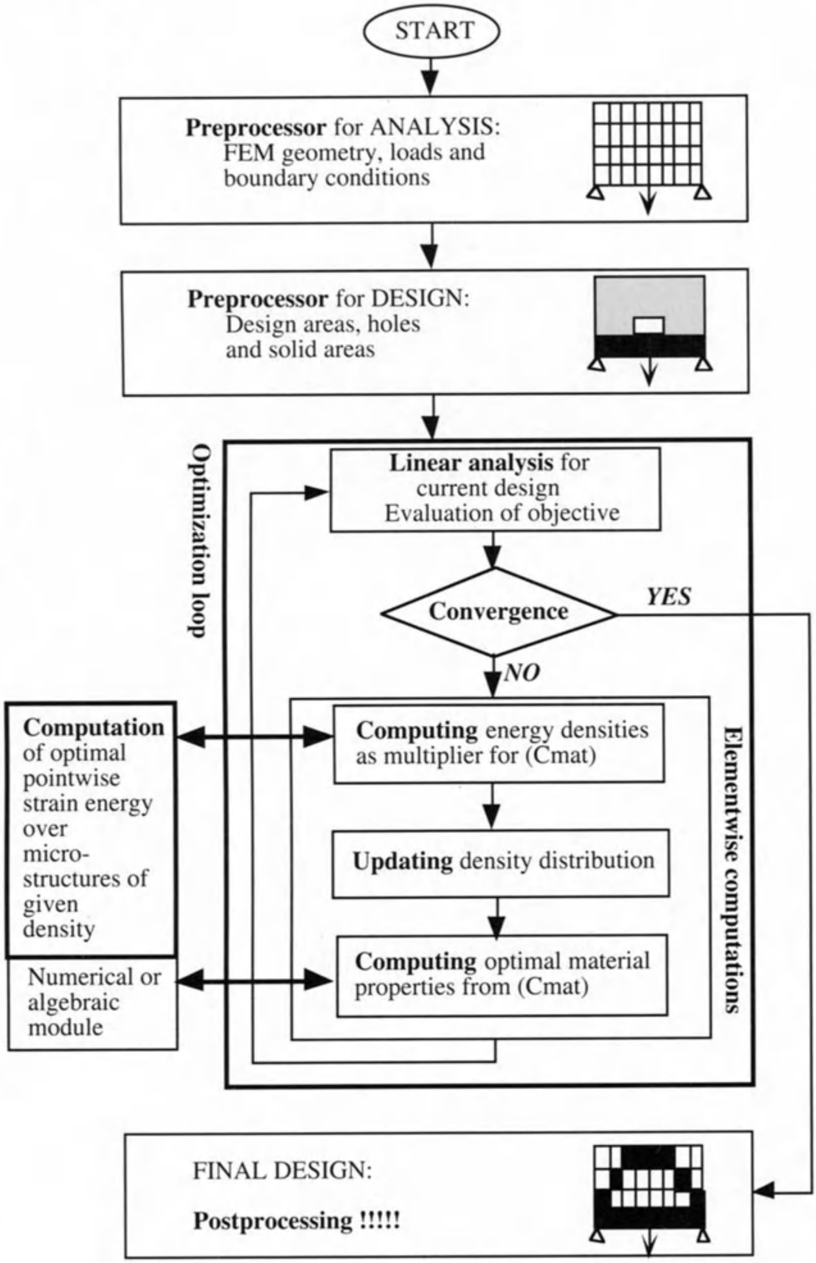

Fig. 2.2. Topology design using explicitly optimized energy functionals, but ignoring the non-linearity introduced by the computation of these optimal energy functionals.

statements as the basis for introducing other types of requirements on the final designs. One possibility that immediately springs to mind is to introduce a penalization on intermediate values of density, trying to obtain 0-1 type designs. Further, a penalization of the perimeter of the design would allow for a control on the number and sizes of holes predicted for the final topology (Jog, Haber and Bendsøe, 1994b). In essence, such constraints would impose some typical post-processing constraints as described in section 1.4 already at the level of the topology design. The type of optimization problem that one would consider for the constraints just mentioned could be of the form

$$\max_{\substack{0<\rho_{\min}\le\rho\le 1\\ \int_\Omega \rho\, d\Omega \le V}} \left\{ \Phi_u(\rho) - \mathrm{X}\Phi_{\text{grey}}(\rho) - \mathrm{Z}\Phi_{\text{per}}(\rho) \right\}$$

with

$$\begin{aligned} \Phi_u(\rho) &= \min_{u\in U} \left\{ \int_\Omega \overline{W}(\rho, \varepsilon_{ij}(u))\, d\Omega - l(u) \right\} \\ \Phi_{\text{grey}}(\rho) &= \int_\Omega \rho(1-\rho)\, d\Omega \\ \Phi_{\text{per}}(\rho) &= \sup\left\{ \int_\Omega \rho \operatorname{div}\varphi\, d\Omega \;\middle|\; \varphi\in C_c^1(\Omega,\mathbf{R}^n),\ |\varphi|\le 1 \right\} \end{aligned} \tag{2.13}$$

Here X, Z are penalty factors for the measure of grey area, Φ_{grey}, and the measure of perimeter, Φ_{per}, respectively. Computational results for such a formulation will be presented in section 2.3.2. These results are based on use of the following smooth realisation of the expression for the perimeter (which holds for a piecewise continuous function ρ)

$$\Phi^{\delta}_{\text{per}}(\rho) = \int_{\Omega\setminus\Gamma_J} \left[|\nabla\rho|^2 + \delta^2 \right]^{1/2} d\Omega + \int_{\Gamma_J} \left[\langle\rho\rangle^2 + \delta^2 \right]^{1/2} d\Gamma$$

where Γ_J is the jump set of the density ρ, $\langle\rho\rangle$ is the jump in ρ across Γ_J and δ is a small parameter that makes the expression smooth in ρ.

2.2 Optimized energy functionals for the homogenization modelling

2.2.1 Basic problem statement

It was shown in the previous sections how alternative computational procedures can be devised if we numerically or analytically can solve the problem

$$\overline{\Pi}(\rho,\sigma_{ij}) = \min_{\substack{\text{microstructure}\\ \text{of density } \rho(x)}} \left\{ \tfrac{1}{2} C_{ijkl}\big(\rho(x),\theta(x),\mu(x),\gamma(x),\ldots\big)\sigma_{ij}\sigma_{kl} \right\} \tag{2.8}$$

for the stress based min-min formulation (1.3) of the single load minimum compliance topology design problem or the problem

$$\overline{W}(\rho,\varepsilon) = \max_{\substack{\text{microstructure}\\ \text{of density } \rho(x).}} \left\{ \tfrac{1}{2} E_{ijkl}\big(\rho(x),\theta(x),\mu(x),\gamma(x),\ldots\big)\, \varepsilon_{ij}\varepsilon_{kl} \right\} \tag{2.6}$$

for the strain based max-min formulation (1.2) of the same topology design problem.

In problem (2.8) we seek the optimal choice of microstructure for which the homogenized effective moduli of the material minimize the complementary energy density for a fixed stress field σ, for all possible composites with a fixed volume fraction of material and void (weak material for the layered materials). Similarly for (2.6) we seek the optimal choice of micro structure for which the homogenized effective moduli of the material maximize the strain energy density for a fixed strain field. A sub-problem of these problems was considered earlier in the form of finding the optimal rotation of an orthotropic material.

In finding a solution to problems (2.6) and (2.8) we are faced with two sub-problems. First, the form of the optimal microstructure has to be found among *all* parametrizations of microstructures. Second, when the class of optimal microstructures have been identified, the problems (2.6) and (2.8) should be solved explicitly for this specific parametrization of design. For the first problem recent results from the theoretical materials science provide the answer for the compliance problems we consider here, while the second problem will be solved analytically below for the single load case in dimension 2.

Studies on bounds on the effective material properties of composite mixtures made of two isotropic materials have shown that for elasticity the strongest (or weakest) material for a single load or multiple load problem can be obtained by a layered medium, with layering at several microscales [21], [23]. For single load problems the strongest material consists of orthogonal layers, with no more than 2 layers for dimension 2 and no more than 3 layers for dimension 3. For multiple load problems the strongest material (for the weighted average formulation) consists of layers that are not necessarily orthogonal, up to 3 for dimension 2 and up to 6 for dimension 3. This result together with the saddle point property (cf., section 2.1.1, and Lipton, 1993a, 1994d)

$$\max_{\substack{E \text{ for layers}\\ \text{of fixed } \rho}} \min_{u\in U} \left\{ \tfrac{1}{2}\int_\Omega E_{ijkl}\,\varepsilon_{ij}(u)\varepsilon_{kl}(u)\,\mathrm{d}\Omega - l(u) \right\}$$

$$= \min_{u\in U} \max_{\substack{E \text{ for layers}\\ \text{of fixed } \rho}} \left\{ \tfrac{1}{2}\int_\Omega E_{ijkl}\,\varepsilon_{ij}(u)\varepsilon_{kl}(u)\,\mathrm{d}\Omega - l(u) \right\}$$

means that we can obtain information of theoretical as well as computational importance by solving problems (2.6) and (2.8) analytically for layered materials.

2.2.2 Rank-2 layered materials in dimension 2

As described above, the strongest material in plane elasticity for a single stress or strain tensor can be obtained by a layered medium, with orthogonal layerings at two different microscales. It was shown in section 1.6 how effective material properties for layered materials can be obtained analytically and for the rank-2 layering two densities γ and μ of layers are needed to define the material properties and the total density of material. Let us briefly recapitulate the construction of the rank-2 layering: First, a (first order) layering of the strong and the weak material (void in the following) is constructed, the thicknesses of the strong and weak layers being γ and $(1-\gamma)$, respectively, in the unit cell, $[0,1]\mathrm{x}\mathbf{R}$ (see Fig. 2.3). This resulting composite material is then used as one of two components in a new layered material, with layers μ thick of the isotropic, strong material and with layers $(1-\mu)$ thick of the composite just constructed; the layers of this composite material are placed perpendicular to the direction of the new layering. The effective properties of the resulting material are computed by one of the methods shown in section 1.6 on homogenization of layered materials, with the moduli computed as the material is constructed, bottom up.

The total density of the strong material in the unit cells of the rank-2 layered material is

$$\rho = \mu + (1-\mu)\gamma = \mu + \gamma - \mu\gamma$$

and if the primary layerings of density μ are placed in the 2-direction of our reference frame, the effective material properties in plane stress are (we impose now that the weak material is void, i.e. $E^{-} \to 0$)

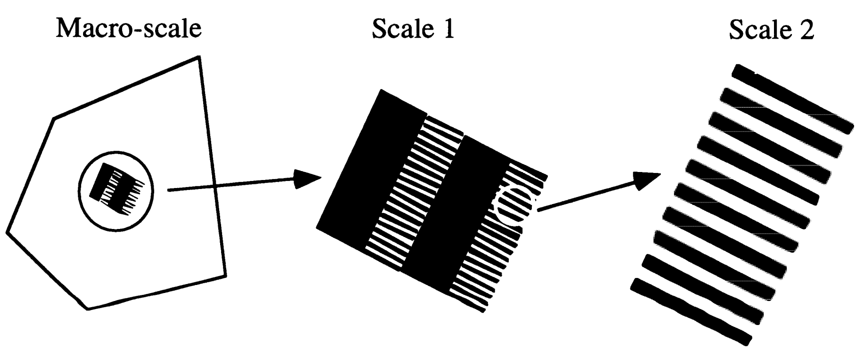

Fig. 2.3. A rank-2 layered material for the single load problem in dimension 2.

$$E_{1111} = \frac{\gamma E}{\mu\gamma(1-\nu^2)+(1-\mu)}, \quad E_{1122} = \mu\nu E_{1111},$$
$$E_{2222} = \mu E + \mu^2\nu^2 E_{1111}, \qquad E_{1212} = 0$$

Here E is Young's modulus and ν is Poisson's ratio. It is straightforward to verify that such a material is weak in shear, i.e. that the material parameters satisfy $E_{1111} + E_{2222} - 2E_{1122} - 4E_{1212} \geq 0$ (cf., definition in section 1.2.1).

The rank-2 materials are not the only composites which achieves the upper bound on stiffness of a mixture of two materials (cf., Grabowski, 1994, Grabovsky and Kohn, 1994a, 1994b, Milton, 1990 and Vigdergauz, 1984). For example, the optimal strain energy for any strain field with principal strains of the same sign can actually be achieved by a composite at a *single* scaling, provided the unit cell can have a general rectangular shape (Vigdergauz, 1984, Grabowski and Kohn, 1994b); this distortion of the cell as compared to the square cell actually provides a second scaling effect. Thus, for example, the single layering can be approximated by long slender cells with slits.

The layered materials are thus not special in the sense of being uniquely optimal, but they are convenient composites as the effective material properties can be expressed as the fairly simple, explicit rational functions of the layer densities displayed above. This is crucial for the developments in the following. It should be noted that the algebraic analysis that we present below for both the stress and the strain based approaches holds for dimension 2 and a single load case *only* (Jog, Haber and Bendsøe, 1994a). For dimension 3, the explicit algebraic solution of the material design problem for a single load has been carried out recently by Allaire, 1994a.

2.2.3 The stress based analysis of optimal layered materials

The results on optimal rotation of orthotropic materials shows that for the minimum compliance problem with a material which is weak in shear, the axes of orthotropy should be aligned with the axes of principal stresses σ_I, σ_{II}. Thus in a structure where the material instantaneously rotates according to this principle, the complementary energy has the form

$$\Pi = \tfrac{1}{2} C_{ijkl}\sigma_{ij}\sigma_{kl} = \frac{1}{2|D|}\left[E_{1111}\sigma_{II}^2 + E_{2222}\sigma_I^2 - 2E_{1122}\sigma_I\sigma_{II}\right]$$

with

$$|D| = E_{1111}E_{2222} - E_{1122}{}^2$$

Here, we have the well-known relations between the principal stresses σ_I, σ_{II}. and the stresses $\sigma_{11}, \sigma_{22}, \sigma_{12}$ in an arbitrary frame:

$$\sigma_I = \frac{1}{2}(\kappa + \omega),\ \sigma_{II} = \frac{1}{2}(\kappa - \omega)$$

$$\kappa = \sigma_{11} + \sigma_{22},\ \omega = \sqrt{(\sigma_{11} - \sigma_{22})^2 + 4\sigma_{12}{}^2}$$

We see that the alignment of axes is consistent with the fact that $E_{1212} = 0$ for the layered material. The vanishing shear stiffness for the layered material plays no role as the material automatically rotates to a frame of zero shear. Also, we have factored out the zero stiffness contribution from this term in the rigidity matrix. Note that the material described by the energy expression above now represents a non-linear material, by virtue of the optimal rotation and the fact that $E_{1111} \neq E_{2222}$. The alignment of the layers and the principal stresses also follows from the work showing the optimality of the layered materials [21].

Here and in the following we use the term 'material' to describe the characteristics of the optimized energy expressions. This should not be interpreted as properties of the layered materials in a physical sense, but expresses the peculiarity of the energy of a structure which automatically assigns the real material in accordance with the applied load (stress/strain field).

We now fix the density ρ fixed and express γ in terms of μ from the relation $\rho = \mu + \gamma - \mu\gamma$. The problem of minimizing the complementary energy is thus reduced to a one-parameter problem. Stationarity of the energy with respect to the layer density μ can now be found by standard but fairly lengthy calculations. We find the stationary layer density μ and corresponding layer density γ to be expressed as:

$$\mu = \frac{\rho|\sigma_{II}|}{|\sigma_{II}| + (1-\rho)|\sigma_I|}\ ;\quad \gamma = \frac{\rho|\sigma_I|}{|\sigma_I| + |\sigma_{II}|}$$

These values turn out to represent minimizing values if the value of μ satisfy the constraints $0 < \mu < \rho$. This implies that the stresses should satisfy $\sigma_I\sigma_{II} \neq 0$ and for such values of stress the optimal layering is a true rank-2 layering. If $\sigma_I\sigma_{II} = 0$ we have a region with an unidirectional, single layering or a solid region corresponding to $\mu = 0,\ \gamma = \rho$ or $\mu = \rho,\ \gamma = 0$. The numerical values of stresses in the formula above indicate that there for the rank-2 regions are two distinct types of layerings depending on the sign of the quantity $\sigma_I\sigma_{II}$:

$$\text{Mode I: } \sigma_{\mathrm{I}}\sigma_{II} < 0 \text{ and } \mu = \frac{\rho\sigma_{II}}{\sigma_{II} - (1-\rho)\sigma_I}\ ;\quad \gamma = \frac{\rho\sigma_I}{\sigma_I - \sigma_{II}}$$

$$\text{Mode II: } \sigma_{\mathrm{I}}\sigma_{II} > 0 \text{ and } \mu = \frac{\rho\sigma_{II}}{\sigma_{II} + (1-\rho)\sigma_I}\ ;\quad \gamma = \frac{\rho\sigma_I}{\sigma_I + \sigma_{II}}$$

We denote the two types of stationary layerings as mode I and mode II materials, and the rank-1 materials as mode III materials.

Note that the expressions above were derived under the assumption that the direction of the outer layer of the rank-2 layering (corresponding to μ) is aligned with σ_{II}, and that no restrictions where imposed on the relative sizes of σ_I and σ_{II}. The analysis shows that the optimization over layer densities automatically assures that the axis of maximal stiffness is aligned with the axis of the largest stress, in accordance with the result on optimal rotations. Also note that a second, equally optimal layering can be obtained by aligning the outer layerings with the stress σ_I; the formulas above now holds with σ_I and σ_{II} interchanged. The effective complementary energy for both optimal microstructures is given by the expressions:

$$\begin{aligned}
&\text{Mode I} \;\;: \;\; \overline{\Pi} = \frac{1}{2E\rho}\left[\sigma_I^2 + \sigma_{II}^2 - 2(1-\rho+\rho\nu)\sigma_I\sigma_{II}\right]; \\
&\text{Mode II} \;: \;\; \overline{\Pi} = \frac{1}{2E\rho}\left[\sigma_I^2 + \sigma_{II}^2 + 2(1-\rho-\rho\nu)\sigma_I\sigma_{II}\right]; \qquad (2.14) \\
&\text{Mode III} : \;\; \overline{\Pi} = \frac{\sigma_I^2}{2E\rho} \text{ if } \sigma_{II} = 0; \;\; \overline{\Pi} = \frac{\sigma_{II}^2}{2E\rho} \text{ if } \sigma_I = 0.
\end{aligned}$$

The material properties of the now optimized microstructure are completely given in terms of the density and the principal stresses. Noting that

$$\begin{aligned}
\sigma_I^2 + \sigma_{II}^2 &= \sigma_{11}{}^2 + \sigma_{22}{}^2 + 2\sigma_{12}{}^2 \\
\sigma_I\sigma_{II} &= \sigma_{11}\sigma_{22} - \sigma_{12}{}^2
\end{aligned}$$

we observe the surprising fact that the optimized energy corresponds to an artificial material which for the regions with two layerings is linearly elastic and quasi isotropic. The compliance tensor $\overline{C}_{ijkl}$ for this material is given through the energy expression $\overline{\Pi}(\rho,\sigma) = \frac{1}{2}\overline{C}_{ijkl}\sigma_{ij}\sigma_{kl}$ and it has in any reference frame the following non-zero elements:

$$\begin{aligned}
\text{Mode I} \;: \;\; &\overline{C}_{1111} = \overline{C}_{2222} = \frac{1}{E\rho}; \;\; \overline{C}_{1212} = (2-\rho+\rho\nu)/2E\rho; \\
&\overline{C}_{1122} = \overline{C}_{2211} = -(1-\rho+\rho\nu)/E\rho. \\
\text{Mode II} : \;\; &\overline{C}_{1111} = \overline{C}_{2222} = \frac{1}{E\rho}; \;\; \overline{C}_{1212} = \rho(1+\nu)/2E\rho; \\
&\overline{C}_{1122} = \overline{C}_{2211} = (1-\rho-\rho\nu)/E\rho.
\end{aligned}$$

For the single layering regions the material is non-linear. Note that the isotropy of the optimized material law is natural in view of the rotation of the rank-2 material. The linearity and isotropy of this extremal material law can be understood in a broader context from the translation method for obtaining optimal bounds on effective moduli of composite materials, Cherkaev, 1993a, Milton, 1990.

The expression (2.14) is the solution to the problem (2.8) for the single load case we consider. Note, however, that for the stress based problem (2.7) a further reduction to a design-free problem is possible, cf., problem (2.11) defined in section 2.1.2. To this end we should optimize with respect to the density of material also. Taking the volume constraint into account for the inner problem of (2.11), we minimize with respect to the bulk density ρ the expression $\overline{\Pi}+\Lambda\rho$, where $\Lambda \geq 0$ is a Lagrange multiplier for the volume constraint. By fairly straightforward algebraic manipulations, we get the following optimality condition for the bulk density ρ:

$$\rho = \frac{|\sigma_I| + |\sigma_{II}|}{\sqrt{2\Lambda E}} \quad \text{in all modes.} \tag{2.15}$$

which can also be computed by direct relaxation of the problem (1.2), Allaire and Kohn, 1993d. In (2.15) the absolute value operators indicate that we have different expressions for mode-I and mode-II materials. The corresponding densities γ and μ are:

$$\mu = \frac{|\sigma_{II}|}{\sqrt{\Lambda E} - |\sigma_I|}, \quad \gamma = \frac{|\sigma_I|}{\sqrt{\Lambda E}}$$

The optimal distribution of the bulk density should satisfy the volume constraint:

$$\int_\Omega \rho \, \mathrm{d}\Omega = \int_\Omega \min\left\{ \frac{|\sigma_I| + |\sigma_{II}|}{\sqrt{2\Lambda E}}, 1 \right\} \mathrm{d}\Omega = V \tag{2.16}$$

This constraint determines the value of the Lagrange multiplier Λ for any relevant volume constraint with value less than the volume of the design domain Ω. This follows from the monotonicity of the ρ as a function of Λ. Thus the volume constraint in our case implies that we can consider Λ as a function of the principal stresses, given via the equation (2.16) and we can write $\Lambda(\sigma_I, \sigma_{II})$. Taking this feature into consideration, the expressions for the complementary strain energy density corresponding to the optimal densities are:

$$\text{if } \frac{|\sigma_I| + |\sigma_{II}|}{\sqrt{2E\Lambda(\sigma_I, \sigma_{II})}} \leq 1 :$$

$$\begin{cases} \hat{\Pi}(\sigma) = \dfrac{1}{2E}\left\{\sqrt{2E\Lambda(\sigma_I,\sigma_{II})}\,(|\sigma_I| + |\sigma_{II}|) + 2(1-\nu)\sigma_I\sigma_{II}\right\}, & \text{if } \sigma_I\sigma_{II} \leq 0 \\ \hat{\Pi}(\sigma) = \dfrac{1}{2E}\left\{\sqrt{2E\Lambda(\sigma_I,\sigma_{II})}\,(|\sigma_I| + |\sigma_{II}|) - 2(1+\nu)\sigma_I\sigma_{II}\right\}, & \text{if } \sigma_I\sigma_{II} \geq 0 \end{cases}$$

and

$$\text{if } \frac{|\sigma_I|+|\sigma_{II}|}{\sqrt{2E\Lambda(\sigma_I,\sigma_{II})}} \geq 1 \ : \ \hat{\Pi}(\sigma) = \frac{1}{2E}\left\{|\sigma_I|^2 + |\sigma_{II}|^2 + 2\nu|\sigma_I||\sigma_{II}|\right\}.$$

By the procedure described above we have reduced the stress based *design* problem (1.3) to a *design independent* non-linear, non-smooth elasticity problem of the form:

$$\min_{\substack{\sigma \\ \operatorname{div}\sigma+p=0 \\ \sigma\cdot n=t}} \left\{ \int_\Omega \hat{\Pi}(\sigma)\, d\Omega \right\} \tag{2.17}$$

This problem is written in terms of a relaxed complementary energy, with a constraint expressing equilibrium. Thus a finite element discretization of this formulation requires the use of higher order elements for the approximation of stresses. Also, non-smooth optimization techniques or smoothing techniques for the objective functional have to be invoked. These features does advocate the use of the strain based formulation, even though this involves keeping the bulk density ρ as a variable of the problem, as we shall see in the proceeding section. Details of a numerical procedure for solving the stress based problem (2.17) can be found in Allaire and Kohn, 1993d.

2.2.4 The strain based problem of optimal layered materials

The optimal rotation of the layered material with the directions of principal strains $\varepsilon_I, \varepsilon_{II}$ results in a non-linear strain energy:

$$W = \tfrac{1}{2} E_{ijkl}\, \varepsilon_{ij}\, \varepsilon_{kl} = \tfrac{1}{2}\left\{E_{1111}\, \varepsilon_I^2 + E_{2222}\, \varepsilon_{II}^2 + 2E_{1122}\, \varepsilon_I\, \varepsilon_{II}\right\}$$

where the relations between principal strains $\varepsilon_I, \varepsilon_{II}$ and the strains ε_{11}, ε_{22}, ε_{12} in an arbitrary frame follows the analogous formulas as for the stress case. The non-linearity of the rotating, adaptive material again follows from the rotation and the fact that the layered material is anisotropic with $E_{1111} \neq E_{2222}$.

The algebra involved in optimizing the microstructure for the strain based formulation is much more complicated than for the stress case and for simplification of presentation in this case, it turns out to be convenient to impose the choice $|\varepsilon_I| \geq |\varepsilon_{II}|$ for the principal strain directions.

In the following we align the outer layer of thickness μ with the ε_{II} strain direction. This does not guarantee that the material satisfies the condition $E_{1111} \geq E_{2222}$ but it turns out that the optimization over μ automatically implies that the optimized micro-structure satisfies this condition, in accordance with the results on optimal rotations of orthotropic materials.

The following step of the analysis is analogous to the procedure for the stress case. That is, we fix the density ρ, express γ in terms of μ and find the stationary points of the strain energy W as a function of μ only. The algebraic manipulations now become very involved, and the use of symbolic manipulations is recommended.

The optimal density μ and corresponding density γ are again given by different expressions, depending on the relative values of the principal strains $\varepsilon_I, \varepsilon_{II}$ as well as the size of the bulk density ρ. We again denote the different expressions as Mode-I, Mode-II and Mode-III regions. The optimal values are:

$$\text{Mode I:} \quad \left\{ \begin{aligned} \mu &= \frac{\varepsilon_I(1+\nu\rho-\rho)+\varepsilon_{II}}{\nu\varepsilon_I+(2-\rho-\nu+\nu\rho)\varepsilon_{II}} \\ \gamma &= \frac{\varepsilon_I+\varepsilon_{II}(1+\nu\rho-\rho)}{(1-\nu)(\varepsilon_I-\varepsilon_{II})} \end{aligned} \right\} \text{ if } \frac{\varepsilon_{\mathrm{I}}+\varepsilon_{II}}{(1-\nu)\varepsilon_I}<\rho<1$$

$$\text{Mode II:} \quad \left\{ \begin{aligned} \mu &= \frac{\varepsilon_I(\nu\rho+\rho-1)+\varepsilon_{II}}{\nu\varepsilon_I+(2-\rho+\nu-\nu\rho)\varepsilon_{II}} \\ \gamma &= \frac{\varepsilon_I+\varepsilon_{II}(\nu\rho+\rho-1)}{(1+\nu)(\varepsilon_I+\varepsilon_{II})} \end{aligned} \right\} \text{ if } \frac{\varepsilon_{\mathrm{I}}-\varepsilon_{II}}{(1+\nu)\varepsilon_I}<\rho<1$$

$$\text{Mode III:} \quad \left\{ \begin{aligned} \mu &= 0 \\ \gamma &= \rho \end{aligned} \right\} \text{ if } 0 \le \rho \le \frac{\varepsilon_{\mathrm{I}}-\varepsilon_{II}}{(1+\nu)\varepsilon_I} \text{ or } 0 \le \rho \le \frac{\varepsilon_{\mathrm{I}}+\varepsilon_{II}}{(1-\nu)\varepsilon_I}$$

Note that the mode-III material (for the lower bound $\mu = 0$) represents a rank-1 layering in the 1-direction. Accordingly, the material can only sustain a uni-axial stress state in mode-III; this is consistent with the choice $|\varepsilon_I| \ge |\varepsilon_{II}|$. Also observe that the upper bound $\mu = \rho$ can only be achieved for the solid material $\rho = 1$. The mode-I, mode-II and mode-III materials reduce all for $\rho = 1$ to the solid $\rho = 1$ material. Moreover, the mode-I, mode-II and mode-III materials satisfy the constraint $\mu \le \rho$ for $\rho \le 1$, so the upper bound constraint on μ can be ignored

In the development above, we made the choice of aligning the outer layer of thickness μ with the ε_{II} strain direction. If we alternatively choose to align this layer with the ε_I strain direction, the optimization over μ results in the same energy expressions as for the expressions given above, i.e. for each strain field there exist two optimal rank-2 microstructures. In essence, aligning with the ε_I direction corresponds to extending the analysis above to the case of $|\varepsilon_I| \le |\varepsilon_{II}|$, and the densities in this situation are also given by the equations above, with the exception of mode-III now being a uni-axial layer in the μ direction corresponding to $\mu = \rho$. The conditions expressing the validity of the different modes also extends readily to this case, but with $\varepsilon_I, \varepsilon_{II}$ interchanged.

The effective strain energy corresponding to either optimal layering is given by the expressions:

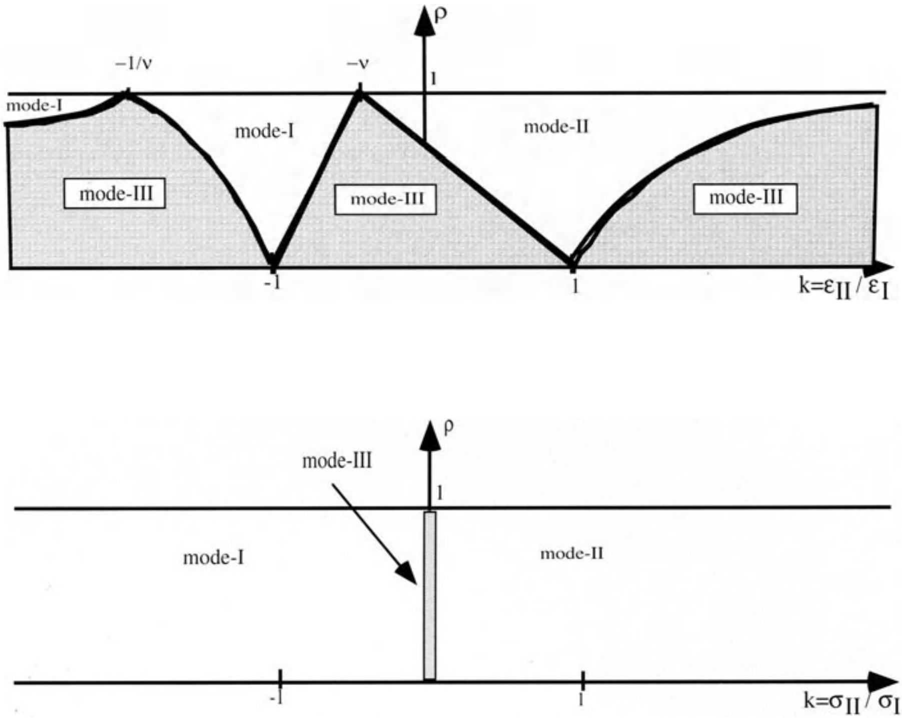

Fig. 2.4. The regions of the different optimal material modes for optimizing a rank-2 material. The modes depend on the given values of ratio of principal strains or stresses and the bulk density ρ. Note that there is a one-to-one correspondence between the strain based case and the stress based case.

$$\text{Mode I} \;:\; \overline{W}(\rho,\varepsilon)=\frac{E}{2(1-\nu)(2-\rho+\nu\rho)}\left[\varepsilon_I^2+\varepsilon_{II}^2+2(1-\rho+\rho\nu)\varepsilon_I\varepsilon_{II}\right];$$

$$\text{Mode II} \;:\; \overline{W}(\rho,\varepsilon)=\frac{E}{2(1+\nu)(2-\rho-\nu\rho)}\left[\varepsilon_I^2+\varepsilon_{II}^2-2(1-\rho-\rho\nu)\varepsilon_I\varepsilon_{II}\right];$$

$$\text{Mode III} \;:\; \overline{W}(\rho,\varepsilon)=\frac{\rho E{\varepsilon_I}^2}{2} \text{ if } |\varepsilon_I|\geq|\varepsilon_{II}|;\;\; \overline{W}(\rho,\varepsilon)=\frac{\rho E{\varepsilon_{II}}^2}{2} \text{ if } |\varepsilon_I|\leq|\varepsilon_{II}|\,.$$

In the Mode-III regions with single layers, the extremal rotated and adapted material is non-linear and, as for the stress based analysis, the rank-2 layered regions of Modes I and II consist of a linearly elastic effective material. This material has the same stiffness matrix as the optimal material obtained in the stress case. This is consistent with the property that for a fixed density ρ we have (see Lipton, 1993a, 1994b)

$$\min_{\substack{div\sigma+p=0\\ \sigma\cdot n=t}} \left\{ \int_{\Omega} \overline{\Pi}(\rho,\sigma)\, d\Omega \right\} = \max_{u\in U} \left\{ l(u) - \int_{\Omega} \overline{W}(\rho,\varepsilon(u))\, d\Omega \right\}$$

i.e., a duality principle holds for the optimized strain and complementary energies when the bulk density is kept fixed.

For completeness we write the rigidity tensor $\overline{E}_{ijkl}$ for the optimized *energy*, $\overline{W}(\rho,\varepsilon) = \frac{1}{2}\overline{E}_{ijkl}\varepsilon_{ij}\varepsilon_{kl}$, for this case also. Writing only the non-zero components, we can use that the energy corresponds to the energy of an isotropic material, so

$$\left.\begin{aligned} &\overline{E}^K_{1111} = \overline{E}^K_{2222} = \tilde{E}_K \\ &\overline{E}^K_{1212} = \overline{E}^K_{2112} = \overline{E}^K_{2121} = \overline{E}^K_{1221} = \tfrac{1}{2}(1-\tilde{\nu}_K)\tilde{E}_K \\ &\overline{E}^K_{1122} = \overline{E}^K_{2211} = \tilde{\nu}_K\tilde{E}_K \end{aligned}\right\} \quad K = I \text{ or } II$$

with

$$\text{Mode I}: \quad \tilde{E}_I = E/\left[(1-\nu)(2-\rho+\rho\nu)\right], \quad \tilde{\nu}_I = (1-\rho+\rho\nu)$$

$$\text{Mode II}: \quad \tilde{E}_{II} = E/\left[(1+\nu)(2-\rho-\rho\nu)\right], \quad \tilde{\nu}_{II} = -(1-\rho-\rho\nu)$$

The optimization of the strain energy with respect to layer directions as well as layer densities results in an optimized strain energy $\overline{W}$ which is convex in the density ρ ; this is readily checked by examining the second derivative of the energy for the different modes. This excludes the possibility of interchanging min and the max in the reduced problem

$$\max_{\substack{\text{density } \rho\\ \int_\Omega \rho\, d\Omega = V}} \; \min_{u\in U} \left\{ \int_{\Omega} \overline{W}(\rho,\varepsilon(u))\, d\Omega - l(u) \right\} \tag{2.18}$$

and this is thus the final reduced form of the strain based formulation.

2.2.5 The limiting case of Michell's structural continua

The layout theory of Michell frames and its extensions to flexural systems is the classical approach to topology and layout design of structures [3], [8], [16]. It has been illustrated earlier that the homogenization method predicts structures that resemble truss-type layouts and Michell continua type layouts, when constrained to small volumes of available material. We show here that this limiting process can be formalized through an asymptotic expansion of the problem under rescaling of the geometric and load data.

A Michell frame is a continuum in dimension two consisting of two mutually orthogonal fields of tension/compression only members that are directed along the principal strain. The total amount of material used is described by two independent densities of material, constrained to satisfy some volume constraint. The problem is a continuum analogue to the single-load truss optimal design problem, and there are a number of equivalent stress or strain based problem statements. The frame is described by a specific strain energy of the form:

$$W = \frac{E}{2}\left[\alpha \varepsilon_I^{\,2} + \beta \varepsilon_{II}^{\,2}\right]$$

where α, ε_I and β, ε_{II} are the densities and corresponding principal strains in the two directions of the continua, and the optimization problem is the one of minimizing compliance for a given volume of material, or equivalently, maximizing of compliance for given constraints on the strains in each bar, cf., Hemp, 1973, Bendsøe, Ben-Tal and Zowe, 1994. Lay-out theory for grid-type structures in general, as treated by Prager and Rozvany, deals with problems with a wider scope of objectives and constraints, but with basically the same energy definition as above.

As noted above the homogenization method for topology design generates designs that are very similar to the well-known examples of Michell structures for small volume fractions ($V <<$ volume of Ω). Also, it can be shown that for the stress-based homogenization formulation as described above, the limiting case of infinitely large Lagrange multiplier Λ for the volume constraint (i.e. small density) corresponds to the stress-based Michell frame lay-out problem formulation, Kohn and Allaire, 1993d. We describe here an asymptotic analysis approach, based on a finite-energy geometric rescaling, that results in the Michell frame limit for both the stress and strain homogenization formulations.

The Michell frame is usually understood as a limiting case for low densities of material, where the interaction of thin members in a planar frame can be ignored. Thus, we are concerned with the limiting situation where the layers in a layered material become 'thin' relative to the cell size of the problem. This can be modelled by letting the density of material tend to zero in an asymptotic expansion. Taking the limit of zero density of material requires a complementary rescaling of the loads and tractions to make the energy limit well posed. We thus introduce a scaling parameter ξ which reduces the layer densities by rescaling the dimensions of the microstructure relative to the unit cell (see Fig. 2.5). The rescaled densities are:

$$\hat{\mu} = \xi^2 \mu; \qquad \hat{\gamma} = \xi^2 \gamma; \qquad \hat{\rho} = \xi^2 \rho.$$

We now use the rescaled densities together with an expansion of the stresses and strains in the expressions for the optimized energies described above, using only the terms of zero order in ξ and requiring that the energies remain finite in the limit of $\xi \to 0$.

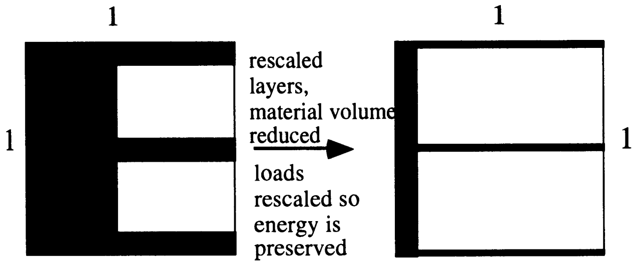

Fig. 2.5. The rescaling of the layerings that leads to the Michell frame limit.

For the stress based case the stress expansion reads:

$$\hat{\sigma}_{ij} = ...+\xi^{-2}\sigma^{-2}{}_{ij} + \xi^{-1}\sigma^{-1}{}_{ij} + \sigma^{0}{}_{ij} + \xi\sigma_{ij} + \xi^{2}\sigma^{2}{}_{ij}+.....$$

For the energy to remain finite in the limit, the expansion in stresses must be of order greater than or equal to 1. The zero-order part of the optimized complementary energy $\overline{\Pi}$ (see section 2.2.3) then becomes (for all modes):

$$\Pi_M = \frac{1}{2E\rho}\,(|\sigma_I| + |\sigma_{II}|)^2$$

corresponding to a rescaling of stress given by $\xi\sigma_{ij}$. This is expected from equilibrium considerations for the unit cell.

The rescaling at the limit of $\xi \to 0$ implies that the upper constraint on bulk density ρ is not active. Thus the optimization over ρ under the volume constraint results in the stress based problem (2.7) reducing to the form,

$$\min_{\substack{\sigma \\ \mathrm{div}\sigma + p = 0 \\ \sigma \cdot n = t}} \left\{ \int_{\Omega} (|\sigma_I| + |\sigma_{II}|)\, d\Omega \right\}$$

This is the classical Michell problem formulated in stresses. Here the specific reference to the volume constraint is not present, as the Lagrange multiplier for this constraint only enters as a scaling parameter, which has no influence on the form of the optimal solution. The problem corresponds to a layout problem, where the cost of carrying the principal stresses is minimized over all statically admissible stress fields. This corresponds directly to the classical stress-based truss optimization problem stated as:

$$\min_{q^+,q^-} \sum_{i=1}^{m} \frac{l_i}{\overline{\sigma}_i}(q_i^+ + q_i^-)$$
$$\text{subject to:}$$
$$\mathbf{B}(q^+ - q^-) = p,$$
$$q_i^+ \geq 0,\ \ q_i^- \geq 0, \quad i = 1,....,m.$$

which is a problem in plastic design. Here, q_i^+, q_i^- are the truss bar member forces in compression and tension, respectively, $\mathbf{B}$ is the compatibility matrix, l the lengths of the bars and $\overline{\sigma}_i$ the yield limit for bar number i. This problem is equivalent to the problem of fixed volume, minimum compliance design of an elastic truss structure with Young's moduli $E_i = \overline{\sigma}_i^2$ and a volume equal to the optimal volume for the plastic problem, thus taking the development 'full circle'. Truss topology design is treated in detail in chapter 4.

For the strain based case, we again use an expansion in the form:

$$\hat{\varepsilon}_{ij} = ...+\xi^{-2}\varepsilon^{-2}{}_{ij} + \xi^{-1}\varepsilon_{ij} + \varepsilon^{0}{}_{ij} + \xi\varepsilon^{1}{}_{ij} + \xi^{2}\varepsilon^{2}{}_{ij} + ...;$$

In the limit of $\xi \to 0$ and using the convention of $|\hat{\varepsilon}_I| \geq |\hat{\varepsilon}_{II}|$, the energy optimized with respect to layer densities becomes

$$\overline{W} = \frac{E\xi^2\rho\hat{\varepsilon}_I{}^2}{(2-\xi^2\rho+\xi^2\nu\rho)} \ \text{ if } \hat{\varepsilon}_I = -\hat{\varepsilon}_{II}; \ \ \overline{W} = \frac{E\xi^2\rho\hat{\varepsilon}_I{}^2}{(2-\xi^2\rho-\xi^2\nu\rho)} \ \text{ if } \hat{\varepsilon}_I = \hat{\varepsilon}_{II};$$
$$\overline{W} = \frac{\xi^2\rho E\hat{\varepsilon}_I{}^2}{2}, \ \text{otherwise}$$

The requirement that the energy $\overline{W}$ remains finite in the limit $\xi \to 0$ implies that the terms in the strain expansion must have degree greater or equal to -1 in ξ. Now taking only the zero order terms of $\overline{W}$ we obtain for all modes ($|\varepsilon_I| \geq |\varepsilon_{II}|$):

$$W_M = \frac{\rho E\varepsilon_I{}^2}{2}$$

corresponding to the term $\frac{1}{\xi}\varepsilon_{ij}$ as a rescaled strain.

We also can arrive at the strain based energy expression by considering the original strain energy expression and performing the optimization over layer densities after taking the limit of $\xi \to 0$. To this end we note that the rigidities are of the form:

$$E_{1111} = \frac{\xi^2 \gamma E}{\xi^2 \mu \gamma (1-\nu^2) + (1-\xi^2 \mu)} = \xi^2 \gamma E + \text{terms of order} \geq 4 \text{ in } \xi,$$
$$E_{1122} = \xi^4 \mu \nu E = 0 + \text{terms of order} \geq 4 \text{ in } \xi, \quad E_{1212} = 0$$
$$E_{2222} = \xi^2 \mu E + \xi^4 \mu^2 \nu^2 E_{1111} = \xi^2 \mu E + \text{terms of order} \geq 4 \text{ in } \xi$$

This implies that the zero order contribution to a finite strain energy has the form:

$$W = \tfrac{1}{2} E \left[\gamma\, \varepsilon_I^2 + \mu\, \varepsilon_{II}^2 \right]$$

corresponding to the Michell continua strain energy described above. Expressing μ in terms of γ and the bulk density ρ we obtain an energy

$$W = \tfrac{1}{2} E \left[\rho\, \varepsilon_I^2 + \mu (\varepsilon_{II}^2 - \varepsilon_I^2) \right]$$

which is linear in the density μ. As we assume $|\varepsilon_I| \geq |\varepsilon_{II}|$, this energy for $|\varepsilon_I| \neq |\varepsilon_{II}|$ is maximal if $\mu = 0$. For all strain variations the optimal energy density becomes again $W_M = \tfrac{1}{2} \rho E \varepsilon_I^{\,2}$, showing by alternative means that the Michell frame corresponds to the low volume fraction strain based rank-2 layering problem.

2.3 Implementation issues and examples

2.3.1 Computational procedure

In this section we will discuss the implementation of a computational solution procedure for the strain based reduced problem (2.18)

$$\max_{\substack{0 < \rho_{\min} \leq \rho \leq 1 \\ \int_\Omega \rho\, d\Omega = V}} \; \min_{u \in U} \left\{ \int_\Omega \overline{W}(\rho, \varepsilon(u))\, \mathrm{d}\Omega - l(u) \right\} \tag{2.18}$$

for the case of a single load case in dimension 2, and based on the analytically derived optimal specific strain energy $\overline{W}(\rho, \varepsilon(u))$ derived in section 2.2.3. We will follow the approach of the basic optimality criteria scheme presented in section 2.1.2 (see also figure 2.1).

The equilibrium problem. The equilibrium problem in (2.18) is a non-linear problem, so the equilibrium problem requires an inner iteration loop at this point. The optimal energy $\overline{W}(\rho, \varepsilon(u))$ is the result of a maximization of pure quadratics in the strains, and thus the equilibrium problem in (2.18) is convex. Moreover, the analysis problem is actually smooth when $0 < \rho_{\min} \le \rho$. This is readily seen by deriving partial derivatives of $\overline{W}(\rho, \varepsilon(u))$ and by noting that the singularity in Mode-III regions for $\varepsilon_{11} = \varepsilon_{22}, \varepsilon_{12} = 0$ is excluded by the constraint $0 < \rho_{\min} \le \rho$.

The analysis problem is actually linear in the solid regions and in regions of Mode-I and II material, while it is non-linear in the Mode-III regions. In the Mode-III regions the tangent stiffness matrix is singular and unsuitable for use in computations. Therefore an iterative solution strategy based on a secant stiffness matrix for the nonlinear equilibrium problem can be adopted. The secant matrix maps total strains into total stresses, in contrast to a map from strain increment to stress increment as for the tangent stiffness. In the rank-2 regions the response is linearly elastic, so here the secant matrix coincides with the linear stiffness matrices shown in the previous chapter. For the Mode-III regions we choose to use a positive definite secant matrix, which generates the correct strain energy and which attains the values of the Mode-I and Mode-II stiffness matrices at the transition to these modes. This turns out to be possible and the resulting secant rigidity tensor is

$$\overline{E}^{III}_{1111} = \overline{E}^{III}_{2222} = \tilde{E}_{III}$$

$$\overline{E}^{III}_{1212} = \overline{E}^{III}_{2112} = \overline{E}^{III}_{2121} = \overline{E}^{III}_{1221} = \tfrac{1}{2}(1 - \tilde{\nu}_{III})\tilde{E}_{III}$$

$$\overline{E}^{III}_{1122} = \overline{E}^{III}_{2211} = \tilde{\nu}_{III}\tilde{E}_{III}$$

with

$$\tilde{E}_{III} = \rho E\left[1 - (\varepsilon_{II}/\varepsilon_{I})^2\right]^{-1}, \quad \tilde{\nu}_{III} = -\,\varepsilon_{II}/\varepsilon_{I} \quad \text{if } |\varepsilon_{I}| \ge |\varepsilon_{II}|$$

$$\tilde{E}_{III} = \rho E\left[1 - (\varepsilon_{I}/\varepsilon_{II})^2\right]^{-1}, \quad \tilde{\nu}_{III} = -\,\varepsilon_{I}/\varepsilon_{II} \quad \text{if } |\varepsilon_{I}| \le |\varepsilon_{II}|$$

For the computations all regions are thus described by isotropic stiffness matrices and the density dependence of the stiffness can be simulated through a variation of Young's modulus as well as the Poisson ratio of an isotropic material. It is the use of the optimal energy functionals that causes this and it makes it fairly simple to implement the computational procedure by iterative use of even the simplest finite element package. This is somewhat surprising as the original design problem in essence is seeking the distribution of an *orthotropic* material.

Note that the effective total stress-strain relation remains nonlinear, as the secant matrix in the Mode-III region is a function of the current state. Accordingly, the secant stiffness must be updated at every equilibrium iteration, according to the local strain at each point in the domain with Mode-III material. Computational experience has shown that, as the optimization over the bulk density is in itself iterative, only one (or a few) equilibrium iterations are needed for each design update.

The design update. Note that we for the density update have to compute the derivative of the strain energy with respect to the density. This derivative is here for the rank-2 case given by the expression

$$\text{For } \frac{\varepsilon_I+\varepsilon_{II}}{(1-\nu)\varepsilon_I}<\rho<1:\ \frac{\partial\overline{W}}{\partial\rho}=\frac{E}{2}\left[\frac{\varepsilon_I-\varepsilon_{II}}{(2-\rho+\nu\rho)}\right]^2;$$
$$\text{For } \frac{\varepsilon_I-\varepsilon_{II}}{(1+\nu)\varepsilon_I}<\rho<1:\ \frac{\partial\overline{W}}{\partial\rho}=\frac{E}{2}\left[\frac{\varepsilon_I+\varepsilon_{II}}{(2-\rho-\nu\rho)}\right]^2;$$

$$\text{For } 0\le\rho\le\frac{\varepsilon_I+\varepsilon_{II}}{(1-\nu)\varepsilon_I}\ \text{or}\ 0\le\rho\le\frac{\varepsilon_I-\varepsilon_{II}}{(1+\nu)\varepsilon_I}:$$
$$\frac{\partial\overline{W}}{\partial\rho}=\frac{E\varepsilon_I^{\,2}}{2}\ \text{if } |\varepsilon_I|\ge|\varepsilon_{II}|;\ \frac{\partial\overline{W}}{\partial\rho}=\frac{E\varepsilon_{II}^{\,2}}{2}\ \text{if } |\varepsilon_I|\le|\varepsilon_{II}|\,.$$

For the design update we also have to solve the equation

$$F(\Lambda)=\int_\Omega \min\left\{\frac{1}{\Lambda}\left[\frac{\partial\overline{W}}{\partial\rho}(\rho,\,\varepsilon(u))\right]\rho\,,\,1\right\}d\Omega=V$$

in the scalar Lagrange multiplier Λ for the volume constraint. In the examples presented in this chapter, this equation was solved using a Newton procedure. With this approach in mind we note that the directional derivative of F can be computed as:

$$\frac{dF}{d\lambda}(\lambda^+)=\int_{\Omega^+\cup\Omega^1}-\frac{1}{\lambda^2}\left[\frac{\partial\overline{W}}{\partial\rho}(\rho,\,\varepsilon(u))\right]\rho\,d\Omega;\ \frac{dF}{d\lambda}(\lambda^-)=\int_{\Omega^+}-\frac{1}{\lambda^2}\left[\frac{\partial\overline{W}}{\partial\rho}(\rho,\,\varepsilon(u))\right]\rho\,d\Omega\,,$$

with:

$$\Omega^+=\left\{x\in\Omega\,\middle|\,\frac{1}{\lambda}\left[\frac{\partial\overline{W}}{\partial\rho}(\rho,\,\varepsilon(u))\right]\rho<1\right\},\quad \Omega^1=\left\{x\in\Omega\,\middle|\,\frac{1}{\lambda}\left[\frac{\partial\overline{W}}{\partial\rho}(\rho,\,\varepsilon(u))\right]\rho=1\right\}$$

2.3.2 Examples

We illustrate here some example design obtained by use of the procedure described above. The examples relate to problems solved earlier by alternative means and which constitute standard test examples.

In figure 2.6 we show that the present method is also prone to the checkerboard problem discussed in section 1.3.2, unless proper precaution is taken. In the examples illustrated in this chapter, checkerboard designs were subdued by using a stable couple of discretizations of density and displacements, namely element wise constant density approximation in connection with Q8 elements for the displacements.

We also illustrate the effect of using a penalization of the density distribution in terms of a perimeter penalization as well as a penalization of intermediate areas (grey areas). These examples are then example solutions of problem (2.13) outlined at the end of section 2.1.2. These examples shows that it is possible to include certain production related constraints already at the level of the topology design phase, thus supplementing the post-processing procedure described in section 1.4.2.

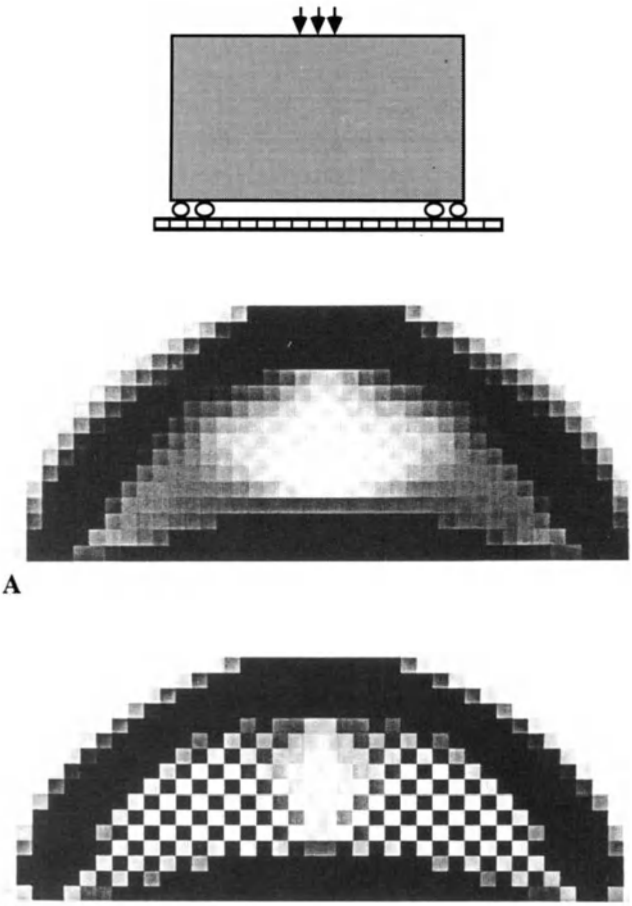

A

B

Fig. 2.6. Optimal design using an optimized rank-2 material strain energy density. Problem is for a rectangular domain loaded at the top, c.f. top picture. *(A)*: Shows the optimal designs using element wise constant density function and a 8-node displacement model. *(B)*: Shows the unstable, checkerboard solution obtained using constant density function and a 4-node displacement model. Jog, Haber and Bendsøe, 1994a.

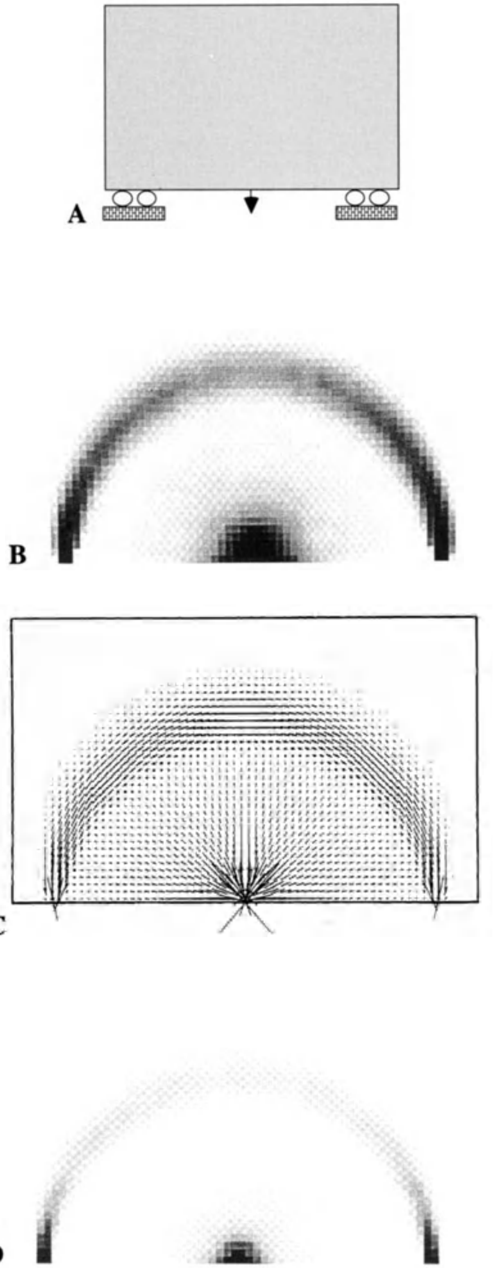

Fig. 2.7. Optimal design using an optimized rank-2 material strain energy density. Problem is for a rectangular domain loaded at mid-span on its bottom edge, c.f. *(A)*. Optimal designs computed using element wise constant density function and a 8-node displacement model. *(B)* and *(C)*: show the density distribution and principal stress distribution for a volume fraction of 20 %. *(D)*: shows the density distribution for a volume fraction of 10 %. Note that grey area is not limited to biaxial response. The bicycle wheel like design has an area with radial uniaxial stress as well as a rim of circumferential uniaxial stress (the rim of a 'wheel'). Jog, Haber and Bendsøe, 1994a.

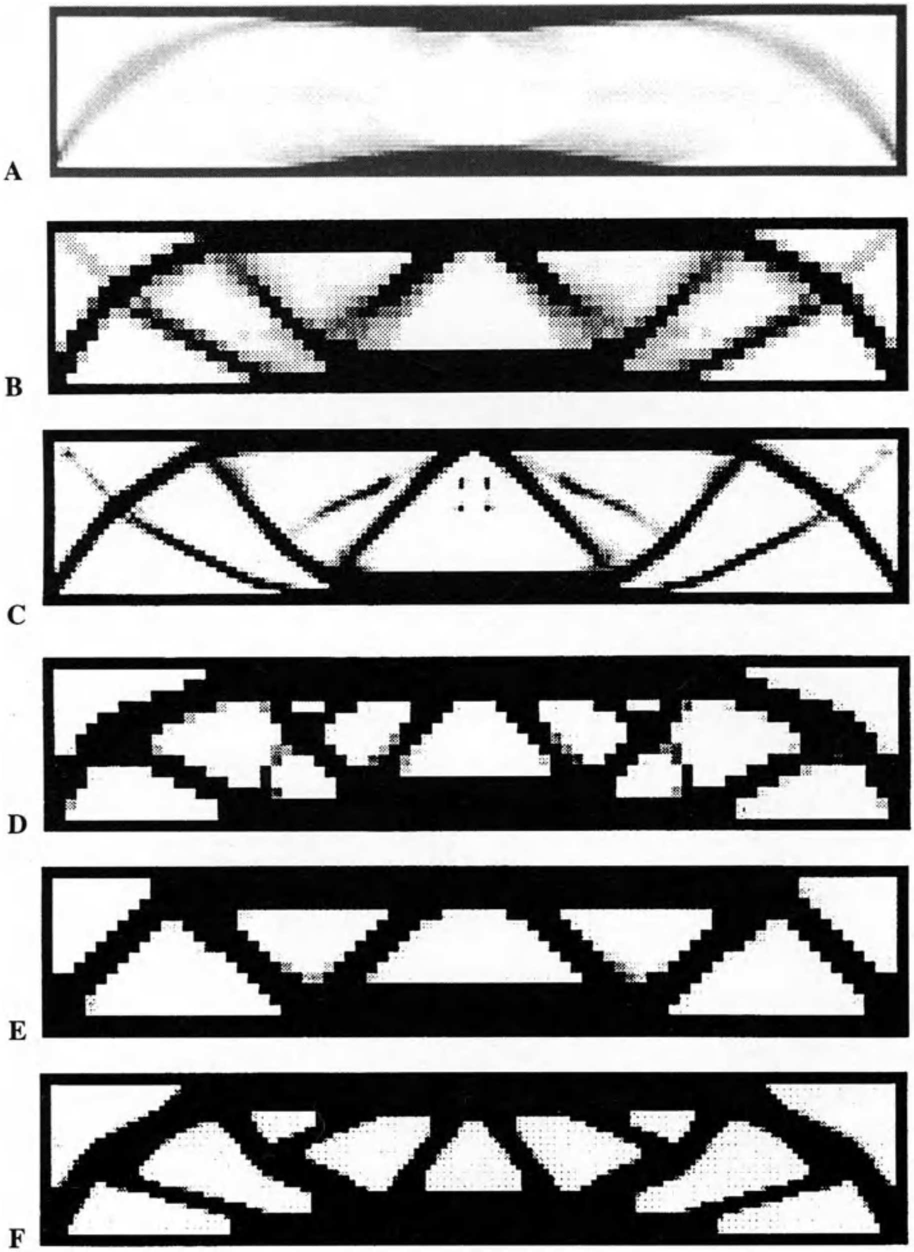

Fig. 2.8. Optimal design using an optimized rank-2 material strain energy density with penalties on intermediate densities and on perimeter (cf. problem 2.13). The problem is the MBB beam described in figure 1.29 of chapter 1. *(A)* shows the density distribution for the unconstrained case. In *(B)* and *(C)* intermediate densities are penalized. In *(D)* to *(F)* intermediate densities and perimeter are penalized, with *(F)* being a fine mesh variant of *(D)*. Jog, Haber and Bendsøe, 1994b.

3 Extremal energy functionals for a free parametrization of material, shape and topology

In a number of recent papers on the optimization of structures, the distribution of material as well as the material properties themselves have been considered as design variables [25]. The goal of these studies is to formulate a structural optimization problem in a form that encompasses the design of structural material in a broad sense, while also encompassing the provision of predicting the structural topologies and shapes associated with the optimum distribution of the optimized materials. This goal is accomplished by representing as design variables the material properties in the most general form possible for a (locally) linear elastic continuum namely as the unrestricted set of positive semi-definite constitutive tensors.

In the modelling of the optimization problem the parameters which describe the structure can be divided into two sets: the parameters defining the local material tensor and those that describe the specific cost of the material. In parallel with the developments in chapter 2, it can be shown that the minimum compliance optimization of a structure with respect to these two sets of parameters can be performed independently. Furthermore, the optimization with respect to the local material tensor parameters can be performed analytically. This derivation is fairly simple for both the single load case and the multiple load problem and for any dimension of the spatial domain. Thus the more general problem statement is considerably simpler as compared to the homogenization topology problem.

The very general framework of optimizing directly on a free parametrization of the material tensor results in developments which provide an attainable global lower bound on the performance of any structure designed for the same loads, boundary conditions and ground structure. At the same time, it provides an attainable global upper variational bound on the effective moduli of any elastic material. Also, the considerable simplifications that can be demonstrated indicate that the broader form of a material design problem, as described and analyzed in this chapter, should constitute effective means for studying the global structural optimization problem involving sizing, shape, topology and material selection.

The results that we can obtain within the assumption of a locally unconstrained configuration of material are informative towards gaining insight into the nature of efficient local structures. For practical reasons it is important to understand how to match a particular local microstructure to the specific form of the elasticity tensors predicted here. One possibility is to formulate this problem as the topology design of a unit cell of a homogenized medium. The objective is then to achieve certain homogenized coefficients (energy expressions) for example with minimum use of a given specified material. As the optimized materials typically will be singular in nature, it is natural to consider truss models for the cells of the homogenization modelling.

The computational results for the inverse material design problem shows that the locally unconstrained configuration of material employed here is actually realizable, provided that fairly complicated composites with microstructure are considered acceptable. Thus a more restrictive modelling of the material is not needed on purely physical grounds but should be considered only as a way to penalize impractical features of the local structure.

3.1 Problem formulation for a free parametrization of design

3.1.1 Modelling considerations

The strong interrelation between the fields of optimal design and materials science has been underlined in the preceding chapters. Thus optimal topology design and optimal design with advanced materials is closely related. The problem of optimal rotation of orthotropic materials provides a natural starting point for considerations for a more general approach to the concurrent design of material and structure, while the lack of existence to the generalized shape design problems provides a natural mathematical angle to the simultaneous design of material and overall structure. In the homogenization modelling the structure is assumed to be made up of an arbitrary composition of a strictly limited number of given materials, and for the special case of topology design one of the given materials is void (usually approximated by a very flexible material). The homogenization modelling predicts a ranked set of 'microstructures' or 'structures with microscale variations' as the optimal material distribution, and this microstructure should be chosen optimally with respect to simple energy criteria (cf. problems (2.6) and (2.8) in chapter 2).

In the homogenization method of topology design, the total volume of material, defined at the micro level, provides a natural cost function for the optimization problem. There is not at first glance a natural cost function for the general material design formulation we consider here, where we allow for all possible positive semi-definite constitutive tensors. Instead, we use certain invariants of the stiffness tensor as the measure of cost, thus ensuring that the optimal design solutions are independent of the choice of reference frame.

For physical reasons, the possible rigidity tensors in the design formulation are restricted to the set of positive semi-definite, symmetric tensors. As discussed above, suitable cost functions must have the property of frame indifference. Since the goal is to optimize the local material properties as well as the global structural response, we choose to consider cost in terms of invariants of the constitutive tensor itself. Specifically, we choose for the developments in the following two invariants as examples of local cost (cf., Bendsøe, Haber, Guedes, Pedersen and Taylor, 1993, and Bendsøe, Díaz, Lipton and Taylor, 1994):

$$\Psi_{\mathrm{A}}(E) = E_{ijij}, \qquad \Psi_{\mathrm{B}}(E) = \left[E_{ijkl}E_{ijkl}\right]^{\frac{1}{2}}$$

i.e., respectively, the trace and the Frobenius norm of the 4-tensor E.

3.1.2 Problem statement

The problem we consider is the multiple load minimum compliance problem (1.4) (cf., section 1.1.1) generalized to the situation where the material properties themselves appear in the role of design variables. This means that we consider a design parametrization in the form

$$\begin{gathered} E \geq 0 \ \text{ in } \Omega \\ E_{ijkl} \in L^{\infty}(\Omega), \ \text{ for all } \ ijkl \\ \int_{\Omega} \Psi(E)\, \mathrm{d}\Omega \leq V \end{gathered} \tag{3.1}$$

Thus we take the minimization over all positive, semi-definite rigidity tensors E_{ijkl} (with the usual symmetry properties) and use the integral over the domain of some invariant $\Psi(E_{ijkl})$ of the rigidity tensor as the measure of cost.

With M load cases (body forces p^k and boundary traction t^k) and with given weighting factors w^k we can, as seen earlier, formulate the minimum compliance problem as

$$\max_{\substack{\text{rigidity } E \geq 0 \\ \int_{\Omega}\Psi(E)d\Omega \leq V}} \ \min_{\substack{u=\{u^1,\ldots,u^M\} \\ u^k \in U,\ k=1,\ldots,M}} \left\{ \mathrm{H}(E,\boldsymbol{u}) = \int_{\Omega} W(E,\boldsymbol{u})\mathrm{d}\Omega - l\,(\boldsymbol{u}) \right\} \tag{3.2}$$

where

$$W(E,\boldsymbol{u}) = \tfrac{1}{2}\sum_{k=1}^{M} w^k E_{ijpq}(x)\varepsilon_{ij}(u^k)\varepsilon_{pq}(u^k), \quad l\,(\boldsymbol{u}) = \sum_{k=1}^{M} w^k l^k(u^k), \quad \boldsymbol{u} = \left\{u^1,\ldots,u^M\right\}.$$

Here we have, as several times earlier, represented the equilibrium requirement via minimization of the potential energy with respect to deformation. Also, we have used that the displacement fields for the individual load cases are independent.

As discussed above in the introduction, suitable cost functions must have the property of frame indifference. Specifically, we choose the following two invariants of the constitutive tensor as examples of local cost:

$$\text{Case A}: \quad \Psi_{\text{A}}(E) = \rho_A = E_{ijij}, \qquad \text{Case B}: \quad \Psi_{\text{B}}(E) = \rho_B = \left[E_{ijkl}E_{ijkl}\right]^{\frac{1}{2}}$$

Note that these measures are homogeneous of degree one. Thus comparing to the conventional 2D problem for the design of material distribution in a sheet (where total cost is proportional to the volume of material), the above 'cost measures' correspond in their role to the sheet thickness.

For the sake of simplifying the derivation, we have introduced the resource density functions, ρ_{A} and ρ_{B} and we choose to restate the design problem in the common form:

$$\max_{\substack{\text{density } \rho \\ 0\le\rho_{\min}\le\rho\le\rho_{\max}<\infty \\ \int_\Omega \rho\, d\Omega \le V}} \quad \max_{\substack{\text{rigidity } E\ge 0 \\ \Psi(E)\le\rho}} \quad \min_{\substack{\mathrm{u}=\{u^1,\ldots,u^M\} \\ u^k\in U,\ k=1,\ldots,M}} \quad \mathrm{H}(E,\mathrm{u}) \tag{3.3}$$

This separation of the design variables provides a separation between the properties of the tensor E that can be optimized locally (at each point in the structure) and those that must be treated as a distributed parameter problem over the full domain. This type of separation was also used in chapter 2 for the single load, homogenization modelling topology design statement. We will here go through similar steps as there, in order to clarify the development for the multiple load case.

In the max-min problems above we have introduced an upper bound on the resource densities in order to ensure that the problem is well posed. A possible non-zero lower bound is also catered for. Note that the resource constraints are convex for both case A and B.

In the developments to follow, we show that an analytical optimization actually can reduce the number of free design variables from 6 in dimension two and 21 in dimension three to only *one* in both dimensions (in any dimension that is).

3.1.3 Splitting the problem into a series of sub-problems

We can perform a further rearrangement of problems (3.3) by exchanging the order of the min and max operations in the two inner problem. This is allowable here as the inner problem in (3.3) satisfies the conditions for existence of a saddle point: the weights w^k are positive, the function $\mathrm{H}(E,\boldsymbol{u})$ is concave (linear) in E and convex in the displacements u^k, and the set $\{E \mid \Psi(E)\le\rho,\ E\ge 0\}$ is closed, convex and weak*-compact in $L^\infty(\Omega)$ (see also section 1.5.1). After the exchange we write

$$\max_{\substack{\text{density } \rho \\ 0\le\rho_{\min}\le\rho\le\rho_{\max}<\infty \\ \int_\Omega \rho\, d\Omega \le V}} \quad \min_{\substack{u=\{u^1,\ldots,u^M\} \\ u^k\in U,\ k=1,\ldots,M}} \quad \max_{\substack{E\ge 0 \\ \Psi(\rho)\le\rho}} \mathrm{H}(E,\mathrm{u}) \tag{3.4}$$

whose solution is, again, the same as that of the original problem. Observe that E is assumed to be independent from point to point in the structure. Thus the inner maximization problem will be solved when the average energy density is maximized in a point-wise sense over Ω. The final form of the problem is then

Optimization Problem. With ρ, E and $\{u^k\}$, $k=1,2,..M$, as variables

$$\max_{\rho\in G}\left\{ \min_{\substack{u=\{u^1,\ldots,u^M\} \\ u^k\in U,\ k=1,\ldots,M}} \left[\int_\Omega \max_{\substack{E\ge 0 \\ \Psi(\rho)\le\rho}} \{W(E,\boldsymbol{u})\} \mathrm{d}\Omega - l\,(\boldsymbol{u}) \right] \right\} \tag{3.5}$$

with the density being restricted to the closed, convex and weak-* compact constraint set G in $L^\infty(\Omega)$:

$$G=\left\{ \rho\in L^\infty(\Omega) \;\middle|\; \int_\Omega \rho \;\mathrm{d}\Omega\le V,\;\; 0\le\rho_{\min}\le\rho\le\rho_{\max}<\infty \right\}$$

It is convenient for the analysis and crucial for the computational procedure to identify in (3.5) three coupled optimization sub problems, which we label here the *local anisotropy*, *equilibrium*, and *material distribution* optimization problems. This is quite analogous to the development described in chapter 2.

Local anisotropy problem. For fixed displacements $u^k\in U$ and resource $\rho\in G$ maximize the weighted average strain energy density over all load cases, i.e.,

$$\overline{W}(\rho,\boldsymbol{u})=\max_{\substack{E\ge 0 \\ \Psi(E)\le\rho}} \left\{ W(E,\boldsymbol{u})=\tfrac{1}{2}\sum_{k=1}^{M} w^k E_{ijpq}(x)\varepsilon_{ij}(u^k)\varepsilon_{pq}(u^k) \right\} \tag{3.6}$$

In the local anisotropy optimization problem the goal is to determine the optimum material distribution given a fixed amount ρ of resource and M independent strain fields $\varepsilon(u^k)$.

This problem corresponds to finding the pointwise strongest material for a set of given strain fields (displacement fields) and a given distribution of 'density' - as discussed earlier, this is the standard problem setting in the theory of variational bounds on effective moduli of anisotropic materials. This signifies that we as a result of our design study as a by-product will identify the 'strongest' materials, among all elastic materials with a certain invariant fixed (here the trace and the 2-norm, respectively).

Equilibrium problem. The equilibrium problem of the structural optimization problem reads

$$\Phi(\rho) = \min_{\substack{u=\{u^1,\ldots,u^M\} \\ u^k \in U,\ k=1,\ldots,M}} \left\{ \int_\Omega \overline{W}(\rho,\boldsymbol{u}) \mathrm{d}\Omega - l(\boldsymbol{u}) \right\}$$

The equilibrium problem seeks kinematically admissible equilibrium displacements for the locally optimum energy functional, for a given distribution of resource ρ.

It should be noted that, since the locally optimum energy $\overline{W}(\rho,\boldsymbol{u})$ depends on the displacement fields $\{u^k\}$ in a complex fashion via (3.6), this equilibrium problem is in fact a constitutively non-linear, non-smooth elasticity problem, except in very special cases. Furthermore, in general, $\overline{W}(\rho,\boldsymbol{u})$ is not a separable function of the u^k's.

Material distribution problem. The local anisotropy and equilibrium problems are solved for a fixed but arbitrary spatial distribution of the resource function ρ. The optimum material distribution problem seeks the resource distribution that minimizes the average mean compliance. It is simply stated as follows:

$$\min_{\rho \in G} \quad \Phi(\rho)$$

3.2 Locally extremal materials

3.2.1 The solution to the optimum local anisotropy problems

In this section we study the solution to the local anisotropy optimization problem

$$\max_{\substack{E \geq 0 \\ \Psi(E) \leq \rho}} \quad W(E, \boldsymbol{u}) \tag{3.6}$$

with $W(E,\boldsymbol{u}) = ½ \sum_{k=1}^{M} w^k E_{ijpq}(x) \varepsilon_{ij}(u^k) \varepsilon_{pq}(u^k)$

We now define the positive semi-definite, symmetric 4-tensor A as

$$A_{ijpq} = \sum_{k=1}^{M} w^k A^k_{ijpq} \ , \quad A^k_{ijpq} = \varepsilon_{ij}(u^k) \varepsilon_{pq}(u^k)$$

and write (3.6) as

$$\max_{\substack{\max \\ E\geq 0 \\ \Psi(E)\leq\rho}} \tfrac{1}{2} E_{ijpq} A_{ijpq} \tag{3.7}$$

The Frobenius norm case. For the norm resource measure, problem (3.7) corresponds to finding the tensor E of given norm that has the largest standard inner product with the given tensor A. The optimal rigidity tensor is thus proportional to A and because of the resource constraint it is given as

$$E^B_{ijpq} = \rho \frac{A_{ijpq}}{\sqrt{A_{mnrs} A_{mnrs}}}$$

and the corresponding extremal energy functional is

$$\overline{W}_B(\rho,\boldsymbol{u}) = \rho\, \breve{W}_B(\boldsymbol{u}) = \frac{\rho}{2}\sqrt{A_{ijpq}A_{ijpq}} = \frac{\rho}{2}\sqrt{\sum_{k,l=1}^{M} w^k w^l \left[\varepsilon_{ij}(u^k)\varepsilon_{ij}(u^l)\right]^2}$$

We have denoted by $\breve{W}$ the optimum energy density function per unit amount of resource ρ . Here and elsewhere we embellish with an upper inverted "hat" ($\breve{W}$) quantities per unit amount of resource.

Note that the optimized material properties represented by E^B_{ijpq} do not possess any specific symmetry properties and the material is thus generally anisotropic for all but very special cases. The optimized material tensor can have zero eigenvalues, and this happens always if the number of load cases that we consider is one or two in dimension 2 or one to five in dimension 3. For more than this number of load cases, the material will generically be stable, with zero eigenvalues only appearing if the strain fields are linearly dependent.

The trace case. For the trace resource measure, problem (3.7) corresponds to solving a linear programming problem, with objective given by the tensor A. In order to find the solution to this problem, introduce the spectral decompositions of E and A. Now let $0 \leq \eta_1 \leq \ldots \leq \eta_N, \sum_{i=1}^{N} \eta_i = \rho$, and $0 \leq \lambda_1 \leq \ldots \leq \lambda_N$ be the ordered eigenvalues of E and A, respectively ($N=3$ in dimension 2 and $N=6$ in dimension 3). From a result on the eigenvalues of positive symmetric matrices (Mirsky, 1959), it follows that

$$E_{ijpq} A_{ijpq} \leq \sum_{i=1}^{N} \eta_i \lambda_i \leq \sum_{i=1}^{N} \eta_i \overline{\lambda} = \rho \overline{\lambda}$$

where $\overline{\lambda}$ denotes the largest eigenvalue of the tensor A, with orthonormal eigentensors $\varepsilon^{\alpha}_{ij}$, $\alpha = 1,..,P$. We observe that the right hand side of these inequalities is achieved by any rigidity tensor E of the form

$$E^A_{ijpq} = \rho \sum_{\alpha=1}^{P} \mu^\alpha \varepsilon^\alpha_{ij} \varepsilon^\alpha_{pq} \text{ , with } \sum_{\alpha=1}^{P} \mu^\alpha = 1$$

so we conclude that the optimal energy in the trace case is

$$\overline{W}_A(\rho,\boldsymbol{u}) = \rho\, \breve{W}_A(\boldsymbol{u}) = \frac{\rho}{2}\overline{\lambda} = \frac{\rho}{2} \cdot \max \operatorname{eig}\left\{ \sum_{k=1}^{M} w^k \varepsilon_{ij}(u^k)\varepsilon_{pq}(u^k) \right\}$$

Note that using only one of the eigenvectors associated with the eigenvalue $\overline{\lambda}$ it is possible to choose an optimal E^A that represents an orthotropic material. Clearly, if $\overline{\lambda}$ *is* a simple eigenvalue, E^A is unique and it corresponds to an orthotropic material. However, these orthotropic materials will have only one non-zero eigenvalue, thus being highly singular.

3.2.2 The single load case

For the case of a single load case (M=1), the optimal energy in the trace and norm case reduce to the same expression, namely

$$\begin{aligned} \overline{W}_1(\rho,u^1) &= \rho\, \breve{W}_1(u^1) = \tfrac{1}{2}\rho\, \varepsilon_{ij}(u^1)\varepsilon_{ij}(u^1) \\ &= \tfrac{1}{2}\rho\, E^0_{ijkl}\, \varepsilon_{ij}(u^1)\varepsilon_{kl}(u^1) \equiv W_0(\rho,u^1) = \rho \breve{W}_0(u^1) \end{aligned}$$

corresponding the energy of an isotropic, zero-Poisson-ratio material, with rigidity tensor ρE^0, which is ρ times the identity tensor. This matrix has norm $\Psi_B(\rho E^0) = \sqrt{N}\ \rho$ and trace $\Psi_A(\rho E^0) = N\rho$ ($N = 3$ in dimension 2 and $N = 6$ in dimension 3). Note however, that the bound $\overline{W}_0$ is achieved with the tensor

$$E^*_{ijkl} = E^A_{ijkl} = E^B_{ijkl} = \rho\ \frac{\varepsilon_{ij}(u^1)\varepsilon_{kl}(u^1)}{\varepsilon_{pq}(u^1)\varepsilon_{pq}(u^1)}$$

which has norm as well as trace equal to ρ. The optimized material represented by E^* is orthotropic, with axes of orthotropy given by the axes of principal strains (and stresses) for the field $\varepsilon_{ij}(u^1)$, in analogy to the results on optimal rotations of orthotropic materials as described in section 1.2.1.

For completeness of presentation, we write for dimension 2 the resulting optimal rigidities in terms of and in the frame of the principal strains ε_I, ε_{II} of the single strain field $\varepsilon_{ij}(v^1)$ (for convenience we have dropped the index "1" for this load case):

$$\left(E^*\right)_{\text{matrix}} = \frac{\rho}{\varepsilon_I^2 + \varepsilon_{II}^2}\begin{pmatrix} \varepsilon_I^2 & \varepsilon_I\varepsilon_{II} & 0 \\ \varepsilon_I\varepsilon_{II} & \varepsilon_{II}^2 & 0 \\ 0 & 0 & 0 \end{pmatrix}$$

Note again that the optimized material is indeed orthotropic, and that the material rigidity tensor has two zero eigenvalues. Thus, the extremization of the strain energy density results in a material which is at the utmost limit of feasibility for satisfying the positivity constraint, and the material can only carry strain fields which are direct scalings of the given strain field for which the optimization was undertaken. This underlines the true optimal nature of the material. Such behaviour of extremized materials was also seen in the homogenization method for topology design with one given material, as described in section 2.2. In dimension 2 and for a single load condition (as here) the optimized material has only one zero eigenvalue corresponding to vanishing shear stiffness. The restriction used in the homogenization approach that the composite material should be constructed from some specified elastic material is a penalty that is thus evident in the form of the optimized strain energy.

For the single load problem we can solve problem (3.6) by a slightly different argument. For a single load problem we have to find the maximum of the term $E_{ijkl}\varepsilon_{kl}\varepsilon_{ij}$. That is, we have to find a semi-definite inner product of fixed trace or Frobenius norm which maximizes the length of the given tensor ε_{ij}. We have that $E_{ijkl}\varepsilon_{kl}\varepsilon_{ij} = (E_{ijkl}\varepsilon_{kl})\,\varepsilon_{ij}$ (an inner product of 2-tensors) is maximal if $E_{ijkl}\varepsilon_{kl}$ is proportional to ε_{ij}, i.e. if ε is an eigentensor for the rigidity tensor E . Moreover, in view of the cost constraint (fixed sum of eigenvalues or the squares of eigenvalues) and from the requirement that E is positive semi-definite, it follows that ε is the only eigentensor for the optimal E with non-zero eigenvalue. This eigenvalue must be equal to ρ for both resource constraints. Thus, the strain energy density for the optimal material has the general expression $\overline{W}(u) = \frac{1}{2}\,\rho\,\varepsilon_{ij}(u)\,\varepsilon_{ij}(u)$ as seen earlier.

The short development above gives the optimized energy but not directly the expressions for the rigidity tensor in the Cartesian tensor basis. For this, we write (in dimension 3) ε in terms of the principal strains $\hat{\varepsilon}_K$, $K = 1,2,3$. In the frame of reference given by the principal strains, the stiffness tensor is written in matrix form as:

$$E = X^T \begin{pmatrix} \mathrm{T}_{3\times3} & 0_{3\times3} \\ 0_{3\times3} & 0_{3\times3} \end{pmatrix} X, \quad \text{with } \mathrm{T} = \begin{pmatrix} \rho & 0 & 0 \\ 0 & 0 & 0 \\ 0 & 0 & 0 \end{pmatrix}$$

where X is an orthogonal transformation from the Cartesian tensor basis to an orthonormal basis of tensors where the first basis tensor is ε. Using the notation

$\hat{\varepsilon} = (\hat{\varepsilon}_I \, , \hat{\varepsilon}_{II}, \hat{\varepsilon}_{III})$, $\|\hat{\varepsilon}\|^2 = \hat{\varepsilon}_I^{\,2} + \hat{\varepsilon}_{II}^{\,2} + \hat{\varepsilon}_{III}^{\,2}$ the resulting rigidity matrix is, as we have already seen

$$E = \begin{pmatrix} E_{3\times3} & 0_{3\times3} \\ 0_{3\times3} & 0_{3\times3} \end{pmatrix} \quad \text{with} \quad E_{3\times3} = \frac{\rho}{\|\hat{\varepsilon}\|^2} \, \hat{\varepsilon} \, \hat{\varepsilon}^T$$

Also, the specific cost function ρ at the optimum can be expressed as $\rho = E_{iiii}$ for both case A and case B.

Note that for the single load case, we have for both resource measures obtained the reduced equivalent problem statement (3.5) in the form

$$\max_{\substack{\text{density } \rho \\ 0 \le \rho_{\min} \le \rho \le \rho_{\max} \\ \int_\Omega \rho \, d\Omega \le V}} \quad \min_{v \in U} \left\{ \tfrac{1}{2} \int_\Omega \rho \, \varepsilon_{ij}(v) \, \varepsilon_{ij}(v) \, d\Omega - l(v) \right\}$$

which not only gives the optimal distribution of material, but also the displacements, strains, stresses and material properties of the optimal structure.

For this problem we can return to the original form of the minimum compliance problem as stated in (1.2), section 1.1.1, taking the development 'full circle'

$$\begin{aligned} &\min_{u,\rho} \, l(u) \\ &\text{subject to:} \\ &\int_\Omega \rho \, \varepsilon_{ij}(u) \, \varepsilon_{ij}(v) \, d\Omega = l(v) \quad \text{for all } v \in U \\ &0 \le \rho_{\min} \le \rho \le \rho_{\max} \, , \ \int_\Omega \rho \, d\Omega \le V \end{aligned}$$

The reduced problem is exactly equivalent to the variable-thickness design problem for a sheet made of an isotropic zero-Poisson-ratio material, with the density ρ playing the role of the thickness of the sheet. This problem was discussed in detail in section 1.5.1, where also the existence of optimal solutions was proved by a fairly straightforward development. Moreover, a finite element discretization of the variable thickness sheet design problems is of the same form as the equivalent problem for trusses and thus a numerical optimization can make use of the very efficient optimization algorithms devised for truss topology problems. Such algorithms will be discussed in chapter 4.

Let us briefly for the single load case consider the stress based formulation (1.3) for the design parametrization used here. This problem can be stated as

$$\inf_{\substack{E > 0 \\ \int_\Omega \Psi(E) \, d\Omega \le V}} \quad \min_{\substack{\operatorname{div}\sigma + p = 0 \text{ in } \Omega \\ \sigma \cdot n = t \text{ on } \Gamma_T}} \left\{ \tfrac{1}{2} \int_\Omega E^{-1}_{ijkl} \, \sigma_{ij} \sigma_{kl} \, d\Omega \right\} \tag{3.8}$$

where we take the infimum with respect to all *positive definite* rigidity tensors, in order to give meaning to $E^{-1}_{ijkl}\sigma_{ij}\sigma_{kl}$. Interchanging the equilibrium minimization with the local minimization of complementary energy (cf. section 2.1.1) and using that we from a spectral decomposition can derive that

$$\inf_{E>0,\Psi(E)=\rho} E^{-1}_{ijkl}\sigma_{ij}\sigma_{kl} = \frac{1}{\rho}\sigma_{ij}\sigma_{ij}$$

for both of our resource measures, we see that the stress based case has a reduced formulation

$$\inf_{\substack{\text{density } \rho \\ 0<\rho\le\rho_{\max} \\ \int_\Omega \rho \, d\Omega \le V}} \min_{\substack{\operatorname{div}\sigma+p=0 \text{ in } \Omega \\ \sigma\cdot n=t \text{ on } \Gamma_T}} \left\{ \tfrac{1}{2}\int_\Omega \frac{1}{\rho}\sigma_{ij}\sigma_{kl} \, d\Omega \right\}$$

as expected in light of the form of the displacements based formulation above.

3.2.3 Comparison bounds for the case of multiple loads

The simplicity of the single load case described above can be exploited to obtain similarly tractable comparison problems even for the case of multiple loads.

For the upper bound we note that

$$\begin{aligned}
\max_{\substack{E\ge0 \\ \Psi(E)\le\rho}} \tfrac{1}{2}E_{ijpq}A_{ijpq} &= \max_{\substack{E\ge0 \\ \Psi(E)\le\rho}} \tfrac{1}{2}\sum_{k=1}^{M} w^k E_{ijpq}A^k_{ijpq} \\
&\le \sum_{k=1}^{M} w^k \max_{\substack{E\ge0 \\ \Psi(E)\le\rho}} \tfrac{1}{2}E_{ijpq}A^k_{ijpq} = \sum_{k=1}^{M} w^k (\tfrac{1}{2}\rho E^0_{ijpq}A^k_{ijpq}) \\
&= \sum_{k=1}^{M} w^k \left(\tfrac{1}{2}\rho\varepsilon_{ij}(u^k)\varepsilon_{ij}(u^k)\right) = W_0(\rho,\boldsymbol{u}) = \rho\breve{W}_0(\boldsymbol{u})
\end{aligned}$$

where $W_0(\rho,\boldsymbol{u})$ corresponds to the weighted average of the strain energies in a structure made of an isotropic, zero-Poisson-ratio material with rigidity tensor ρE^0. As noted above, this is not in the set of feasible tensors (its 2-norm is $\sqrt{N}\,\rho$ and its trace is $N\rho$) and it is easy to see that the bound cannot be achieved. To obtain a lower bound, note that the rigidity tensor $\frac{1}{\sqrt{N}}\rho E^0$ has 2-norm equal to ρ, and that the rigidity tensor $\frac{1}{N}\rho E^0$ has trace equal to ρ. This, together with the bound shown above, implies that we for our cost measures have the bounds:

$$\frac{1}{N} W_0(\rho,\boldsymbol{u}) \le \overline{W}_A(\rho,\boldsymbol{u}) \le W_0(\rho,\boldsymbol{u}) \quad \text{and} \quad \frac{1}{\sqrt{N}} W_0(\rho,\boldsymbol{u}) \le \overline{W}_B(\rho,\boldsymbol{u}) \le W_0(\rho,\boldsymbol{u})$$

Thus we have a fairly tight upper and lower bound given in terms of the weighted average $W_0(\rho,\boldsymbol{u})$ of the strain energies for an isotropic, zero-Poisson-ratio material. We shall see later that using $W_0(\rho,\boldsymbol{u})$ we can build a 'reference' problem that is easy to solve and provides useful bounds on the solution of the original full optimization problem.

3.2.4 Construction of the extremal material parameters

In the context of the design problem setting above it is of course very interesting to know if the predicted extremal materials can be constructed, and for the problem (3.2) to make sense we should in principle seek a construction of materials with any positive semi-definite rigidity tensor. This question has been answered in the affirmative in recent research (Milton and Cherkaev, 1993 and Sigmund, 1994a, 1994b). In Milton and Cherkaev, 1993, layered materials constructed from an infinitely strong phase and an infinitely weak phase is used to construct any rigidity tensor, while Sigmund, 1994a, 1994b, treats the problem numerically as an inverse homogenization problem of generating the topology of a unit cell of a periodic medium.

Consider now a given positive semi-definite rigidity tensor E and consider the problem of finding the minimum weight truss or continuum topology for a unit cell Y in a periodic medium which as homogenized coefficients have precisely the rigidity E . This is an optimal design problem of generating an optimal topology for materials used in topology design, making the dog bite its tail.

Using standard notation for homogenization, as described in chapter 1, the material design problem can be written as a topology design problem for a unit cell. Denoting, as there, the pre-stretching of the cell (in dimension 2) by the fields $y^{11}=(y_1,0)$, $y^{12}=(y_2,0)$, $y^{21}=(0,y_1)$ and $y^{22}=(0,y_2)$, and the mean strain energy of the cell by the energy bilinear form $a_Y(u,v)=\int_Y D_{ijkl}(y)\varepsilon_{ij}(u)\varepsilon_{kl}(v)\mathrm{d}Y$,

we write the material design problem as

$$\min_{D\in \mathrm{E}_{ad},\ \chi^{ij}} \{\text{Volume of cell } Y\}$$

subject to :

$$\left.\begin{array}{l} E^{\mathbf{H}}_{ijkl} \equiv \dfrac{1}{|Y|} a_Y(y^{ij}-\chi^{ij}, y^{kl}-\chi^{kl}) = E^{\text{given}}_{ijkl} \\ \chi^{ij}\in U_{Y\text{-periodic}},\ \ a_Y(y^{ij}-\chi^{ij},\ \varphi)=0 \ \text{ for all } \varphi\in U_{Y\text{-periodic}} \end{array}\right\} i,j,k,l=1,2(,3) \qquad (3.9)$$

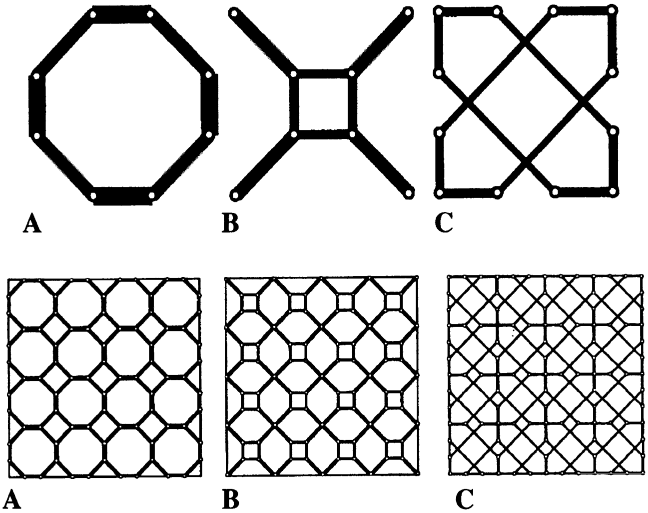

$$\left(E^*\right)_{\mathrm{matrix}} = \begin{pmatrix} 1 & 1 & 0 \\ 1 & 1 & 0 \\ 0 & 0 & 0 \end{pmatrix}$$

Fig. 3.1. Minimum weight 2-D microstructures (upper row shows the unit cells, lower row an assemblage of cells) for obtaining materials with the indicated rigidity in the axis of the cell, corresponding the optimal material for a single strain field $\varepsilon = (1,1,0)$. This is an isotropic material with Poisson's ratio 1.0. The three designs all have the same weight and are obtained using a 4 by 4 equidistant nodal lay-out in a square cell. All 120 possible connections between the nodal points are considered as potential members. Members not shown for the optimum cell (and structure) are at the minimum gauge which is 10^5 times smaller than the maximum gauge. The different designs are obtained by penalization of the lengths of the bars. By courtesy of Ole Sigmund.

Problem (3.9) can be interpreted as a topology design problem in the form studied in chapter 1. Notice that the condition on the homogenized coefficients in (3.9) is an (strain) energy criterion, making (3.9) equivalent to a multiple load minimum compliance problem. Here, however, the volume of material is to be minimized under conditions of specified compliance, for a number of independent load cases (in the form of pre-strains). In Sigmund, 1994a, the continuum problem is solved for the 2-D case by parametrizing the design of the cell as a variable thickness sheet.

In order to achieve the extremal materials described above for the free material design, it is natural to consider (3.9) for 'thin' structures, which may exhibit mechanism type behaviour, for example truss structures. To this end, the continuum problem for the 'thin' structure is discretized using 2-node truss elements. Also, the combined fields $(y^{ij} - \chi^{ij})$ are used as the basic state variables. This approach means that we are thinking of the problem in the setting of the so-called ground structure approach to topology design of trusses, in which

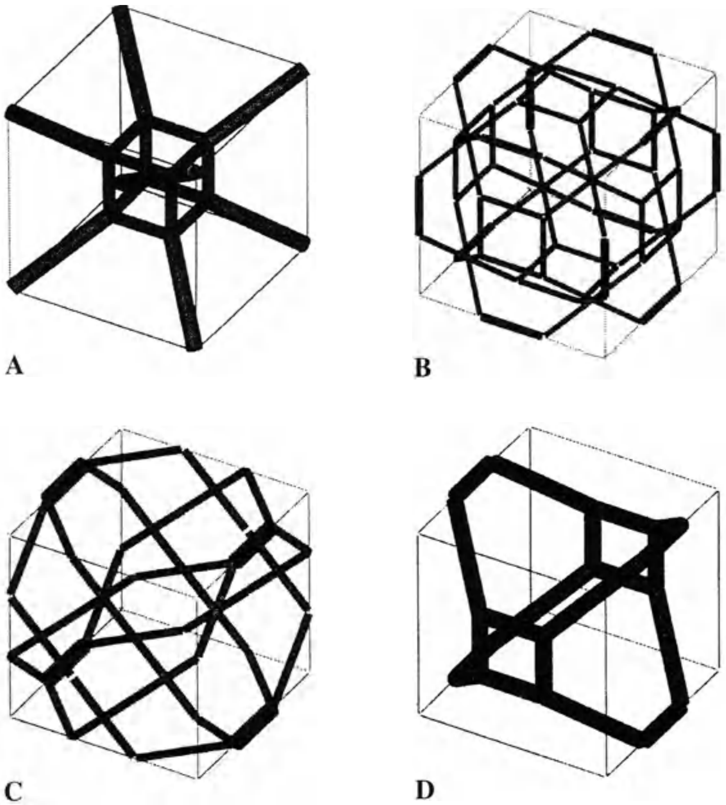

$$\left(E^{*}\right)_{\text{matrix}} = \begin{pmatrix} 1 & 1 & 1 & 0 & 0 & 0 \\ 1 & 1 & 1 & 0 & 0 & 0 \\ 1 & 1 & 1 & 0 & 0 & 0 \\ 0 & 0 & 0 & 0 & 0 & 0 \\ 0 & 0 & 0 & 0 & 0 & 0 \\ 0 & 0 & 0 & 0 & 0 & 0 \end{pmatrix}$$

Fig. 3.2. Minimum weight microstructures in dimension 3 for obtaining materials which corresponds to the optimal material for a single strain field $\varepsilon = (1,1,1,0,0,0)$. The three designs all have the same weight and are obtained using a 4 by 4 by 4 equidistant nodal lay-out in a cubic cell. All 2016 possible connection between the nodal points are considered as potential members. Members not shown for the optimum cell (and structure) are at the minimum gauge. The different designs are obtained by penalization of members with certain lengths. The topologies in *(A)* and *(B)* have full cubic symmetry. The topology in *(C)* have bars on the surface of the cell only and is not cubic symmetric, even though the effective parameters are isotropic. Notice the similarity between the 3-D microstructures and the 2-D microstructures shown in figure 3.1. By courtesy of Ole Sigmund.

one seeks the minimum weight trusses among all trusses that consist of certain connections between a lay-out of chosen nodal points (see chapter 4). For the homogenization formulas to make sense no bars can vanish in the ground structure, but they can be made infinitely thin; this is of course consistent with the use of a optimality criteria optimization algorithm where such an constraint is necessarily enforced. We should mention here that the use of truss models in the homogenization studies for thin structures can be formalized on the basis of asymptotic studies and rigorous convergence analysis [25]. The material design problem for the truss case can be formulated as

$$\min_{t_i \geq t_{\min},\, i=,..,m;\ [u^{ij}]} \quad \sum_{i=1}^{m} t_i$$

$$\text{subject to:} \qquad \left.\begin{array}{l} E^{\mathbf{H}}_{ijkl} \equiv \left[u^{ij}\right]^T \mathbf{K}(t)\left[u^{kl}\right] = E^{\text{given}}_{ijkl} \\ \left[u^{ij} - y^{ij}\right] \text{ is } Y\text{-periodic} \\ [\varphi]^T \mathbf{K}(t)\ \left[u^{kl}\right] = 0, \ \forall\ [\varphi]_{Y\text{-periodic}} \end{array}\right\} i,j,k,l = 1,2(,3) \tag{3.10}$$

in terms of bar volumes t_i. In (3.10), $[u]$ is the nodal displacement vector and $\mathbf{K}(t) = \sum_{i=1}^{m} t_i \mathbf{K}_i$ is the stiffness matrix, written as a sum of (global) element stiffness matrices.

The numerical results by Sigmund, 1994a, 1994b, implies that any positive semi-definite rigidity tensor can be generated using 'thin' structures. In particular, it is seen that the possibility of mechanism like behaviour of such structures means that the extremal materials described above can indeed be constructed. In figures 3.1 and 3.2 we show some example materials.

3.3 Analysis of the reduced problems

3.3.1 The equilibrium problem for the optimized energy

The solution to the local anisotropy problems has shown that the equilibrium problem with the optimized strain energy functions for both cases we consider can be written as

$$\min_{\substack{\boldsymbol{u}=\{u^1,\ldots,u^M\} \\ u^k \in U,\ k=1,\ldots,M}} \left\{ \int_\Omega \rho \breve{W}(\boldsymbol{u})\, d\Omega - l(\boldsymbol{u}) \right\} \tag{3.11}$$

This is a coupled, non-linear problem for all the load cases at once, the coupling arising through the optimized strain energy functional.

We note here that the function $\breve{W}(u^1,...,u^M)$ of the displacements is homogeneous of degree two, that is, under proportional loading the optimized material behaves as a linearly elastic material. Moreover, $\breve{W}$ is a convex function. This follows from the fact that $\breve{W}$ is given as a maximization of convex functions of the displacements.

For the Frobenius norm resource measure, we note that $\breve{W}_B$ is a smooth function, except at the origin $(u^1,...,u^M)=(0,....,0)$ when all displacements are zero. For the trace resource measure the optimized strain energy functional involves an eigenvalue problem, which implies that the functional $\breve{W}_A$ is only differentiable at sets of displacements for which the maximal eigenvalue of the tensor A is not repeated, and it is non-differentiable at displacements for which the maximal eigenvalue is multiple. This includes the origin $(u^1,...,u^M)=(0,....,0)$ where all displacements are zero.

The Hessian (tangent stiffness matrix) for the strain energy $\breve{W}(u^1,...,u^M)$ is (where it is defined) of the block form

$$\mathbf{H}^* = \begin{pmatrix} \mathbf{H}_{11} & \cdots & \mathbf{H}_{1M} \\ \vdots & & \vdots \\ \mathbf{H}_{M1} & \cdots & \mathbf{H}_{MM} \end{pmatrix}$$

where all the blocks are non-zero almost everywhere. This underlines the coupling between the displacements for the different loads present in problem (3.11). For comparison, we note that for the quadratic bounding energy functional $W_0(\rho,\boldsymbol{u})$ defined above for the zero-Poisson-ratio material, the tangent stiffness matrix is the block diagonal matrix

$$\mathbf{H}_0 = \begin{pmatrix} \rho\mathbf{D}_0 & \cdots & \mathbf{0} \\ \vdots & \ddots & \vdots \\ \mathbf{0} & \cdots & \rho\mathbf{D}_0 \end{pmatrix}$$

where $\mathbf{D}_0$ is the identity matrix. This implies that problem (3.11) with this energy functional decouples into M uncoupled, linear equilibrium problems, one for each load case. Finally remark that for the single load case, the equilibrium problem (3.11) is just a single linear equilibrium problem for a structure made of a zero-Poisson-ratio material with varying Young moduli, as described through the variable ρ.

3.3.2 The optimization problem in resource density

The reduced optimization problem is as described earlier

$$\max_{\substack{\text{density } \rho \\ 0 \le \rho_{\min} \le \rho \le \rho_{\max} \\ \int_\Omega \rho \, d\Omega \le V}} \left[\Phi(\rho) = \min_{\substack{u=\{u^1,\ldots,u^M\} \\ u^k \in U,\ k=1,\ldots,M}} \left\{ \int_\Omega \rho \breve{W}(\boldsymbol{u}) \mathrm{d}\Omega - l(\boldsymbol{u}) \right\} \right] \tag{3.12}$$

This is of the form of a variable thickness sheet problem for a sheet made of a non-linear elastic material. Here the function $\Phi(\rho)$ of the density distribution ρ is defined through the non-linear equilibrium problem discussed in the previous section. Since $\Phi(\rho)$ is given as a minimization of concave (linear) functions in ρ , $\Phi(\rho)$ is in itself concave. Thus (3.12) is a convex minimization problem in the density variable ρ . The condition of optimality for ρ is

$$\begin{gathered} \breve{W}(u^1,\ldots,u^M) = \Lambda - \gamma_- + \gamma_+ \\ \gamma_- \ge 0, \quad \gamma_- \rho_{\min} = 0 \\ \gamma_+ \ge 0, \quad \gamma_+ \rho_{\max} = 0 \end{gathered}$$

where Λ ,γ_-,γ_+ are Lagrange multipliers for the resource constraint and the lower and upper bound on ρ , respectively, and where $(u^1,\ldots,u^M)$ is the solution to the equilibrium problem.

The reduced problem (3.12) is also a saddle point problem in the resource density ρ and displacements { u^k }. As shown in section 1.5.1, the existence of a saddle point is assured and we can thus find an optimal solution of the optimization problem (3.12) by solving:

$$\min_{\substack{u=\{u^1,\ldots,u^M\} \\ u^k \in U,\ k=1,\ldots,M}} \left\{ \hat{W}(\boldsymbol{u}) - l(\boldsymbol{u}) \right\}, \qquad \text{where } \hat{W}(\boldsymbol{u}) = \max_{\substack{\text{density } \rho \\ 0 \le \rho_{\min} \le \rho \le \rho_{\max} \\ \int_\Omega \rho \, d\Omega \le V}} \int_\Omega \rho \breve{W}(\boldsymbol{u}) \mathrm{d}\Omega$$

Using again a Lagrange multiplier Λ for the resource constraint, the globally optimized weighted strain energy functional $\hat{W}(\boldsymbol{u})$ can be expressed as:

$$\hat{W}(\boldsymbol{u}) = \min_{\Lambda \ge 0} \left\{ \int_\Omega \max\left\{ \rho_{\min} \left[\breve{W}(\boldsymbol{u}) - \Lambda \right],\ \rho_{\max} \left[\breve{W}(\boldsymbol{u}) - \Lambda \right] \right\} \mathrm{d}\Omega + \Lambda V \right\} \tag{3.13}$$

This implies that the design variables can be removed entirely from the problem, and the resulting problem becomes a non-linear and non-smooth, convex, analysis-only problem. Note that even the single load case problem has this nature if the design variables are removed entirely from the problem. In this case the final reduced problem is

$$\min_{\substack{\Lambda\geq 0\\ u\in U}} \left\{ \int_\Omega \max\left\{\rho_{\min}\left[\tfrac{1}{2}\varepsilon_{ij}(u)\varepsilon_{ij}(u)-\Lambda\right],\ \rho_{\max}\left[\tfrac{1}{2}\varepsilon_{ij}(u)\varepsilon_{ij}(u)-\Lambda\right]\right\} \mathrm{d}\Omega + \Lambda V - l(u) \right\}$$

3.3.3 An extension to contact problems

It is clear from the analysis above that all steps can be performed without restriction for problems that include design independent, convex displacement constraints in the equilibrium statement. Thus design problems including unilateral contact can be treated by a similar analysis.
Now let Γ_C denote the boundary of potential contact and let $u \cdot n \geq 0$ on Γ_C be the unilateral contact condition; this is a convex constraint. Then the design problem for minimum compliance under multiple loads can be stated as (see also section 4.2.3)

$$\max_{\substack{\text{rigidity } E\geq 0\\ \int_\Omega \Psi(E)d\Omega \leq V}} \ \min_{\substack{u=\{u^1,\ldots,u^M\}\\ u^k\in U,\ u^k\cdot n\geq 0 \text{ on } \Gamma_C}} \left\{ \int_\Omega W(E,\boldsymbol{u})\mathrm{d}\Omega - l\,(\boldsymbol{u}) \right\}$$

where the inner problem is the minimum potential energy principle expressed for a contact problem. For both resource measures this problem can be reduced to the forms seen earlier, the only change being the addition of the contact condition on the admissible displacements. Also, the optimal materials are given by the same expressions.

3.3.4 The problem of a segmented design domain

The problems treated so far in our developments have been characterized by a set of pointwise varying design variables. We will now consider a problem where the material properties are supposed to be fixed in a finite number of *sub-domains* (design segments) of the total design area. Let us now consider the problem of finding the optimal material for each of these sub-domains, as well as the optimal distribution of material between these areas. Studies of segmented design problems can be found in the literature for several distributed problems (Prager, 1974, Taylor, 1987) and the present presentation is strongly inspired by recent work of Cherkaev, 1993d, who used this idea to generate areas of stable microstructures for generalized shape design. Here we use these ideas for the free parametrization of design.

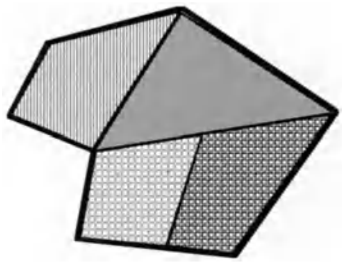

Fig. 3.3. A design domain consisting of four sub-areas, each with the same material in all points

The design domain now consists of a finite number of sub-domains Ω_q, $q = 1,\dots,Q$ such that $\Omega = \bigcup_{q=1}^{Q} \Omega_q$, $\mathrm{int}(\Omega_q) \bigcap \mathrm{int}(\Omega_p) = \varnothing$ for $q \neq p$. In each of these sub-domains we have fixed material properties throughout, so the design parametrization is of the form

$$
\begin{aligned}
&E(x) = E^q \geq 0 \ \text{ for } x \in \Omega_q\,, \ q = 1,..,Q \\
&\int_\Omega \Psi(E)\, \mathrm{d}\Omega = \sum_{q=1}^{Q} \Psi(E^q) \int_{\Omega_q} 1\, \mathrm{d}\Omega \leq V
\end{aligned}
\tag{3.14}
$$

Treating only a single load condition, the minimum compliance problem is then

$$
\max_{\substack{E^q \geq 0,\ q=1,\dots,Q; \\ \sum_{i=1}^{Q} \Psi(E^q)|\Omega_q| \leq V}} \ \min_{u \in U} \left\{ \sum_{q=1}^{Q} (\tfrac{1}{2} E^q_{ijkl} \int_{\Omega_q} \varepsilon_{ij}(u)\varepsilon_{kl}(u)\mathrm{d}\Omega) - l\,(u) \right\}
\tag{3.15}
$$

where we have made use of the segment-wise constant rigidities. Problem (3.15) is in nature quite similar in nature to the multiple load problem (3.2) and is as that problem concave-convex. An interchange of operators results in

$$
\max_{\substack{\text{density } \rho^q,\ q=1,\dots,Q; \\ \sum_{i=1}^{Q} \rho^q |\Omega_q| \leq V}} \ \min_{u \in U} \left\{ (\sum_{q=1}^{Q} \max_{\substack{E^q \geq 0 \\ \Psi(E^q) \leq \rho^q}} \left[\tfrac{1}{2} E^q_{ijkl} A^q_{ijkl} \right]) - l\,(u) \right\}
$$

with

$$
A^q_{ijkl} = \int_{\Omega_q} \varepsilon_{ij}(u)\varepsilon_{kl}(u)\mathrm{d}\Omega, \ q = 1,..,Q
$$

denoting the segment averages of the dyadic products $\varepsilon_{ij}(u)\varepsilon_{kl}(u)$. Here the fact that the rigidities are independent from sub-domain to sub-domain has been utilized to move the maximization with respect to rigidity under the summation sign. Now note that the inner maximization problems

$$\max_{\substack{E^q \geq 0 \\ \Psi(E^q) \leq \rho^q}} \left[\tfrac{1}{2} E^q_{ijkl} A^q_{ijkl} \right], \quad q = 1,..,Q$$

are precisely of the form solved in section 3.2. For the Frobenius norm case the optimal material properties are then given as

$$E^q_{ijkl} = \rho^q A^q_{ijkl} \left(A^q_{mnrs} A^q_{mnrs} \right)^{-\frac{1}{2}}, \quad q = 1,..,Q$$

As the tensor A^q_{ijkl} is the average over the domain Ω_q of the tensor $\varepsilon_{ij}(u)\varepsilon_{kl}(u)$, the optimal materials will typically be non-singular. However, the optimal materials will also typically be anisotropic, with very little likelihood of orthotropy. The main interest of the present analysis is actually the conclusion that we typically can expect stable materials for each sub-region.

Now for convenience, set for all $q = 1,..,Q$

$$\Xi^q(u) = \frac{1}{2\left|\Omega_q\right|} \sqrt{A^q_{ijkl}(u) A^q_{ijkl}(u)},$$

$$t^q = \rho^q \left|\Omega_q\right|, \; t^q_{\min} = \rho_{\min}\left|\Omega_q\right|, \; t^q_{\max} = \rho_{\max}\left|\Omega_q\right|$$

We can then for the Frobenius norm case write reduced problem statements as

$$\max_{\substack{0 \leq t^q_{\min} \leq t^q \leq t^q_{\max} \\ \sum_{i=1}^{Q} t^q \leq V}} \; \min_{u \in U} \left\{ \sum_{q=1}^{Q} t^q \, \Xi^q(u) - l(u) \right\} \tag{3.16}$$

$$\min_{u \in U} \left\{ \sum_{q=1}^{Q} \max\left\{ t^q_{\min}\left[\Xi^q(u) - \Lambda\right], t^q_{\max}\left[\Xi^q(u) - \Lambda\right] \right\} + \Lambda V - l(u) \right\} \tag{3.17}$$

The development of (3.16) and (3.17) seems to have mainly academic interest, as these problems consists of non-smooth and non-linear equilibrium problems which couples all the degrees of freedom in each sub-domain Ω_q (each sub-domain is assumed to consist of many elements in a discretization). This implies that these problems should be very hard to solve computationally. Also, the original problem (3.15) will only have a fair number of design variables if the number of sub-domains is moderate. Thus it is more reasonable to do computations for this problem directly. On the other hand, the conclusion that we typically can expect stable materials for each sub-region may suggest that each sub-region could consist just of a few finite elements, and in that case it may be competitive to consider solving (3.16) along the lines described for the multiple load problem in the coming sections.

3.4 Numerical implementation and examples

The analysis to follow will show that the presence of multiple load cases introduces significant complications in the problem of determining the material configuration that minimizes an average measure of the compliance in a structure. These complications arise because the locally optimal material couples deformations associated with the different load cases in a complex way that, as we have already seen, involves non-linear, non-smooth energy functionals which depend on all the load cases simultaneously. This will stand in sharp contrast with the solution of the problem of design for a single load case, where the energy in the optimal material can be computed through a straight forward linear analysis involving an isotropic, zero-Poisson-ratio material.

3.4.1 Computational procedure for the general case

In this section we discuss a computational procedure for solving problem (3.12) as a design problem for a structure with non-linear elastic behaviour. The solution of (3.12) involves the application of two distinct computational strategies: an optimality criterion based algorithm used to solve the material distribution problem (3.12) and a finite element based non-linear analysis used to solve the equilibrium problem (3.11) for fixed ρ . This separation of analysis and design computations is standard in optimal structural design. As an alternative, the solution of (3.13) requires a restructuring of the finite element analysis procedure, but apart from this difficulty, algorithms developed for truss topology design as described in the coming chapter are directly applicable.

In order to solve problem (3.12) we use a finite element procedure based on a discretization of the domain Ω into m elements Ω_e, each with n_e nodes, for a total of n nodes. For simplicity we use an element-wise constant approximation of ρ. The approximation of the displacement field will not be specified.

With

$$\Phi(\rho_e) = \min_{u^1,..,u^M} \left\{ \sum_{e=1}^{m} \rho_e \breve{W}_e(u_e^1,..,u_e^M) - \sum_{k=1}^{M} p^{k^T} u^k \right\} \quad \text{and} \quad \breve{W}_e(\boldsymbol{u}_e) = \int_{\Omega_e} \breve{W}(\boldsymbol{u}_e) d\Omega$$

the discretized form of the optimization problem (3.12) is (here we invoke $\rho_{\min} > 0$)

$$\max_{\rho_e} \Phi(\rho_e)$$

subject to:

$$\sum_{e=1}^{m} \rho_e V_e = V$$

$$0 < \rho_{\min} \leq \rho_e \leq \rho_{\max} < \infty, \; e = 1,....,m$$

Here V_e is the element area (2D) or volume (3D), p^k represents the equivalent nodal loads for the k-th load, and $\rho_e \breve{W}_e(u_e^1,..,u_e^M)$ is the element strain energy computed using the discrete strains and nodal displacements $\boldsymbol{u}_e = (u_e^1,..,u_e^M)$ of element e.

Solution of the Non-Linear Equilibrium Problem. The energy functionals $\overline{W}$ are *not* pure quadratic functions of the strains. Therefore the solution of the equilibrium problem for fixed ρ requires an iterative scheme such as a Newton method or a secant method. Here we choose to rely on the simplicity of the latter approach since $\overline{W}$ is homogeneous of degree two. However, recent experience has shown that the complicated non-smoothness for the trace resource case prevents the use of this secant method, and solving (3.11) requires the use of techniques from non-smooth optimization for this case. For this reason the developments that follow are for the *norm case only*.

The energy $\overline{W}_B$ couples the M displacement fields. Therefore, in a discretization of n nodes in an n_d-dimensional elasticity problem, at each iteration one must solve a linear system involving a $(n_d \cdot M \cdot n) \times (n_d \cdot M \cdot n)$ stiffness matrix, assembled from $(n_d \cdot M \cdot n_e) \times (n_d \cdot M \cdot n_e)$ element stiffness matrices $\mathbf{K}_e$*. The element stiffnesses $\mathbf{K}_e$* are a discretized version of the Hessian $\mathbf{H}$* of the energy defined in section 3.3.1. One iteration in the solution of the equilibrium problem requires that the full $(n_d \cdot M \cdot n) \times (n_d \cdot M \cdot n)$ system be solved. This is a prohibitive task for a realistic discretization and more than a few load cases, so here a secant method is used where only the diagonal blocks of the element stiffness matrix are retained , i.e., as an approximate element stiffness one employs the matrices

$$\mathbf{K}_e^{\text{approx}} = \begin{pmatrix} \mathbf{K}_{11}^e & \mathbf{0} & \mathbf{0} \\ \mathbf{0} & \ddots & \mathbf{0} \\ \mathbf{0} & \mathbf{0} & \mathbf{K}_{MM}^e \end{pmatrix}$$

This has the effect of uncoupling the individual load cases. Using these block element stiffness matrices at each iteration one has to solve an $(n_d \cdot n) \times (n_d \cdot n)$ linear system for each of the M load cases and thus a significant reduction in computational effort has been achieved. Note that each load case has a different stiffness matrix, as in general $\mathbf{K}_{kk}^e \neq \mathbf{K}_{ll}^e$ if $k \neq l$. This means that each load case requires an independent assembly and factorization of the global stiffness matrix. Also note that the simplification achieved using the block diagonal approximation only uncouples the load cases at each step of the iterative secant method, but the coupling persists between iteration steps, as the values of the entries of the matrices $\mathbf{K}^e_{kk}$ depend on the current values of *all* the strain fields.

To gain a perspective on the effort involved in the solution of this problem it is useful to compare the solution to the equilibrium problem with coupled displacement fields to the solution of the zero-Poisson-ratio material 'reference' problem. For the reference problem we have the energy functional W_0 instead of $\overline{W}_B$, i.e., using the element strain energy functional $\breve{W}_e^0(\boldsymbol{u}_e) = \int_{\Omega_e} \breve{W}_0(\boldsymbol{u}_e) d\Omega$. In this case the computational effort required to solve the equilibrium problem is reduced dramatically since the corresponding stiffness matrix $\mathbf{K}_e$ *is* block-diagonal and the diagonal blocks $\mathbf{K}^e_{kk}$ are the same for all the load cases. As a result, the 'reference' problem requires only one assembly and factorization of the common stiffness matrix. Also, since W_0 is a pure quadratic function, the corresponding equilibrium problem is linear and no iterations are required to obtain equilibrium solutions for fixed ρ.

Solution of the Material Distribution Problem. To complete the solution of the optimization problem we use an optimality criterion method to solve the optimization of material resource ρ. In the k-th iteration step, given ρ^k and the corresponding equilibrium energy $\breve{W}_e^k$, the density is updated according to the the standard updating formula

$$\rho_e^{k+1} = \max\left\{\rho_{\min},\ \min\left\{\left[\frac{1}{\Lambda^k}\breve{W}_e^k\right]^\eta \rho_e^{\,k},\ \rho_{\max}\right\}\right\}$$

with the Lagrange multiplier Λ^k determined by the constraint $\sum_{e=1}^{m} \rho_e^{\,k+1} V_e = V$.

This optimality criterion algorithm is similar to what has been presented earlier, see sections 1.2.2 and 2.1.2. We remark that experience in computations has shown that, as the optimization over the density is in itself an iterative procedure, only a limited number of (secant) equilibrium iterations need to be used for each design update (cf., section 2.3.1). For the examples shown below eight equilibrium iterations were used for each estimate of the density distribution and fewer iterations would most probably suffice in most practical situations.

3.4.2 Computational procedure for the single load case

For the single load case both the trace and Frobenius norm resource measures lead to the same reduced problem of what amounts to a variable thickness sheet problem for a sheet made of a zero-Poisson-ratio material. Since the optimized strain energy W_0 is a pure quadratic function in this case, we can write the discretized problem in the form

$$\begin{aligned}
&\max_{t} \min_{u} \left\{ \frac{1}{2} \sum_{e=1}^{m} t_e u^T \mathbf{K}_e u - p^T u \right\} \\
&\text{subject to:} \\
&0 < t_{\min} \le t_{\min}^e \le t_e \le t_{\max}^e < \infty, \; e = 1, \ldots, m \\
&\sum_{e=1}^{m} t_e = V
\end{aligned}$$

Here $\mathbf{K} = \sum_{e=1}^{m} t_e \mathbf{K}_e$ is the assembled stiffness matrix $t_e = \rho_e V_e$ is the amount of resource in element *e*, and *u, p* are the vectors of nodal displacements and applied nodal forces, respectively. This problem can also be written as

$$\begin{aligned}
&\min_{t,\, u} \; p^T u \\
&\text{subject to:} \\
&\sum_{e=1}^{m} t_e \mathbf{K}_e u = p^T \\
&\sum_{e=1}^{m} t_e = V, \quad 0 < t_{\min} \le t_{\min}^e \le t_e \le t_{\max}^e < \infty, \; e = 1, \ldots, m
\end{aligned}$$

This shows that we in this case have a design problem that shares important features with minimum compliance problems for trusses, the most important property being that all constraints are linear in the design variable *t*. We shall see in the coming chapter that this can be employed to devise other types of very efficient algorithms for such problems.

3.4.3 Examples

We include here a number of different examples of computational results for plane stress problems. Solutions for single load as well as for multiple load problems are included. For the multiple load case we include the following options:

- Alternative 1. Using an isotropic, zero-Poisson-ratio material and solving the multiple load 'reference' problem introduced in the previous sections. While the solution to this problem is *not* a feasible solution of the original problem, it does provide bounds on the optimum compliance, as stated in section 3.2.3.
- Alternative 2. Using the homogenization method with layered materials and solving the multiple load problem as described in chapter 1.

It is remarkable in the multi-load example that the *spatial* distribution of resource is similar in all cases. However, in interpreting these results one must be careful to recognize that the details of how this resource is utilized to determine the *local* anisotropy are different in each case. In the problem discussed in this part, resource is assigned with the most freedom, as each of the entries of the material tensor can be designed independently. In the 'reference' problem, as well as in the solutions based on homogenization modelling, the assignment is limited to mixtures of isotropic materials.

The appearance of checkerboard patterns (as discussed in section 1.3.2) is observed in all solutions, albeit less pronounced in the single load examples. The phenomenon is more acute when the homogenization modelling is used, but it is present even when solving the problem using the material model discussed in this chapter. The methods to control the appearance of checkerboard patterns as described in section 1.3.2 were not applied here.

The similarities observed in computations between the optimal allocation of resource and the solution of the much simpler 'reference' problem can be exploited to simplify computations. The material distribution in the 'reference' problem is a reasonable approximation to the true optimal material distribution. In addition, the 'reference' problem is of particular interest in its own right, since through its solution one can compute with a modest effort upper and lower bounds on the optimum compliance. As a result, through the analysis presented here one gains a broad insight into the characterization of optimal structures under multiple loads. Since the solution presented here is optimal with respect to *any* composite, it provides a lower bound on the average compliance of similar structures built using elements from a more restricted set of materials. Furthermore, as the 'reference' problem provides a lower bound *even* on the compliance of structures built with optimized materials, its solution yields a measure of optimality of any structure subjected to multiple loads against which all design strategies can be measured.

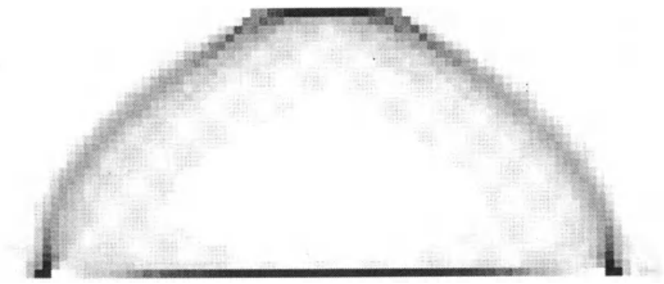

Fig. 3.4. Distribution of resource for the design of a deep beam using optimal materials. The single load, boundary conditions etc. are described in figure 2.6. Bendsøe and Guedes, 1994.

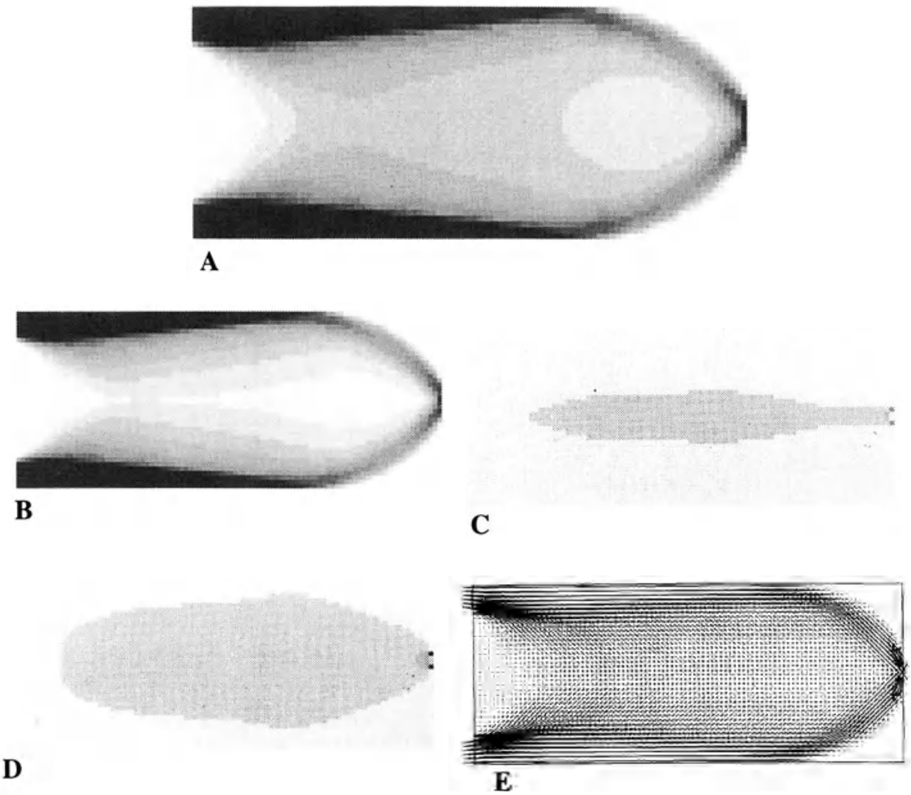

Fig. 3.5. The design of a medium aspect ratio cantilever using optimal materials. Single load case. Vertical load at mid right-hand point, supports at left hand vertical line. *(A)*: Distribution of resource. *(B)*: Distribution of E_{1111}. *(C)*: Distribution of E_{2222}. *(D)*: Distribution of $|E_{1122}|$. *(E)*: Directions and sizes of principal strains; directions correspond to direction of material axes. Compare with figure 1.15, 1.16 and 1.26. Bendsøe and Guedes, 1994.

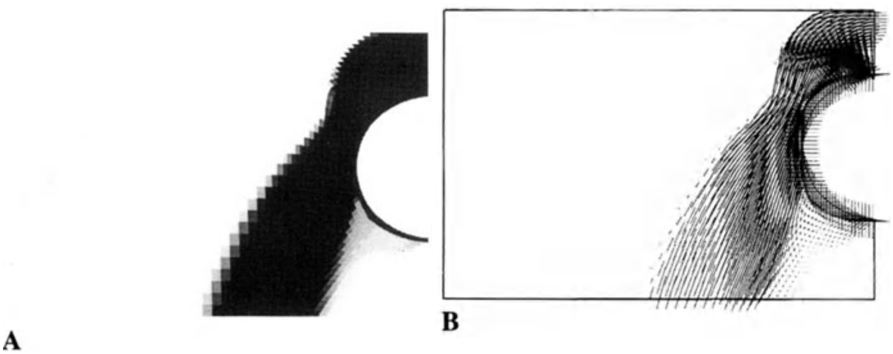

Fig. 3.6. The design of a bearing pedestal using optimal materials. The single load, boundary conditions etc. are described in figure 1.27. *(A)*: Distribution of resource. *(B)*: Directions and sizes of principal strains. Compare with figure 1.27. Bendsøe and Guedes, 1994.

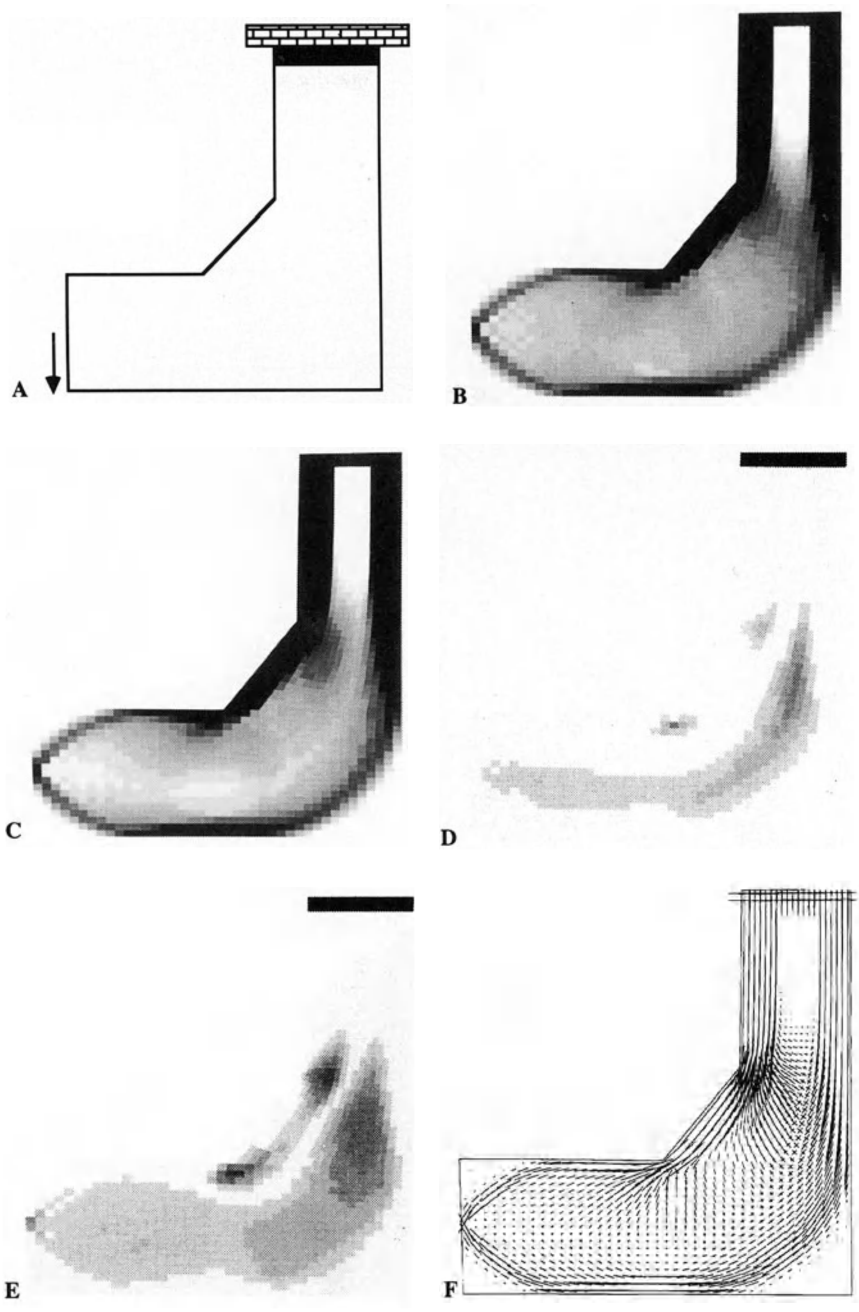

Fig. 3.7. The design of a L-shaped cantilever *(A)* using optimal materials. Single load case. The upper, black part at the support is considered as fixed. *(B)*: Distribution of resource. *(C)*: Distribution of E_{1111}. *(D)*: Distribution of E_{2222}. *(E)*: Distribution of $|E_{1122}|$. *(F)* Directions and sizes of principal strains; directions correspond to direction of material axes. Compare with figure 1.30. Bendsøe and Guedes, 1994.

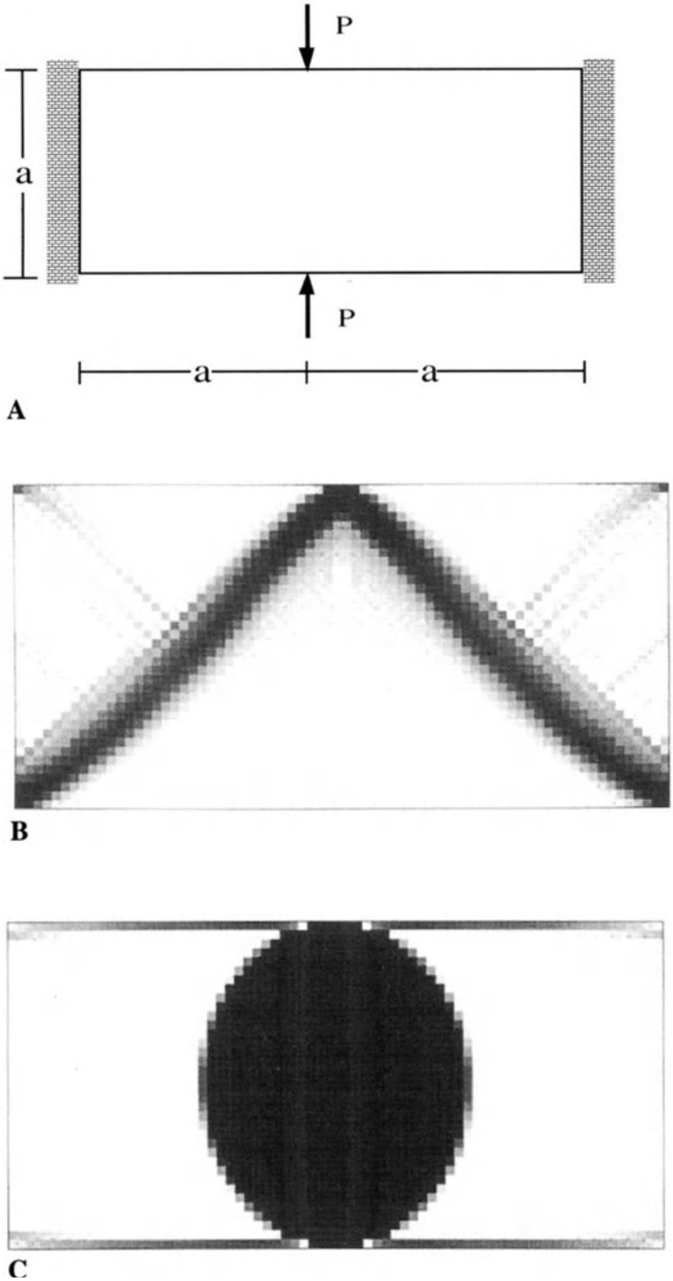

Fig. 3.8a. Design for multiple loads using optimal materials. *(A)*: Geometry and boundary conditions. *(B)*: Distribution of optimal zero-Poisson-ratio material when only upper load is acting. *(C)*: Distribution of optimal zero-Poisson-ratio material when the two loads are treated as acting simultaneously. Bendsøe, Díaz, Lipton and Taylor, 1994.

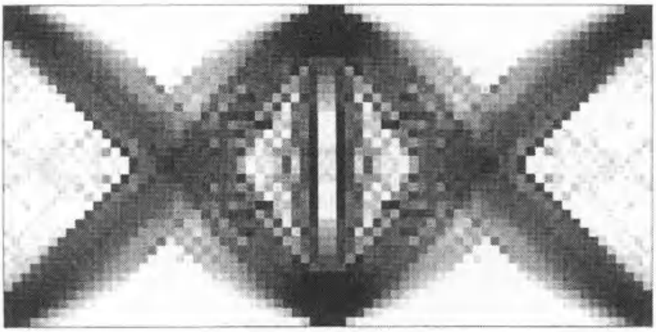

A

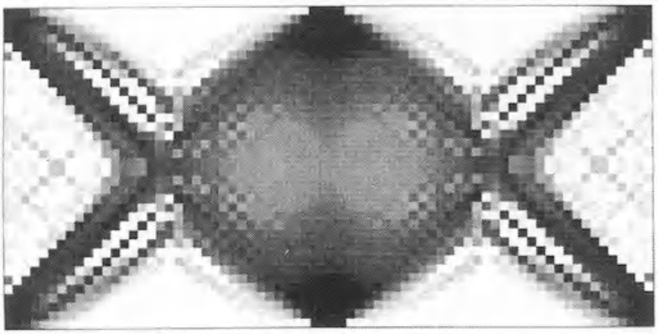

B

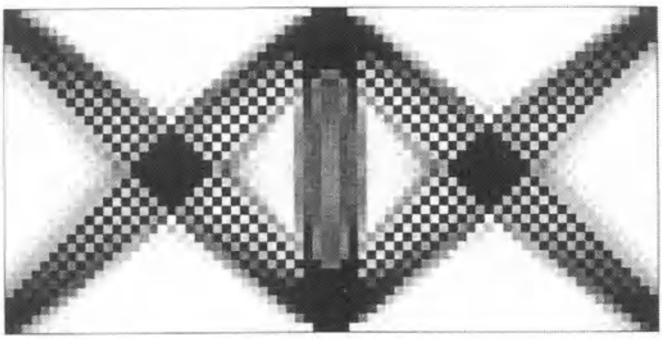

C

Fig. 3.8b. Design for multiple loads using optimal materials. Geometry and boundary conditions as in figure 3.8a. *(A)*: Distribution of optimal material. *(B)*: Distribution of a zero-Poisson-ratio material. *(C)*: Distribution of a rank-2 layered material. Bendsøe, Díaz, Lipton and Taylor, 1994.

4 Topology design of truss structures

Topology optimization of trusses in the form of grid-like continua is a classical subject in structural design. The study of fundamental properties of optimal grid like continua was pioneered by Michell, 1904, but this interesting field has only much later developed into what is now the well-established lay-out theory for frames and flexural systems [3], [8], [16]. The application of numerical methods to discrete truss topology problems and similar structural systems, which is the subject of this chapter, has a shorter history with early contributions in, for example, Dorn, Gomory and Greenberg, 1964 and Fleron, 1964 (see also [26]). The development of computationally efficient methods is not only of great importance for the truss topology problem in itself. It is likewise of interest for solving the reduced problems which arise in the study of simultaneous design of material and structure, as described in chapter 3.

The optimization of the geometry and topology of trusses can conveniently be formulated with the so-called ground structure method. In this approach the lay-out of a truss structure is found by allowing a certain set of connections between a fixed set of nodal points as potential structural or vanishing members. For the truss topology problem the geometry allows for using the continuously varying cross-sectional bar areas as design variables, including the possibility of zero bar areas. This implies that the truss topology problem can be viewed as a standard sizing problem. This sizing reformulation is possible for the simple reason that the truss as a continuum geometrically is described as one dimensional. Thus for both planar and space trusses there are extra dimensions in physical space that can describe the extension of the truss as a true physical element of space, simplifying the basic modelling for truss topology design as compared to topology design of three dimensional continuum structures.

Truss topology design problems were in early work formulated in terms of member forces, ignoring kinematic compatibility to obtain a linear programming problem in member areas and forces. The resulting topology and force field are then often employed as a starting point for a more complicated design problem formulation, with heuristics, branch and bound techniques, etc. being used to link the two model problems [8]. Alternatively, when displacement formulations are used, then (small) non zero lower bounds on the cross-sectional areas have been imposed in order to have a positive definite stiffness matrix. This means that standard techniques for optimal structural design can be used, albeit imposing very tight restrictions on the size of problem that can be handled. Also, it allows for the use of optimality criteria methods for large scale design problems involving compliance, stress, displacement and eigenvalue objectives [26]. In the simultaneous analysis and design approach the design variables and state variables are not distinguished so the full problem is solved by one unified numerical optimization procedure. However, unless specially developed numerical solution procedures are used, only very small problems can be treated [26]. A recent interesting development is the use of simulated annealing and genetic algorithm techniques for the topology problems in their original formulation as discrete selection problems, but also these fairly general approaches are with the present technology restricted to fairly small scale problems [28].

In this chapter we will investigate various formulations of and numerical methods for truss topology design [27]. We seek specifically to be able to handle problems with a large number of potential structural elements, using the ground structure approach. For this reason we consider, as in the continuum setting, the simplest possible optimal design problem, namely the minimization of compliance (maximization of stiffness) for a given total mass of the structure. The analysis is general enough to encompass multiple load problems in the worst-case and weighted-average formulation, the case of self-weight loads and the problem of determining the optimal topology of the reinforcement of a structure as for example seen in fail-safe design. In direct analogy with the continuum setting, these problems can be given in a number of equivalent problem statements, among them problems in the nodal displacements only or in the member forces only. With these reformulations at hand it is possible to devise very efficient algorithms that can handle large scale problems. Also, as we have seen in earlier chapters, the formulations can be obtained through duality principles and the resulting formulations in displacements or stresses correspond to equilibrium problems for an optimally global strain energy and an optimally global complementary energy, respectively.

4.1 Problem formulation for minimum compliance truss design

The ground structure approach allows the truss topology design problem to be viewed as a sizing problem. However, the topology problem is unusual as a structural optimization problem as the number of design variables is typically several magnitudes bigger than the number of state variables describing the equilibrium of the structure. For most structural optimization problems described in the literature the opposite is the case. Also, for truss topology design the stiffness matrix of the full ground structure with certain members at zero gauge can be singular. This implies that most optimal designs have a singular stiffness matrix when described as part of the full ground structure, thus excluding the possibility of invoking standard structural optimization techniques.

4.1.1 The basic problem statements in displacements

In the ground structure approach for truss topology design a set of n chosen nodal points (N degrees of freedom) and m possible connections are given, and one seeks to find the optimal substructure of this structural universe. In some papers on the ground structure approach, the ground structure is always assumed to be the set of all possible connections between the chosen nodal points, but here we allow the ground structure to be any given set of connections (see Fig. 4.1). This approach may lead to designs that are not the best ones for the chosen set of nodal points, but the approach implicitly allows for restrictions on the possible spectrum of possible member lengths (see, e.g. Fig. 4.1B. where only two bar lengths appear) as well as for the study of the optimal subset of members of a given truss-layout.

Let a_i, l_i denote the cross-sectional area and length of bar number i, respectively, and we assume that all bars are made of linear elastic materials, with Young's moduli E_i. The volume of the truss is

$$V = \sum_{i=1}^{m} a_i l_i$$

In order to simplify the notation at a later stage, we introduce the bar volumes $t_i = a_i l_i$, $i = 1,\dots,m$, as the fundamental design variables. Static equilibrium is expressed as

$$\mathbf{B}q = p$$

where q is the member force vector and p is the nodal force vector of the free degrees of freedom. The ground structure is chosen so that the compatibility matrix $\mathbf{B}$ has full rank and so that $m \geq N$, excluding mechanisms and rigid body motions. The stiffness matrix of the truss is written as

$$\mathbf{K}(t) = \sum_{i=1}^{m} t_i \mathbf{K}_i$$

where $t_i\mathbf{K}_i$ is the element stiffness matrix for bar number i, written in global coordinates. Note that $\mathbf{K}_i = \frac{E_i}{l_i^2} b_i b_i^T$ where b_i is the i'th column of $\mathbf{B}$.

The problem of finding the minimum compliance truss for a given volume of material (the stiffest truss) has the well-known formulation (cf., the continuum setting)

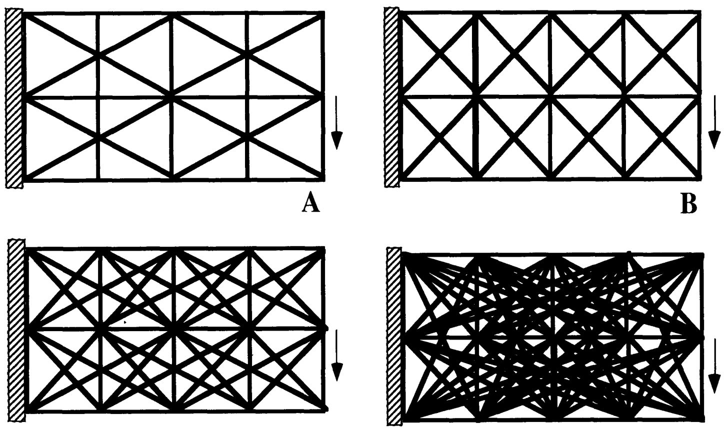

Fig. 4.1. Ground structures for transmitting a vertical force to a vertical line of supports. Truss ground structures of variable complexity in a rectangular domain with a regular 5 by 3 nodal layout. In *(D)* all the connections between the nodal points are included.

$$\begin{aligned} &\min_{u,t} p^T u \\ &\quad \text{subject to :} \\ &\quad \sum_{i=1}^{m} t_i \mathbf{K}_i u = p \\ &\quad \sum_{i=1}^{m} t_i = V, \quad t_i \geq 0, \quad i = 1,\ldots,m \end{aligned} \tag{4.1}$$

Problem (4.1) is well studied in the case of an imposed non-negative lower bound on the volumes t_i [8]. In this case the stiffness matrix $\mathbf{K}(t)$ is positive definite for all feasible t and the displacements can be removed from the problem. The resulting problem in bar volumes turns out to be convex and existence of solutions is assured (Svanberg, 1984). Allowing for zero lower bounds complicates the analysis, but it also provides valuable insight. The zero lower bound on the variables t_i thus means that bars of the ground structure can be removed and the problem statement thus covers topology design. Problem (4.1) can result in an optimal topology that is a mechanism; this mechanism is in equilibrium under the given load, and infinitesimal bars can be added to obtain a stable structure. Also, if the optimal topology has straight bars with inner nodal points, these nodal points should be ignored. The resulting truss maintains the stiffness and the equilibrium of the original optimal topology.

The zero lower bound in problem (4.1) implies that the stiffness matrix is not necessarily positive definite and the state vector u cannot be removed by a standard adjoint method. Removing u from the formulation is not very important for the size of the problem, as, typically, the number m of bars is much greater than the number of degrees of freedom. In the complete ground structure we connect all nodes, having $m = n(n-1)/2$, while the degrees of freedom are only of the order $2n$ or $3n$ (for planar and 3-D trusses). For the complete ground structure we also have a fully populated stiffness matrix lacking any sparsity and bandedness.

Our aim here is to develop methods which can be applied to large scale truss topology problems and for this reason we employ, as in the continuum setting, the simplest possible design formulation as stated in problem (4.1). For more general problem statements involving for example stress and displacement constraints, a suitable formulation is to use a full parametrization of the state of the system in terms of independent fields of member forces, member strains and displacements (an extended simultaneous analysis and design formulation for this case is discussed in Sankaranaryanan, Haftka and Kapania, 1993). Such an approach also allows to incorporate such constraints in a consistent way (Cheng and Jiang, 1992). Local buckling of the individual bars of the ground structure can also be treated in this framework. The formulation of a suitable problem statement that covers global buckling and also caters for the shift of member lengths in the buckling expressions when inner nodes can be removed from the truss has yet to be seen.

The extended problem statements can be solved by a number of methods, all of which presently suffer from the inability to handle general large scale problems. For only a very few active displacement constraints an optimality criteria approach seems to be viable [26]. Use of a conjugate gradient method for a penalized version of the general statement has also been investigated (Sankaranaryanan, Haftka and Kapania, 1993), as has the use of interior penalty methods together with sparse matrix techniques (Ringertz, 1988). For the case of a single load, local stability constraints can be efficiently handled in a force formulation and solved by a modified simplex algorithm, as described in Pedersen, 1993c, d, Smith, 1994.

In the case of *multiple loads*, we formulate also for trusses the problem of minimizing a weighted average of the compliances. For a set of M different load cases p^k, $k = 1,...,M$ and weights w^k, $k = 1,...,M$, the multiple load problem reads

$$\begin{aligned}
&\min_{u,t} \sum_{k=1}^{M} w^k p^{k^T} u^k \\
&\text{subject to :} \\
&\sum_{i=1}^{m} t_i \mathbf{K}_i u^k = p^k, \quad k = 1,......,M \\
&\sum_{i=1}^{m} t_i = V, \quad t_i \geq 0, \quad i = 1,\ldots,m.
\end{aligned} \tag{4.2}$$

Note that in problem (4.2) it is possible to refer each load case to a distinct ground sub-structure, and that it thus is possible to cover *fail-safe design* along the lines described in Taylor, 1987.

Let us introduce an extended displacement vector

$$\hat{u} = (u^1, \dots, u^M)$$

of all the displacement vectors u^k, $k = 1, \dots, M$, an extended force vector

$$\hat{p} = (w^1 p^1, \dots, w^M p^M)$$

of the weighted force vectors $w^k p^k$, $k = 1, \dots, M$, and the extended element stiffness matrices as the block diagonal matrices

$$\hat{\mathbf{K}}_i = \begin{pmatrix} w^1 \mathbf{K}_i & & \\ & \ddots & \\ & & w^M \mathbf{K}_i \end{pmatrix}$$

Then problem (4.2) can be written as

$$\begin{aligned} & \min_{u,t} \hat{p}^T \hat{u} \\ & \quad \text{subject to :} \\ & \quad \sum_{i=1}^{m} t_i \hat{\mathbf{K}}_i \hat{u} = \hat{p} \\ & \quad \sum_{i=1}^{m} t_i = V, \quad t_i \geq 0, \quad i = 1, \dots, m \end{aligned} \tag{4.3}$$

which is precisely of the same form as problem (4.1).

The problem of *worst case* minimum compliance design for multiple loads p^k, $k = 1, \dots, M$, reads:

$$\begin{aligned} & \min_{u^k,t} \max_{k=1,\dots,M} \; p^{kT} u^k \\ & \quad \text{subject to :} \\ & \quad \sum_{i=1}^{m} t_i \mathbf{K}_i u^k = p^k, \quad k = 1, \dots, M \\ & \quad \sum_{i=1}^{m} t_i = V, \quad t_i \geq 0, \quad i = 1, \dots, m \end{aligned} \tag{4.4}$$

where u^k, $k = 1, \dots, M$, are again the displacements corresponding to the different load cases. The discrete optimization over the compliance values can be converted into a smooth maximization by introducing a convex combination of weighting parameters λ^k, $k = 1, \dots, M$, so that the problem becomes:

$$
\begin{aligned}
&\min_{u^k,t} \quad \max_{\substack{\lambda^k \ge 0,\ k=1,\dots,M \\ \sum_{i=1}^{m} \lambda^k = 1}} \quad \sum_{k=1}^{M} \lambda^k p^{k^T} u^k \\
&\quad \text{subject to :} \\
&\quad \sum_{i=1}^{m} t_i \mathbf{K}_i u^k = p^k, \quad k = 1,\dots,M \\
&\quad \sum_{i=1}^{m} t_i = V; \quad t_i \ge 0, \quad i = 1,\dots,m
\end{aligned}
$$

which is similar in form to the weighted average formulation.

We note that the problem formulation (4.1) covers the finite element formulation of the minimum compliance design of continuum problems that exhibit a linear relation between rigidity and the relevant design variable, as exemplified by design of variable thickness sheets, the design of sandwich plates or the simultaneous design of structure and material (cf., Chapt. 3). In these cases the matrices $\mathbf{K}_i$ should be interpreted as the specific element stiffness matrices, and the design variables t_i are the element thicknesses (volumes). For these cases and for the multiple load formulation (4.3), the element stiffness matrices no longer have the form of dyadic products. In order to cover all three cases by one formulation we will write in the following (4.1) in a generalized form

$$
\begin{aligned}
&\min_{u,t} p^T u \\
&\quad \text{subject to :} \\
&\quad \sum_{i=1}^{m} t_i \mathbf{A}_i u = p \\
&\quad \sum_{i=1}^{m} t_i = V, \quad t_i \ge 0, \quad i = 1,\dots,m
\end{aligned}
\tag{4.5}
$$

where $\mathbf{A}_i$ are positive semi-definite, symmetric matrices that satisfy that the matrix $\mathbf{A}(t) = \sum_{i=1}^{m} t_i \mathbf{A}_i$ is positive definite if all t_i's are positive. For trusses this means that the number of bars in the ground structure exceeds the number of degrees of freedom and that the compatibility matrix has full rank.

In analogy to the continuum problems treated earlier in chapters 1-3, it is also in this discretized case convenient to rewrite the problem statements in terms of a minimum potential energy formulation of the equilibrium constraint. Thus problem (4.5) can be rewritten as a max min problem in the form:

$$
\max_{\substack{t \ge 0 \\ \sum_{i=1}^{m} t_i = V}} \ \min_{u} \left\{ \frac{1}{2} u^T \left(\sum_{i=1}^{m} t_i \mathbf{A}_i \right) u - p^T u \right\} \tag{4.6}
$$

This is a saddle point problem for a concave-convex problem, and we shall also for the truss problem in the following use that the max and min operator in (4.6) can be interchanged.

4.1.2 The basic problem statements in member forces

For the continuum formulations of topology design we formulated a stress based minimum compliance problem using the minimum complementary energy principle (cf., problem (1.3) in section 1.1.1). Writing here for the single load truss problem we have the problem

$$\begin{aligned}
&\inf_{t} \min_{q} \quad \frac{1}{2}\sum_{i=1}^{m} \frac{l_i^2}{E_i}\frac{(q_i)^2}{t_i} \\
&\text{subject to:} \\
&\mathbf{B}q = p \quad ; \\
&\sum_{i=1}^{m} t_i = V, \quad t_i > 0, \ i = 1,\dots,m.
\end{aligned} \tag{4.7}$$

where we have to take the infimum over all positive bar volumes in order to have a well-posed problem. In (4.7), q is the vector of member forces. For a given t the solution q^* to the inner problem of (4.7) satisfies $q_i^* = \frac{E_i}{l_i^2} t_i \, b_i^T u^*$, where u^* is the displacement of the truss, i.e., u^* is the solution to the inner problem of (4.6). Note that problem (4.7) is a problem which is simultaneous convex in member forces and member volumes.

The traditional formulation of truss topology design in terms of member forces is for single load, *plastic* design [8]. This problem is normally stated as a minimum weight design problem, for all trusses that satisfy static equilibrium within certain constraints on the stresses in the individual bars. With the same stress constraint value σ_i for both tension and compression, the formulation is in the form of a linear programming problem

$$\begin{aligned}
&\min_{q,t} \sum_{i=1}^{m} t_i \\
&\text{subject to:} \\
&\mathbf{B}q = p, \\
&-\sigma_i t_i \le l_i q_i \le \sigma_i t_i, \quad i = 1,\dots,m, \\
&t_i \ge 0, \quad i = 1,\dots,m.
\end{aligned} \tag{4.8}$$

Notice that in problem (4.8) the stress constraints are written in terms of *member forces*. This turns out to be important in order to give a consistent formulation. For some truss problems, the stress in a number of members will converge to a finite non-zero level as the member areas converge to zero, but the member forces will converge to zero, Cheng and Jiang, 1992, Kirsch, 1992. This fact should be observed for any truss design problem involving stress constraints.

Problem (4.8) is a formulation purely in terms of statics, with no kinematic compatibility included in the formulation. However, a basic solution to this LP problem will automatically satisfy kinematic compatibility, a rather puzzling fact. We note here that (4.8) can be extended to cover cost of supports and to problems involving local stability constraints (buckling etc.) while maintaining the basic properties of (4.8), albeit not the LP form, Pedersen, 1993c, d. This extension will not be discussed here.

With the change of variables $t_i = \frac{l_i}{\sigma_i}(q_i^+ + q_i^-)$, $q = (q^+ - q^-)$ we can write (4.8) in standard LP form, as

$$\begin{aligned}
&\min_{q^+,q^-} \sum_{i=1}^{m} \frac{l_i}{\sigma_i}(q_i^+ + q_i^-) \\
&\text{subject to:} \\
&\mathbf{B}(q^+ - q^-) = p, \\
&q_i^+ \geq 0, \;\; q_i^- \geq 0, \quad i = 1,....,m.
\end{aligned} \tag{4.9}$$

Here q_i^+, q_i^- can be interpreted as the member forces tension and compression, respectively. It is easy to see from the necessary conditions of optimality that the problem (4.8) gives rise to fully stressed designs, i.e. designs for which all bars with non-zero bar area have stresses at the maximum allowed level σ_i. Thus one can often in the literature find (4.9) stated directly without reference to (4.8), as for a fully stressed design, the objective function of (4.9) is precisely the weight of the structure. We shall in a later section revert to these formulation and will show that (4.8), (4.7), and (4.1) are all equivalent in a certain sense.

The plastic design formulation can easily be extended to a multiple load situation as

$$\begin{aligned}
&\min_{q^k,t} \sum_{i=1}^{m} t_i \\
&\text{subject to:} \\
&\mathbf{B}q^k = p^k + \sum_{i=1}^{m} t_i g_i, \;\; k = 1,...,M \\
&-\sigma_i t_i \leq l_i q_i^k \leq \sigma_i t_i, \quad i = 1,....,m, \;\; k = 1,...,M \\
&t_i \geq 0, \quad i = 1,....,m.
\end{aligned} \tag{4.10}$$

where self-weight loads in the form $\sum_{i=1}^{m} t_i g_i$ are also considered (see below for details on notation). This problem is also a linear programming problem. However for this case the precise relation between this problem and the minimum compliance problem is not known.

4.1.3 Problem statements including self-weight and reinforcement

The formulations given above in section 4.1.1 lend themselves to natural extensions, such as to the problem of finding the optimal topology of the reinforcement of a given structure and the optimal topology problem with self-weight taken into consideration.

For the reinforcement problem, see, e.g. Olhoff and Taylor, 1983, using the ground structure approach, we divide a given ground structure into the set S of bars of fixed size and the set R of possible reinforcing bars. Typically S and R will be chosen as disjoint. We prefer here to allow R to contain (a part of) S as a subset; in this way non-zero lower bounds on the design variables can easily be included in the general problem analysis. The bars (elements) of the given structure have given bar volumes s_i, $i \in S$, and the optimal reinforcement t_i, $i \in R$, is the solution of the minimum compliance problem

$$\begin{aligned} &\min_{u,t} p^T u \\ &\quad \text{subject to :} \\ &\sum_{i \in R} t_i \mathbf{A}_i u + \sum_{i \in S} s_i \mathbf{A}_i u = p \\ &\sum_{i \in R} t_i = V, \quad t_i \geq 0, \quad i \in R \end{aligned} \tag{4.11}$$

This problem can be solved by analogous means as can be used for the other topology design problems formulated above. Note that a reinforcement formulation in connection with a multiple load formulation with distinct sub-ground structures of a common ground structure will allow for a very general fail-safe design formulation.

For the important case of optimization with loads due to the weight of the structure taken into account, we employ the standard assumption that the weight of a bar is carried equally by the joints at its ends, thus neglecting bending effects. With g_i denoting the specific nodal gravitational force vector due to the self-weight of bar number i, the problem of finding the optimal topology with self-weight loads and external loads takes the form:

$$
\begin{aligned}
&\min_{u,t}\left\{p^T u + (\sum_{i=1}^{m} t_i g_i)^T u\right\} \\
&\text{subject to :} \\
&\sum_{i=1}^{m} t_i \mathbf{A}_i u = p + \sum_{i=1}^{m} t_i g_i \\
&\sum_{i=1}^{m} t_i = V, \quad t_i \geq 0, \quad i = 1,\dots,m
\end{aligned}
\tag{4.12}
$$

Note that for the problem with self-weight, any feasible truss design for which the self-weight load equilibrates the external load is an optimal design with compliance zero and zero displacement field (compliance is non-negative in all cases). Thus to avoid trivial situations, it is natural to assume that the following set is empty:

$$
\left\{t_i \,\middle|\, \sum_{i=1}^{m} t_i = V, \ t_i \geq 0, \quad i = 1,\dots,m, \ p + \sum_{i=1}^{m} t_i g_i = 0\right\} = \emptyset
$$

We complete this exposition of problem statements by stating the reinforcement problem, with self-weight loads, and general stiffness matrices and loads, so that all cases above are covered as special cases:

$$
\begin{aligned}
&\min_{u,t}\left\{p^T u + (\sum_{i\in R} t_i g_i)^T u + (\sum_{i\in S} s_i g_i)^T u\right\} \\
&\text{subject to :} \\
&\sum_{i\in R} t_i \mathbf{A}_i u + \sum_{i\in S} s_i \mathbf{A}_i u = p + \sum_{i\in R} t_i g_i + \sum_{i\in S} s_i g_i \\
&\sum_{i\in R} t_i = V, \quad t_i \geq 0, \quad i \in R
\end{aligned}
\tag{4.13}
$$

Here the max-min formulation (4.6) is for this general case of the form:

$$
\max_{\substack{t\geq 0 \\ \sum_{i\in R} t_i = V}} \min_u \left\{\frac{1}{2} u^T\left(\sum_{i\in R} t_i \mathbf{A}_i + \sum_{i\in S} s_i \mathbf{A}_i\right)u - \left(p + \sum_{i\in R} t_i g_i + \sum_{i\in S} s_i g_i\right)^T u\right\} \tag{4.14}
$$

maintaining the concave-convex nature of the basic problem (4.6).

4.2 Problem equivalence and globally optimized energy functionals

4.2.1 Conditions of optimality

For the sake of completeness of the presentation, we will in this section derive the optimality conditions for the general minimum compliance truss topology problem (4.12) with self-weight. These conditions constitute the basis for the well-known optimality criteria method for the numerical solution of the general lay-out and topology design problem which we will describe under a general discussion on computational procedures in a later section.

In order to obtain the necessary conditions for optimality for problem (4.12) we introduce Lagrange multipliers $\tilde{u}$, Λ, μ_i, $i = 1,....,m$, for the equilibrium constraint, the volume constraint and the zero lower bound constraints, respectively. The necessary conditions are thus found as the conditions of stationarity of the Lagrangian:

$$L = (p + \sum_{i=1}^{m} t_i g_i)^T u - \tilde{u}(\sum_{i=1}^{m} t_i \mathbf{A}_i u - p - \sum_{i=1}^{m} t_i g_i) + \Lambda(\sum_{i=1}^{m} t_i - V) + \sum_{i=1}^{m} \mu_i(-t_i)$$

By differentiation we obtain the necessary conditions:

$$\sum_{i=1}^{m} t_i \mathbf{A}_i \tilde{u} = p + \sum_{i=1}^{m} t_i g_i;\ \tilde{u}^T(\mathbf{A}_i u - 2g_i) = \Lambda - \mu_i,\ \mu_i \geq 0,\ \mu_i t_i = 0, i = 1,...,m;\ \ \Lambda \geq 0.$$

If we impose a small non-negative lower bound on the areas, the stiffness matrix $\mathbf{A}$ is positive definite and thus u is the unique Lagrange multiplier for the equilibrium constraint, but the situation without a lower bound is not so straightforward.

Now let $\Lambda^*(u)$ denote the maximum of the specific energies $u^T(\mathbf{A}_i u - 2g_i)$ (with self-weight) of the individual bars, i.e.

$$\Lambda^*(u) = \max\{u^T(\mathbf{A}_i u - 2g_i) \mid i = 1,...,m\}$$

and let $J(u)$ denote the set of bars for which the specific energy attains this maximum level:

$$J(u) = \{i \mid u^T(\mathbf{A}_i u - 2g_i) = \Lambda^*(u)\}$$

We also define non-dimensional element volumes $\tilde{t}_i = t_i / V$. Then the necessary conditions are satisfied with

$$\tilde{u} = u;\ t_i = \tilde{t}_i V,\ i \in J(u);\ t_i = 0,\ i \notin J(u);\ \Lambda = \Lambda^*(u);$$
$$\mu_i = 0,\ i \in J(u);\ \mu_i = \Lambda^*(u) - u^T(\mathbf{A}_i u - 2g_i),\ i \notin J(u). \tag{4.15a}$$

provided that there exist a displacement field u with corresponding set $J(u)$ and non-dimensional element volumes $\tilde{t}_i$, $i \in J(u)$, such that

$$V \sum_{i\in J(u)} \tilde{t}_i \mathbf{A}_i u = p + V \sum_{i\in J(u)} \tilde{t}_i g_i; \qquad \sum_{i\in J(u)} \tilde{t}_i = 1 \tag{4.15b}$$

The optimality conditions (4.15b) states that a convex combination of the gradients of the quadratic functions $V(\frac{1}{2}u^T\mathbf{A}_i u - g_i^T u)$, $i \in J(u)$, equals the load vector p.

It can be shown (see below) that there does indeed exist a pair (u, t) which is a solution to the reduced optimality conditions (4.15). This implies that there exists an optimal truss that has bars with constant specific energies and the set $J(u)$ is the set of these active bars. Note that a pair (u,t) satisfying the necessary conditions (4.15) for problem (4.5) is automatically a minimizer for the non-convex minimum compliance problem. This can be shown by copying the proof of Taylor, 1969, who treated the case with a uniform, positive lower bound on the areas. For any design $\tilde{s}_i$, $i = 1,\ldots,m$ satisfying the volume constraint and with corresponding displacement field v, we have that:

$$\begin{aligned}
(p + \sum_{i=1}^m t_i g_i)^T u &= 2(p + \sum_{i=1}^m t_i g_i)^T u - \sum_{i=1}^m t_i u^T \mathbf{A}_i u = 2p^T u - \sum_{i=1}^m t_i u^T(\mathbf{A}_i u - 2g_i) \\
&= 2p^T u - \sum_{i=1}^m t_i \Lambda^*(u) = 2p^T u - V\Lambda^*(u) = 2p^T u - \sum_{i=1}^m \tilde{s}_i \Lambda^*(u) \\
&\le 2p^T u - \sum_{i=1}^m \tilde{s}_i u^T(\mathbf{A}_i u - 2g_i) \\
&\le 2\max_w \left\{ (p + \sum_{i=1}^m \tilde{s}_i g_i)^T w - \frac{1}{2}\sum_{i=1}^m \tilde{s}_i w^T \mathbf{A}_i w \right\} \\
&= 2(p + \sum_{i=1}^m \tilde{s}_i g_i)^T v - \sum_{i=1}^m \tilde{s}_i v^T \mathbf{A}_i v = (p + \sum_{i=1}^m \tilde{s}_i g_i)^T v
\end{aligned}$$

where we have invoked the extremum principle for equilibrium. Finally note that the existence of solutions to the optimality conditions (4.15) shows that there always exists an optimal solution with no more active bars than the degrees of freedom (dimension of u) plus 1; this follows from Caratheodory's theorem on convex combinations (see, e.g. Achtziger et al, 1992).

4.2.2 Reduction to problem statements in bar volumes only

It was noted earlier that the truss topology problem is an unusual structural optimization problem, as the acceptance of zero bar volumes implies that the stiffness matrix of the problem can be singular. Thus the standard gradient/adjoint methods of structural optimization which view the problems as optimization problems in the design variables only cannot be invoked directly. However, if we accept to consider the topology optimization problem as a limes inferior problem for a series of optimal design problems with decreasing positive lower bounds on the design variables we can remove the displacement from the formulation.

Rewriting (4.5) and imposing positive element volumes as a perturbation of the original problem, we can remove the displacement variables by solving for the now unique displacements:

$$\inf_{\substack{t_i>0 \\ \sum_{i=1}^m t_i = V}} \left\{ \Phi(t) \equiv p^T \left[\sum_{i=1}^m t_i \mathbf{A}_i \right]^{-1} p = \max_u \left[2p^T u - u^T \sum_{i=1}^m t_i \mathbf{A}_i u \right] \right\} \tag{4.16}$$

Note that we have exchanged the min-operator with the inf-operator as well as changing the constraint $t_i \geq 0$ to $t_i > 0$. Problem (4.16) is a formulation which is more standard in structural optimization, but from a computational point of view it is still unusual, as the stiffness matrix in truss topology optimization typically will be dense.

It was earlier pointed out that problem (4.16) is convex (see also Svanberg, 1984). This follows from the fact that the compliance function $\Phi(t)$, as a function of the design variables by the second expression in (4.16) is expressed as the supremum (maximum) over a family of convex (linear in this case) functions. Note that the gradient of the objective function $\Phi(t)$ is easy to compute and is given as

$$\frac{\partial \Phi}{\partial t_i} = -u^T \mathbf{A}_i u, \quad \text{with } \sum_{i=1}^m t_i \mathbf{A}_i u = p$$

Note that we for the multiple load problem in its worst-case setting also have a convex formulation in bar volumes only :

$$\inf_{\substack{t_i>0,\ i=1,\dots,m \\ \sum_{i=1}^m t_i = V}} \ \max_{k=1,\dots,M} \ p^{kT} \left[\sum_{i=1}^m t_i \mathbf{A}_i \right]^{-1} p^k \tag{4.17}$$

4.2.3 Reduction to problem statements in strains only

We will now use the max-min formulation (4.14) of the truss topology design problem to derive a globally optimal strain energy functional that describes the energy of the optimal truss. This leads to an alternative, equivalent convex, but non-smooth formulation of the problem, for which a number of computationally effective algorithm can be devised. The derivation is in concept and results similar to the derivation for simultaneous design of structure and material as described in chapter 3, but the dyadic nature of the stiffness matrix for trusses means that one can go somewhat further, as will be shown in the coming sections.

We recall that problem (4.14) has the form

$$\max_{\substack{t\geq 0 \\ \sum_{i\in R} t_i = V}} \min_{u} \left\{ \frac{1}{2} u^T \left(\sum_{i\in R} t_i \mathbf{A}_i + \sum_{i\in S} s_i \mathbf{A}_i \right) u - \left(p + \sum_{i\in R} t_i g_i + \sum_{i\in S} s_i g_i \right)^T u \right\}$$

and this problem is linear in the design variable and convex in the displacement variable. Thus the problem is concave-convex (with a convex and compact constraint set in t) and we can interchange the max and the min operators, to obtain:

$$\min_{u} \max_{\substack{t\geq 0 \\ \sum_{i\in R} t_i = V}} \left\{ \frac{1}{2} u^T \left(\sum_{i\in R} t_i \mathbf{A}_i + \sum_{i\in S} s_i \mathbf{A}_i \right) u - \left(p + \sum_{i\in R} t_i g_i + \sum_{i\in S} s_i g_i \right)^T u \right\}$$

The inner problem is now a linear programming problem in the t variable. To solve this problem, note that with $t \geq 0$, $\sum_{i\in R} t_i = V$ we have the inequality

$$\sum_{i\in R} t_i (u^T \mathbf{A}_i u - 2 g_i^T u) \leq \sum_{i\in R} t_i \max_{i\in R} \left\{ u^T \mathbf{A}_i u - 2 g_i^T u \right\} = V \max_{i\in R} \left\{ u^T \mathbf{A}_i u - 2 g_i^T u \right\}$$

Here the equality holds if all material is assigned to a bar with maximum specific energy $u^T \mathbf{A}_i u - 2 g_i^T u$. Thus we see that the problem (4.14) can be reduced to (Ben-Tal and Bendsøe, 1992):

$$\min_{u} \max_{i\in R} \left\{ \frac{V}{2} \left[u^T \mathbf{A}_i u - 2 g_i^T u \right] - \left[p + \sum_{i\in S} s_i g_i - \sum_{i\in S} \frac{1}{2} s_i \mathbf{A}_i u \right]^T u \right\} \tag{4.18}$$

This is an unconstrained, *convex* and *nonsmooth* problem in the displacement variable u only, with optimal value minus one half of the optimal value for the problem (4.13). For completeness let us state the equivalent problems for the specific cases discussed in section 4.1. For the single load case we have

$$\min_{u}\left[\max_{i=1,\dots,m}\left\{\frac{V}{2}u^{T}\mathbf{A}_{i}u-p^{T}u\right\}\right] \tag{4.19}$$

which for the weighted average, multiple load case this can also be written as:

$$\min_{u^{k}}\left[\max_{i=1,\dots,m}\left\{\sum_{k=1}^{M}w^{k}(\frac{V}{2}u^{k^{T}}\mathbf{K}_{i}u^{k}-p^{k^{T}}u^{k})\right\}\right] \tag{4.20}$$

One can think of the resulting displacements only problems shown above as equilibrium problems for a structure with a non-smooth, convex strain energy. This strain energy is the strain energy for a self-optimized structure which automatically adjusts its topology and sizing so as to minimize compliance for the applied load(s). This feature was also prominent in the study of extremal strain energy functionals described in chapter 2 and 3.

It is possible to show existence of solutions to the problems (4.18)-(4.20) and to prove the equivalence between problem statements of the form (4.1)-(4.6) and (4.18)-(4.20) (Ben-Tal and Bendsøe, 1993). There is no uniqueness in the solutions and it is quite well-known that there are normally 'many' solutions (actually subspaces of solutions). The equivalence of the problems is understood in the sense that for a solution u to for example problem (4.19) and the corresponding set $J(u)$ of active bars, there exists a corresponding set of bar volumes t satisfying the optimality condition

$$\sum_{i\in J(u)}t_{i}\mathbf{A}_{i}u=p;\qquad \sum_{i\in J(u)}t_{i}=V$$
$$t_{i}=0,\, i\notin J(u);\quad t_{i}\geq 0,\, i=1,\dots,m$$

and these optimality conditions are precisely the optimality conditions for the min-max problem (4.19).

For the worst case multiple load problem it is possible to generate a displacements only formulation in the form (Achtziger, 1992, 1993a, 1993b):

$$\min_{\substack{u^{k},\lambda^{k}\geq 0\\ \sum_{k=1}^{M}\lambda^{k}=1.}}\left[\max_{i=1,\dots,m}\left\{\sum_{k=1}^{M}\lambda^{k}(\frac{V}{2}u^{k^{T}}\mathbf{A}_{i}u^{k}-p^{k^{T}}u^{k})\right\}\right] \tag{4.21}$$

where we have used weighting parameters $\lambda^{k}\geq 0,\ k=1,..,M$. Solutions to this problem can likewise be proved to exist and the optimal value of problem (4.21) equals minus one half the extremal value of problem (4.4) The direct equivalence between the two problems (in the sense discussed for the single load problem) may fail if a multiplier λ^k equals zero in the optimal solution to problem (4.21). In this case we cannot guarantee equilibrium for this load condition, as the equilibrium will not necessarily be enforced by the necessary conditions of optimality. However, a set of bar areas can be identified by considering the loads with non-zero multipliers, and a minimum compliance truss will be generated for these loads. This makes it natural to consider a slightly perturbed version of (4.4) and (4.21), where the multipliers are constrained as $\lambda^k \geq \varepsilon > 0,\ \ k = 1,\dots,M$. For the resulting perturbed version of problem (4.21) we can write:

$$\min_{\substack{\lambda^k \geq \varepsilon \\ \sum_{k=1}^{M} \lambda^k = 1}} \left(\min_{u^k} \left[\max_{i=1,\dots,m} \left\{ \sum_{k=1}^{M} \lambda^k \left(\frac{V}{2} u^{kT} \mathbf{A}_i u^k - p^{kT} u^k \right) \right\} \right] \right) \tag{4.22}$$

indicating that the inner problem in the displacements could be solved using the methods described in the preceding sections, with the outer problem solved using algorithms for convex non-differentiable optimization problems; this is described in detail in Achtziger, 1992, 1993a, 1993b.

4.2.4 Linear programming problems for single load problems

In the preceding section the minimum compliance truss topology problem was reformulated as a non-smooth, convex problem in the displacements only. This can now be used as a basis for generating a range of other equivalent problem statements.

The problem (4.18) is, by introducing a bound formulation, equivalent to the convex problem

$$\begin{aligned} &\min_{u,\mu} \left\{ \sum_{i \in S} \frac{1}{2} s_i u^T \mathbf{A}_i u - p^T u - \sum_{i \in S} s_i g_i^T u + \mu^2 \right\} \\ &\text{subject to:} \\ &\frac{V}{2}\left[u^T \mathbf{A}_i u - 2 g_i^T u \right] \leq \mu^2 \ , i \in R \end{aligned} \tag{4.23}$$

which is a smooth, quadratic, positive semi-definite optimization problem with a large number of constraints. This problem lends itself to numerical treatment by invoking a *sparse* SQP method specially suited for problems with many constraints.

For the simpler case of the pure topology problem (no structure to reinforce), the problem becomes, up to a scaling,

$$\min_{u,\mu} \left\{-p^T u\right\}$$
subject to:
$$\frac{V}{2}\left[u^T \mathbf{A}_i u - 2g_i^T u\right] \leq 1 \ , i = 1,\ldots,m.$$

Finally, if also self-weight is absent, the problem statement reduces further to:

$$\min_{u}\left\{-p^T u\right\}$$
subject to: (4.24)
$$\frac{V}{2} u^T \mathbf{A}_i u \leq 1, \quad i = 1,\ldots.,m$$

i.e. a maximization of compliance, with constraints on the specific strain energies.

For the single load truss problem the element stiffness matrices are dyadic products and we get for the specific energies

$$u^T \mathbf{K}_i u = \left(\frac{\sqrt{E_i}}{l_i} b_i^T u\right)^2.$$

This special form of the element specific energies implies that (4.24) can be written in LP- form as (Achtziger et. al., 1992):

$$\min_{u}\left\{-p^T u\right\}$$
subject to: (4.25)
$$-1 \leq \sqrt{\frac{V E_i}{2}} \frac{b_i^T u}{l_i} \leq 1, \quad i = 1,\ldots.,m$$

which is a problem of maximizing the compliance with constraints on the strains $\varepsilon_i = l_i^{-1} b_i^T u$ in all bars. For suitable stress constraint values σ_i it turns out that problem (4.25) is the dual of the force formulation (4.9)

$$\min_{\substack{q_i^+ \geq 0,\ q_i^- \geq 0, \\ i=1,\ldots.,m, \\ \mathbf{B}(q^+ - q^-) = p}} \sum_{i=1}^{m} \frac{l_i}{\sigma_i}(q_i^+ + q_i^-) \tag{4.9}$$

for single load, plastic design (cf. section 4.1.2). Here the tension/compression forces q_i^+, q_i^- are the multipliers for the strain inequality constraints of (4.25). As seen in section 4.1.2, problem (4.9) is, after a change of variables, precisely the traditional minimum mass plastic design formulation (4.8).

The developments described above show that the minimum compliance design problem for a single load case is equivalent to a minimum mass plastic design formulation, in the sense that for a solution t,q to the minimum mass plastic design problem with data V,σ_i, there corresponds a solution t_C,x_C to the minimum compliance problem with data V_C,E_i. The precise relations are (cf. Achtziger et. al., 1992)

$$\sigma_i = \sqrt{E_i} \ , \ t_C = \frac{V_C}{V} t \ , \ x_C = \frac{V_C}{V} x \ ,$$

where x is the dual variable of the minimum mass plastic design problem corresponding to the static equilibrium constraint $\mathbf{B}q = p$.

The member force formulations (4.8) and (4.9) are, as described earlier, the traditional formulations for single load truss topology optimization. These are, of course, very efficient formulations and could be solved using *sparse*, primal-dual LP-methods. The force methods are at first glance problems in plastic design, as kinematic compatibility is ignored, and their use in elastic design is justified by the possibility of finding statically determinate solutions. The equivalence between the force methods and the minimum compliance problem for the *single load case* shows that *any* solution to the force LP-formulation leads to a minimum compliance topology design, within the frame-work of elastic designs. Such designs are uniformly stressed designs, as well as having a constant specific energy in all active bars. The existence of basic solutions to the linear programming problem (4.9) implies that there exist minimum mass truss topologies with a number of bars not exceeding the degrees of freedom. If there exists such a basic solution with only non-zero forces (areas), this is a statically determinate truss. Otherwise, the truss will have a unique force field for the given load but will be kinematically indeterminate. In other words the truss may have rigid body (mechanism) response to certain loads other than the load for which it is designed; this may be the case even after nodes with no connected bars are removed (see also Kirsch, 1992, for a discussion on this).

The equivalence between problems (4.8), (4.9) and (4.25) can also be found in Dorn, Gomory and Greenberg, 1964, and the equivalence between problems (4.1) and (4.8) is indicated in Hemp, 1973, among other places. In Dorn, Gomory and Greenberg, 1964, one can also find a lengthy discussion on how the force formulations are convenient for studying an eventual static determinacy of the solutions.

The derivation of the linear programming formulations above holds only for the case of pure topology truss design with unconstrained design variables, a single load case and excluding self-weight. Thus, the natural extension of the plastic design situation to problem (4.10) which caters for multiple loads and self-weight loads does not seem to have a natural equivalent statement in terms of displacements and compliances. Also, it is well known that in the case of multiple load plastic design, it is most common that statically indeterminate solutions result, thus imposing a requirement for further redesign if kinematic compatibility is required, as for elastic design (Kirsch, 1989, 1992, Topping, 1992).

For the sake of completeness of presentation, note that in the reinforcement case without self-weight, the single load case problem can be reduced to a quadratic optimization problem with linear constraints:

$$\begin{aligned} &\min_{u,\mu}\left\{\frac{1}{2}u^T\left(\sum_{i\in S} s_i \mathbf{K}_i\right)u - p^T u + \mu^2\right\} \\ &\text{subject to:} \\ &-\mu \le \sqrt{\frac{VE_i}{2l_i}}\, b_i^T u \le \mu, \quad i \in R \end{aligned} \tag{4.26}$$

Notice here that the matrix $\sum_{i\in S} s_i \mathbf{K}_i$ is positive semi-definite, but usually not positive definite. The problem statement (4.26) also represents a simplification of the minimum compliance problem for a single load case (no self-weight) and with lower bounds on the variables; the vector s represents the vector of lower bounds on the design variables.

4.2.5 Reduction to problem statements in stresses only

In the following we will base our developments on the worst-case multiple load design formulation

$$\min_{\substack{\lambda^k \ge \varepsilon \\ \sum_{k=1}^M \lambda^k = 1}} \left(\min_{u^k} \left[\max_{i=1,\dots,m} \left\{ \sum_{k=1}^M \lambda^k \left(\frac{V}{2} u^{kT} \mathbf{A}_i u^k - p^{kT} u^k\right) \right\} \right] \right) \tag{4.22}$$

In order to simplify notation we will refrain from covering the problem of reinforcement and the self-weight problem will also play a minor role in the following. However, we begin with a general treatment that covers truss, variable thickness sheet and sandwich plate design.

Now returning to problem (4.22) we note that by a change of variables of u^k to $\frac{1}{\lambda^k}u^k$, this problem can be stated as

$$\inf_{\substack{\lambda^k > 0 \\ \sum_{k=1}^M \lambda^k = 1}} \left(\min_{u^k} \left[\max_{i=1,\dots,m} \left\{ \sum_{k=1}^M \left(\frac{V}{2}\frac{1}{\lambda^k} u^{kT} \mathbf{A}_i u^k - p^{kT} u^k\right) \right\} \right] \right) \tag{4.27}$$

which is now jointly convex on the feasible set in both the multipliers λ^k and the displacements. Here we have used the inf-operator to indicate the use of a decreasing sequence of lower bounds on the multipliers λ^k. The presence of the infimum over the multipliers indicates that it is a natural choice to use interior penalty methods for a computational procedure for solving of this problem, as will be described later.

We shall now show that by deriving the dual formulations of (4.27) one can for the truss case generate what amounts to stress based min-max minimum compliance formulations. The basis for this derivation is again, as in the earlier development, the dyadic structure of the individual member stiffness matrices. Expressing the maximization over the bar numbers (the inner problem) with a bounding variable and using auxiliary variables $c^k{}_i = b_i^T u^k$ (the member elongations), the equivalent convex dual problem can be derived to have the form:

$$\begin{aligned}
&\inf_{t} \ \min_{q^k} \left[\max_{k=1,\dots,M} \left\{ \frac{1}{2} \sum_{i=1}^{m} \frac{l_i^2}{E_i} \frac{(q^k{}_i)^2}{t_i} \right\} \right] \\
&\text{subject to:} \\
&\mathbf{B} q^k = p^k, \ \ k = 1,\dots,M; \\
&\sum_{i=1}^{m} t_i = V, \quad t_i > 0, \ i = 1,\dots,m.
\end{aligned} \tag{4.28}$$

With $\bar{\lambda}^k$, $\bar{u}^k$ denoting the Lagrange multipliers for a bound constraint formulation of the maximization over k and the equilibrium constraint, respectively, we can for an optimum q^k, t of (4.28) with $\bar{\lambda}^k > 0, k = 1,..,M$, identify $u_k = \bar{u}^k / \bar{\lambda}^k, t$ as a solution to our original problem statement (4.4) in displacements and bar areas. Also, we can show, from the Karush-Kuhn-Tucker optimality conditions that $q^k{}_i = \frac{E_i}{l_i^2} t_i \, b_i^T u^k$, i.e. compatibility of stresses and displacements is automatically assured.

The problem (4.28) is actually the minimum compliance problem formulated in terms of the complementary energy, written for the worst-case multiple load situation. For the single load situation, the formulation (4.28) reduces to problem (4.7) which was stated in section 4.1.2.

Finally, we will consider the elimination of the bar volumes from the problem (4.28), by directly solving for these variables. This corresponds to the elimination of bar volumes in the displacements (strain) based formulation as carried out in the preceding section 4.2.2. Expressing the maximization over load cases by a maximization over a convex combination of weighting factors:

$$\min_{\substack{q^k \\ \mathbf{B}q^k=p^k}} \inf_{\substack{t>0 \\ \sum_{i=1}^m t_i=V}} \max_{\substack{\lambda^k\geq 0 \\ \sum_{k=1}^M \lambda^k=1}} \left\{ \sum_{k=1}^M \lambda^k \left[\frac{1}{2} \sum_{i=1}^m \frac{l_i^2}{E_i} \frac{(q^k{}_i)^2}{t_i} \right] \right\} \tag{4.29}$$

we can derive the optimal values of the bar volumes as:

$$t_i = V \sqrt{\frac{l_i^2}{E_i} \sum_{k=1}^M \lambda^k (q^k{}_i)^2} \cdot \left[\sum_{i=1}^m \sqrt{\frac{l_i^2}{E_i} \sum_{k=1}^M \lambda^k (q^k{}_i)^2} \right]^{-1} \tag{4.30}$$

Inserting in (4.29) we obtain the following problem in the member forces only:

$$\begin{aligned} &\min_{q^k} \max_{\substack{\lambda^k\geq 0 \\ \sum_{k=1}^M \lambda^k=1}} \left\{ \frac{1}{2V} \left[\sum_{i=1}^m \left(\frac{l_i}{\sqrt{E_i}} \sqrt{\sum_{k=1}^M \lambda^k (q^k{}_i)^2} \right) \right]^2 \right\} \\ &\text{subject to:} \\ &\mathbf{B}q^k = p^k \ , \ k = 1,\dots,M. \end{aligned} \tag{4.31}$$

For the single load case we recover the traditional linear programming formulation (4.9) in the disguised form :

$$\min_{\substack{q \\ \mathbf{B}q=p}} \left\{ \frac{1}{2V} \left[\sum_{i=1}^m \left(\frac{l_i}{\sqrt{E_i}} |q_i| \right) \right]^2 \right\} \tag{4.32}$$

Rescaling the objective function and taking the square root of the objective function results in (4.9). Note that we have again seen that the stress constraint values for the plastic topology problem should be chosen as $\sqrt{E_i}$. Also, as (4.32) was obtained by direct duality without rescaling, one can see that the optimal value Π of the optimal compliance will relate to the optimal value Ψ of the minimum mass plastic design problem as

$$\Psi^2 = \Pi \cdot V$$

This relation has also been reported recently by Rozvany, 1993.

Note that (4.32) is the natural formulation for the stress only reformulation of the minimum compliance problem stated in terms of stresses and the complementary energy. Problem (4.32) can be viewed as a corresponding equilibrium problem for a structure with a non-smooth, convex complementary energy. This energy arises from a truss for which the bars automatically adjust their sizing and connectivities with the purpose of minimizing the compliance of the currently applied load. This is completely analogous to the situation described for continuum problems in chapter 2 and 3.

4.2.6 Extension to contact problems

The discussion above can be extended to problems involving unilateral contact, as we shall briefly outline in the following (cf., section 3.3.3). Truss topology design in this context has recently been studied by Klarbring, Petersson and Rönnqvist, 1993, Petersson and Klarbring, 1994. Here we present some slight generalization of their results. The most natural setting for unilateral contact problems is a displacement based formulation. For an unilateral contact condition of the form $\mathbf{C}u \leq 0$, the minimum compliance problem (4.14) for contact problems becomes

$$\max_{\substack{t \geq 0 \\ \sum_{i \in R} t_i = V}} \min_{\substack{u \\ \mathbf{C}u \leq 0}} \left\{ \frac{1}{2} u^T \left(\sum_{i \in R} t_i \mathbf{A}_i + \sum_{i \in S} s_i \mathbf{A}_i \right) u - \left(p + \sum_{i \in R} t_i g_i + \sum_{i \in S} s_i g_i \right)^T u \right\} \tag{4.33}$$

where only the inner equilibrium problem is altered. In Klarbring, Petersson and Rönnqvist, 1993, the problem of finding the stiffest structure among all structures with constant contact pressure is also considered and in this case the unilateral constraint should be of the scalar form $\mathbf{1}_C \mathbf{C}u \leq 0$, corresponding to a total gap constraint $\mathbf{1}_C d = 0$, where d is an initial gap which is designed to achieve constant pressure (see also Klarbring, 1992). This case is also covered by the statement (4.33), by proper choice of $\mathbf{C}$.

The introduction of *design independent* constraints in the inner problem of (4.33) does not change the saddle point property of the problem. As shown in Klarbring, Petersson and Rönnqvist, 1993, it does not make sense for contact problems to assume that the stiffness matrix is positive definite for at least one design. Instead, one has to assume that the applied force does not give raise to rigid body motions and that the applied force is not entirely applied at the potential contact nodes. With this assumption we have existence of solution and an equivalent displacements only problem in the form

$$\min_{\substack{u \\ \mathbf{C}u \leq 0}} \max_{i \in R} \left\{ \frac{V}{2} \left[u^T \mathbf{A}_i u - 2 g_i^T u \right] - \left[p + \sum_{i \in S} s_i g_i - \sum_{i \in S} \frac{1}{2} s_i \mathbf{A}_i u \right]^T u \right\} \tag{4.34}$$

Consider now the worst-case multiple load problem in the formulation which includes contact

$$\inf_{\substack{\lambda^k > 0 \\ \sum_{k=1}^{M} \lambda^k = 1}} \left(\min_{\substack{u^k \\ \mathbf{C}^k u^k \leq 0}} \left[\max_{i=1,\dots,m} \left\{ \sum_{k=1}^{M} \left(\frac{V}{2} \frac{1}{\lambda^k} u^{k^T} \mathbf{A}_i u^k - p^{k^T} u^k \right) \right\} \right] \right) \tag{4.35}$$

Here we have related each load case to a potentially different contact condition. Computing the dual of the equilibrium problem, we obtain the complementary energy formulation in the form

$$\inf_{t} \min_{q^k, f^k} \left[\max_{k=1,\dots,M} \left\{ \frac{1}{2} \sum_{i=1}^{m} \frac{l_i^2}{E_i} \frac{(q^k{}_i)^2}{t_i} \right\} \right]$$

subject to :

$$\mathbf{B} q^k = p^k - \mathbf{C}^{k^T} f^k, \; f^k \geq 0, \; k = 1, \dots, M;$$

$$\sum_{i=1}^{m} t_i = V, \quad t_i > 0, \; i = 1, \dots, m.$$

where the contact forces f^k also enter as variables. As for the non-contact case we can compute the optimal bar volumes (given again by formula (4.30)) and the resulting force-only formulation only change by the addition of the contact forces in the equilibrium constraint. For the single load case we get the disguised linear programming problem:

$$\min_{\substack{q, f \geq 0 \\ \mathbf{B} q = p - \mathbf{C}^T f}} \left\{ \frac{1}{2V} \left[\sum_{i=1}^{m} \left(\frac{l_i}{\sqrt{E_i}} |q_i| \right) \right]^2 \right\}$$

For the displacement formulation one has, likewise, the LP formulation

$$\min_{u} \{ -p^T u \}$$

subject to :

$$\mathbf{C} u \leq 0$$

$$-1 \leq \sqrt{\frac{V E_i}{2}} \frac{b_i^T u}{l_i} \leq 1, \quad i = 1, \dots., m$$

taking the development "full circle". A similar development for piecewise linear elasto-plasticity will be covered in section 5.2 for continuum structures.

We close this section by remarking that the minimum compliance problem with unilateral contact formulated as a

$$\sup_{\substack{t > 0 \\ \sum_{i \in R} t_i = V}} \left[\Phi(t) = \min_{\substack{u \\ \mathbf{C} u \leq d}} \left\{ \frac{1}{2} u^T \left(\sum_{i \in R} t_i \mathbf{A}_i + \sum_{i \in S} s_i \mathbf{A}_i \right) u - \left(p + \sum_{i \in R} t_i g_i + \sum_{i \in S} s_i g_i \right)^T u \right\} \right]$$

for positive definite stiffness matrices is actually a C^1-smooth problem in the bar volumes (see also Haslinger and Neittaanmäki, 1988). Here we consider that an initial non-zero gap d is given, so that the unilateral constraint is $\mathbf{C} u \leq d$. The derivatives of the compliance functional $\Phi(t)$ are given as

$$\frac{\partial}{\partial t_i}\Phi(t) = \left\{\frac{1}{2}u_*^T\mathbf{A}_i u_* - g_i^T u_*\right\}, \text{ with}$$

$$u_* = \arg \min_{\substack{u \\ \mathbf{C}u \le d}} \left\{\frac{1}{2}u^T\left(\sum_{i\in R} t_i\mathbf{A}_i + \sum_{i\in S} s_i\mathbf{A}_i\right)u - \left(p + \sum_{i\in R} t_i g_i + \sum_{i\in S} s_i g_i\right)^T u\right\}$$

Note, however, that the displacements are not differentiable as functions of bar volumes, as the displacements are non-smooth at designs were there are active contact nodes with zero contact forces. This feature means that most other design problems which involves contact conditions are non-smooth problems.

In order to complete the presentation let us briefly state the result on sensitivity analysis of the displacement solution to the contact problem with positive definite stiffness matrix (cf., Bendsøe, Olhoff and Sokolowski, 1985). To this end let u_*, f be the displacement and associated contact force, and identify the potential contact nodes according to

$$I_C = \{i \mid (\mathbf{C}u_*)_i = d_i \text{ and } f > 0\}$$
$$I_{C0} = \{i \mid (\mathbf{C}u_*)_i = d_i \text{ and } f = 0\}$$
$$I_N = \{i \mid (\mathbf{C}u_*)_i < d_i\}$$

Now consider a design perturbation of the form $t + \delta \cdot \Delta t$. Then the sensitivity u_*' of the displacement in the direction Δt is given as the solution of the auxiliary problems:

For $\delta > 0$:

$$u_*' = \arg \min_{\substack{v \\ (\mathbf{C}v)_i \le 0 \text{ for } i\in I_{C0} \\ (\mathbf{C}v)_i = 0 \text{ for } i\in I_C}} \left\{\frac{1}{2}v^T\left(\sum_{i\in R} t_i\mathbf{A}_i + \sum_{i\in S} s_i\mathbf{A}_i\right)v - \left(\sum_{i\in R}(\Delta t)_i[g_i + \mathbf{A}_i u_*]\right)^T v\right\}$$

For $\delta < 0$:

$$-u_*' = \arg \min_{\substack{v \\ (\mathbf{C}v)_i \le 0 \text{ for } i\in I_{C0} \\ (\mathbf{C}v)_i = 0 \text{ for } i\in I_C}} \left\{\frac{1}{2}v^T\left(\sum_{i\in R} t_i\mathbf{A}_i + \sum_{i\in S} s_i\mathbf{A}_i\right)v + \left(\sum_{i\in R}(\Delta t)_i[g_i + \mathbf{A}_i u_*]\right)^T v\right\}$$

It is readily seen that the displacements are differentiable when the set

$$I_{C0} = \{i \mid (\mathbf{C}u_*)_i = d_i \text{ and } f = 0\}$$

is empty, i.e., no nodes in contact have zero contact force.

4.3 Computational procedures and examples

The availability of efficient methods to solve large (sparse) LP problems makes it natural to solve the single load truss topology design problem using the LP formulations. For problems with multiple loads and/or bounded bar areas, for the reinforcement problem as well as for the FEM case, we cannot obtain a linear programming formulation of the minimum compliance problem and we are forced to solve problems of the type (4.1)-(4.6), (4.11)-(4.13), (4.18)-(4.22) or (4.23)-(4.24) directly.

Problems of the form (4.1)-(4.6) and (4.11)-(4.13) generalize most easily to more general design situations involving stress and displacement constraints but they are large scale and non-convex. The optimality criterion method is a good and easily programmed option for solving this problem in the minimum compliance setting, if suitable lower bounds on the bar volumes are imposed. Problems (4.18)-(4.22) and (4.23)-(4.24) are convex and have the size of the degrees of freedom of the ground structure; (4.18)-(4.22) are non-differentiable and unconstrained and (4.23)-(4.24) are differentiable, but at the cost of a high number of constraints. Below we shall present a specialized algorithm for solving problem (4.18), which can be easily implemented to take advantage of the sparsity of the matrices $\mathbf{A}_i$. General purpose algorithms for min-max optimization or non-differentiable optimization can also be employed, but comparison is difficult for problem sizes where sparsity plays an important role; also most general purpose methods have enormous computer storage requirements. Likewise, problems (4.23)-(4.24) can be solved by general purpose algorithms (SQP etc.), but again sparsity and the fact that the number of variables is much lower than the number of constraints should be utilized.

It should be emphasized that the truss topology design problem is a very challenging mathematical programming problem with structure and properties which are a test for even the best of algorithm.

4.3.1 An optimality criteria method

For the continuum problems treated earlier the optimality criteria method is an effective and general mean for solving minimum compliance problems. Also for truss topology design this is a simple and effective computational procedure [18]. In physical terms the method assigns material to members proportionally to the specific energy of each member in order to reach the situation of constant specific energy in the active bars. Thus each iteration step consists of the following:

$$\text{For } t_i^{k-1} \text{ given, compute displacement } \mathrm{u}_{k\text{-}1} \text{ from equilibrium eqs.} \tag{4.37a}$$

$$\text{Find } \Lambda \text{ so } \sum_{i=1}^{m} \max\left\{ t_i^{k-1} \frac{u_{k-1}{}^T \mathbf{A}_i u_{k-1}}{\Lambda},\ t_{\min} \right\} = V. \tag{4.37b}$$

$$\text{Update } t_i^k = \max\left\{ t_i^{k-1} \frac{u_{k-1}{}^T \mathbf{A}_i u_{k-1}}{\Lambda},\ t_{\min} \right\}. \tag{4.37c}$$

The linearity of stiffness and volume in bar areas implies that the optimality criteria algorithm for the single load case can be viewed as a fully stressed design algorithm, and it is as such a fix point algorithm, Levy, 1991. Also, the method can be viewed as an implementation of a sequential quadratic programming technique for the topology design problem; this is discussed in detail in Svanberg, 1992a, 1994a, 1994b.

The optimality criteria method involves assembly of the global stiffness matrix as well as the solving the equilibrium problem at each iteration step, and this part of the algorithm is the most time consuming. Note, that for $t_{\min} \sim 0.0$ the algorithm can utilize that the volume is linear in the design variables so that satisfying the volume constraint is just a rescaling of variables. However, the algorithm does not take advantage of the fact that also the stiffness matrix is linear in the design variables. Also for the single load case truss topology problem (4.1) we have that the matrices $\mathbf{A}_i$ are dyadic products and this is not used either.

4.3.2 A non-smooth descent method

It turns out that it is advantageous to consider algorithms for the equivalent problems (4.18)-(4.22) and we will here describe an "ε-steepest descent" method for the non-smooth problems (Demyanov and Malozemov, 1974, Ben-Tal and Bendsøe, 1993). The algorithm is not the most effective that can be devised (see next section), but it is physically intuitive, and it is closely related to the optimality criteria algorithm.

The algorithm solves a problem in the displacement variables only, as the design variables have been removed through a duality argument. However, the algorithm generates the solution u as well as the bar volumes t. Note that the standard procedure in design problems is to solve for the design variables, with the displacements removed via the state equation and adjoint equation.

For generality we describe the algorithm for the general reinforcement problem with external loads as well as loads due to self-weight. The algorithm consists of the following very intuitive steps.

The algoritm for problem (4.18):

$$\min_u \left[F(u) = \frac{V}{2} \max_{i\in R} \left\{ u^T \mathbf{A}_i u - 2 g_i{}^T u \right\} + \frac{1}{2} \sum_{l\in S} s_l (u^T \mathbf{A}_l u - 2 g_l{}^T u) \ - p^T u \right]$$

0. Compute an initial guess of displacement field u , for example by solving the equilibrium equations for a feasible set of bar volumes t .

1. For present u, compute $\Lambda^*(u) = \max_{i\in R}\{\, u^T\mathbf{A}_i u - 2g_i^T u \,\}$, indices

$$J(u) = \left\{ i \in R \mid u^T\mathbf{A}_i u - 2g_i^T u \geq \Lambda^*(u) - \varepsilon \right\}$$

$$J_U(u) = \left\{ i \in R \,\middle|\, u^T\mathbf{A}_i u - 2g_i^T u \geq \Lambda^*(u) - C\varepsilon \right\},\; C \approx 10$$

and the displacement dependent load $f = p + \sum_{l\in S} s_l g_l - \sum_{l\in S} s_l \mathbf{A}_l u$

2. Compute descent direction d as

$$d = -\left[\sum_{i\in J} t_i \left[\mathbf{A}_i u - g_i\right] - f \right]$$

where $t_i,\, i \in J$ are found from

$$\min_{\substack{t_i \geq 0,\, i\in J \\ \sum_{i\in J} t_i = V}} \left\{ \left\| \sum_{i\in J} t_i \left[\mathbf{A}_i u - g_i\right] - f \right\|^2 - \sum_{i\in J} t_i u^T \left[\mathbf{A}_i u - 2g_i\right] \right\}$$

3. If $\|d\| \leq \delta$, stop. Else go to 4.

4. Compute a step size α^* for the update $u := u + \alpha d$, by a line search with the function

$$\Psi(\alpha) = F(u + \alpha d) = \max_{i\in R} \left\{ \bar{a}_i \alpha^2 + \bar{b}_i \alpha + \bar{c}_i \right\},$$

$$\bar{a}_i = \frac{V}{2} d^T\mathbf{A}_i d + \frac{1}{2}\sum_{l\in S} s_l d^T\mathbf{A}_l d, \qquad \bar{b}_i = \left[V(\mathbf{A}_i u - g_i) - f\right]^T d$$

$$\bar{c}_i = \left[\frac{V}{2}(\mathbf{A}_i u - 2g_i) - (f + \frac{1}{2}\sum_{l\in S} s_l \mathbf{A}_l u) \right]^T u$$

5. Update, $u := u + \alpha^* d$, and go to step 1.

Here, ε is a relaxation on the activity set J which is crucial to guarantee the convergence of the algorithm, and δ determines the accuracy of the solution. Each iteration loop of the algorithm consists of first finding the set of almost active bars (Step 1). The descent direction (Step 2) is then found by first finding the bar volumes of these bars which minimizes the error in equilibrium for the given estimate of displacement. This is a quadratic programming problem. The error is measured in a least squares sense and the descent direction is given as the vectorial error with this best fit of bar volumes. For ε small enough, the set of almost active bars equals the set of actually active bars, so it is natural to work with a decreasing sequence of the relaxation parameter ε, as well as with a decreasing sequence of equilibrium errors δ. The line search for the non-smooth function $\Psi(\alpha)$ (Step 4) is most conveniently carried out using a Golden Section method, using the set J_U of almost active bars as the basis for the search. A search with a full set of bars is only invoked if the update with this reduced set of bars does not result in an improvement of the functional.

Note that the algorithm above lends itself to an implementation that takes the fullest advantage of sparsity both in storage and computations. An efficient storage strategy is to store the bar-connectivity matrix (m by 2 matrix of integers) and the bar cosines (m by 2 or 3 matrix of reals) for all information on the matrices $\mathbf{A}_i$, $i = 1,\dots,m$, and to base computations of the data such as $\mathbf{A}_i u$, $u^T\mathbf{A}_i u$ on this information. Finally note that the least squares sub problem of step 2 are sparse problems in the t_i variables. For a proof of the convergence of the algorithm, we refer to Ben-Tal and Bendsøe, 1993, where also the case of constrained bar areas is treated in full detail. An example of the use of this algorithm for the layout design of aircraft wings can be found in Balabanov and Haftka, 1994.

The algorithm above is conceptually similar to the algorithm given in Taylor and Rossow, 1977, for the single load case, the difference being in the update scheme, which here is based on the formal identification of the equivalence between problems (4.13) and (4.18).

4.3.3 Interior point methods

It is the provision of a lower bound on the bar volumes that allows for the use of the very effective optimality criterion method. A similar efficiency can be obtained by considering the problem of taking the infimum of the compliances for all truss structures with positive bar volumes:

$$\inf_{\substack{t_i > 0 \\ \sum_{i=1}^m t_i = V}} \left\{ \Phi(t) = p^T \left[\sum_{i=1}^m t_i \mathbf{K}_i \right]^{-1} p \right\} \tag{4.38}$$

As shown earlier this problem is convex and this in combination with the inf-form makes it ideally suited for interior point barrier methods (Ben-Tal and Nemirovskii, 1993, 1994, Ringertz, 1988, 1993), as this will imply that the positivity constraint on the bar volumes will be satisfied automatically. Problem (4.38) does not lend itself to the use of sparse techniques, as the Hessian of the objective function $\Phi(t)$ is full, while the Hessian of the constraint $\sum_{i=1}^m t_i \mathbf{A}_i u = p$ is very sparse. Thus sparsity can be utilized if the problem

$$\begin{aligned}
&\inf_{u,t} p^T u \\
&\quad \text{subject to :} \\
&\quad \sum_{i=1}^{m} t_i \mathbf{K}_i u = p \qquad\qquad (4.39) \\
&\quad \sum_{i=1}^{m} t_i = V, \quad t_i > 0, \quad i = 1,\dots,m
\end{aligned}$$

in both the displacement and design variables is solved using an interior point method. Even though the latter problem is not convex, finding a stationary solution provides also a stationary point for problem (4.38), and thus a minimizer for this convex problem (Ringertz, 1993). This approach extends readily to all the problem types described above. Note, however, that the use of an interior barrier method for problems (4.38) or (4.39) involves the use of a suitable sequence of penalty parameters, which in effect corresponds to imposing a constraint of the type $t_i \geq t_{\min} > 0, \quad i = 1,\dots,m$ for a suitable small lower bound value $t_{\min}$. This can make it troublesome to identify precisely which bars are active in the optimal topology. However, convergence of the designs (and relevant displacements) as we take the limit $t_{\min} \to 0$ is guaranteed, see Achtziger 1993b, 1994.

For the worst-case multiple load problem (4.4), formulated as a smooth problem using a bound formulation with bounding variable α, a possible logarithmic barrier function is of the form:

$$\min_{t,\alpha}\left\{-\sum_{k=1}^{M}\ln(\alpha - p^{kT}\left[\sum_{i=1}^{m} t_i \mathbf{A}_i\right]^{-1} p^k) - \sum_{i=1}^{m}\ln(t_i) - \ln(\alpha_{\max} - \alpha)\right\}$$

where $\alpha_{\max}$ is a suitable guaranteed upper bound on the optimal value of the problem. Further details on the use of such interior point methods can be found in for example Ben-Tal and Nemirovskii, 1993, 1994.

Barrier function methods and so-called "Penalty/Barrier/Multiplier (PBM) Method" can also to great advantage be used for the displacements only formulations of the form (4.18) (Bendsøe, Ben-Tal and Zowe, 1993). We will here briefly describe the Penalty/Barrier/Multiplier Method for a general non-linear program (for details, see Ben-Tal and Zibulevsky, 1993, and Zibulevsky and Ben-Tal, 1993). Thus we write a general convex and non-linear program

$$\min_{x}\left\{f_0(x) \mid f_i(x) \leq 0, i \in I\right\} \qquad (4.40)$$

and consider the strictly increasing and strictly convex, smooth function

$$\varphi_\rho(t) = \begin{cases} \dfrac{1}{8\rho} t^2 + t & \text{if } t \geq -2\rho \\ -\rho\left[\log(\dfrac{t}{-2\rho}) + \dfrac{3}{2}\right] & \text{if } t < -2\rho \end{cases}$$

composed of a logarithmic branch and a quadratic branch. Since $\varphi_\rho(t) \leq 0$ if and only if $t \leq 0$, it follows that the problem (4.40) is equivalent to the problem,

$$\min_x \left\{ f_0(x) \mid \varphi_\rho[f_i(x)] \leq 0,\ i \in I \right\} \tag{4.41}$$

The Lagrangian corresponding to problem (4.41) is:

$$F_\rho(x,\mu) = f_0(x) + \sum_{i \in I} \mu_i \varphi_\rho[f_i(x)] \tag{4.42}$$

and the PBM method consists in minimizing this combined penalty, barrier and multiplier function. At the j-th iteration step of the PBM method the penalty parameter $\rho_j > 0$ and the current estimate of the Lagrange multipliers $\{\mu_i^j : i \in I\}$ are given. The update of the variables x^j are computed by a Newton method for the minimization of (4.42), i.e.,

$$x^{j+1} = \arg\min_x F_{\rho^j}(x, \mu^j).$$

The multipliers are then updated by the rule

$$\mu_i^{j+1} = \mu_i^j \frac{d\varphi_{\rho^j}}{dt}\left[f_i(x^{j+1})\right],\ i \in I.$$

and the penalty parameter by the update formula $\rho_{j+1} = \alpha \rho_j$, with a parameter α, $0 < \alpha < 1$. For details on motivation, convergence properties and implementation of the PBM method we refer to Ben-Tal, Yuzefovich, and Zibulevsky, 1992, and Zibulevsky and Ben-Tal, 1993.

In order to apply the PBM method to for example the min-max multiple load truss topology design problem, the formulation (4.27) is used in a form where the discrete maximization over bar numbers is removed by a bound formulation

$$\inf_{\substack{\lambda^k>0, u^k, \tau \\ \sum_{k=1}^{M} \lambda^k = 1}} \left\{ V\tau - \sum_{k=1}^{M} p^{k^T} u^k \right\}$$

$$\text{subject to :} \qquad (4.43)$$

$$\sum_{k=1}^{M} \frac{1}{2\lambda^k} u^{k^T} \mathbf{A}_i u^k - \tau \leq 0 \,, \; i = 1,\ldots,m.$$

Note that (4.43) is a smooth convex optimization problem. It can be shown from the Karush-Kuhn-Tucker conditions of problem (4.43), that the Lagrange multipliers for the constraints on the specific energies are precisely the optimal volumes of the bars in the optimal topology. Hence the optimal bar volumes are approximated directly at each iteration step of the PBM method by the Lagrange multipliers for these constraints. Notice that a further reformulation is handy, namely the formulation

$$\inf_{\substack{s^k \geq 0, x^k, \tau \\ \sum_{k=1}^{M} (s^k)^2 = 1}} \left\{ V\tau - \sum_{k=1}^{M} s^k p^{k^T} x^k \right\}$$

$$\text{subject to :} \qquad (4.44)$$

$$\sum_{k=1}^{M} x^{k^T} \mathbf{A}_i x^k - 2\tau \leq 0 \,, \; i = 1,\ldots,m.$$

which is derived from (4.43) by the transformation $s^k = \sqrt{\lambda^k}$, $x^k = u^k / \sqrt{\lambda^k}$ of variables.

Table 4.1 contains typical run-time results for solving single and multiple load truss topology design problems by the Penalty/Barrier/Multiplier (PBM) method. For the single load case, the problem solved was the formulation (4.24) and for the multiple load, worst case design formulation the problem solved was problem (4.44). For a truss with N degrees of freedom, m potential bars and M load cases, problem (4.24) has N variables and m constraints, while problem (4.44) has $NM+M+1$ variables and m non-linear constraints. The main computational effort in applying the PBM method is the minimization of the unconstrained penalty/barrier function. This is done using a Newton method. Therefore the number of Newton steps reported in Table 4.1 reflects well the number of main iterations; note that each Newton step corresponds to solving a linear system of equations, which for the single load case is comparable in size to the linear system solved for one full equilibrium analysis step of the "Optimality Criteria Method". For all problems the starting point was $\tau = 0$, $u^k = 0$ and $\lambda^k = 1/M$ for $k = 1,..,M$. The algorithm was stopped when 6 digits of accuracy of the objective function was obtained. The examples used for the table are all for ground structures in a rectangular domain in the plane with a fairly regular layout of nodal points. As potential connections all non-overlapping connections were used

Example	Degrees of freedom (number of variables)	Number of bars	Number of load cases	Number of Newton steps	CPU time (SUN-4-s.3 computer)	See figure no.
13 x 13	334 (334)	8744	1	34	4'	4.7A
13 x 13	334 (334)	8744	1	34	4'	4.7B
13 x 13	334 (1002)	8744	3	58	2 h	4.7B
3 x 33	194 (582)	2818	3	70	35'	4.6
21 x 11	458 (458)	16290	1	37	11'	4.8
21 x 11	458 (1374)	16290	3	69	6 h 4'	-

Table 4.1. Typical performance of the Penalty/Barrier/Multiplier method for truss topology design. The ground structures include all non-overlapping connections. For details, see text.

4.3.4 Examples

In the following we illustrate some prominent features of truss topology design for single loads, for multiple loads and for the case of reinforcement as well as self-weight problems. The main purpose is to illustrate the effect of various modelling choices on the geometry of the lay-outs. Space does not permit an exhaustive discussion on this subject, as many features influence the final designs, such as the choice of nodal points as well as the geometry and connectivities of the ground structure, the geometry of the loads, the geometry of the supports, etc. More examples of large scale truss topology optimization can be found in the literature [26], [27].

In most of the examples the ground structures consist of all possible connections (as in Fig.4.1D) or of only connections to the neighbouring points (as in Fig.4.1B). For problems with all possible connections, the possibility of redundant, overlapping bar members entering the ground structure should be avoided by removing overlapping bars, in the sense that for any two nodal points the straight line connection between the two points always consists of the connection through eventual other nodal points lying on the line connecting the two points. For problems with self-weight, overlapping bars do not represent a redundancy, as a connection through an extra nodal point introduces the possibility of self-weight loads at such extra nodes. This underlines a weakness in the simple modelling of self-weight loads in trusses.

For the truss topology problem with a single load case it is possible to generate a catalogue of optimal topologies. Problem (4.1) is made up of expressions that are element wise linear in all variables, except geometric data. Thus, for a specific choice of ground structure geometry and load vector direction, the optimal topology needs only to be computed for one set of assigned values of Young's modulus E , volume V , load size, and one geometric scale; for any other values of these variables, the optimal values of the design variables t , the deformation u and the compliance $p^T u$ can be derived by a simple scaling; the non dimensional parameter

$$\Phi = \frac{(p^T u) V E}{\|p\|^2 L^2}$$

is a constant for optimal topologies generated with equivalent topologies of the ground structure, with L being a measure of scale. A similar non-dimensional parameter can be devised for the multiple load case, the case of self-weight loads, etc., but here the catalogue will depend on a further range of parameters, such as the ratios between the sizes of the different applied loads.

A very important feature of the truss topology method is the prediction of Michell frame type lay-outs in certain cases, if such a structure is natures best topology with the given loads, supports and ground structure, as illustrated in figures 4.3 and 4.14. These figures illustrates the varied topologies that can be created for the simple problem of transmitting a single vertical load to a vertical line of supports, through ground structures of rectangular lay-out of different aspect ratios. The range of topologies goes from the optimal two-bar truss with two bars at $\pm 45^\circ$ to long slender Michell frame lay-outs which at a global scale behaves like a sandwich beam in bending. The transition from 'true' trusses to Michell truss continua for this setting has been studied by analytical means in Lewinski, Zhou and Rozvany, 1993. Note that we in these examples (as in all cases) clearly see that the topology optimization not only predicts the optimal lay-out of the structures, but also finds the optimal use of the prescribed possible support conditions. The examples in figure 4.3 are for a ground structure with total freedom. The possible strong influence of choice of ground structure is illustrated in figure 4.4.

It was mentioned earlier that truss topology compliance optimization under a single load condition leads to statically determinate solutions, but the resultant structures are more often than not mechanisms, which are stable under the applied load. This feature can in most cases be avoided by designing the truss for multiple load cases, either in the weighted average formulation or in the worst case, min-max formulation. Figure 4.5 shows that it is important to consider multiple load situations and figure 4.7 shows the difference between treating three nodal loads as one, combined load, or as three independent load cases. Note that we through the multiple load formulation avoid the mechanisms, at the expense of much more complicated topologies. Figure 4.7 also illustrates the differences that occur due to the relative position of the possible supports and the applied loads. In figure 4.6 we show, for a similar load and support condition in a different ground structure the (small) difference between multiple load designs achieved through the weighted average formulation and the min-max formulation. That multiple load conditions can also simplify the lay-out of the optimal topology is illustrated in figure 4.9. In all examples with multiple load, worst case design, the nature of the applied loads is here such that all loads have compliance value at the maximal value. This is usually not the case for problems where the optimal structure for one of the applied loads can carry the other loads.

Examples of large truss topology optimization results are shown in figures 4.8 and 4.13, again illustrating the important effect of support conditions. One of the interesting features of topology design is that the extreme freedom of the design setting immediately reveals any weakness or misinterpretation of support and load conditions. Thus a topology design method is a very effective interactive tool in the initial steps of a design process.

Finally, in figures 4.10 and 4.11 we show examples of truss topology design with self-weight loads included in the formulation, in figure 4.12 we show a optimal topology for a complicated lay-out of the ground structure and in figure 4.14 we show the similarity between results of a homogenization topology design of a 'thin' structure and the topology design of a truss.

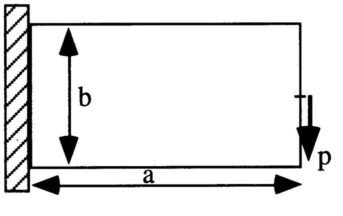

Figures 4.3, 4.4, 4.14

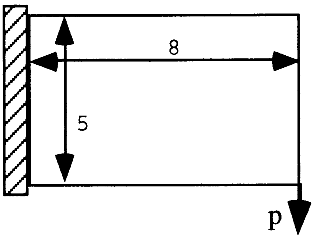

Figure 4.10

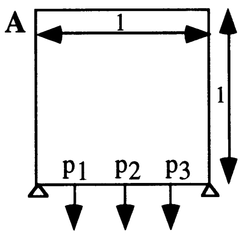

Figures 4.6, 4.7A

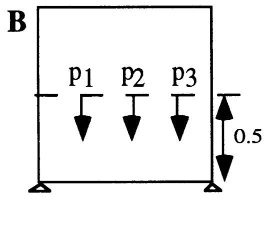

Figure 4.7B

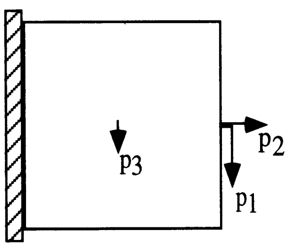

Figure 4.9

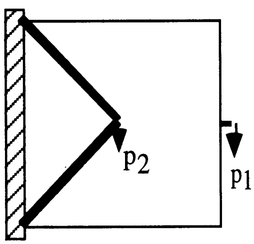

Figure 4.11

Fig. 4.2. The ground structure geometry, load and support conditions used in the examples.

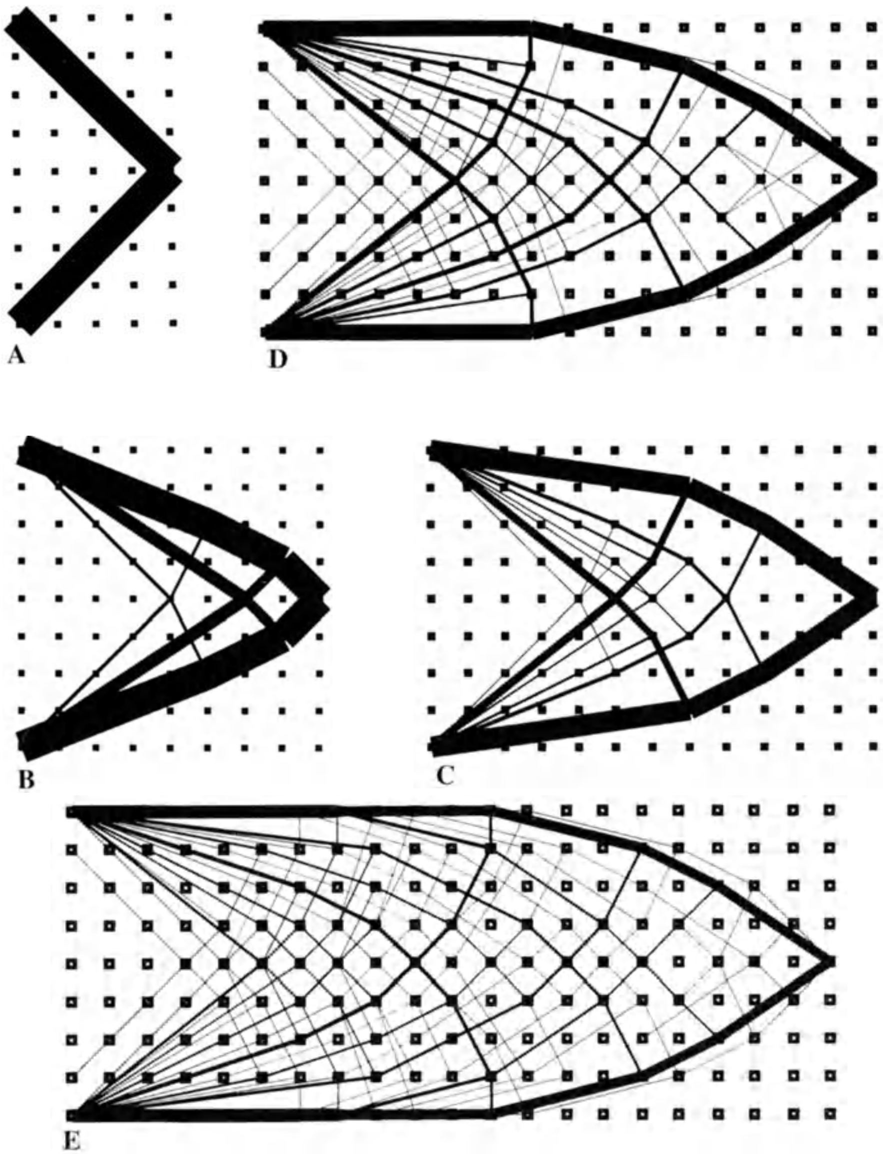

Fig. 4.3. The influence of the ground structure geometry on the optimal topology. Optimal truss topologies for transmitting a single vertical force to a vertical line of supports (see Fig. 4.2). The ground structures consist of all possible non-overlapping connection between the nodal points of a regular mesh in rectangles of varying aspect ratios R=a/b. *(A)*: 632 potential bars for 5 by 9 nodes in a rectangle with R=0.5. Optimal non-dimensional compliance Φ= 4.000. *(B)*: 2040 potential bars, 9 by 9 nodes, R=1.0, Φ= 5.975. *(C)*: 4216 potential bars, 13 by 9 nodes, R=1.5, Φ= 9.1676. *(D)*: 7180 potential bars, 17 by 9 nodes, R=2.0, Φ= 12.5756. *(E)*: 10940 potential bars, 21 by 9 nodes, R=2.5, Φ= 16.4929. Bendsøe, Ben-Tal and Zowe, 1993.

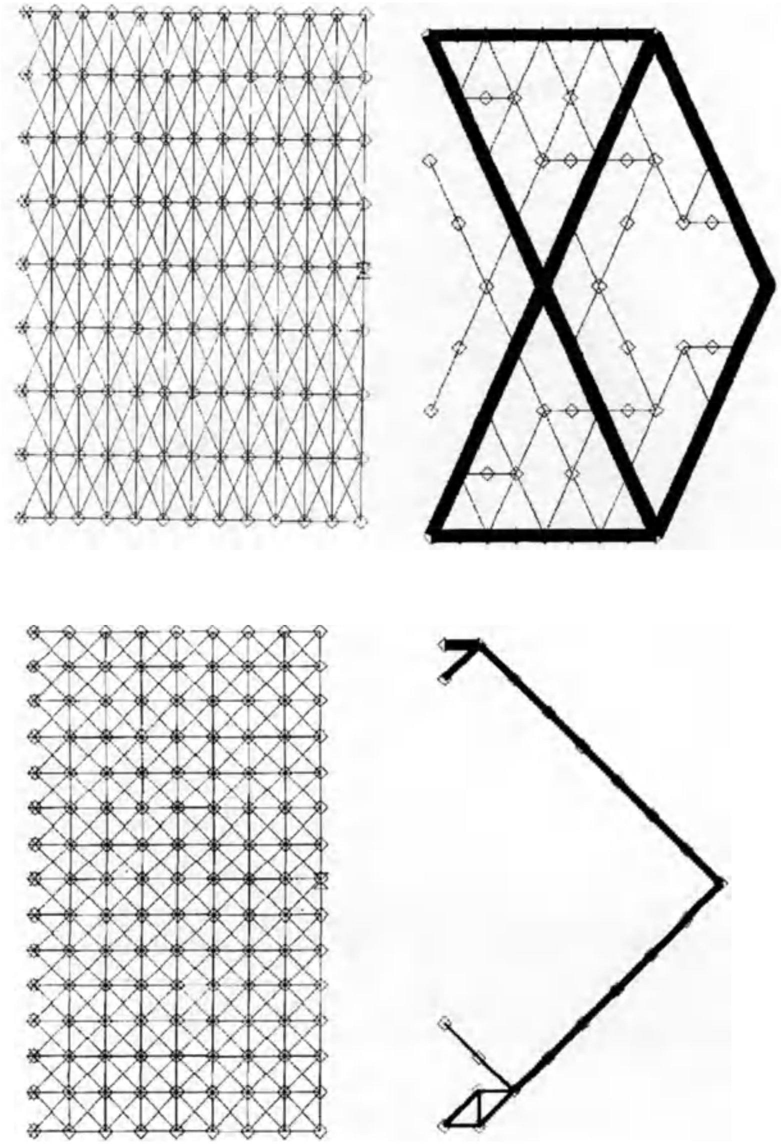

Fig. 4.4. The strong dependence of the topology of the optimal solution on the suitable choice of ground structure. For both examples we have one vertical load at the middle of the right hand side, and all nodes at the left hand side are possible supports. Top pictures show the ground structure and resulting optimal design for a 13 by 9 layout of nodes in a rectangular domain. The special form of the optimal topology is caused by the inability to transmit the force to the supports along direct 45^0 bars. The bottom pictures show the ground structure and resulting optimal design for a 9 by 15 layout of nodes in a rectangular domain. Here it is almost possible, but not quite possible to transmit the force to the supports along direct 45^0 bars. The ground structure in the lower figure is slightly asymmetric, resulting in an asymmetric design.

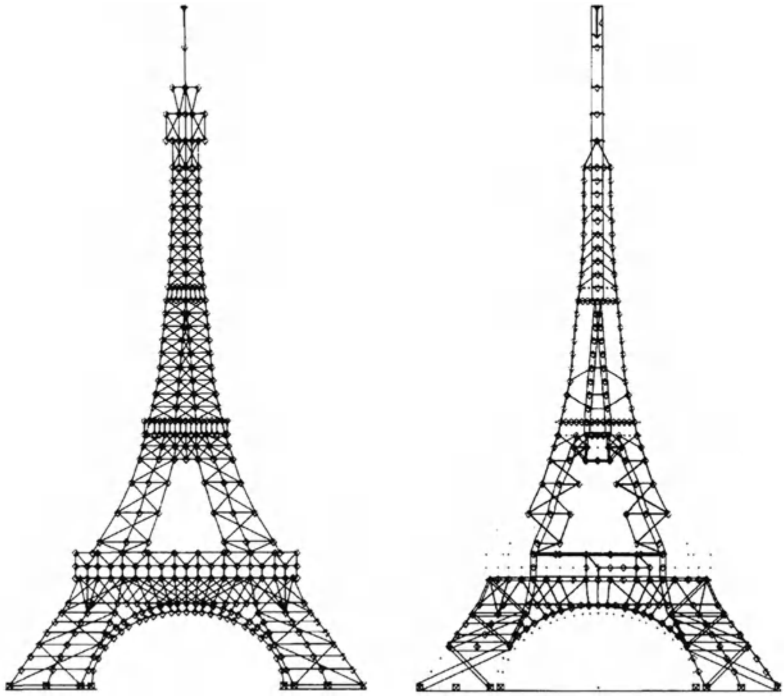

Fig. 4.5. The flexibility in choice of ground structure. Optimal design of a well-known structure. Left hand picture shows the ground structure and the right hand picture the optimal topology for a single downward load at the top of the structure. The example shows that it is reasonable to consider multiple load cases for realistic structures. By courtesy of M. Kocvara and J. Zowe.

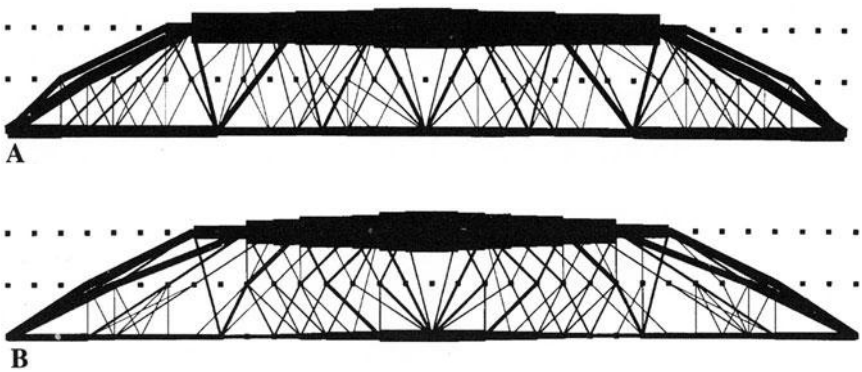

Fig. 4.6. The difference (and similarity) between multiple load case treated in the weighted average formulation (equal weights) *(A)* and treated in the worst case min-max formulation *(B)*. Optimal truss topologies for transmitting three vertical forces to two fixed supports as in Fig. 4.7A (cf. Fig. 4.2), but for a long slender rectangular ground structure of aspect ratio 16 (like a long span bridge), with 33 by 3 equidistant nodes and all 2818 possible non-overlapping connections. In the figures, the vertical scale has been distorted in order to being able to show the results. Bendsøe, Ben-Tal and Zowe, 1993.

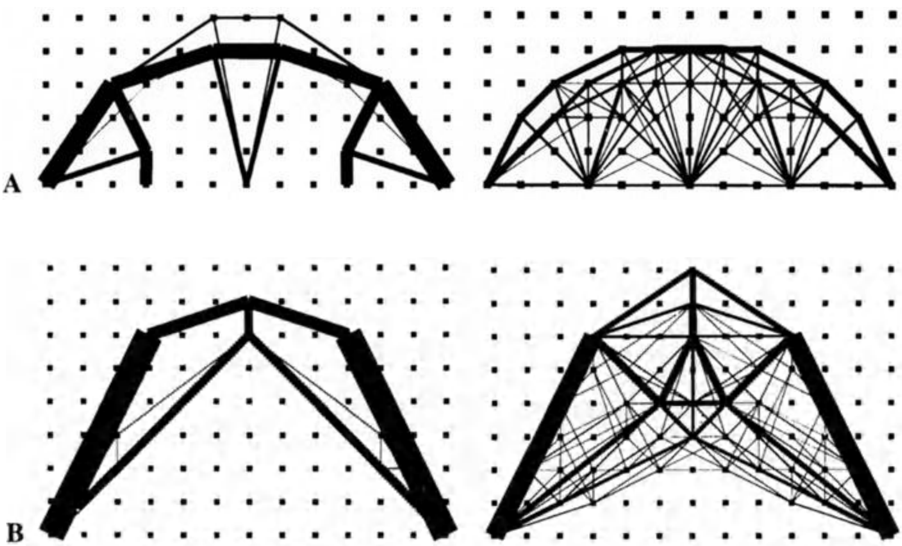

Fig. 4.7. The difference between multiple load and single load case problems. Optimal truss topologies for transmitting three vertical forces to two fixed supports. Two positions of the loads are considered and the trusses are optimized with the loads treated as a single load as well as three individual load cases for a min-max, worst case design situation. The ground structures consist of all 8744 possible non-overlapping connections between the nodal points of a regular 13 by 13 mesh in a square domain. The loads are vertical unit loads at three equidistant nodes along the lower line of nodes *(A)* or across the middle of the ground structure *(B)* (see also Fig. 4.2). The left hand column shows the single load results, the left hand column the multiple load, worst case results.. We do not show the uppermost rows of nodes, as these are not part of the optimal structure. A slight asymmetry of the ground structure is reflected in the optimal truss topologies. Bendsøe, Ben-Tal and Zowe, 1993.

Fig. 4.8. A detailed study situation of Fig. 4.7A, but with only the mid-span load applied. The ground structure is restricted to a rectangular domain of aspect ratio 2, and with the number of nodes increased to a 21 by 11 layout, with 16290 possible non-overlapping connections. Note that the supports have been moved in by two nodes from each vertical side, in order to identify an eventual restriction of having the supports at the extreme points of the ground-structure. Bendsøe, Ben-Tal and Zowe, 1993.

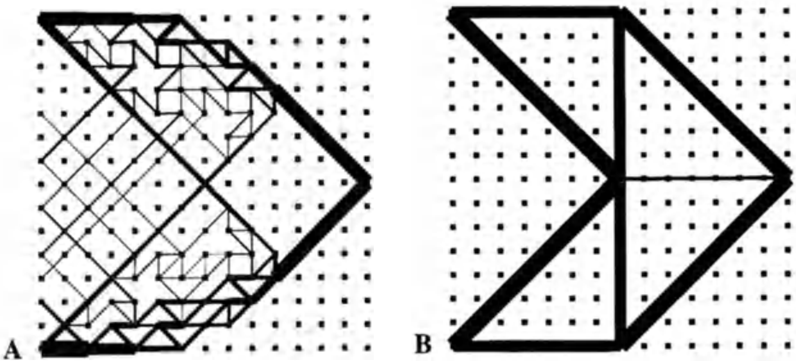

Fig. 4.9. A case where the introduction of multiple loads simplify the optimal lay-out. Also an example of the optimal topology for a ground structure with only neighbouring nodes in a square, regular 15 by 15 lay-out being connected (see Fig. 4.1B); this results in only 788 potential bars. All nodes at the left hand side are potential supports (see Fig. 4.2). *(A)*: The optimal topology for a single vertical load at the mid right hand node. *(B)*: The optimal topology for three load cases including the load of the single load problem. The load of the single load example is twice as large as the two other loads, one of which is a horizontal load at the mid right hand node while the last load is a vertical load at the centre of the ground structure. This is for a weighted average formulation with equal weights. The compliance for the load case number 1 increases by only 2.6%, as compared to *(A)*, which is optimal for this load only. Bendsøe, Ben-Tal and Zowe, 1993.

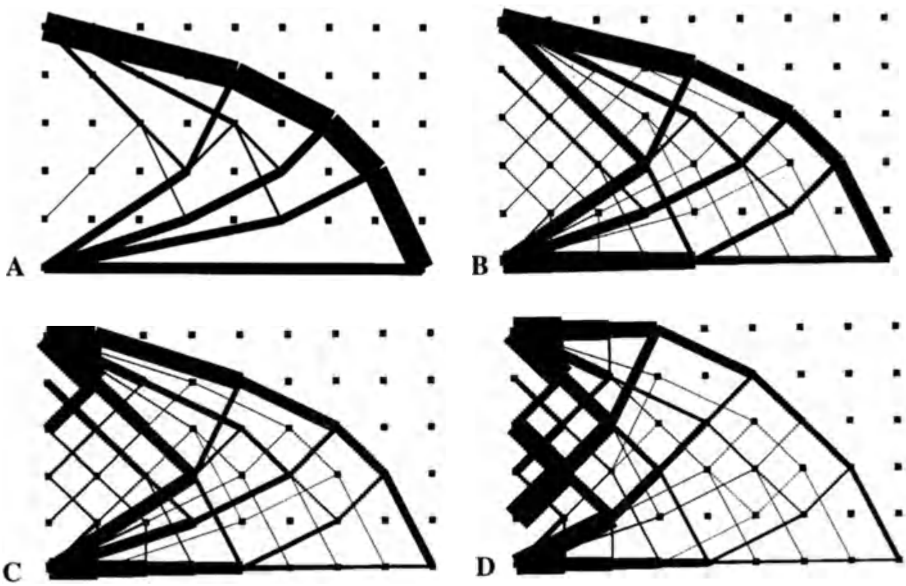

Fig. 4.10. The effect of self-weight loads. Optimal truss topologies for transmitting a single vertical force to a vertical line of supports (see Fig. 4.2). The figures show the variation for increasing specific self-weight loads, corresponding to increasing real lengths of the structures. In *(A)* self-weight is ignored, in *(B)* self-weight is present, increased by 2 times to the design *(C)*. These designs are obtained for a 9 by 6 equidistant nodal lay-out in a rectangular domain of aspect ratio 1.6, and all 919 possible *non-overlapping* connections. If all 1431 possible connections are used, the design *(C)* is modified to the design *(D)*. Bendsøe, Ben-Tal and Zowe, 1993.

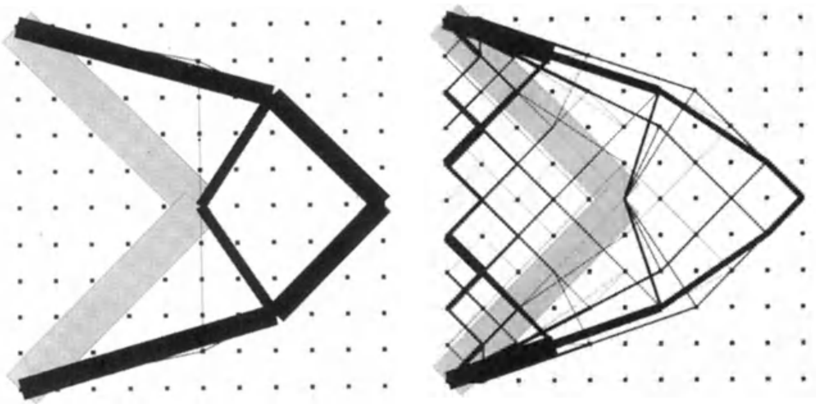

Fig. 4.11. A reinforcement example. Optimal truss topologies for transmitting two vertical forces to a vertical line of supports (see Fig. 4.2). The given structure is the optimal two-bar truss for carrying the load case number two at the centre of the ground structure. We then seek the optimal reinforcement of this structure, with the purpose of carrying load number one as well. The reinforcement problem is treated as a weighted average, multiple load problem, without (left) or with self-weight taken into account (right). The ground structure for reinforcement is the 11 by 11 equidistant nodal lay-out in a square, with all 4492 possible non-overlapping connections. Bendsøe, Ben-Tal and Zowe, 1993.

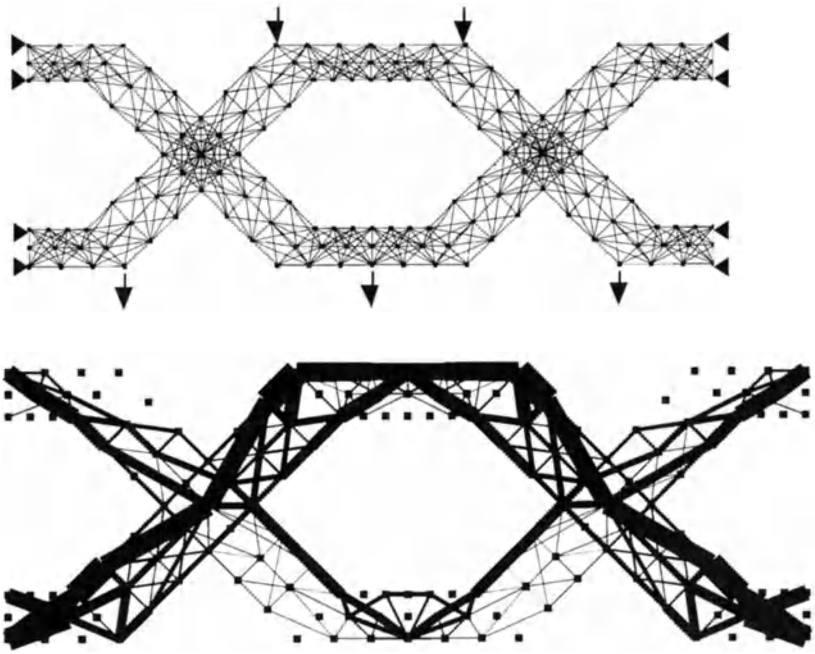

Fig. 4.12. An example of a complicated ground structure geometry, with 156 nodal points and 660 potential bars. The ground structure, supports and five loads are shown at the top. The resulting topology for a weighted average, multiple load problem formulation is shown below. The ground structure was generated by an interactive CAD-based programme, see Smith, 1994. Bendsøe, Ben-Tal and Zowe, 1993.

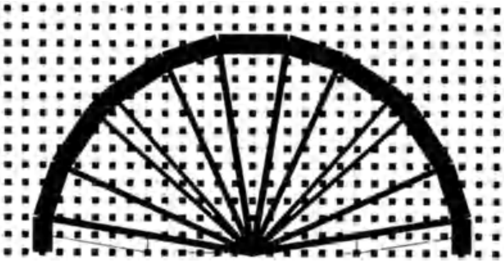

Fig. 4.13. The influence of the boundary conditions. A detailed study of the situation in Fig. 4.8 (single load case), but with the right hand support changed from a fixed support to a 'rolling' support which restricts movements in the vertical direction only. Also the number of nodes is increased to a 29 by 15 lay-out with all 57770 possible non-overlapping connections. Compare with Fig. 2.7. Bendsøe, Ben-Tal and Zowe, 1993.

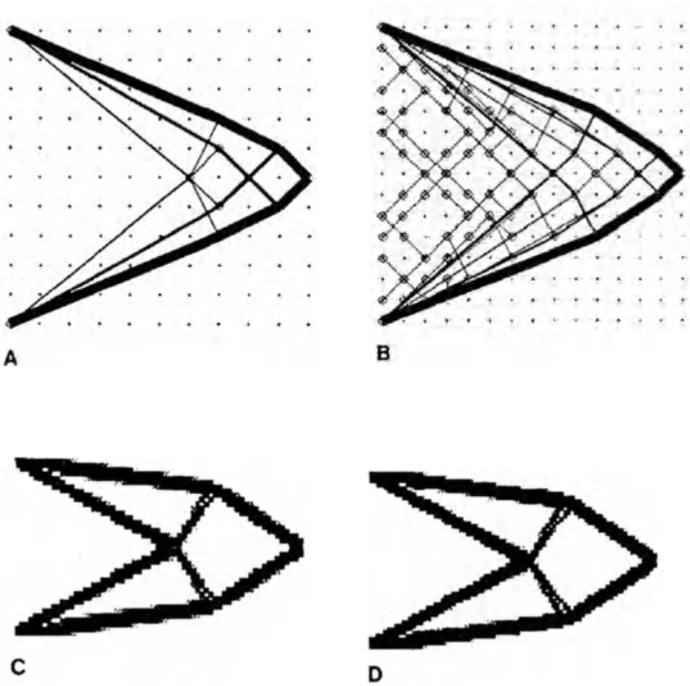

Fig. 4.14. The similarity between the results obtained by the homogenization method and truss topology design for 'thin' structures. Optimal topologies for transmitting a vertical force to a vertical line of supports, with a design domain whose vertical extension is less than or equal to its horizontal extension (cf., figure 4.2). *(A), (B)*: The optimal truss topology in a square with 11 by 11 and 15 by 15 nodes, respectively (7260 and 25200 potential bars, respectively). *(C), (D)*: The optimum continuum structural topologies for a 8 by 5 rectangular domain, a volume constraint of 25% and a FEM discretization of 64 by 40 and 80 by 50 quadrilateral elements, respectively. Continuum topologies obtained by the homogenization method, using square cells with rectangular holes for the microstructure.

5 Extensions of topology design methodologies

The topology design problems treated so far have all been characterized by being compliance problems for structures with linearly elastic response. The reason for this is the simplifications that are implied for analysis and numerical algorithms. However, we have also seen that these problems in their apparent simplicity are fairly complicated to treat because of the large scale nature of the problems and because of the need to relax the continuum formulations.

In a number of recent works we have seen a series of new developments in topology design of continuum problems, extending the methodology to more complex analysis models and to more complex design problem settings. Many studies are concerned with the understanding of the nature of optimal topologies for such more complicated design situations, with the homogenization modelling seen as a tool for generating continuous design parameters. The use of exact relaxed formulations or exact optimal microstructures is not central in these works. As history showed for the 2-D continuum problem, it is hoped that more theoretical work in the materials science and the theory of variational problems will at a later stage provide the answer to these questions.

The extensions of the topology design methodology can roughly be classified in two groups of problem types. One is the treating of more complicated design situations in the context of simple linear elasticity, an example being the design for vibration problems. The other type of extensions is the use of the basic minimum compliance formulation for more complicated analysis formulations, e.g., thermoelastic problems and elasto-plastic problems. In the coming chapters some of these extensions are described. The main topic will be the modelling problems associated with the extensions for continuum problems. The numerical issues related to treating these more complicated problems will be mentioned only briefly and we refer to the references for details on these issues. One promising approach in many cases is the use of optimality criteria methods or new specialized mathematical programming algorithms

5.1 Topology and material design for vibration problems

Eigenvalue optimization is a problem of particular interest in structural design, in the context of buckling analysis and in analysis of structural response in free-vibration (see for example Olhoff, 1987, for a review of this subject). Recently, the use of a homogenization method for layout optimization for this type of problem has been discussed by Díaz and Kikuchi, 1992 and Ma et. al., 1993, in the case of vibrations and by Neves, Guedes and Rodrigues, 1993, 1994, in the case of buckling. The design for specified spectral properties is not only important for suppression of vibration response of structures. The last decade has seen an increasing interest in structural control, and here the spectral properties are critical for the performance of the structure and associated control systems. Such issues are for example discussed in Bendsøe, Olhoff and Taylor, 1987, in the context of integrated design of structure and control system.

We shall here first consider the problem of free material design for vibration problems, and then briefly discuss the use of the homogenization modelling for such situations.

5.1.1 Optimization of material properties for improved frequency response

In this section we discuss the formulation and solution of an eigenvalue structural optimization problem where the design variables include the constitutive tensors that characterize material properties, as also described in chapter 3. Here, we focus our attention on the problem of maximizing the lowest eigenvalue of the structure in free vibration (Bendsøe and Díaz, 1994).

We consider a design problem in two or three dimensional elasticity where the elastic properties of the medium are represented by the constitutive tensor E, and its mass is characterised by a scalar function m. As the goal is to find optimum material distributions, both E and m are functions of the spatial co-ordinate x that may vary over the spatial domain Ω. We seek to maximize the lowest eigenvalue of the structure, namely, to maximize the solution to the problem

$$\lambda_1 = \min_{u \in U} \left[\int_\Omega E_{ijkl}\, \varepsilon_{ij}(u)\varepsilon_{kl}(u)\, \mathrm{d}\Omega \right] \left[\int_\Omega m u \cdot u \, \mathrm{d}\Omega \right]^{-1}$$

Formally, we may pose the optimization problem as follows:

$$\begin{aligned} &\max_{E,m} \ \lambda_1 \\ &\text{subject to :} \\ &\int_\Omega I_i \, \mathrm{d}\Omega \le V_i \quad i = 1,2,3; \qquad \int_\Omega m \, \mathrm{d}\Omega \le V_m \\ &E \ge 0, \qquad m \ge m_0 > 0 \end{aligned} \tag{5.1}$$

The parameters m_0, V_i and V_m are data for the problem. Inspired by the analysis in chapter 3, we use the *principal invariants* of the tensor E to measure the amount of available material, thus insuring that the formulation is independent of the choice of co-ordinate-system. The 3 principal invariants (in 2-D problems) can be expressed as

$$I_1 = \mathrm{tr}(\mathbf{D}) \qquad I_2 = -\frac{1}{2}[\mathrm{tr}(\mathbf{D}^2) - \mathrm{tr}(\mathbf{D})^2] \qquad I_3 = \det(\mathbf{D})$$

where $\mathbf{D}$ is a symmetric matrix representation of the symmetric tensor E with respect to any orthonormal basis of symmetric second order tensors. The constraint $E \geq 0$ implies that $I_i \geq 0$. Notice that six invariants are needed in 3-D problems, but for simplicity of exposition we restrict the presentation to 2-D problems.

It is crucial for the analysis to characterize the relation between elastic properties and mass. Both from practical considerations and to preserve well-posedness, E and m cannot be designed *independently*. However, to assume *a-priori* the existence of a one-to-one relationship between m and E would appear to be too restrictive. Fortunately, this is not necessary for the analysis, and we simply assume a point-to–set relation $m \in M(E) \subset R$. The set $M = M(E)$ is bounded below by zero and we assume here that it is closed. Elements in M are materials with the same elastic properties but different mass. Furthermore, as E is uniquely characterized by its principal invariants (up to a rotation that does not affect the mass), we may write $m \in M(I_1, I_2, I_3)$.

We notice now that for fixed E and u and M closed and bounded below, the quotient

$$R = \min_{u \in U} \left[\int_\Omega E_{ijkl}\ \varepsilon_{ij}(u)\varepsilon_{kl}(u)\ \mathrm{d}\Omega \right] \left[\int_\Omega m u \cdot u\ \mathrm{d}\Omega \right]^{-1}$$

is maximized by $\hat{m}$, the *smallest* element of M. Therefore, problem (5.1) can be written in terms of E only as:

$$\begin{aligned}
&\max_E\ \lambda_1 \\
&\text{subject to :} \\
&\int_\Omega I_i\ \mathrm{d}\Omega \leq V_i \quad i = 1,2,3; \quad \int_\Omega \hat{m}(I_1, I_2, I_3)\mathrm{d}\Omega \leq V_m \qquad (5.2) \\
&E \geq 0, \qquad \hat{m}(I_1, I_2, I_3) \geq m_0 > 0 \\
&\hat{m} = \min_{m \in M(D)} m
\end{aligned}$$

Finally, we need to impose some restrictions on the function $\hat{m}\,(I_1, I_2, I_3)$. We exclude a "frivolous" utilization of the mass and assume here that $\hat{m}$ is an increasing function of the three principal invariants of E. In words, of all materials with the same elastic properties, the one with the lowest mass is such that it cannot be made stiffer without making it heavier.

To simplify the notation, in what follows we drop the caret from $\hat{m}$ but keep in mind that $m(I_1,I_2,I_3)$ corresponds to the *lowest* mass realization among all materials with invariants (I_1,I_2,I_3).

Following the approach of previous developments, we introduce the *resource* measure $\boldsymbol{\rho}=(\rho_1,\rho_2,\rho_3)$ and replace problem (5.2) by the equivalent problem

$$\max_{\substack{E\geq 0\\ \int_\Omega I_i\,\mathrm{d}\Omega\leq V_i\\ \int_\Omega m(I_i)\,\mathrm{d}\Omega\leq V_m}} \lambda_1 = \max_{\boldsymbol{\rho}\in G}\ \max_{\substack{E\\ I_i(E)=\rho_i}}\ \min_{u\in U}\ \left[\int_\Omega E_{ijkl}\ \varepsilon_{ij}(u)\varepsilon_{kl}(u)\ \mathrm{d}\Omega\right]\left[\int_\Omega m(I_i)\ u\cdot u\,\mathrm{d}\Omega\right]^{-1} \tag{5.3}$$

where the feasible set G is defined as (cf., chapter 3)

$$G=\left\{\boldsymbol{\rho}\in\mathbf{R}^3\ \middle|\ \int_\Omega \rho_i\ \mathrm{d}\Omega\leq V_i, \int_\Omega m(\boldsymbol{\rho})\ \mathrm{d}\Omega\leq V_m,\ 0\leq\rho^i_{\min}\leq\rho_i\leq\rho^i_{\max}<\infty,\ m(\boldsymbol{\rho})\geq m_0\right\}$$

We now proceed as in chapter 3 to interchange the various minimization and maximization operations. The appearance of the rigidity dependent mass in the denominator precludes the direct application of a saddle point theorem, so instead we proceed in a slightly different manner. To this end, we can write

$$\max_{\boldsymbol{\rho}\in G}\ \max_{\substack{E\\ I_i(E)=\rho_i}}\ \min_{u\in U}\ \frac{\int_\Omega E_{ijkl}\ \varepsilon_{ij}(u)\varepsilon_{kl}(u)\ \mathrm{d}\Omega}{\int_\Omega m u\cdot u\ \mathrm{d}\Omega}\leq \max_{\boldsymbol{\rho}\in G}\ \min_{u\in U}\ \max_{\substack{E\\ I_i(E)=\rho_i}}\ \frac{\int_\Omega E_{ijkl}\ \varepsilon_{ij}(u)\varepsilon_{kl}(u)\ \mathrm{d}\Omega}{\int_\Omega m u\cdot u\ \mathrm{d}\Omega}$$

Since m depends only on the invariants, the term on the right-hand side may be expressed as follows:

$$\max_{\boldsymbol{\rho}\in G}\ \min_{u\in U}\ \max_{\substack{E\\ I_i(E)=\rho_i}}\ \frac{\int_\Omega E_{ijkl}\ \varepsilon_{ij}(u)\varepsilon_{kl}(u)\ \mathrm{d}\Omega}{\int_\Omega m u\cdot u\ \mathrm{d}\Omega}=\max_{\boldsymbol{\rho}\in G}\ \min_{\substack{u\in U\\ \int_\Omega m u\cdot u\ \mathrm{d}\Omega=1}}\ \max_{\substack{E\\ I_i(E)=\rho_i}}\ \int_\Omega E_{ijkl}\ \varepsilon_{ij}(u)\varepsilon_{kl}(u)\ \mathrm{d}\Omega$$

Also, since the material tensor can be chosen independently, point by point in Ω,

$$\begin{aligned}&\max_{\boldsymbol{\rho}\in G}\ \min_{\substack{u\in U\\ \int_\Omega m u\cdot u\ \mathrm{d}\Omega=1}}\ \max_{\substack{E\\ I_i(E)=\rho_i}}\ \int_\Omega E_{ijkl}\ \varepsilon_{ij}(u)\varepsilon_{kl}(u)\ \mathrm{d}\Omega\\ &\quad\leq \max_{\boldsymbol{\rho}\in G}\ \min_{\substack{u\in U\\ \int_\Omega m u\cdot u\ \mathrm{d}\Omega=1}}\ \int_\Omega\ \max_{\substack{E\\ I_i(E)=\rho_i}}\left\{E_{ijkl}\ \varepsilon_{ij}(u)\varepsilon_{kl}(u)\right\}\mathrm{d}\Omega\end{aligned}$$

Now focus on the inner problem in the right-hand side, which is similar to the problem (3.6) studied in section 3.2.1. Relaxing the constraints on the invariants, we have,

$$\max_{\substack{E \\ I_i(E)=\rho_i}} \left\{ E_{ijkl} \; \varepsilon_{ij}(u)\varepsilon_{kl}(u) \right\} \leq \max_{\substack{E \\ I_i(E)\leq\rho_i}} \left\{ E_{ijkl} \; \varepsilon_{ij}(u)\varepsilon_{kl}(u) \right\}$$

The solution to the right hand side problem follows from the treatment of the single load problem in section 3.2.2 and we have that

$$\max_{\substack{E \\ I_i(E)\leq\rho_i}} \left\{ E_{ijkl} \; \varepsilon_{ij}(u)\varepsilon_{kl}(u) \right\} = \rho_1 \; \varepsilon_{ij}(u)\varepsilon_{ij}(u) = \rho_1 \, E^0_{ijkl} \; \varepsilon_{ij}(u)\varepsilon_{kl}(u)$$

and the solution to the maximization problem is the orthotropic, rank-1 tensor

$$E^*_{ijkl} = \rho_1 \; \frac{\varepsilon_{ij}(u)\,\varepsilon_{kl}(u)}{\varepsilon_{pq}(u)\,\varepsilon_{pq}(u)}$$

for which we notice that $I_2(E^*_{ijkl}) = 0$, $I_3(E^*_{ijkl}) = 0$. Above, we have for reference written the optimal energy $\rho_1 \, \varepsilon_{ij} \, \varepsilon_{ij}$ in terms of the identity tensor E^0, which corresponds to an isotropic, zero-Poisson-ratio material. Combining the inequalities above, we get the following inequalities:

$$\begin{aligned} \max_{\rho\in G} \max_{\substack{E \\ I_i(E)=\rho_i}} \min_{u\in U} \frac{\int_\Omega E_{ijkl} \; \varepsilon_{ij}(u)\varepsilon_{kl}(u) \; \mathrm{d}\Omega}{\int_\Omega m u\cdot u \; \mathrm{d}\Omega} &\leq \max_{\rho\in G} \min_{u\in U} \frac{\int_\Omega \rho_1 \, \varepsilon_{ij}(u)\varepsilon_{ij}(u) \; \mathrm{d}\Omega}{\int_\Omega m(\boldsymbol{\rho}) \; u\cdot u \; \mathrm{d}\Omega} \\ &\leq \max_{\rho_1\in G_1} \min_{u\in U} \frac{\int_\Omega \rho_1 \, \varepsilon_{ij}(u)\varepsilon_{ij}(u) \; \mathrm{d}\Omega}{\int_\Omega m(\rho_1, 0, 0) \; u\cdot u \; \mathrm{d}\Omega} \end{aligned}$$

where the last inequality follows since m is an increasing function of the second and third invariants. Here we have introduced the feasible set

$$G_1 = \left\{ \rho_1 \;\middle|\; \begin{array}{l} \int_\Omega \rho_1 \; \mathrm{d}\Omega \leq V, \; \int_\Omega m(\rho_1, 0, 0) \; \mathrm{d}\Omega \leq V_m, \\ 0 \leq \rho^1_{\min} \leq \rho_1 \leq \rho^1_{\max} < \infty, \; m(\rho_1, 0, 0) \geq m_0 \end{array} \right\}$$

The last max-min problem is an eigenvalue problem for an elastic material of Poisson ratio zero, thickness ρ_1 and mass $m(\rho_1, 0, 0)$ and we may write

$$\min_{u\in U} \frac{\int_\Omega \rho_1\, \varepsilon_{ij}(u)\varepsilon_{ij}(u)\ \mathrm{d}\Omega}{\int_\Omega m(\rho_1,0,0)\ u\cdot u\ \mathrm{d}\Omega} = \min_{u\in U} \frac{\int_\Omega \rho_1\, E^0_{ijkl}\varepsilon_{ij}(u)\varepsilon_{kl}(u)\ \mathrm{d}\Omega}{\int_\Omega m(\rho_1,0,0)\ u\cdot u\ \mathrm{d}\Omega} = \mu_1(\rho_1)$$

where μ_1 is the lowest eigenvalue in this auxiliary problem.

To show that the inequalities above are in fact achieved, let $\rho_1 \in G_1$ be an arbitrary feasible density distribution and let ε^0 the be the strain field corresponding to the eigenmode u^0 for the auxiliary zero-Poisson-ratio problem with resource ρ_1. Now consider a design with

$$\boldsymbol{\rho}^0 = (\rho_1,0,0), \quad E^{\#}_{ijkl} = \rho_1 \frac{\varepsilon^0_{ij}\,\varepsilon^0_{kl}}{\varepsilon^0_{pq}\varepsilon^0_{pq}}$$

Clearly, this design is feasible for our original problem, as $\boldsymbol{\rho}^0 \in G$ and $I_1(E^{\#}_{ijkl}) = \rho_1$, $I_2(E^{\#}_{ijkl}) = 0$, $I_3(E^{\#}_{ijkl}) = 0$. Therefore

$$\min_{u\in U} \frac{\int_\Omega E^{\#}_{ijkl}\varepsilon_{ij}(u)\varepsilon_{kl}(u)\ \mathrm{d}\Omega}{\int_\Omega m(\rho_1,0,0)\ u\cdot u\ \mathrm{d}\Omega} \le \max_{\boldsymbol{\rho}\in G} \max_{\substack{E\\ I_i(E)=\rho_i}} \min_{u\in U} \frac{\int_\Omega E_{ijkl}\ \varepsilon_{ij}(u)\varepsilon_{kl}(u)\ \mathrm{d}\Omega}{\int_\Omega m u\cdot u\ \mathrm{d}\Omega}$$

But since

$$(E^{\#}\varepsilon^0)_{ij} = \rho_1 \frac{\varepsilon^0_{ij}\,\varepsilon^0_{kl}}{\varepsilon^0_{pq}\,\varepsilon^0_{pq}}\varepsilon^0_{kl} = \rho_1\varepsilon^0_{ij} = (\rho_1 E^0\varepsilon^0)_{ij}$$

we have that

$$\min_{u\in U} \frac{\int_\Omega E^{\#}_{ijkl}\varepsilon_{ij}(u)\varepsilon_{kl}(u)\ \mathrm{d}\Omega}{\int_\Omega m(\rho_1,0,0)\ u\cdot u\ \mathrm{d}\Omega} = \mu_1(\rho_1)$$

Therefore,

$$\max_{\rho_1\in G_1} \mu_1(\rho_1) \le \max_{\rho_1\in G_1} \min_{u\in U} \frac{\int_\Omega E^{\#}_{ijkl}\varepsilon_{ij}(u)\varepsilon_{kl}(u)\ \mathrm{d}\Omega}{\int_\Omega m(\rho_1,0,0)\ u\cdot u\ \mathrm{d}\Omega}$$

$$\le \max_{\mathbf{r}\in G} \max_{\substack{E\\ I_i(E)=\rho_i}} \min_{u\in U} \frac{\int_\Omega E_{ijkl}\ \varepsilon_{ij}(u)\varepsilon_{kl}(u)\ \mathrm{d}\Omega}{\int_\Omega m u\cdot u\ \mathrm{d}\Omega}$$

Furthermore, we have that

$$\max_{\rho\in G} \max_{\substack{E \\ I_i(E)=\rho_i}} \min_{u\in U} \frac{\int_\Omega E_{ijkl}\, \varepsilon_{ij}(u)\varepsilon_{kl}(u)\, \mathrm{d}\Omega}{\int_\Omega m u\cdot u\, \mathrm{d}\Omega}$$

$$\leq \max_{\rho_1\in G_1} \min_{u\in U} \frac{\int_\Omega \rho_1\, \varepsilon_{ij}(u)\varepsilon_{ij}(u)\, \mathrm{d}\Omega}{\int_\Omega m(\rho_1,0,0)\, u\cdot u\, \mathrm{d}\Omega} = \max_{\rho_1\in G_1} \mu_1(\rho_1)$$

so the *equalities* in fact, hold throughout. Indeed, the optimum resource allocation of ρ_1 in the original problem (5.1) can be obtained from the solution of the *auxiliary* eigenvalue maximization problem

$$\max_{\rho_1\in G_1} \mu_1(\rho_1) = \max_{\rho_1\in G_1} \min_{u\in U} \frac{\int_\Omega \rho_1\, \varepsilon_{ij}(u)\varepsilon_{ij}(u)\, \mathrm{d}\Omega}{\int_\Omega m(\rho_1,0,0)\, u\cdot u\, \mathrm{d}\Omega}$$

This is a problem of maximization of the fundamental frequency of a sheet of variable thickness ρ_1 and mass m, made of an isotropic material of zero Poisson ratio. Computationally, this is a much simpler problem to solve than (5.1), as it involves the determination of the spatial distribution of a single scalar variable, ρ_1.

This analysis shows that when the goal is to maximize a fundamental frequency, the generalization of more conventional layout optimization formulations to include the design of the material carries along surprisingly few complications. The solution of the problem is available from an *auxiliary* problem involving a variable thickness sheet and an isotropic material of zero Poisson ratio, a surprising simplification that is also present in problems of compliance minimization, as we have seen in chapter 3. This is available under assumptions that bear further study, particularly in connection with the relation between the stiffness and mass properties of a material. In the coming section we will restrict the admissible tensor to those available through homogenization with a single, isotropic base material. For this case the relation between the stiffness and mass is simple to specify.

5.1.2 Optimization of frequency response using the homogenization method

Using the homogenization modelling, the problem of maximizing the lowest eigenfrequency has the form

$$\max_{\rho,\mu,\gamma,\theta} \min_{u\in U} \frac{\int_\Omega E^H_{ijkl}(\rho,\mu,\gamma,\theta)\, \varepsilon_{ij}(u)\varepsilon_{kl}(u)\, \mathrm{d}\Omega}{\int_\Omega \alpha\rho u\cdot u\, \mathrm{d}\Omega}$$

$$\text{subject to :} \tag{5.4}$$

$$\int_\Omega \rho\ \mathrm{d}\Omega \leq V$$

$$0 \leq \rho(x) \leq 1,\ \ x\in\Omega$$

where α is the specific mass of the basis material.

This is now a standard sizing problem involving eigenfrequencies, albeit with a large number of design variables. For a solution where the optimal eigenvalue is single modal the necessary conditions of optimality are very similar to the conditions for a minimum compliance design and the use of an optimality criteria algorithm is a straightforward and reliable solution procedure (Olhoff, 1970. 1974, 1976, Díaz and Kikuchi, 1992). However, if the solution is multi-modal, the eigenvalue is a non-differentiable function of design and the derivations of necessary conditions of optimality becomes more cumbersome and special algorithms from non-smooth analysis are required. These questions are too involved to address here, so the reader is referred to the literature [29].

Note here that the problem (5.4) as stated is not well-posed. One can in this problem as stated remove the structure completely, obtaining an infinite frequency. Thus (5.4) should normally be considered in the framework of reinforcement of a given structure, given through a fixed given distribution of a material (or structure) described by a rigidity and associated mass $E^0_{ijkl}(x)$, $m_0(x)$. Thus the problem statement becomes

$$\max_{\rho,\mu,\gamma,\theta} \min_{u\in U} \frac{\int_\Omega \left[E^0_{ijkl} + E^H_{ijkl}(\rho,\mu,\gamma,\theta)\right] \varepsilon_{ij}(u)\varepsilon_{kl}(u)\, \mathrm{d}\Omega}{\int_\Omega \left[m_0 + \alpha\rho\right]\, u\cdot u\, \mathrm{d}\Omega}$$

$$\text{subject to :} \tag{5.5}$$

$$\int_\Omega \rho\ \mathrm{d}\Omega \leq V$$

$$0 \leq \rho(x) \leq 1,\ \ x\in\Omega,$$

We remark here that the limit problem of eigenvalue problems for a material with microstructure is described by the homogenized elasticity operator and the bulk density ρ, as the weak limit of the mass distribution [29]. Thus (5.5) is consistent with the limiting process of introducing finer and finer details in a 0-1 type design.

Moreover, we note that we in (5.5) have that the density ρ is independent of the local pointwise distribution of material, so that extremal composites and extremal strain energies take on a similar meaning as for the minimum compliance problem, as discussed in chapter 3. We can thus write an upper bound problem as

$$\max_{\rho} \quad \min_{\substack{u \in U \\ \int_\Omega [m_0 + \alpha\rho]\, u \cdot u \, d\Omega = 1}} \quad \int_\Omega \left[E^0_{ijkl}\varepsilon_{ij}(u)\varepsilon_{kl}(u) + \max_{\substack{\mu,\gamma,\theta \\ \mathrm{vol}(\mu,\gamma)=\rho}} E^H_{ijkl}(\rho,\mu,\gamma,\theta)\varepsilon_{ij}(u)\varepsilon_{kl}(u) \right] d\Omega$$

subject to :

$$\int_\Omega \rho \ d\Omega \leq V$$

$$0 \leq \rho(x) \leq 1, \quad x \in \Omega,$$

where the inner maximization of local strain energy density was derived in detail in section 2.2.

The frequency problem will not be covered in further detail here; the reader is referred to the references and literature cited therein [29]. However to indicate what type of results that can be obtained, two examples of optimal topologies of reinforcement for improved vibration response are included below.

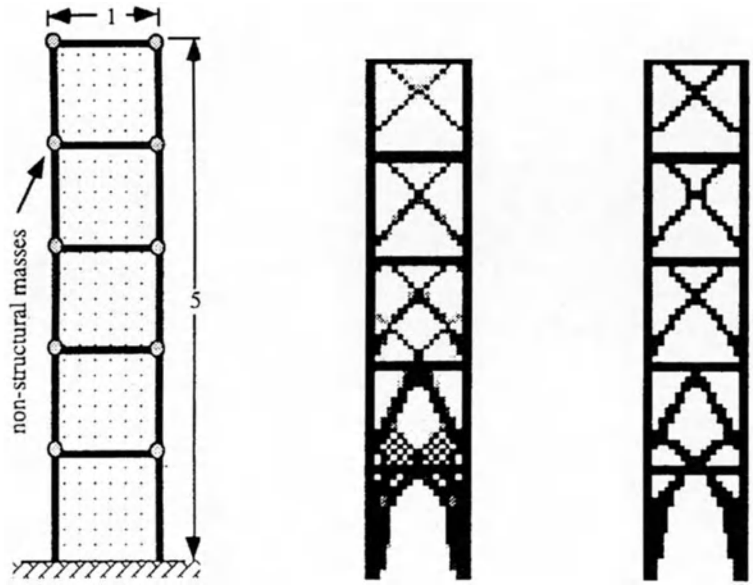

Fig. 5.1. Optimal reinforcement of a 5 bay truss tower structure for increase of the fundamental frequency. Non-structural masses are attached to the nodes. The problem geometry is shown to the left. The reinforcement corresponds to 18% of the design domain, which is discretized using a 100 by 20 mesh of Q4 elements. The optimum topology of reinforcement and a postprocessed black/white design is shown to the right; here the eigenvalue has been increased by 9.1 (and 7.7) times in relation to the unreinforced structure. No checkerboard control was used. By courtesy of A. R. Díaz and N. Kikuchi.

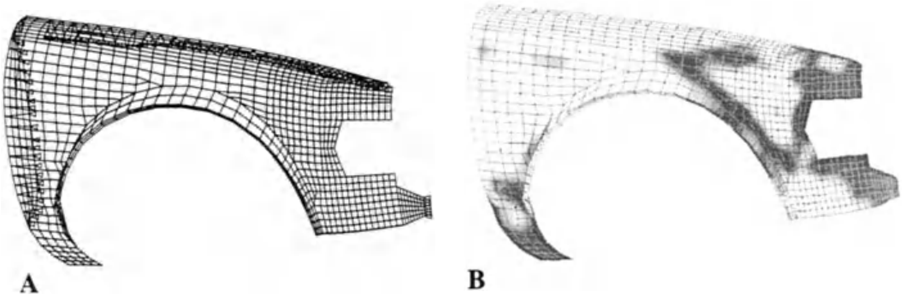

Fig. 5.2. Optimal reinforcement of a car fender (mudguard) for increase of the fundamental frequency. *(A)* shows the problem geometry and *(B)* the optimum topology of reinforcement. By courtesy of A. R. Díaz.

5.2 Topology and material design for materials with piece wise linear elastic behaviour

In chapter 3 we dealt with the design of material properties in the context of global structural optimization to provide, in analytical form, a prediction of the optimal material tensor distributions for two or three dimensional continuum structures. The model developed is extended here to cover the design of a structure and associated material properties for a system composed of a generic form of *nonlinear softening material.* As was established in the earlier study on design with linear materials, the formulation for combined 'material and structure' design with softening materials can also be expressed as a convex problem. However, the optimal distribution of material properties predicted in the nonlinear problem depends on the magnitude of load, in contrast to the case with linear material.

5.2.1 Problem statement

The purpose here is to treat, in analytical form, the design problem for simultaneous prediction of material properties and structure for a structure composed of a generic form of nonlinear softening material (Bendsøe, Guedes, Plaxton and Taylor, 1994). The relevant mechanics is represented in terms of a generalized complementary energy principle and the design objective is likewise based on complementary energy. Net material properties of the softening medium reflect a superposition of properties associated with each of a number of material constituents, and the collection of these properties, expressed through the rigidity tensors for each of these constituents, provides the problem with a set of design parameters. Analytical forms of the optimal material tensor as well as for the global distribution of material can be derived, in much the same way as described earlier for linear materials and the results have an analogous structure. If the design parameters are removed entirely from the problem, the reduced problem is an equilibrium only problem, albeit with a nonlinear and non-smooth (optimal) complementary energy functional. However, by only solving analytically for the optimal local properties, the reduced problem is a smooth and convex problem combining analysis and the determination of the optimal distribution of bulk resource.

As indicated above, it is the availability of an extremum problem formulation for the analysis part of the problem that makes it possible to treat the design of nonlinear materials conveniently. The type of formulation used in the following development, which amounts to a generalized form of complementary energy principle, is presented in detail in Taylor, 1993a. It is described briefly here to set the stage for the subsequent extension to cover design. The portrayal of a general form of nonlinear softening material relies on a feature in the model that has total stress expressed via a superposition of an arbitrary number of independent (constituent) fields. Each field is represented to be arbitrarily heterogeneous and anisotropic. Overall material properties are then determined by a set of parameters that appear as data in the problem statement. These parameters serve to govern the individual constituent fields, and therefore how the softening material is modelled by these fields in combination.

The formulation for equilibrium analysis is stated here first in terms of mixed stress and deformation fields. With the superposition of M softening components and one purely elastic basis component to make up the total stress, the problem has the form:

$$
\begin{aligned}
&\max_{\alpha,\sigma^k,u}\ \alpha \\
&\text{subject to:} \\
&\operatorname{div}\Big(F_{ijrs}\varepsilon_{rs}(u)+\sum_{k=1}^{M}\sigma_{ij}^{k}\Big)+\alpha\, p=0 \\
&\Big(F_{ijrs}\varepsilon_{rs}(u)+\sum_{k=1}^{M}\sigma_{ij}^{k}\Big)\cdot n=\alpha t \quad \text{on} \quad \Gamma_T,\ u=0 \ \text{ on } \ \Gamma_0 \\
&\sigma^k\in \mathbf{K}_k\ ,\ k=1,\dots,M \\
&\tfrac{1}{2}\int_{\Omega}\Big(F_{ijrs}\,\varepsilon_{ij}(u)\varepsilon_{rs}(u)+\sum_{k=1}^{M}C_{ijrs}^{k}\,\sigma_{ij}^{k}\,\sigma_{rs}^{k}\Big)\,\mathrm{d}\Omega\le\Phi
\end{aligned}
$$

Here $C_{ijrs}^{k}={E_{ijrs}^{k}}^{-1}$ are the compliance tensors for the M softening components and F is the rigidity tensor for the basis component. The stresses for the softening components are denoted σ_{ij}^{k} and the displacement of the continuum by u. The convex sets of admissible stresses σ_{ij}^{k} for the softening components are denoted by $\mathbf{K}_k$. The problem is written for a given material, and the combined compliance tensors, rigidity tensor, and the information that serves to define sets $\mathbf{K}_k$ comprise the data by which overall material properties are set. For the design of material properties to be considered below, one or more of these items of data are treated as design variables.

As an alternative, the basic equilibrium analysis problem can be stated in terms of stresses alone as:

$$
\begin{aligned}
&\max_{\alpha,\sigma^k,\gamma} \ \alpha \\
&\text{subject to}: \\
&\operatorname{div}(\gamma_{ij} + \sum_{k=1}^{M} \sigma_{ij}^k) + \alpha\, p = 0 \\
&(\gamma_{ij} + \sum_{k=1}^{M} \sigma_{ij}^k) \cdot n = \alpha t \quad \text{on} \quad \Gamma_T, \\
&\sigma^k \in \mathbf{K}_k \ , \ k = 1,\ldots,M \\
&\tfrac{1}{2}\int_\Omega (D_{ijrs}\gamma_{ij}\gamma_{rs} + \sum_{k=1}^{M} C_{ijrs}^k \sigma_{ij}^k \sigma_{rs}^k)\, \mathrm{d}\Omega \le \Phi
\end{aligned}
$$

where $D_{ijrs} = F_{ijrs}^{\ \ -1}$. This form of the problem statement is a parametrized complementary energy formulation for the general softening material. The solution to this problem predicts a bound to the equilibrium load within the limit Φ on total complementary energy.

Let us now consider the design of the nonlinear material for maximization of load carrying capacity. Using the rigidity tensors as free design variables, this design problem has the form:

$$
\begin{aligned}
&\sup_{E^k,\, F} \ \max_{\alpha,\sigma^k,\gamma} \ \alpha \\
&\text{subject to}: \\
&\operatorname{div}(\gamma_{ij} + \sum_{k=1}^{M} \sigma_{ij}^k) + \alpha\, p = 0 \\
&(\gamma_{ij} + \sum_{k=1}^{M} \sigma_{ij}^k) \cdot n = \alpha t \quad \text{on} \quad \Gamma_T, \\
&\sigma^k \in \mathbf{K}_k \ , \ k = 1,\ldots,M \\
&\tfrac{1}{2}\int_\Omega (F_{ijrs}^{\ \ -1}\gamma_{ij}\gamma_{rs} + \sum_{m=1}^{M} E_{ijrs}^{k\ \ -1} \sigma_{ij}^k \sigma_{rs}^k)\, \mathrm{d}\Omega \le \Phi \qquad (5.6) \\
&E^k > 0, \ F > 0, \\
&\int_\Omega \Psi(F)\, \mathrm{d}\Omega \le V_0, \ \int_\Omega \Psi(E^k)\, \mathrm{d}\Omega \le V_k, \ k = 1,\ldots,M
\end{aligned}
$$

As in earlier developments the design is to be optimal with respect to sets covering all positive definite rigidity tensors, and 'material resource' is measured in terms of invariants of these tensors (Ψ is the trace or the Frobenius norm, cf., chapter 3). Notice that we take the supremum over the rigidity tensors, as we are using a stress based formulation; this is inherent to the analysis case under study. Also, each phase has a limited total amount of resource.

In the formulation above it is assumed that the softening constraints for the softening components σ^k of total stress are *design independent*. Thus the solution predicts the optimal distribution of rigidities within these specified softening limits (optimal design with the limits themselves as design variables is treated for arbitrary trussed structures in Taylor, 1993c).

In the case of truss structures modelled as above, design for maximum load carrying capacity using member cross-sectional areas as design variables has been studied in Bendsøe, Olhoff and Taylor, 1993, for the case of an elasto-plastic formulation; in this case the design covers the elasto-plastic design as well as limit load design, depending on the relative size of the parameters of the problem. The type of results that are obtained by such studies are shown in figure 5.3, below. Truss design for the general softening material is reported in Taylor and Logo, 1993 and Taylor, 1993c.

Problem (5.6) is simultaneously convex in stress and design variables and is (up to a rescaling factor on the load) equivalent to the convex problem:

$$
\begin{aligned}
&\inf_{E^k,\,F}\ \min_{\sigma^k,\gamma}\ \tfrac{1}{2}\int_\Omega \Big(F_{ijrs}^{-1}\gamma_{ij}\gamma_{rs} + \sum_{k=1}^{M} E_{ijrs}^{k\ -1}\sigma_{ij}^k\sigma_{rs}^k\Big)\,\mathrm{d}\Omega \\
&\text{subject to:} \\
&\operatorname{div}\Big(\gamma_{ij} + \sum_{k=1}^{M}\sigma_{ij}^k\Big) + \overline{\alpha}\,p = 0 \\
&\Big(\gamma_{ij} + \sum_{k=1}^{M}\sigma_{ij}^k\Big)\cdot n = \overline{\alpha}\,t \quad \text{on} \quad \Gamma_{\mathrm{T}}, \\
&\sigma^k \in \mathbf{K}_k\,,\ k = 1,\ldots,M \qquad\qquad (5.7)\\
&E^k > 0,\ F > 0, \\
&\int_\Omega \Psi(F)\,\mathrm{d}\Omega \le V_0,\ \int_\Omega \Psi(E^k)\,\mathrm{d}\Omega \le V_k,\ k = 1,\ldots,M
\end{aligned}
$$

This is a generalized complementary energy formulation of the design of structures with piecewise linear behaviour.

For further discussions on analysis models and sizing and shape design for elasto-plastic problems we refer to the bibliographical notes [30] and the references of the literature mentioned there.

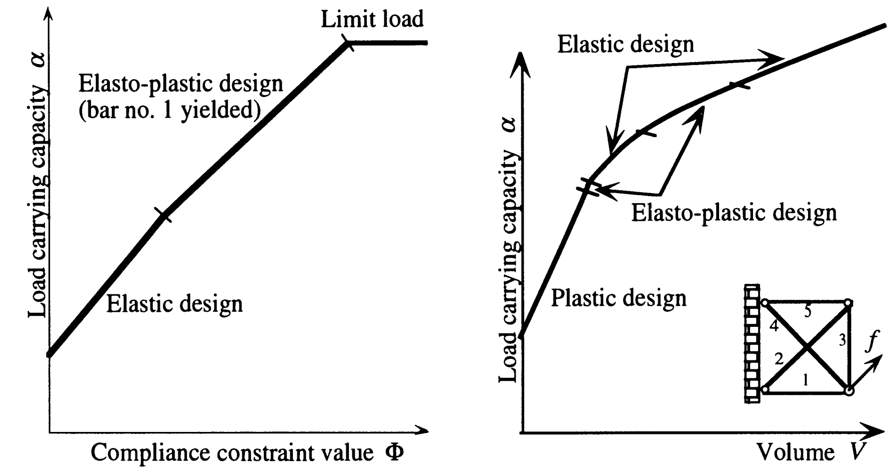

Fig. 5.3. Optimal design of a 5-bar truss for maximum load carrying capacity over the elastic, elasto-plastic and limit load range (cf., problem (5.6) above). Upper constraints on bar areas are enforced. Left hand graph is for fixed volume, right hand graph for fixed compliance constraint. Bendsøe, Olhoff and Taylor, 1993

5.2.2 Analytical reduction of the problem

Along the lines of the analysis in chapters 2 and 3, parameters that describe the structure are now divided into two groups, namely those parameters that measure the amount of resource assigned to each point of the domain, and a second set that delineates how this resource is used to form the local material tensor. This division leads to the following multi-level formulation of the problem:

$$\inf_{\substack{\rho_k,\ \rho_0 \\ \int_\Omega \rho_0 \, d\Omega \le V_0,\ \int_\Omega \rho_k \, d\Omega \le V_k}} \ \inf_{\substack{E^k > 0,\ F > 0, \\ \Psi(F) \le \rho_0, \\ \Psi(E^k) \le \rho_k}} \left\{ \begin{array}{l} \min\limits_{\sigma^k, \gamma} \frac{1}{2} \int\limits_\Omega (F_{ijrs}^{-1} \gamma_{ij} \gamma_{rs} + \sum\limits_{k=1}^{M} E_{ijrs}^{k\ -1} \sigma_{ij}^k \sigma_{rs}^k) d\Omega \\ \text{subject to:} \\ \operatorname{div}(\gamma_{ij} + \sum\limits_{k=1}^{M} \sigma_{ij}^k) + \bar{\alpha}\, p = 0 \\ (\gamma_{ij} + \sum\limits_{k=1}^{M} \sigma_{ij}^k) \cdot n = \bar{\alpha}\, t \quad \text{on} \quad \Gamma_T, \\ \sigma^k \in \mathbf{K}_k, \ k = 1, \ldots, M \end{array} \right\} \tag{5.8}$$

Here the static admissibility conditions of the inner problem are independent of the design variables. Thus minimization with respect to the pointwise variation of the rigidity tensors can be represented in the form:

$$\inf_{\substack{E^k>0,\ F>0, \\ \Psi(F)\le\rho_0, \\ \Psi(E^k)\le\rho_k}} \left\{ F_{ijrs}^{\ -1}\gamma_{ij}\gamma_{rs} + \sum_{k=1}^{M} E_{ijrs}^{k\ \ -1}\sigma_{ij}^{k}\sigma_{rs}^{k} \right\}$$

This characterization is consistent with the assumption of pointwise independent variation of the tensors within fixed values ρ_0, ρ_k of resource. As noted in section 3.2.2, we have that

$$\inf_{E>0,\Psi(E)\le\rho} E_{ijkl}^{-1}\sigma_{ij}\sigma_{kl} = \frac{1}{\rho}\sigma_{ij}\sigma_{ij}$$

for any stress field and any rigidity tensor. This result applies for both the trace and Frobenius norm measures of resource and this optimal energy expression coincides with the energy of a linearly elastic, zero-Poisson-ratio material of density ρ. This infimum is not achieved, but the infimum can be realized by the *singular compliance* tensor (compare with section 3.2.2)

$$C_{ijkl} = \frac{1}{\rho}\frac{1}{\sigma_{pq}\sigma_{pq}}\sigma_{ij}\sigma_{kl}$$

With the introduction of the optimal local energy expression, the problem (5.8) can be reduced to the convex problem:

$$\begin{aligned}
&\inf_{\rho_k>0,\ \rho_0>0}\ \min_{\sigma^k,\gamma}\ \tfrac{1}{2}\int_{\Omega}\left(\frac{1}{\rho_0}\gamma_{ij}\gamma_{ij} + \sum_{k=1}^{M}\frac{1}{\rho_k}\sigma_{ij}^{k}\sigma_{ij}^{k}\right)\mathrm{d}\Omega \\
&\text{subject to:} \\
&\operatorname{div}\Big(\gamma_{ij} + \sum_{k=1}^{M}\sigma_{ij}^{k}\Big) + \bar{\alpha}\,p = 0 \\
&\Big(\gamma_{ij} + \sum_{k=1}^{M}\sigma_{ij}^{k}\Big)\cdot n = \bar{\alpha}\,t \quad \text{on } \Gamma_T, \qquad\qquad (5.9) \\
&\sigma^k \in \mathbf{K}_k,\ k = 1,\dots,M \\
&\int_{\Omega}\rho_0\,\mathrm{d}\Omega \le V_0,\ \int_{\Omega}\rho_k\,\mathrm{d}\Omega \le V_k,\ k = 1,\dots,M
\end{aligned}$$

In (5.9) the energy measure for each constituent corresponds to the complementary energy of a linear elastic, zero-Poisson-ratio material of density equal to the locally assigned resource value.

In problem (5.9) we can solve for the resource densities, facilitated by the fact that the static admissibility conditions of the inner equilibrium problem are independent of the design variables. Combining the optimality condition with the (active) resource constraints the resource densities can be expressed as:

$$\rho_0 = V_0 \frac{\sqrt{\gamma_{ij}\gamma_{ij}}}{\int\limits_{\Omega} \sqrt{\gamma_{ij}\gamma_{ij}}\ \mathrm{d}\Omega}\ ,\ \rho_k = V_k \frac{\sqrt{\sigma_{ij}^k \sigma_{ij}^k}}{\int\limits_{\Omega} \sqrt{\sigma_{ij}^k \sigma_{ij}^k}\ \mathrm{d}\Omega}$$

With the insertion of this result in problem statement (5.9), the equivalent but now design independent problem takes the form:

$$\begin{aligned}
&\min_{\sigma^k,\gamma} \ \frac{1}{2V_0}\left[\int_\Omega \sqrt{\gamma_{ij}\gamma_{ij}}\ \mathrm{d}\Omega\right]^2 + \sum_{k=1}^{M} \frac{1}{2V_k}\left[\int_\Omega \sqrt{\sigma_{ij}^k\sigma_{ij}^k}\ \mathrm{d}\Omega\right]^2 \\
&\text{subject to:} \\
&\operatorname{div}(\gamma_{ij} + \sum_{k=1}^{M} \sigma_{ij}^k) + \bar{\alpha}\, p = 0 \\
&(\gamma_{ij} + \sum_{k=1}^{M} \sigma_{ij}^k)\cdot n = \bar{\alpha}\, t \quad \text{on} \quad \Gamma_{\mathrm{T}}, \\
&\sigma^k \in \mathbf{K}_k\ ,\ k = 1,\ldots,M
\end{aligned}$$

This (convex) problem is a generalized minimum complementary energy statement that is applicable for a linear-softening material with a non-smooth energy functional, one that is not simply quadratic. However, the energy functional is homogeneous of degree two, meaning that the energy functional under proportional load resembles the energy of a elastic-softening material with linear material components. This problem constitutes a generalization of the classical plastic design formulations (cf., chapter 4) for truss structures, the extension here covering linear-softening materials in a continuum setting. The counterpart for truss structures with linear-softening material can be stated in the form (with the notation of chapter 4):

$$\begin{aligned}
&\min_{\sigma^k,\gamma} \ \frac{1}{2V_0}\left[\sum_{i=1}^{m} a_i l_i |\gamma_i|\right]^2 + \sum_{k=1}^{M}\left(\frac{1}{2V_k}\left[\sum_{i=1}^{m} a_i l_i |\sigma_i^k|\right]^2\right) \\
&\text{subject to:} \\
&\mathbf{B}_{ij}\ (a_i\gamma_i + \sum_{k=1}^{M} a_i\sigma_i^k) = \bar{\alpha}\, p_j \\
&|\sigma_i^k| \le \bar{\sigma}^k\ ,\ k = 1,\ldots,M
\end{aligned}$$

The computational results presented below are obtained using a code for smooth optimization problems, to solve examples that are interpreted in the form of the (convex and smooth) problem (5.9). The smoothness is obtained at the expense of an increased number of variables. Alternatively, one can revert to the original problem form of finding the maximal load carrying capacity, i.e. the problem:

$$
\begin{aligned}
&\max_{\rho_k,\,\rho_0} \quad \max_{\alpha,\sigma^k,\gamma} \quad \alpha \\
&\text{subject to:} \\
&\operatorname{div}(\gamma_{ij} + \sum_{k=1}^{M} \sigma_{ij}^k) + \alpha\, p = 0 \\
&(\gamma_{ij} + \sum_{k=1}^{M} \sigma_{ij}^k)\cdot n = \alpha t \quad \text{on} \quad \Gamma_T, \\
&\sigma^k \in \mathbf{K}_k \,,\; k = 1,\dots,M \\
&\tfrac{1}{2}\int_\Omega (\frac{1}{\rho_0}\gamma_{ij}\gamma_{ij} + \sum_{k=1}^{M} \frac{1}{\rho_k}\sigma_{ij}^k \sigma_{ij}^k)\,\mathrm{d}\Omega \;\le \Phi \\
&\int_\Omega \rho_0 \,\mathrm{d}\Omega \le V_0 ,\; \int_\Omega \rho_k \,\mathrm{d}\Omega \le V_k ,\; k = 1,\dots,M \\
&0 < \rho_0^{\min} \le \rho_0 \le \rho_0^{\max} < \infty \\
&0 < \rho_k^{\min} \le \rho_k \le \rho_k^{\max} < \infty \,,\; k = 1,\dots,M
\end{aligned}
$$

Bounds are imposed here on the range of variation of the resource variables in order to facilitate the computational work.

5.2.3 A problem with elastic/stiffening material

For the sake of completeness of presentation we will very briefly outline how the analysis above can be performed for an analogous problem of designing a structure made of a general type of *elastic/stiffening* material. The analysis model is a displacement based equivalent to the models used above. A detailed description of the model can be found in Taylor, 1993b. With the analysis model written as an inner problem (as above), the design problem with free material parametrization becomes

$$
\begin{aligned}
&\max_{E^k,\,F} \quad \min_{\substack{\varepsilon^k, k=0,\dots,M,\\ u}} \left\{ \int_\Omega (\tfrac{1}{2} F_{ijrs}\, \varepsilon_{ij}^0\, \varepsilon_{rs}^0 + \sum_{k=1}^{M} \tfrac{1}{2} E_{ijrs}^k\, \varepsilon_{ij}^k\, \varepsilon_{rs}^k - p u)\,\mathrm{d}\Omega - \int_{\Gamma_T} t u \,\mathrm{d}\Gamma \right\} \\
&\text{subject to:} \\
&(\varepsilon_{ij}^0 + \sum_{k=1}^{M} \varepsilon_{ij}^k) = \frac{1}{2}(\frac{\partial u_i}{\partial x_j} + \frac{\partial u_j}{\partial x_i}) \;\text{ in }\; \Omega, \\
&\varepsilon^k \in \mathbf{H}_k \,,\; k = 1,\dots,M \\
&F \ge 0,\; \int_\Omega \Psi(F)\,\mathrm{d}\Omega \le V_0 , \\
&E^k \ge 0,\; \int_\Omega \Psi(E^k)\,\mathrm{d}\Omega \le V_k ,\; k = 1,\dots,M
\end{aligned}
\qquad (5.10)
$$

The analysis here covers the possibility of locking, with total strain consisting of a superposition of M possible locking phases and one basic non-locking phase. The admissible strains for the locking phases belong to convex sets $\mathbf{H}_k$. The inner analysis problems constitutes a generalized minimum potential energy formulation, and the design problem a generalization of the problem of minimizing the compliance (maximizing stiffness) of a structure, subject to a single load condition. Assuming that the sets $\mathbf{H}_k$ are design independent, problem (5.10) satisfy a saddle point condition if additional pointwise bounds on the resource are included (cf. chapter 3). This means that we can solve for the local properties and the optimization problem reduces to

$$
\begin{aligned}
&\max_{\rho_k,\rho_0} \min_{\substack{\varepsilon^k,k=0,..,M,\\ u}} \left\{ \int_\Omega \Big(\sum_{k=0}^{M} \tfrac{1}{2}\rho_k \varepsilon_{ij}^k \varepsilon_{ij}^k - pu\Big)\mathrm{d}\Omega - \int_{\Gamma_T} tu\,\mathrm{d}\Gamma \right\} \\
&\text{subject to:} \\
&\sum_{k=0}^{M} \varepsilon_{ij}^k = \frac{1}{2}\Big(\frac{\partial u_i}{\partial x_j} + \frac{\partial u_j}{\partial x_i}\Big) \text{ in } \Omega, \\
&\varepsilon^k \in \mathbf{H}_k \,,\; k = 1,\dots,M \\
&0 \le \rho_{\min}^k \le \rho_k \le \rho_{\max}^k < \infty,\; k = 0,1,\dots,M \\
&\int_\Omega \rho_k \,\mathrm{d}\Omega \le V_k,\; k = 0,1,\dots,M
\end{aligned}
$$

This (auxiliary) problem corresponds to a problem of optimal design of a structure made of an elastic/stiffening material modelled with zero-Poisson-ratio constituents only. Note that we here have included the bounds on the resource densities. Solving for the resource densities as well, we have a formulation

$$
\begin{aligned}
&\min_{\substack{\varepsilon^k,\Lambda_k,\,k=0,..,M,\\ u}} \left\{ \sum_{k=0}^{M} \hat{W}_k(\varepsilon^k) - \int_\Omega pu\,\mathrm{d}\Omega - \int_{\Gamma_T} tu\,\mathrm{d}\Gamma \right\} \\
&\text{subject to:} \\
&\sum_{k=0}^{M} \varepsilon_{ij}^k = \frac{1}{2}\Big(\frac{\partial u_i}{\partial x_j} + \frac{\partial u_j}{\partial x_i}\Big) \text{ in } \Omega, \\
&\varepsilon^k \in \mathbf{H}_k \,,\; k = 1,\dots,M
\end{aligned}
$$

where the optimal strain energies are given as

$$
\hat{W}_k(\varepsilon^k) = \min_{\Lambda_k \ge 0} \left\{ \int_\Omega \max\Big[\big(\tfrac{1}{2}\varepsilon_{ij}^k \varepsilon_{ij}^k - \Lambda_k\big)\rho_{\min}^k, \big(\tfrac{1}{2}\varepsilon_{ij}^k \varepsilon_{ij}^k - \Lambda_k\big)\rho_{\max}^k\Big]\mathrm{d}\Omega + \Lambda_k V_k \right\}
$$

Here we have introduced Lagrange multipliers Λ_k for the resource constraints.

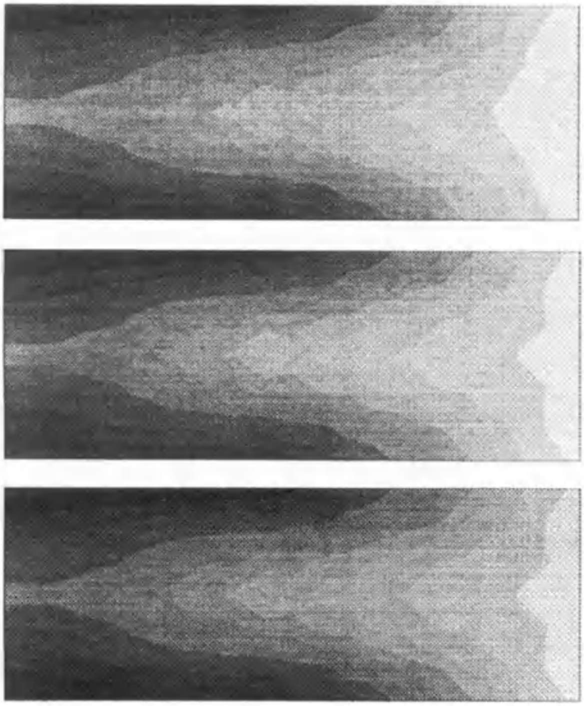

Fig. 5.4. The design of a medium aspect ratio cantilever using optimal materials and an elasto/softening model. Single load case. Vertical load at mid right-hand point, supports at left hand vertical line, cf. figure 3.5. Only the base, linear constituent is allowed to vary and the pictures show the distribution of this fase for two different load levels (low load level at top). Bendsøe, Guedes, Plaxton and Taylor, 1994.

5.2.4 Example

The computational solution procedure that was employed for the example shown above was based on an FEM approximation of stresses as well as resource densities, combined with the use of a mathematical programming routine for solving the associated discrete, convex optimization problem. The FEM discretization was based on the simplest possible, consisting of elements simultaneously constant in stresses and resource densities, with equilibrium being enforced in the weak sense. For the optimization, a sequential quadratic programming algorithm NLPQL, Schittkowski, 1985, was used and the design problem was solved as a combined optimization problem involving stresses simultaneously with densities as variables in the optimization routine. For the procedure, it was important to provide the mathematical programming algorithm with a feasible point, this being achieved by performing an equilibrium only analysis for a feasible density distribution at the outset of each design calculation.

We note that an alternative and equally simple computational procedure is to base the iterative scheme on the optimal values of the densities expressed in terms of stresses only, and thus using NLPQL for only the analysis. Details of the solution of the analysis part of the problem can be found in Plaxton and Taylor, 1993.

We also remark here that it is possible to improve the efficiency of the computational solution procedure considerably. The convexity of problem (5.9) implies that the problem could be solved by use of interior point methods, as described in section 4.3.3. Also, the FEM approximation used is fairly crude. Finally we note that the FEM discretized versions of problem (5.9) will exhibit extensive sparsity which could be exploited in order to improve computational efficiency.

5.3 Topology and material design for plate problems

The studies by Cheng and Olhoff, 1981, 1982, Cheng, 1981 and Olhoff et al, 1981, on the problem of variable thickness plate design and the appearance of stiffeners in such design problems have played a crucial role in the developments in optimal structural design with materials with microstructure, and the homogenization method for topology design can be seen as a natural extension of Cheng and Olhoff's work on plates. In this sense this exposition of topology design methods is reversed relative to history, but with recent developments in mind it is more natural to consider plate design as a special variation of the general framework. In this chapter we will also begin by considering free material design for Mindlin plates of fixed thickness, only later treating the more classical problem of variable thickness design of Kirchhoff plates.

The design of variable thickness Kirchhoff plates is at first glance just another sizing problem of finding the optimal continuously varying thickness of the plate. The close connection with the 0-1 topology design problems is not entirely evident, but the cubic dependence of plate rigidity on the thickness of the plate implies that the optimal design prefers to achieve either of the bounds on the thickness, in essence a plate with integral stiffeners. This in turn implies non-existence of solutions unless fields of infinitely many stiffeners are included, for example in the form of a rank-2 structure of stiffeners.

The optimal design of plates takes an extra twist when the analysis modelling is taken into account. The design problem and its associated relaxation can be viewed as a purely mathematical question of achieving well-posedness, but as any plate model is an approximate model, it is natural to question the validity of the relaxation in relation to the modelling restrictions/assumptions made to achieve the plate model under consideration. In order to limit the length of the exposition we here take the approach of trying to achieve existence of solutions within the framework of a given plate model, irrespective of the assumptions made to obtain that model. For further discussion of the plate design problem, the derivation of plate models in the framework of asymptotic expansions and the relation between plate models and the relaxed design spaces we refer to the vast amount of literature on this subject (cf., [31] which contains a partial list).

5.3.1 Optimization of material properties for Mindlin plate design

In the following we consider the design of Mindlin plates of fixed thickness by considering the simultaneous design of material and structure, as an extension of the approach described in chapter 3 (Bendsøe and Díaz, 1993). The main issue is here how the unrestricted set of positive semi-definite constitutive tensors of the plate enter the model for the Mindlin plate and it turns out that the minimum compliance problem is, from an analysis point of view, basically a multiple load problem. For recent related work that use the homogenization method on the optimal layout of plates and shells in Mindlin and Kirchhoff theories we refer to Soto and Díaz, 1993a, 1993b, 1993c, 1993d, Lipton, 1994a, 1994d, and Díaz, Lipton and Soto, 1994.

The minimum potential energy statement for a *constant thickness* Mindlin plate constructed from one material is of the form*

$$\min_u \left\{ \begin{array}{l} \frac{1}{2}\int_\Omega h\, E^0_{ijkl}\varepsilon_{ij}(u)\varepsilon_{kl}(u)\,\mathrm{d}\Omega + \frac{1}{2}\int_\Omega \frac{h^3}{12} E^0_{ijkl}\kappa_{ij}(u)\kappa_{kl}(u)\,\mathrm{d}\Omega \\ +\frac{1}{2}\int_\Omega h\, D^S_{ij}\gamma_i(u)\gamma_j(u)\,\mathrm{d}\Omega - \left(\int_\Omega p u\,\mathrm{d}\Omega + \int_{\Gamma_t} t u\,\mathrm{d}\Gamma \right) \end{array} \right\}$$

where p is the transverse and t the in-plane load. The thickness of the plate is denoted by h and we assume that the mid-plane is a plane of symmetry . Also, E^0_{ijkl} is the plane stress elasticity tensor and D^S is the transverse shear stiffness matrix and the entries of these tensors will be the design variables of our problem.

In Mindlin plate theory generalized displacements of the plate $u=(u_1,u_2,w,\theta_1,\theta_2)$ consist of the in-plane displacements (u_1,u_2), the fibre rotations (θ_1,θ_2) and the transverse displacement of the mid-plane w. The associated membrane, bending, and transverse shear strains are, respectively,

$$\varepsilon_{ij} = \frac{1}{2}\left(\frac{\partial u_i}{\partial x_j} + \frac{\partial u_j}{\partial x_i}\right) \quad \kappa_{ij} = \frac{1}{2}\left(\frac{\partial \theta_i}{\partial x_j} + \frac{\partial \theta_j}{\partial x_i}\right) \quad \text{and} \quad \gamma_i = \frac{\partial w}{\partial x_i} - \theta_i$$

The optimization problem we will consider is the minimization of compliance and it will be formulated for a two dimensional design domain Ω and the design variable is the point-wise varying stiffness of the plate, described by the element $D=\{E^0, D^S\}$ in the product space $\mathbf{S}^{(4,0)} \times \mathbf{S}^{(2,0)}$ of symmetric (4,0) tensors on Ω and symmetric (2,0) tensors on Ω; these two parts of D are independent if we

* Here and elsewhere in this section (section 5.3) all indices range over 1 and 2.

consider the physical material to be freely parametrized in 3-space. The thickness is maintained fixed. For physical reasons we restrict D to be positive semi-definite, that is $E^0 \geq 0, D^S \geq 0$. The total resource of material is measured by the integral of the 2-norm (the Frobenius norm) $\|D\|_2 = \sqrt{\langle D, D\rangle}$ of D over the domain. Here the standard inner product $\langle D, A\rangle$, of two elements $D = \{E^0, D^S\}$ and $A = \{A^0, A^S\}$ of $\mathbf{S}^{(4,0)} \times \mathbf{S}^{(2,0)}$ is defined as

$$\langle D, A\rangle = E^0_{ijkl}\, A^0_{ijkl} + D^S_{ij}\, A^S_{ij}$$

Following the procedure of chapter 2 and 3, we introduce a 'density' function $\rho = \|D\|_2$ and state the minimum compliance problem as

$$\max_{\rho \in G} \; \max_{\substack{D \geq 0 \\ \|D\|_2 \leq \rho}} \; \min_u \left\{ \frac{1}{2} \int_\Omega \upsilon(D,u)\, \mathrm{d}\Omega - l(u) \right\} \tag{5.11}$$

where

$$\upsilon(D,u) = h\, E^0_{ijkl} \varepsilon_{ij}(u) \varepsilon_{kl}(u) + \frac{h^3}{12} E^0_{ijkl} \kappa_{ij}(u) \kappa_{kl}(u) + h\, D^S_{ij}\, \gamma_i(u) \gamma_j(u)$$

and

$$l(u) = \int_\Omega p u \,\mathrm{d}\Omega + \int_{\Gamma_t} t u \,\mathrm{d}\Gamma.$$

Here the convex and weak-* compact set G in $L^\infty(\Omega)$ given as

$$G_1 = \left\{ \rho \in L^\infty(\Omega) \;\middle|\; \int_\Omega \rho \,\mathrm{d}\Omega \leq V \;,\;\; 0 \leq \rho_{\min} \leq \rho \leq \rho_{\max} < \infty \right\}$$

restricts the range of feasible densities and ensures that the problem is well-posed.

As has been seen earlier, it is allowable to exchange the order the min and max operations of the innermost problem leading to the final form of the problem

$$\max_{\rho \in G} \; \min_u \left\{ \frac{1}{2} \int_\Omega \max_{\substack{D \geq 0 \\ \|D\|_2 \leq \rho}} \upsilon(D,u) d\Omega - l(u) \right\} \tag{5.12}$$

Notice that the first two terms of the specific energy expression $\upsilon(D,u)$ is the sum of energies arising from the same part of the rigidity tensor, thus making the problem analogous to the multiple load problem treated in chapter 3. We shall now briefly describe the solution of the inner problem and the effects this has on a computational procedure to determine the optimal allocation of resource ρ . To this end, notice that the inner problem of (5.12) is

$$\max_{\substack{\|D\|_2 \le \rho \\ D \ge 0}} \left\{ \frac{1}{2} \upsilon(D) = \frac{1}{2} \langle D, A \rangle \right\} \tag{5.13}$$

where $A = \left\{ h\varepsilon_{ij}\varepsilon_{kl} + \frac{h^3}{12}\kappa_{ij}\kappa_{kl} \ , \ h\gamma_i\gamma_j \right\}$.

As seen in section 3.2.1 a solution to (5.13) in terms of A can be readily found. We have that

$$\max_{\substack{D \ge 0 \\ \|D\|_2 \le \rho}} \langle D, A \rangle = \rho \|A\|_2$$

with an optimal design D^* given by

$$D^* = \{E^0, D^S\}^* = \frac{\rho}{\|A\|_2} A = \frac{\rho}{\|A\|_2} \left\{ h\varepsilon_{ij}\varepsilon_{kl} + \frac{h^3}{12}\kappa_{ij}\kappa_{kl} \ , \ h\gamma_i\gamma_j \right\}$$

Note that the optimized material properties represented by D^* do not possess any specific symmetry properties and the material is thus generally anisotropic. Furthermore note that the membrane stiffness depends on the bending and transverse shear strains, and that similar coupling exists for the other stiffnesses. At D^* the optimum energy function is

$$\upsilon^* = \rho \breve{\upsilon}^*$$

with

$$\breve{\upsilon}^* = \|A\|_2 = \sqrt{(h\varepsilon_{ij}\varepsilon_{kl})^2 + (\frac{h^3}{12}\kappa_{ij}\kappa_{kl})^2 + \frac{h^4}{6}\kappa_{ij}\kappa_{kl}\varepsilon_{ij}\varepsilon_{kl} \ + \ h^2\gamma_i\gamma_i\gamma_j\gamma_j}$$

Using the locally optimum material properties the min problem of (5.12) is

$$\min_u \ [\frac{1}{2}\int_\Omega \rho \breve{\upsilon}^*(u) \, d\Omega - l(u)] \tag{5.14}$$

This is non-linear equilibrium problem which couples the bending, membrane and transverse strains in a complex way. Note, however, that the function $\breve{\upsilon}^*(u)$ of the displacements is homogeneous of degree two, that is, under proportional loading the optimized material behaves as a linearly elastic material. Moreover, $\breve{\upsilon}^*(u)$ is a convex function and a smooth function, except at the origin. The Hessian of $\breve{\upsilon}^*(u)$ is of the block form

$$\mathbf{H}^* = \begin{pmatrix} \mathbf{H}_{\varepsilon\varepsilon} & \mathbf{H}_{\varepsilon\kappa} & \mathbf{H}_{\varepsilon\gamma} \\ \mathbf{H}_{\kappa\varepsilon} & \mathbf{H}_{\kappa\kappa} & \mathbf{H}_{\kappa\gamma} \\ \mathbf{H}_{\gamma\varepsilon} & \mathbf{H}_{\gamma\kappa} & \mathbf{H}_{\gamma\gamma} \end{pmatrix}$$

where all the blocks are non-zero almost everywhere. This underlines the coupling between the displacements for the different strains present in problem. A finite element implementation of this problem would involve using an element that reflects this coupling, e.g. one whose tangent stiffness matrix is a discretized version of **H***. Such finite element model would accommodate the coupling, while an appropriate iterative procedure, e.g. a Newton method, would be needed to handle the non-linear nature of the problem.

The reduced optimization problem,

$$\max_{\substack{\rho \\ \int_\Omega \rho \, d\Omega \le V \\ 0 \le \rho_{\min} \le \rho \le \rho_{\max}}} \quad \min_u \, [\frac{1}{2}\int_\Omega \rho \breve{\upsilon}^*(u) \, d\Omega - l(u)]$$

is now of the form of a variable thickness sheet problem for a sheet made of a non-linear elastic material and would be solved by a standard optimality criterion algorithm.

For comparison purposes and computational reasons the following upper bound on υ^* is useful:

$$\begin{aligned} \upsilon^* &= \max_{\substack{D \ge 0 \\ \|D\|_2 \le \rho}} \left[\langle D, \{h\varepsilon_{ij}\varepsilon_{kl}, 0\}\rangle + \left\langle D, \{\frac{h^3}{12}\kappa_{ij}\kappa_{kl}, 0\} \right\rangle + \langle D, \{0, h\gamma_i\gamma_j\}\rangle \right] \\ &\le \max_{\substack{D \ge 0 \\ \|D\|_2 \le \rho}} \left[\langle D, \{h\varepsilon_{ij}\varepsilon_{kl}, 0\}\rangle\right] + \max_{\substack{D \ge 0 \\ \|D\|_2 \le \rho}} \left[\left\langle D, \{\frac{h^3}{12}\kappa_{ij}\kappa_{kl}, 0\} \right\rangle \right] + \max_{\substack{D \ge 0 \\ \|D\|_2 \le \rho}} \left[\langle D, \{0, h\gamma_i\gamma_j\}\rangle\right] \\ &\le \rho \left[h\varepsilon_{ij}\varepsilon_{ij} + \frac{h^3}{12}\kappa_{ij}\kappa_{ij} + h\gamma_i\gamma_i \right] = \rho \breve{\upsilon}_0^* = \upsilon_0^* \end{aligned}$$

Here $\frac{1}{2}\upsilon_0^*$ corresponds to the strain energies in a plate made of an isotropic, zero-Poisson-ratio material with rigidity $\rho D_{\nu=0} = \rho\{\delta_{ik}\delta_{jl}, \delta_{ij}\}$. The 2-norm of this tensor is $\sqrt{5}\,\rho$ so this bound is not achievable. A trivial lower bound can be obtained by the observation that the rigidity $\frac{1}{\sqrt{5}}\rho D_{\nu=0}$ has 2-norm equal to ρ. Thus we have an upper and a lower bound on the optimal compliance given simultaneously in terms of a problem which involves a linear analysis with *uncoupled* membrane, bending and transverse strains:

$$\frac{1}{\sqrt{5}} \max_{\substack{\text{density } \rho \\ 0<\rho_{\min}\le\rho\le\rho_{\max} \\ \int_\Omega \rho\, d\Omega \le V}} \min_u \left[\frac{1}{2}\int_\Omega \rho \breve{v}_0 * (u)\, d\Omega - l(u)\right]$$

$$\le \max_{\substack{\text{density } \rho \\ 0<\rho_{\min}\le\rho\le\rho_{\max} \\ \int_\Omega \rho\, d\Omega \le V}} \min_u \left[\frac{1}{2}\int_\Omega \rho \breve{v} * (u)\, d\Omega - l(u)\right]$$

$$\le \max_{\substack{\text{density } \rho \\ 0<\rho_{\min}\le\rho\le\rho_{\max} \\ \int_\Omega \rho\, d\Omega \le V}} \min_u \left[\frac{1}{2}\int_\Omega \rho \breve{v}_0 * (u)\, d\Omega - l(u)\right]$$

5.3.2 Variable thickness design of Kirchhoff plates

The minimum potential energy statement for a Kirchhoff plate is of the form

$$\min_w \left\{ \frac{1}{2}\int_\Omega \frac{h^3}{12} E^0_{ijkl}\kappa_{ij}(w)\kappa_{kl}(w)\mathrm{d}\Omega - \int_\Omega p w \,\mathrm{d}\Omega \right\}$$

where p is the transverse load. The thickness of the plate is denoted by h and we assume that the mid-plane is a plane of symmetry. The deformation of the plate is described by the transverse displacement of the mid-plane w, with associated (linearized) curvature tensor

$$\kappa_{ij} = \frac{\partial^2 w}{\partial x_i \partial x_j}$$

and the relationship between the curvature tensor and moment tensor M is given as

$$M_{ij} = D_{ijkl}\kappa_{kl} \quad \text{with} \quad D_{ijkl} = \frac{h^3}{12} E^0_{ijkl}$$

where E^0_{ijkl} is the plane stress elasticity tensor of the given material. The similarity between the curvature-moment relation for plates and the strain-stress relation in elasticity hides the fundamental difference that the Kirchhoff plate is governed by a fourth order scalar equation, while standard linear elasticity is governed by a system of second order equations.

The problem we will consider here is also the minimization of compliance. The use of a free parametrization of material is covered by the preceding section, so this will not be discussed separately here. The main focus here will be the design of the thickness of the plate, which here automatically provides the plate design problem with a continuous design variable. The most natural problem to consider is thus

$$\max_{D \in \mathrm{PE}_{ad}} \min_{w} \left\{ \frac{1}{2} \int_{\Omega} D_{ijkl} \kappa_{ij}(w) \kappa_{kl}(w) \, d\Omega - \int_{\Omega} p w \, d\Omega \right\} \tag{5.15}$$

with the set PE_{ad} given as

$$\begin{gathered} D_{ijkl} = \frac{h^3}{12} E^0_{ijkl}, \quad h \in L^{\infty}(\Omega), \\ 0 \le h_{\min} \le h \le h_{\max} < \infty, \quad \int_{\Omega} h \, d\Omega \le V \end{gathered} \tag{5.16}$$

However, problem (5.15) with the design set (5.16) is not well posed, and the existence of solution is not always assured. This was first vividly demonstrated by Cheng and Olhoff, 1981, who discovered the formation of stiffeners in numerically computed 'optimal' solutions for high ratios of $h_{\max} / h_{\min}$ and $h_{\max} / h_{\mathrm{unif}}$, where $h_{\mathrm{unif}} = V / \int_{\Omega} d\Omega$, see figure 5.5. The number of stiffeners increase when the discretization of design is refined, with a resulting (substantial) decrease in compliance, see figure 5.6.

In order to regularize problem (5.15) we are thus forced either to relax the problem or to restrict the design space. As compared to the variable thickness design problem for sheets, this is caused by the cubic dependence of the stiffness of the plate on the thickness. Physically, this dependence makes it advantageous to move as much material as possible away from the mid-plane of the plate, for example in the form of integral stiffeners.

Taking a restriction of the design space first, we achieve existence by restricting the variation of the thickness function, for example in the form of a constraint on the slope (gradient) of the thickness function [31]. From section 1.5.2 we thus know that with the design set PE_{ad} given as

$$\begin{gathered} D_{ijkl} = \frac{h^3}{12} E^0_{ijkl}, \quad h \in H^1(\Omega) \\ \| h \|_{H^1} = \left[\int_{\Omega} (h^2 + (\nabla h)^2) \, d\Omega \right]^{1/2} \le M \\ 0 < h_{\min} \le h \le h_{\max} < \infty, \quad \int_{\Omega} h \, d\Omega \le V \end{gathered} \tag{5.17}$$

existence of solutions is assured. Example solutions with a point wise bound on the slope of the thickness of a rotational symmetric plate can be found in Niordson, 1983.

For a relaxation of the design problem we have to consider plates with infinitely many, infinitely thin integral stiffeners ([31]) in the form of a rank-2 structure of stiffeners of height $h_{\max}$ on a solid plate of variable thickness h, i.e. a planar rank-2 layering of the weak tensor $\frac{h^3}{12}E^0_{ijkl}$ and the strong tensor $\frac{h_{\max}{}^3}{12}E^0_{ijkl}$ (see Fig. 5.7).

For the relaxed design problem we thus need to state the homogenization formulas for Kirchhoff plates, more specifically the effective material parameters for rib-stiffened plates. With these formulas at hand (see below), the computational procedure for computing optimal designs is completely analogous to the procedure described in section 1.3. The optimality criteria are equivalent to those derived in section 1.2, with strains and stresses interpreted as curvatures and moments (this also encompasses the result on optimal rotations).

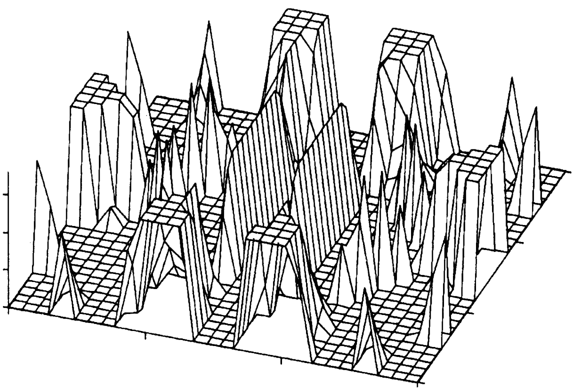

Fig. 5.5. Optimal thickness design of a clamped plate subject to uniform transverse load. Here $h_{\max}/h_{\min} = 5.0$ and $h_{\max}/h_{\text{unif}} = 2.84$. Only the thickness variation over the minimum gauge $h_{\min}$ is shown.

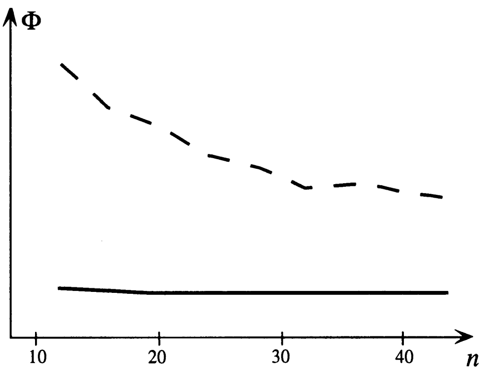

Fig. 5.6. The dependence of the minimum compliance on the fineness of the finite element mesh used for optimal thickness design of a clamped plate. The dashed curve is for thickness only design, the solid curve for a rib-stiffened plate. The mesh is a n by n mesh on a rectangular plate.

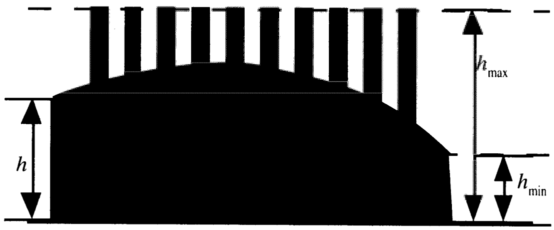

Fig. 5.7. Cross-section of the upper half of a rib-stiffened plate with one field of stiffeners running along the normal of the cutting plane.

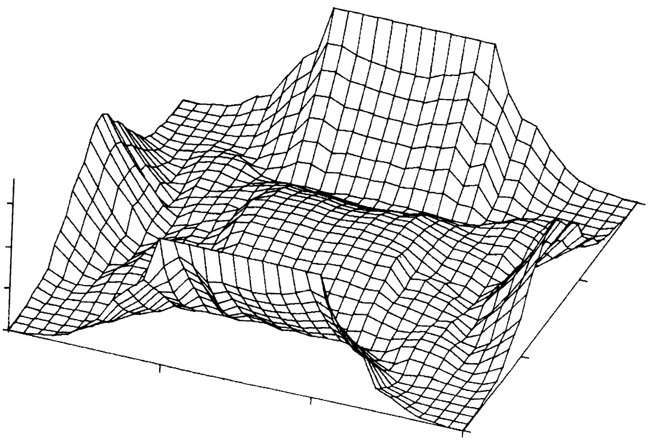

Fig. 5.8. Optimal distribution of material (bulk density) in a clamped plate with two fields of stiffeners. The design data is $h_{\max}/h_{\min} = 5.0$ and $h_{\max}/h_{\text{unif}} = 2.84$ and the plate is subject to a uniform transverse load; compare with figure 5.5. Only the bulk density variation over the minimum gauge $h_{\min}$ is shown.

5.3.3 Homogenization formulas for Kirchhoff plates

The homogenization formulas for Kirchhoff plates can be derived by an asymptotic expansion approach, as outlined for plane elasticity in section 1.1.3. As we are now dealing with a scalar equation of order four, the result becomes (see Duvaut and Metellus, 1976, Duvaut, 1976):

$$\begin{aligned} D^{\mathrm{H}}_{ijkl} &= \min_{\varphi \in U_Y} \frac{1}{|Y|} \int_Y D_{pqrs}(y) \kappa_{pq}(y^{ij} - \varphi) \kappa_{rs}(y^{kl} - \varphi) \, \mathrm{d}Y \\ &= \frac{1}{|Y|} \int_Y D_{pqrs}(y) \kappa_{pq}(y^{ij} - \chi^{ij}) \kappa_{rs}(y^{kl} - \chi^{kl}) \, \mathrm{d}Y \end{aligned} \tag{5.18}$$

Here U_Y denotes the space of Y-periodic virtual displacement fields on the unit cell Y, while χ^{kl} is a microscopic deflection that is given as the Y-periodic solution of the scalar cell-problem

$$\frac{1}{|Y|}\int_Y D_{pqrs}(y)\kappa_{pq}(y^{ij}-\chi^{ij})\kappa_{rs}(\varphi)\,\mathrm{d}Y = 0 \quad \text{for all } \varphi \in U_Y \tag{5.19}$$

with reference deflections

$$y^{11} = \frac{1}{2}y_1{}^2,\ y^{12} = y^{21} = y_1 y_2 \ \text{ and } \ y^{22} = \frac{1}{2}y_2{}^2.$$

For a plate with one field of stiffeners, the effective bending rigidity can be computed from these formulas in a way analogous to the method used for plane elasticity in section 1.6.1. However, it is more instructive to consider the smear-out approach, as described in section 1.6.2. To this end. let $D^-_{ijkl} = \frac{h^3}{12}E^0_{ijkl}$ denote the bending stiffness of the solid core of the plate and let $D^+_{ijkl} = \frac{h_{\max}{}^3}{12}E^0_{ijkl}$ denote the bending stiffness of the stiffened part of the plate, with stiffeners of density μ in the direction t (coordinate 2) with normal n (coordinate 1). For the developments it is now important that the plate equation under consideration is a scalar equation and of fourth order in the deflection. This implies that the continuity conditions across the interface are for the tangential part of the curvature (a regularity condition) and for the normal component of the normal moment (the variational jump condition); compare with (1.30), section 1.6.3:

$$\begin{aligned} \kappa^+_{ij}t_it_j &= \kappa^-_{ij}t_it_j \\ \kappa^+_{ij}t_in_j &= \kappa^-_{ij}t_in_j \\ M^+_{ij}n_in_j &= M^-_{ij}n_in_j \end{aligned} \tag{5.20}$$

Compared to plane elasticity, the *algebraic* form of these interface conditions are such that the moment tensor plays the role of the *strain* tensor, the curvature tensor plays the role of the *stress* tensor and the roles of the vectors *n, t* defining the interface are reversed (cf. conjugate beam theory). However, the similar structure allows us to obtain the homogenized rigidity components directly from the results obtained for plane elasticity. Specifically, the homogenized bending rigidity can be read off from the homogenized *compliance* tensor as

$$D^{\mathrm{H}}_{ijkl} = M(D_{ijkl}) - \frac{\mu(1-\mu)}{N(D_{rstu}n_rn_sn_tn_u)}\left[D^+_{ijpq} - D^-_{ijpq}\right]\left[D^+_{mnkl} - D^-_{mnkl}\right]n_mn_n\,n_pn_q$$

Here we have used the notation

$$M(f) = \mu f^+ + (1-\mu) f^-, \quad N(f) = (1-\mu) f^+ + \mu f^-$$
$$\text{when } f(y) = \begin{cases} f^+ & \text{in stiffener} \\ f^- & \text{in solid plate} \end{cases}$$

as introduced in section 1.6.2. For the case of orthotropic constituents, the different elements of $D^{\mathbf{H}}_{ijkl}$ are given as

$$D^{\mathbf{H}}_{1111} = \left[M\left(\frac{1}{D_{1111}} \right) \right]^{-1}$$

$$D^{\mathbf{H}}_{2222} = M(D_{2222}) - \left[M\left(\frac{D_{1122}{}^2}{D_{1111}} \right) \right] + \left[M\left(\frac{D_{1122}}{D_{1111}} \right) \right]^2 \left[M\left(\frac{1}{D_{1111}} \right) \right]^{-1}$$

$$D^{\mathbf{H}}_{1122} = \left[M\left(\frac{D_{1122}}{D_{1111}} \right) \right] \left[M\left(\frac{1}{D_{1111}} \right) \right]^{-1}; \quad D^{\mathbf{H}}_{1212} = M\left(D_{1212}\right)$$

These expressions are, except for the 1212 term, exactly the same as for the rigidity tensor in the plane elasticity case (see section 1.1.3 or section 1.6.3). Moreover, the optimal rotation of the orthotropic plate means that the 1212 term plays *no* role, making the plate problem completely analogous to the plane elasticity problem when it comes to deriving the optimal material properties for stiffened plates with stiffeners at multiple scales.

We remark here that the use of thin, high stiffeners in a Kirchhoff plate model is in fact a violation of the assumptions under which this model can be derived from 3-D elasticity. Thus the developments above should be seen in the framework of achieving regularization strictly within the Kirchhoff plate framework, ignoring eventual modelling restrictions. The modelling problem should by no means be dismissed but lies outside the scope of this presentation. The reader is referred to the literature [31] for further information on this problem as well as to studies of optimal thickness design of Mindlin plates.

5.3.4 Design of perforated Kirchhoff plates

The design of plates consisting of areas of two distinct thicknesses only or the design of perforated plates of fixed thickness are problems that are directly related to the topology design problems discussed in chapter 1.

In particular, the similarity of the effective material parameters for layered material and for stiffened plates demonstrated above implies that results for the design of perforated plates can be read off directly from the analysis of the topology problem for plane elasticity. Thus the analysis and derivation of optimal

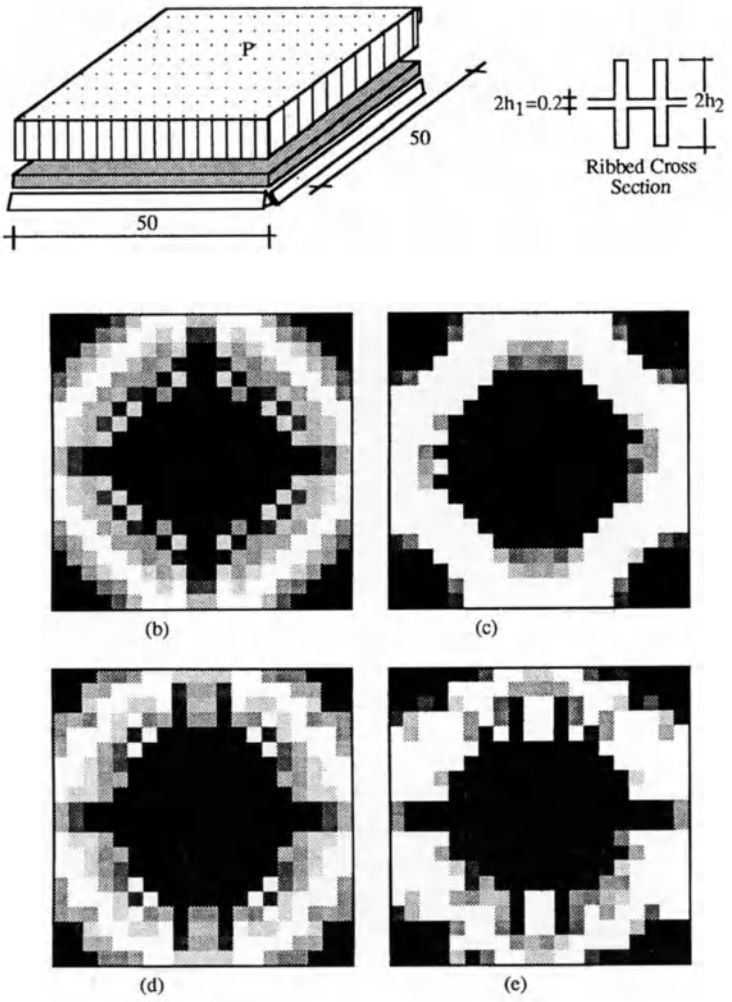

Fig. 5.9. Optimal distribution of material in simply supported rib-stiffened plate subject to uniform transverse load. Comparison of the effect of various models of the plate for $h_{max}/h_{min} = 5.0$ and $h_{max}/h_{unif} = 2.0$. *(b)* is for a Mindlin plate and *(c)* is for a Kirchhoff plate, both with a rank-2 stiffener system. *(d)* and *(e)* are for a laminate Mindlin plate model, for which the effective characteristics of the microstructure from plane elasticity are integrated over the thickness. *(d)* is for a rank-2 microstructure, *(e)* for a rectangular hole type microstructure of stiffeners at one microscale. By courtesy of C. Soto and A. Diaz.

layer densities performed in section 2.2 can be repeated ad verbatim, replacing stresses/strains by moments/curvatures. Moreover, the results of section 2.2.5 show that the design of low volume perforated plates corresponds directly to the classical lay-out theory for flexural systems as described in for example Rozvany, 1976 and Prager, 1985. We will not here repeat the results of section 2.2, as the interpretation of the results in a plate setting is straightforward.

We close this brief exposition of plate design problems by showing some analytical results for the design of circular, perforated plates using rank-2 microstructures. This problem was analyzed in detail by Rozvany, Ong, Szeto, Olhoff and Bendsøe, 1987, for Poisson ratio zero materials, and extended by Ong, Rozvany and Szeto, 1988, for non-zero Poisson ratio materials. In the former paper a moment based analysis was used to show that for a uniformly transversely loaded axially symmetric clamped plate no region contains two-way ribs. Also, the types of designs that can appear all have a solid centre, transforming into radial ribs towards the rim of the plate. For high volume fractions the rim itself will be solid. These results are illustrated in figures 5.10 and 5.11 below.

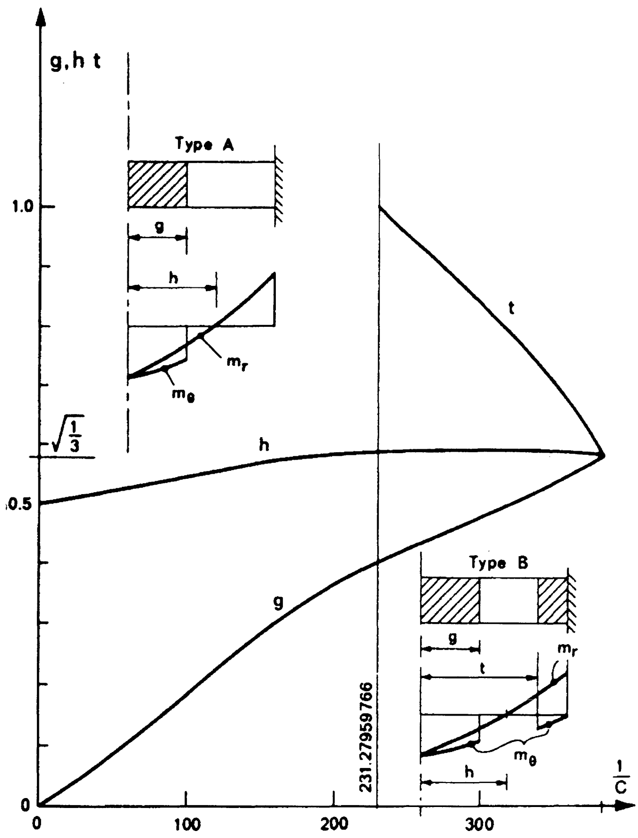

Fig. 5.10. Details of the the geometry of optimal designs for the problem described in figure 5.11. The graphs show the extension of the solid and perforated regions as well as the position of the zero radial bending moment as a function of the inverse of the optimal compliance. Rozvany, Ong, Szeto, Olhoff and Bendsøe, 1987.

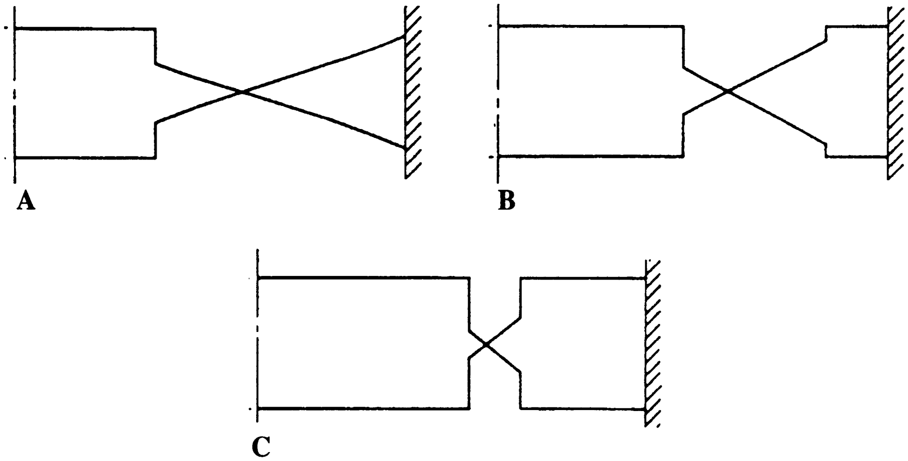

Fig. 5.11. The two basic types of optimal designs that can appear for the optimal design of axisymmetric clamped perforated plates of fixed thickness and with a zero Poisson ratio material. The plate is subject to a uniform transverse load. The figures show the radial distribution of material, the maximum thickness being solid material and the other zone being an area of radial ribs. *(A)* is for low volume fractions, while *(B)* and *(C)* are for higher volume fractions. The point of zero material coincides with a zero radial bending moment. Rozvany, Ong, Szeto, Olhoff and Bendsøe, 1987.

5.4 Hierarchical topology and geometry design

The topology design methods considered so far all employ the basic idea of a ground structure or reference design domain to obtain problem statements that are sizing problems for a fixed geometry. The choice of this reference geometry influences the result of the topology optimization making it important to consider sensitivity analysis of the optimal designs with respect to variation of the reference geometry, and even optimal design of this reference geometry may be fruitful in some situations. This is especially important for truss design problems and is necessary for a proper treatment of continuum topology design problems with pressure loads.

5.4.1 Combined truss topology and geometry optimization

In the ground structure approach to topology design of trusses the positions of nodal points are not used as design variables. This means that a high number of nodal points should be used in the ground structure to obtain efficient topologies. A drawback of the method is that the optimal topologies can be very sensitive to the layout of nodal points, at least if the number of nodal points is relatively low (see for example figure 4.4). This makes it natural to consider an extension of the ground structure approach and to include the optimization of the nodal point location for a given number and connectivity of nodal points [19]. With very efficient tools at hand for the topology design with fixed nodal positions it seems natural to treat the variation of nodal positions as an outer optimization in a two-level hierarchical formulation. As the optimal value function of the topology compliance depends on the geometry variables in a non-smooth way, this outer minimization requires non-smooth optimization techniques.

The 'ultimate best truss' should clearly be obtained by combining topology optimization with a possibility of optimizing simultaneously the positions of the nodal points (or for a FEM model, a possibility of optimizing at the same time the shape of the finite elements and the distribution of material to these elements, see later). For the combined topology and geometry problem for trusses we have as the simplest formulation (using the notation of chapter 4)

$$\begin{aligned}
&\min_{u,a,x} p^T u \\
&\quad \text{subject to :} \\
&\quad \sum_{i=1}^{m} a_i\, l_i(x) \mathbf{A}_i(x) u = p \\
&\quad \sum_{i=1}^{m} a_i\, l_i(x) = V \\
&\quad a_i \geq 0, \quad i = 1,\ldots,m \\
&\quad b_j^k \leq x_j^k \leq c_j^k, \quad j = 1,\ldots\ldots,n \;, \;\; k = 1,2,(3)
\end{aligned} \tag{5.21}$$

which is just problem (4.5) rewritten as a problem depending also on the nodal positions x_j, $j = 1,\ldots\ldots,n$. The nodal positions are restricted to lie within certain bounds that should be chosen to make the resultant trusses realizable. As the member volumes are dependent on the nodal positions we have here reverted to the cross-sectional areas of the individual bars as design variables. Problem (5.21) can be solved as a unified problem considering the problem either as a unified analysis and design problem or as a standard structural optimization problem that can be solved through an adjoint method in the areas and nodal positions only (this requires the application of small lower bounds on the cross sectional areas). An alternative solution procedure is to apply a multilevel approach to the combined problem, treating the topology problem as the inner problem. Because of the size of the topology problem, earlier work has usually involved some form of heuristics to speed up the very significant amount of computations involved [8]. By combining the effective truss topology design methods described in chapter 4 with appropriate tools from non-smooth analysis the multilevel approach can be put in a framework of non-smooth optimization.

For a fixed set of nodal positions we choose here the displacements only form (4.19) of the topology design problem and thus write (5.21) as a two-level problem

$$\max_{\substack{x \\ b \le x \le c}} \left(\min_{u} \left[\max_{i=1,\ldots,m} \left\{ \frac{V}{2} u^T \mathbf{A}_i(x) u - p^T u \right\} \right] \right) \tag{5.22}$$

The inner topology problem in the displacements u can effectively be solved (for fixed x) by one of the computational methods described in chapter 4. The main part remaining is then, of course, the minimization of the so-called master function

$$F(x) := \min_{u} \left[\max_{i=1,\ldots,m} \left\{ \frac{V}{2} u^T \mathbf{A}_i(x) u - p^T u \right\} \right]$$

on the outer level. The number of variables (the nodal positions) in this outer problem will usually be moderate. However, there are two decisive drawbacks. There is no reason for F to be convex and F is not differentiable everywhere. Hence we cannot expect to find more than a local minimum of F and we have to work with codes from non-smooth optimization (e.g. bundle methods, Schramm and Zowe, 1992). These codes require that for each iterate x we can compute a so-called sub-gradient as a substitute for the gradient. Using tools from non-smooth calculus it is easily seen that this causes no difficulties for the above min-max function F (see also section 5.4.2). We add that it is straightforward to show that each local minimizer x^* of F together with the associated t^* and u^* which solve the topology problem for the fixed nodal positions x^* , gives a local minimizer $[u^*, a^*, x^*]$ (with $a_i^* = t_i^* / l_i(x_i^*)$) for problem (5.21).

The two-level approach becomes especially attractive if we consider the single load truss topology problem for which the member stiffness matrices are dyadic products. Then $F(x)$ reduces to the parametrized linear programming problem (compare with (4.25) in section 4.2.2)

$$F(x) = \min_{u} \left\{ -p^T u \;\middle|\; -1 \le \sqrt{\frac{VE_i}{2}} \frac{b_i(x)^T u}{l_i(x)} \le 1, \quad i = 1,\ldots,m \right\}$$

The sub-gradient in this case is basically the derivative with respect to x of the Lagrange function for this LP-problem. Hence we get a sub-gradient 'for free' when solving (4.25) for a given set of nodal positions x . For details we refer to Ben-Tal, Kocvara and Zowe, 1993.

5.4.2 Shape sensitivity analysis of optimal compliance functionals

The approach to topology design of continuum structures considered so far is based on a specific choice of a reference geometry, the ground structure of this method. This geometry should be chosen so that loads and boundary conditions can be properly defined. If the final structure does not seem to be constrained by the geometry chosen, the sensitivity to the precise shape of the geometry is usually

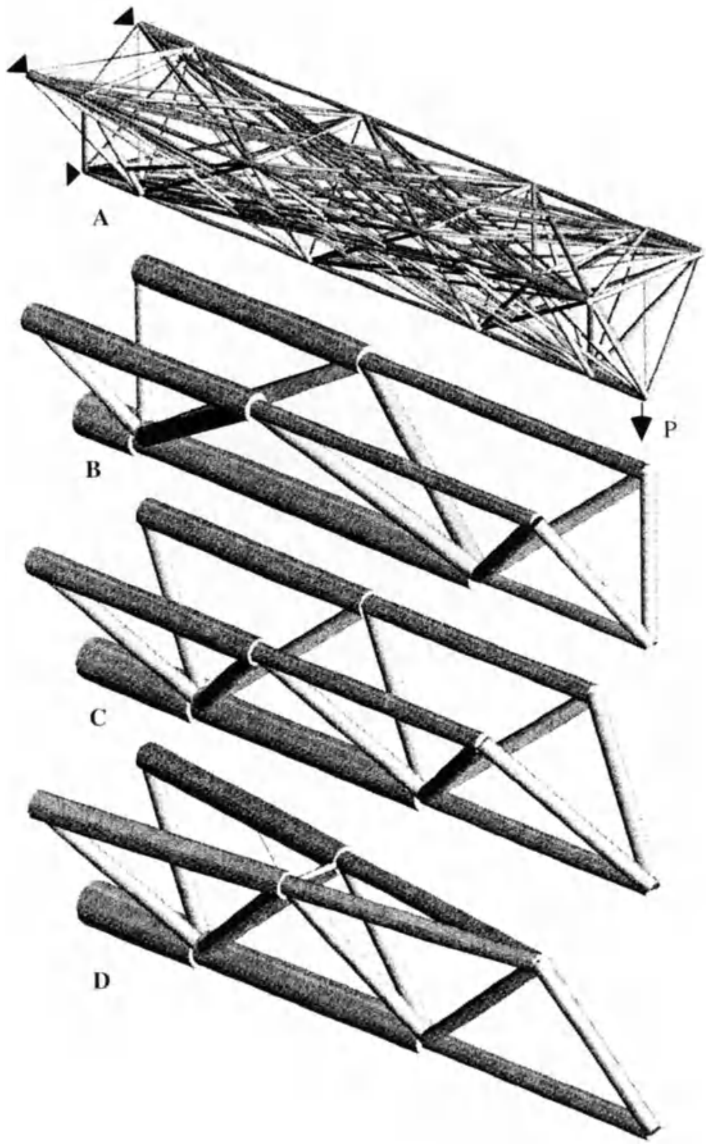

Fig. 5.12. An example of a 3-D topology and geometry optimization for a beam carrying a single load. In *(A)* we show the ground structure of nodal points and potential bars. Note that the ground structure has non-equidistant nodal point positions along the length axis of the 'beam'. In *(B)* we see the optimal topology for the fixed nodal lay-out of the ground structure, in *(C)* a combined geometry and topology optimization with nodal positions restricted to move along the length axis of the 'beam'. Finally, in *(D)* the result of a combined geometry and topology optimization with totally free nodal positions is shown. The compliance values of the optimized designs are 6.944, 6.563 and 6.326, respectively. Bendsøe, Ben-Tal and Zowe, 1993.

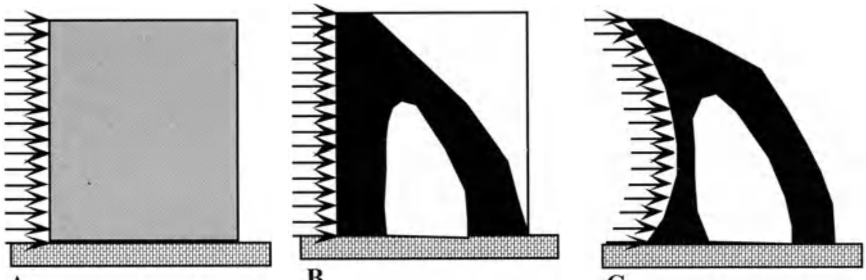

Fig. 5.13 The philosophy behind changing the shape of the reference domain. *(A)* shows the reference domain, with boundary conditions and *pressure* loads. *(B)* is a possible optimal topology for fixed reference geometry. *(C)* is a possible optimal design were the loaded surface of the reference domain is allowed to vary.

---

negligible (see for example Bendsøe, Diaz and Kikuchi, 1993). However, as in any design problem it is important to evaluate the sensitivity of the solution with respect to variations of the given data, which for the topology problems is the shape of the reference domain only.

Apart from the importance of the sensitivity information in its own right, we note that the use of a given reference geometry for defining loads and boundary conditions excludes the possibility of handling some design problems involving pressure loads. In many cases the surface carrying the pressure loads should also be considered as a design parameter, thus requiring simultaneous design of the shape of reference domain as well as topology (see figure 5.13). This simultaneous design could be approached by the hierarchical method outlined above for trusses, and for this we need the shape sensitivity analysis of the compliance of the optimal topology for fixed reference shape. Here, however, we will only outline the form of the sensitivity analysis

In order to exemplify the derivation of shape sensitivity analysis, we consider the problem of free material design for a single load, in its equivalent formulation of variable thickness design of sheet made from a zero-Poisson ratio material. We will consider this problem in the form (see section 3.3.2)

$$J(\Omega) = \min_{\substack{\Lambda \geq 0 \\ u \in U, \\ u \cdot n \geq 0 \text{ on } \Gamma_C}} \left\{ \int_\Omega \max \left\{ \begin{matrix} \rho_{\min} \left[\tfrac{1}{2} \varepsilon_{ij}(u) \varepsilon_{ij}(u) - \Lambda \right], \\ \rho_{\max} \left[\tfrac{1}{2} \varepsilon_{ij}(u) \varepsilon_{ij}(u) - \Lambda \right] \end{matrix} \right\} d\Omega + \Lambda V - l(u) \right\} \quad (5.23)$$

where we include the possibility of a contact condition. As noted earlier, the solution displacement field to this problem is unique if we have that $\rho_{\min} > 0$, but we will include the more general situation in the following. Note that the optimal displacement as well as the optimal density depends on the shape of the reference domain, so even for a unique displacement the sensitivity analysis is slightly more complicated than standard shape sensitivity analysis.

The complications for the sensitivity analysis are the possible dependence of load on shape, the non-smoothness of the domain dependent functional $J(\Omega)$ as well as the possible non-uniqueness of the optimal displacement field.

For the sensitivity analysis of $J(\Omega)$ we consider a one-parameter family of domains $\Omega_s = \varphi(s,\Omega)$ defined through the C^∞-flow $\varphi(s,x)$ associated with a perturbation C^∞-vector field V (i.e., $\frac{\partial}{\partial s}\varphi(s,x) = V(\varphi(s,x))$, $\varphi(0,x) = x$). We first observe that for a situation with non-unique solution to (5.23), the sensitivity can be evaluated by minimization over the sensitivities obtained in the following for each solution. Thus we now consider just one solution (u,λ). For this solution we define

$$\varepsilon'(u) = \frac{1}{2}\left[\nabla(\nabla V \cdot u) + (\nabla(\nabla V \cdot u))^T - \nabla u \cdot \nabla V - (\nabla V)^T \cdot (\nabla u)^T\right]$$

and (compare with the developments in section 4.2.3)

$$\Omega_1 = \Omega_= \cup \Omega_> \quad , \quad \Omega_2 = \Omega \setminus \Omega_1 \qquad \text{with}$$

$$\Omega_= = \left\{x \in \Omega \,\middle|\, \tfrac{1}{2}\varepsilon_{ij}(u)\varepsilon_{ij}(u) = \Lambda,\ \varepsilon'_{ij}(u)\varepsilon_{ij}(u) > 0\right\},\ \Omega_> = \left\{x \in \Omega \,\middle|\, \tfrac{1}{2}\varepsilon_{ij}(u)\varepsilon_{ij}(u) > \Lambda\right\}$$

By transforming the functional as well as the boundary conditions to make these dependent of the reference domain only, we can derive the Eulerian derivative of $J(\Omega)$ with respect to the parameter t at $t = 0^+$ (see Bendsøe and Sokolowski, 1995, for details):

$$\begin{aligned}
dJ(\Omega;V) &= \lim_{s\to 0^+} \frac{1}{s}\left[J(\Omega_s) - J(\Omega)\right] \\
&= \int_\Omega \left[\rho_{\max} 1_{\Omega_1} + \rho_{\min} 1_{\Omega_2}\right]\varepsilon'_{ij}(u)\varepsilon_{ij}(u)\,d\Omega \\
&\quad + \int_\Omega \max\left\{\rho_{\min}\left[\tfrac{1}{2}\varepsilon_{ij}(u)\varepsilon_{ij}(u) - \Lambda\right], \rho_{\max}\left[\tfrac{1}{2}\varepsilon_{ij}(u)\varepsilon_{ij}(u) - \Lambda\right]\right\} \operatorname{div} V\, d\Omega \\
&\quad - \int_\Omega \left[(\nabla p \cdot V)\cdot u + p\cdot(\nabla V \cdot u) + (p \cdot u)\operatorname{div} V\right] d\Omega \\
&\quad - \int_{\Gamma_T} \left[(\nabla t \cdot V)\cdot u + t\cdot(\nabla V \cdot u) + (t \cdot u)\operatorname{div}_\Gamma V\right] d\Gamma
\end{aligned}$$

Note that the shape derivative fails to be linear in the perturbation field V if the measure of the set $\left\{x \in \Omega \,\middle|\, \tfrac{1}{2}\varepsilon_{ij}(u)\varepsilon_{ij}(u) = \Lambda\right\}$ is not zero.

5.5 Other examples of design using a homogenization modelling

The material in this monograph is concerned with structural applications of the design of topology and material. For the continuum setting the basic approach and many results have an equivalent form for other physical and technical situations governed by elliptic equations and with the design parameter entering the highest order term of the elliptic operator [34]. Special mention should here be given to the problem of heat or electromagnetic conduction. Studies of this slightly simpler problem have constituted the basis for the developments and applications in elasticity especially regarding the theoretical aspects [34].

In the following we will briefly describe three cases of applications of the topology design philosophy used in the homogenization method. First we describe an extension of topology design for thermo-elastic problems. Second, we discuss some modelling aspects of treating stability constraints and finally, a simple conceptual model of damage is related to the problem of topology design.

5.5.1 Topology optimization of structures subject to thermal loads

In this section we consider a computational model for the topology optimization problem for elastic 2-D solids subjected to thermal loads. The approach is the one of the homogenization method, using any material model that allows for a material distribution. This problem has been considered by Rodrigues and Fernandez, 1993a, 1993b, and we describe their approach in the following.

Basing our developments on the notation introduced in chapter 1, we now consider a structural component which, apart from body forces and surface tractions is also subjected to a static, known spatial temperature variation T. With thermal expansion properties denoted by β_{ij}, the minimum compliance problem takes the form

$$\max_{E,\beta\in \mathrm{TE}_{ad}} \quad \min_{u\in U} \left\{ \frac{1}{2}\int_{\Omega} E^{\mathrm{H}}_{ijkl}(x)\,\varepsilon_{ij}(u)\varepsilon_{kl}(u)\,\mathrm{d}\Omega - \int_{\Omega} T(x)\,\beta^{\mathrm{H}}_{ij}(x)\,\varepsilon_{kl}(u)\,\mathrm{d}\Omega - l(u) \right\} \quad (5.24)$$

Here the rigidity tensor as well as the thermal expansion tensor arise as the homogenized coefficients defined by the generalization of the admissible set (1.8) (see section 1.1.2):

$$\begin{gathered} E^{\mathrm{H}}_{ijkl}(x) = E^{\mathrm{H}}_{ijkl}(\mu(x),\gamma(x),\ldots,\theta(x)), \qquad \beta^{\mathrm{H}}_{ij}(x) = \beta^{\mathrm{H}}_{ij}(\mu(x),\gamma(x),\ldots,\theta(x)), \\ \text{Geometric variables } \mu,\gamma,\ldots \in L^{\infty}(\Omega), \text{ Angle } \theta \in L^{\infty}(\Omega) \\ \text{Density of material } \rho(x) = \rho(\mu(x),\gamma(x),\ldots) \\ \int_{\Omega} \rho(x)\,\mathrm{d}\Omega \le V; \qquad 0 \le \rho(x) \le 1,\ x\in\Omega \end{gathered} \quad (5.25)$$

It should be noticed that for thermo-elastic problems the compliance is directly dependent of design. This will imply that in some situations the optimal structure will not fully use the available material.

In (5.25) the homogenized stiffness is given by the standard formula applicable for elasticity, while the homogenized thermal expansion material properties are given by the expression (see Francfort, 1983, Brahlm-Otsmane, Francfort and Murat, 1989)

$$\beta_{ij}^{\mathbf{H}}(x) = \frac{1}{|Y|} \int_Y \left[\beta_{ij}(x,y) - \beta_{pq}(x,y) \frac{\partial \chi_p^{ij}}{\partial y_q} \right] \mathrm{d}y$$

where χ^{kl} is the solution of the cell-problem for the elasticity coefficients (cf., section 1.1.3). This result simplifies the evaluation of the effective parameters as only the cell problems for the elasticity case need to be solved.

The problem (5.25) can be solved by analogous means as the pure elasticity case, see chapter 1. Note that (5.25) because of the thermal term in the energy is similar in structure to a multiple load problem. With suitable modifications the optimality criteria described in section 1.2 should then be applied for this case. This also implies that there is no simple relation between material angle and the principal stress or principal strain frames, even for the single load case as formulated here (compare also with the Mindlin plate problem, section 5.3.1). That the volume constraint may not be active means that the optimality algorithms described for the pure elasticity cases treated till now are not directly applicable. Instead, Rodrigues and Fernandez, 1993a, 1993b, employ an Augmented Lagrangian method which is strongly related to the optimality criteria method. For further information on the thermo-elasticity design problem we refer to their papers.

It is important to note that the precise form of optimal microstructures for the thermo-elasticity problem has not yet been identified. Also, for a problem of free design of material a suitable, physically realistic relation between elastic and thermal material properties needs to be identified (or postulated for later verification) as it is probably not correct to assume completely independent properties. If independent properties are assumed, the derivation of optimal material properties is straightforward and follows directly the path laid in earlier sections.

We close this brief exposition by an illustrating example computed using square micro-cells with rectangular holes, see figure 5.14. From the figures we observe that even for the simple model of a given temperature field the optimal topologies are strongly dependent on the temperature variation. Also we see that with an increase of temperature the volume of the optimal structure decreases, resulting in not all the available material being used. Finally we note that the checkerboard problem persists for this case also.

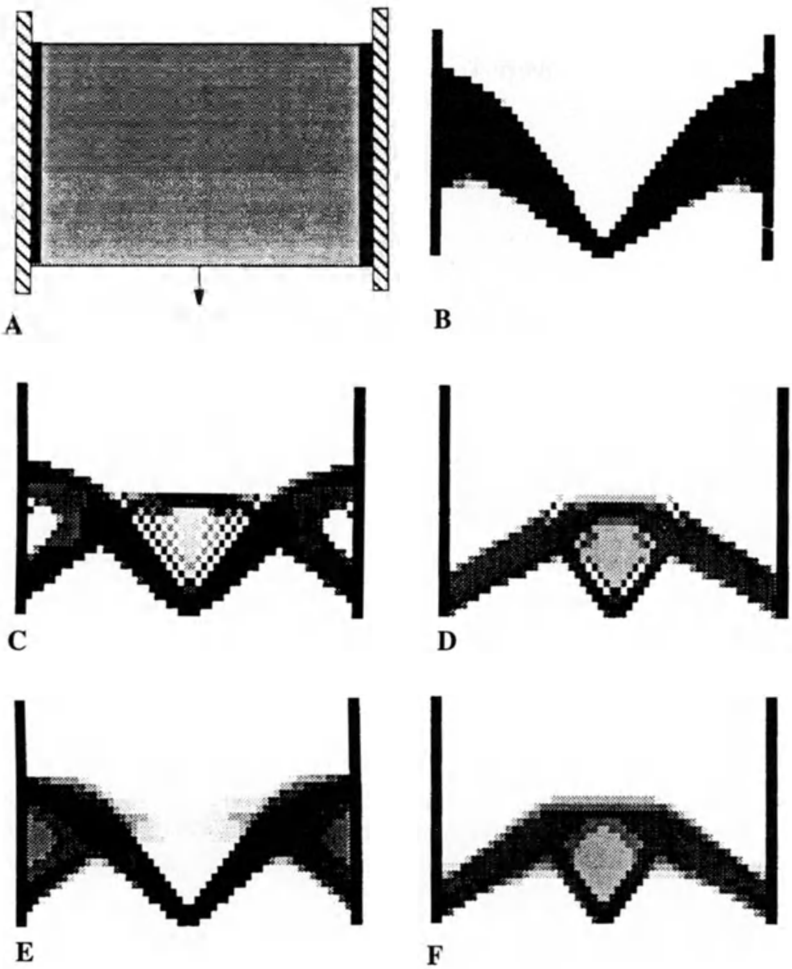

Fig. 5.14. The design of a structure subject to a constant field of thermo loads and with a volume constraint equalling 40% of the total volume of the design area. *(A)* shows the design problem. The black regions identify non-design areas (full material). *(B)* shows the optimum design without temperature effects. *(C)* and *(D)* show optimal design results for increasing temperatures, using a 4-node finite element mesh for analysis. For comparison, *(E)* and *(F)* show the same cases solved using a 9-node element. By courtesy of Rodrigues and Fernandez

5.5.2 Topology optimization of structures under stability constraints

The statement 'optimization of structures under stability constraints' is in this section understood as the design for maximal critical load (buckling load). For the framework of topology design this problem has not attracted much attention in the literature, even though the amount of work on structural design under stability constraints is quite immense [33]. In lay-out theory and truss design local stability of the individual members of the lay-out can be taken into consideration by modification of the cost function in a force (stress) formulation (Pedersen, 1993d, Rozvany, 1989). These models do not, however, account for the change of stability model that arise if two aligned members are connected through a nodal point connected to these two bars only. Global stability is also not accounted for. For the case of continuum models, Neves, Guedes and Rodrigues, 1993, 1994, have recently used the homogenization approach to topology design of planar structures, considering uni-modal, macroscopic critical loads only.

Let us here formulate a critical load design problem for a Kirchhoff plate with stiffeners or perforated with microstructure. With the notation of sections 1.1.1 and 5.3.2, this problem for linearized buckling analysis can be stated as

$$\max_{\substack{\text{design}\\ \text{with}\\ \text{microstructure}}} \left\{ \lambda_{\text{crit}} = \min_{w} \frac{\int_\Omega D^{\mathbf{H}}_{ijkl}\, \kappa_{ij}(w)\kappa_{kl}(w)\, \mathrm{d}\Omega}{\int_\Omega E^{\mathbf{H}}_{ijkl}\ \varepsilon_{kl}(u)\dfrac{\partial w}{\partial x_i}\dfrac{\partial w}{\partial x_j}\mathrm{d}\Omega} \right\} \tag{5.26}$$

with

$$u = \arg\min_{u\in U} \left\{ \frac{1}{2}\int_\Omega E^{\mathbf{H}}_{ijkl}\ \varepsilon_{ij}(u)\varepsilon_{kl}(u)\ \mathrm{d}\Omega - l(u) \right\}$$

Here the pre-stress $E^{\mathbf{H}}_{ijkl}\ \varepsilon_{ij}(u)$ is modelled as design dependent (for homogenization of the buckling problem, consult Mignot, Puel and Suquet, 1980, Suquet, 1981a). The pre-stress arises due to an in-plane load condition, so that both the homogenized plate tensor $D^{\mathbf{H}}_{ijkl}$ and the homogenized plane elasticity tensor $E^{\mathbf{H}}_{ijkl}$ appear in the problem formulation.

Design for critical loads is, as it is well known, a difficult problem because the objective function is an eigenvalue. This was also mentioned under the earlier discussion of vibration problems, see section 5.1.2. For topology design one additional computational problem is encountered, namely the (unphysical) occurrence of local modes in low density regions of the reference domain. Such modes should be filtered out, as low density areas are not to be considered as part of the final structure. Further discussion on this and the critical load problem in the large can be found in Neves, Guedes and Rodrigues, 1993, 1994.

We have earlier remarked that the use of stiffened plate models in some sense is in conflict with the basic assumptions for such models (see section 5.3.3). In a way a similar objection could be raised here against the use of the homogenized linear buckling equations for the prediction of the buckling load of the continuum with microstructure. For any finite dimension of the microstructure, a local buckling of the microstructure can be the critical mode, but by the limiting process only macroscopic modes remain as part of the model (the critical load for the microstructure becomes infinitely high, in the limit of infinitely small microstructure, see Mignot, Puel and Suquet, 1980, Suquet, 1981a).

The occurrence of local buckling modes in a full non-linear asymptotic analysis has been the subject of a number of studies, see for example Bendsøe and Triantafyllidis, 1990, Geymonat, Müller and Triantafyllidis, 1993, Triantafyllidis and Schnaidt, 1993, and references therein. In Bendsøe and Triantafyllidis, 1990, an infinite planar frame was analyzed using a Bloch expansion method (see also Turbe, 1982). In this way the local modes and global modes can be identified. The microstructure can remain finite as the limiting process of small scale microstructure here is achieved through the infinity of the frame. The local modes are defined as modes with periodicity of the order of one cell size, while a global mode is defined as a mode with periodicity that far exceeds the unit cell size. Having expressed the buckling mode in terms of geometric data, an optimization of the buckling loads can be performed with the purpose of identifying design domains for which the optimal buckling mode is a global mode. The complete analysis requires huge parametric studies, as the optimization problem is non-smooth and even not continuous in some cases. The optimization was carried out for fixed density of material and chosen shape variable (defined in figure 5.16) and for the simplified case of equal bar areas in the two directions of the frame. The results show that for this particular case, the safe region for using the homogenization modelling with global modes is well defined and almost independent of the ratio of the applied stresses, see figure 5.17. For further studies on these issues, we refer to the literature mentioned above.

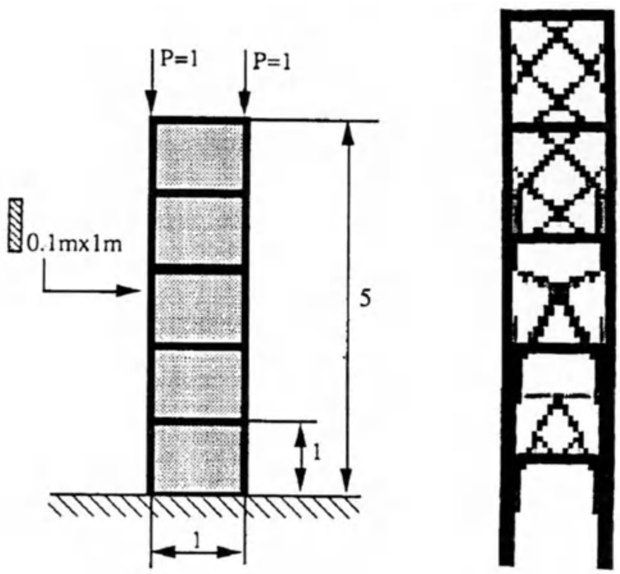

Fig. 5.15. Design (reinforcement) of a five-story frame with respect to buckling. Left hand picture shows the reference design, load and boundary condition. Right hand picture shows the final design, computed in a 22 by 100 9-node finite element mesh. The buckling load is increased to 1.47 times the original critical load. Note that the reinforcement is performed with stubby bars; compare with the vibration result in figure 5.1. By courtesy of M. Neves, J. M. Guedes and H. C. Rodrigues.

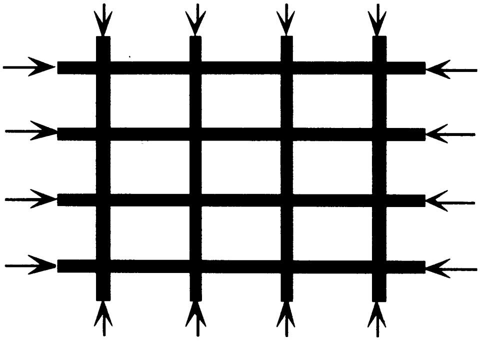

Fig.5.16. Geometry of an infinite frame. The frame is characterized by the density ρ and shape coefficient $c = \sqrt{I_1^2 + I_2^2} / A$ (I_i is the moment of inertia of the bars in direction i, and A is the area of the bars).

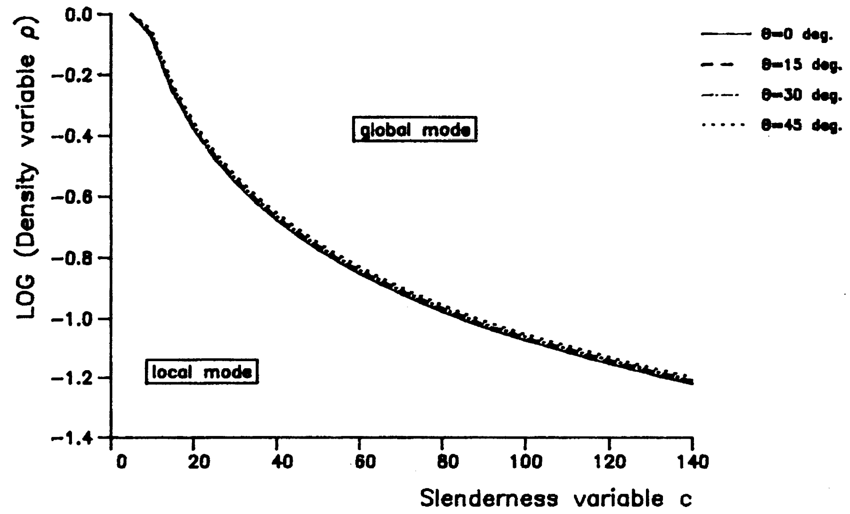

Fig. 5.17. Identification of data for the frame in figure 5.15 for which a maximization of the lowest buckling with respect to aspect ratio and relative moments of inertia of the frame results in global or local modes. The separating curves are for different ratios of applied stress. Bendsøe and Triantafyllidis, 1990.

5.5.3 A simplified homogenization model of damage

We close this monograph on topology design methods by considering a very simple model for damage of structures. Such problems can be related directly to design problems and in this framework involve similar mathematical and computational tools. The model takes the form of a design problem involving the lay-out of a structure made from two materials, a strong material and a weak, damaged material. The model we will consider is a simplification of models described by for example Francfort and Marigo, 1991, 1993, and we refer to the latter reference for a survey of various damage models which are related to the present setting. The simplifications we introduce here are imposed in order to relate the problem directly to the problems we have considered in earlier sections.

The structure we consider is made of a linearly elastic material with elasticity tensor E^+_{ijkl}. Due to loading the material is damaged in some parts of the structure, leaving a weaker material with elasticity tensor E^-_{ijkl} in these parts of the structure. By weaker, we mean that $E^+ - E^- > 0$. Modelling the distribution of damage as a design problem, we say that for a certain load and a certain amount of damage, this damage is distributed so that the compliance of the structure is *maximized*, making the structure as *weak* as possible among all distributions of damage. This problem is formulated as a topology design problem as

$$\begin{aligned}&\underset{u\in U,\, E}{\text{maximize}} \quad l(u)\\&\text{subject to :}\\&\int_\Omega E_{ijkl}(x)\varepsilon_{ij}(u)\varepsilon_{kl}(v)\,\mathrm{d}\Omega = l(v), \quad \text{for all } v\in U,\\&E\in \mathrm{E}_{ad}\end{aligned} \tag{5.27}$$

or

$$\min_{E\in\mathrm{E}_{ad}} \min_{u\in U} \left\{ \tfrac{1}{2}\int_\Omega E_{ijkl}(x)\varepsilon_{ij}(u)\varepsilon_{kl}(v)\,\mathrm{d}\Omega - l(u) \right\} \tag{5.28}$$

Here the set of admissible tensors is given by the relations

$$\begin{aligned}&E_{ijkl} = 1_{\Omega^-}E^-_{ijkl} + (1-1_{\Omega^-})E^+_{ijkl} = \begin{cases} E^+_{ijkl} & \text{if } x\in \Omega\setminus\Omega^- \\ E^-_{ijkl} & \text{if } x\in\Omega^- \end{cases}\\&E_{ijkl}\in L^\infty(\Omega), \quad \int_\Omega 1_{\Omega^-}\,\mathrm{d}\Omega = \mathrm{Vol}(\Omega^-) = V\end{aligned} \tag{5.29}$$

where Ω^- is the damaged zone.

The model described lacks any notion of history of the development of damage. As such, the model is in philosophy related to holonomic elasto-plastic models for proportional loading, as used in section 5.2. However, the present model presents one further limitation as the rate of damage is not governed by load magnitude, but only by the volume of damage allowed. A notion of history dependence can be introduced by considering (5.28) for an increasing sequence $0 < V_1 < V_2 < \ldots < V_n < \ldots$ of damage volumes, with an additional constraint for the $(i+1)$'th problem of the form $[\Omega^-{}_i]^* \subseteq \Omega^-{}_{i+1}$, where $[\Omega^-{}_i]^*$ is the domain of damage for the i'th problem, see Francfort and Marigo, 1993. Nevertheless, we just consider the simpler problem (5.27) in the following, as this problem is similar to the topology design problem described in chapter 1. It is actually rather surprising that this very simple model is capable of capturing some essential features of the development of damage, see figure 5.18 below.

As for the topology problem of minimizing compliance, the present problem requires relaxation in order to obtain existence of solutions. From studies of optimal bounds on the effective material properties we know also in this case that layered materials will provide the weakest composites, and thus a required relaxation [21-23]. For plane elasticity, the weakest composite consists of a non-orthogonal rank-2 layering with the *strong* material being the inner material.

For computations an optimality criteria algorithm can be used for this problem also, mimicking the procedure described in chapter 1. Typically, convergence is more difficult to achieve and some experimenting with tuning parameters and move limits is required.

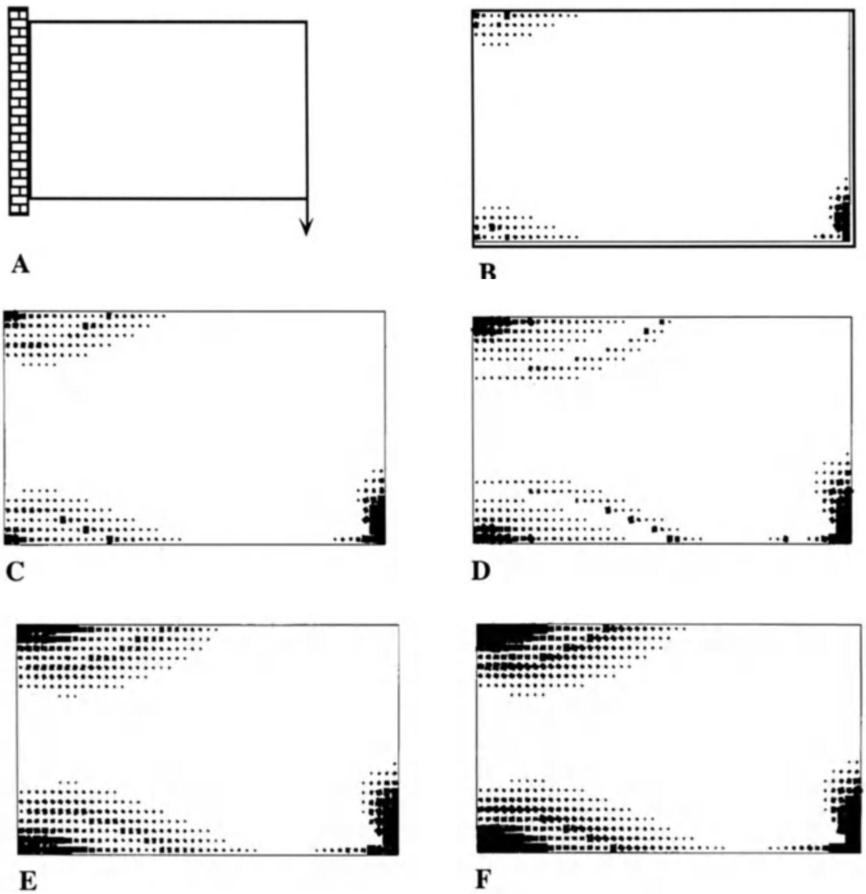

Fig. 5.18. The distribution of damage in an increasingly damaged plane domain (*(B)* through *(F)*). *(A)* shows the structural domain, boundary and load conditions.

6 Bibliographical notes

The bibliography consists of two parts, bibliographical notes and the list of references at the end of the book.

The list of references is concentrated on literature central for the developments described in this monograph, supplemented with background material in order to ease access to work in related fields. The list of references is by no means complete, and should more be seen as a supplement to dedicated survey papers and other monographs.

The purpose of these bibliographical notes is two-fold. The primary purpose is to serve as a guide to the literature in the field of topology design and related subjects. A secondary purpose is to function as a list of references grouped according to subject. In this way long lists of references have been avoided in the main text of the monograph, reference instead being made to these bibliographical notes.

The bibliographical notes cover the various sub-fields of topology design, the groups being largely defined by the structure of the presentation in the main text of the monograph. The entries are divided into books, survey papers and other publications, with a more elaborate division into sub-fields for the latter category of publications. The bibliographical notes do not cover all entries of the list of references, as this list also contains specific references used in the main text.

6.1 Books

[1] On optimal design in general. There exist quite a number of excellent books treating optimal structural design in a broader sense. As a recent textbook we mention Haftka, Gürdal and Kamat, 1993, while Kamat, 1993, is a recent edited research monograph that covers most subjects of the field. For a recent overview of software systems for optimal design, consult Hörnlein and Schittkowski, 1993. Haug, Choi and Komkov, 1986 contains detailed information on sensitivity analysis. A very convenient overview of the developments in the field over the last decade can be gained by consulting the books edited by Haug and Cea, 1981, Morris, 1982, Mota Soares, 1987, and Rozvany , 1993, all of which are based on lecture notes produced for NATO Advanced Summer Schools. Of other books we mention Banichuk, 1983, Banichuk, 1990 and Save and Prager, 1985, 1990 as being closely related to several developments described in this monograph. Very recent proceedings are edited by Herskovits 1993a, 1993b, and Pedersen, 1993, with the latter specializing on design with advanced materials.

[2] **On classical shape design methods.** Example research monographs are Pironneau, 1984, Bennett and Botkin, 1986, and Haslinger and Neittaanmäki, 1988. Sensitivity analysis for shape design problems is treated in detail in Sokolowski and Zolesio, 1992.

[3] **On topology design and layout optimization.** Classical books on this subject are Hemp, 1973, and Rozvany, 1976. A recent survey of lay-out theory can be found in Rozvany, 1989, while Rozvany, 1992, and Bendsøe and Mota Soares, 1993, cover the subject in a broad sense, with the latter emphasizing more the mathematical aspects.

[4] **On homogenization, effective media theory and optimal bounds.** A general introduction on the mechanics of composite materials can be found in, e.g., Christensen, 1991, and Aboudi, 1991. Classical books on the theory of homogenization are Bensoussan, Lions and Papanicolaou, 1978, and Sanchez-Palencia, 1980. Lions, 1981, contains a nice introduction to the subject, also in the context of control theory and Eriksen et al, 1986, is a collection of papers closely related to the contents of the present monograph. Finally, Dal Maso and Dell'Antonio, 1991, is a recent book containing papers on this subject and its relations to relaxation and design.

[5] **On relaxation of functionals in the calculus of variations.** Example research monographs are Attouch, 1984, Buttazzo, 1989, Dacorogna, 1989, Lurie, 1993d, and Dal Maso, 1993. The latter contains a very detailed bibliography.

6.2 Survey papers

[6] **On optimal design in general.** Example survey papers are Banichuk, 1982, Olhoff, and Taylor, 1983, and Taylor, 1987. The crucial influence of material choice on design is vividly described in Ashby, 1991, and Lakes, 1993. A recent overview of issues in structural optimization, encompassing topology, shape and sizing optimization can be found in Ramm et al, 1994.

[7] **On classical shape design methods.** Example survey papers are Vanderplaats, 1984, Ding, 1986, Haftka and Gandhi, 1986.

[8] On topology design and layout optimization. Example survey papers on lay-out theory are Rozvany, 1984, Rozvany, 1993, Rozvany, Zhou and Sigmund, 1994, Rozvany, Bendsøe and Kirsch, 1994. Surveys of numerical methods for truss-type structures are for example Bennett, 1980, Topping, 1983, 1992, 1993, and Kirsch, 1989a. The topology design of structures using the homogenization modelling is covered by Bendsøe, Díaz and Kikuchi, 1993, and Bendsøe and Kikuchi, 1993.

[9] On homogenization, effective media theory and optimal bounds, relaxation of functionals. Homogenization theory as applied to composite materials in elasticity is described in Duvaut, 1976, Lions, 1978, Francu, 1982. The relation between homogenization, smear-out techniques and other theories for effective media is discussed in Fishman and McCoy, 1980. The relaxation of functionals and related topics are covered in Zhikov, Kozlov, Oleinik and Ngoan, 1979. For a survey of the theory of optimal bounds and optimal design, see for example Kohn, 1988, 1991.

6.3 Papers

[10] The homogenization method for topology design, basic methodology. The basic idea of finding the topology of a structure by searching for the optimal indicator function of the material set is discussed briefly in for example Cea, Gioan and Michel, 1973, and Tartar, 1977. The numerical implementation of the homogenization idea was first described in Bendsøe and Kikuchi, 1988, and a closely related idea was pursued in Zochowski, 1988. Further developments of the homogenization idea for topology design can be found in Bendsøe, 1989, Kikuchi and Suzuki, 1991, 1992, Suzuki and Kikuchi, 1991a, 1991b, 1992, 1993, Thomsen, 1991. Details of the implementation of these ideas can also be found in the manuals Suzuki, Kikuchi and Bendsøe, 1988, and Bendsøe and Rodrigues, 1989. Extensions to multiple loads can be found in Díaz and Bendsøe, 1992, and extension to topology design with more than one material is treated numerically in Thomsen, 1992, Olhoff, Krog and Thomsen, 1993, and Olhoff, Thomsen and Rasmussen, 1993. Extensions to shell problems is described in Fukishima, Suzuki and Kikuchi, 1993, Kikuchi, Suzuki and Fukishima, 1991, Suzuki and Kikuchi, 1990, 1991c, while the relation between truss topology design and the homogenization modelling is discussed in Díaz and Belding, 1993. A recent report on industrial testing of the methodology can be found in Chirehdast et al, 1994.

[11] The homogenization method for topology design, the checkerboard problem. The control of the checkerboards in topology design has been discussed in Bendsøe, Díaz and Kikuchi, 1993, Jog, Haber and Bendsøe, 1993a, 1993b, and Rodrigues and Fernandez, 1993a. Recent detailed analyses of the problem can be found in Jog and Haber, 1994, Díaz and Sigmund, 1994. Background material on the similar problem for saddle point problems in analysis can be found in for example Hughes, 1987, and Brezzi and Fortin, 1991.

[12] The theory of homogenization of periodic media. Supplementing the books mentioned above, we mention the description of the dual method for homogenization in Suquet, 1981b, 1982, and the recent alternative two-scale convergence theory for the convergence of homogenized functionals as described in e.g., Allaire, 1992. For the topology design problem, the results on homogenization for problems with voids in Cioranescu and Saint Jean Paulin, 1979, are of crucial importance. Of interest for design is also the relation between cell symmetries and symmetries of composite media as described in, e.g. Lene and Duvaut, 1981, and the shape sensitivity analysis of the effective properties described in Sokolowski, 1993.

[13] Numerical computations of effective media characteristics using homogenization. Computational implementations of the homogenization method for computing effective media characteristics are described in for example Bourgat, 1977, Begis, Duvaut and Hassim, 1981, Guedes and Kikuchi, 1990, Guedes, 1992, and Dvorak, 1993a.

[14] Alternative parametrizations for topology design. The idea of using a variable thickness sheet model to predict topology was first suggested by Rossow and Taylor, 1973; see also Didenko, 1981. A recent application of this idea is by Walther and Mattheck, 1993, where the Young modulus of a material plays the role of thickness and where this method is combined with a basic technique of cutting away under-stressed elements (areas) of a structure; such a method is also is described in Atrek, 1989, 1993. The penalized variable thickness approach for numerically approximating the 0-1 design problem of topology design was tested in Bendsøe, 1989, and has since been used extensively in e.g. Rozvany, Sigmund, Zhou and Birker, 1993, Rozvany and Zhou, 1993a, Rozvany, Zhou, Birker and Sigmund, 1993. Related to this idea and also to the homogenization method is the use of approximate effective energies as used by Mlejnek, Jehle and Schirrmacher, 1991, Mlejnek, 1992, Mlejnik and Schirrmacher, 1993, while Reiter, Rammerstorfer and Böhm, 1993, used ideas from bone adaptation models to predict topology. Of entirely different methodologies are: the search for optimal placement of new holes in a structure (Eschenauer, Kobelev and Schumacher, 1994, Eschenauer, Schumacher and Vietor, 1993), the imbedding method of transforming the problem to a boundary control problem (Haslinger, 1992, Haslinger, Hoffmann and Kocvara, 1992) and the related fictitious domain method (Tiba, Neittaanmäki and Mäkinen, 1990, Tiba, 1991, Neittaanmäki, and Tiba, 1992), and finally the dimensional similarity method proposed by Rosyid and Caldwell, 1991. Finally we mention the important theoretical work by Ambrosio and Buttazzo, 1993, covering topology design with a perimeter penalization.

[15] On boundary shape design methods. The principal introduction to this field can be found in the books and survey papers mentioned above. Of recent developments directed more at CAD integrated shape design we mention Braibant and Fleury, 1984, Kikuchi, Chung Torigaki and Taylor, 1986, Rodrigues, 1988, Rajan, Belegundu and Budiman, 1988, Rasmussen, 1988, 1990, 1991, Rasmussen, Lund and Birker, 1992, Rasmussen, Lund, Birker and Olhoff, 1993, most of which are concerned with two or two and a half dimensional structures described by curves and surfaces. The very recent papers by Rasmussen, Lund and Olhoff, 1993a, 1993b, deals with parametric solid modelling techniques for shape design. For some of the original work on shape sensitivity analysis we refer to Murat and Simon, 1976, Simon, 1980, Haug and Rousselet, 1980a, 1980b, Rousselet and Haug, 1983 and Zolesio, 1981.

[16] Classical layout theory. The classical reference here is Michell, 1904. Modern lay-out theory was founded by Prager and Rozvany and is described in for example Prager, 1963, Prager, 1974, Prager and Rozvany 1977, Prager, 1985a, 1985b, as well as in books mentioned above. The mathematical problems involved in lay-out theory is discussed in for example Lagache, 1981, and Strang and Kohn, 1981, Stavroulakis and Tzaferopoulos, 1994. Recent developments are described in Lewinski, Zhou and Rozvany, 1993, Rozvany, Sigmund, Lewinski, Gerdes and Birker, 1993, Rozvany, Zhou, Lewinski and Sigmund, 1993.

[17] Optimal design with anisotropic materials. Optimal design with orthotropic materials and the problem finding the optimum angle of material rotation is discussed in Rasmussen, 1979, Seregin and Troitskii, 1982, Banichuk, 1983, Fedorov and Cherkaev, 1983, Pedersen, 1989, 1990, Rovati and Taliercio, 1991, Cinquini and Rovati, 1993. Studies on the simultaneous design of thickness and material angle can be found in, e.g, Pedersen, 1991, 1993a, 1993b. Closely related to the moment formulation of design of layered materials is the work of Fukanaga and Vanderplaats, 1991, Grenestedt, Gudmundson, 1993, Miki and Sugiyama, 1993, on design of (engineering) laminates by variations of ply angles and ply lay-up.

[18] Optimality criteria methods in optimal design. The development of optimality criteria algorithms for continuum problems can be traced back to for example Wasiutynsky, 1960, Prager and Taylor, 1968, Taylor, 1969, Masur, 1970. The use of such algorithms for continuum design problems can be found in for example Olhoff, 1970, Olhoff, 1974, Taylor and Rossow, 1977, Olhoff and Taylor, 1979, Cheng, 1981, Cheng and Olhoff, 1981, 1982, Olhoff, Lurie, Cherkaev and Fedorov, 1981, Bendsøe, 1986, Bendsøe and Kikuchi, 1988, Holnicki-Szulc, 1989. Levy, 1991, discusses a fixed point algorithm interpretation of the optimality criteria algorithms, while recent developments in the use of such algorithms are described in Rozvany, Lewinski, Sigmund, Gerdes and Birker, 1993, Rozvany and Zhou, 1991a, 1991b, 1993a, 1993b, Sigmund, Zhou and Rozvany, 1991, Zhou and Rozvany, 1991, Rozvany, Sigmund and Birker, 1993. For the relation between optimality criteria update schemes and models for bone adaptation (adaptive bone-remodelling), see, e.g., Cowin, 1990, Reiter and Rammerstorfer, 1993, Reiter and Rammerstorfer, Böhm, 1993, Weinans, Huiskes and Grootenboer, 1992, Senger, 1993.

[19] Integration of boundary shape optimization and topology design. Integration of the homogenization method for topology design and classical shape design is described in Papalambros and Chirehdast, 1990, 1993, Bendsøe and Rodrigues, 1991, Bremicker, et al 1992, Olhoff, Bendsøe and Rasmussen, 1992, Olhoff, Lund and Rasmussen, 1993, Olhoff, Thomsen and Rasmussen, 1993, Rasmussen, Lund, Birker and Olhoff, 1993, Rasmussen, Thomsen and Olhoff, 1993, Maute and Ramm, 1994. Bendsøe and Rodrigues, 1989, is a manual for such an integrated system. For trusses, integrated geometry and topology design is described in for example Pedersen, 1970, and Nishino and Duggal, 1990, using hierarchical methods. The use of gradient information between the different phases has been considered in Ben-Tal, Kocvara and Zowe, 1993, Bendsøe, Ben-Tal and Zowe, 1994. The use of perimeter constraints in the basic homogenization formulation is discussed in Jog, Haber and Bendsøe, 1993b, 1994b.

[20] Existence of solutions to optimal design problems. Of papers addressing in a survey form the problem of non-existence in optimal design problems we mention here Murat, 1977, 1985, Lurie, 1980, Sokolowski, 1981a, Goebel, 1981, Velte and Villaggio, 1982, Stadler, 1986, Cabib and Dal Maso, 1988, Chenais, 1993. These papers also discuss the two possibilities of achieving existence of solutions: relaxation (see below) or restricting the design space to a compact set. The latter is described in a vast number of papers on for example classical shape design (see books on this subject). A fundamental study on the existence of solution in shape design can be found in Chenais, 1975.

[21] Effective media theory and optimal bounds. We include here only work which is fundamental for topology design as described in this book, i.e., the optimality of ranked layered materials. Such work includes among others (for elasticity) Francfort and Murat, 1986, Lurie and Cherkaev, 1986, Gibiansky and Cherkaev, 1987, Avellaneda, 1987, Kohn and Lipton, 1988, Milton and Kohn, 1988, Lipton, 1988, Avellaneda, 1989, Avellaneda and Milton, 1989, Milton, 1990, Lipton, 1990, Lipton, 1991, Allaire and Kohn, 1993a, 1993b, Lipton, 1993b, 1993c, 1994c. The use of other types of microstructures for optimal bounds are described in for example Vigdergauz, 1986, Milton, 1990, Grabovsky, 1994 and Grabovsky and Kohn, 1994a, 1994b.

[22] Relaxation of functionals in the calculus of variations. The crucial notion of G-convergence of elliptic operators is discussed in De Giorgi and Spagnolo, 1973, Spagnolo, 1976, Raitum, 1978, 1979, Simon, 1979, Spagnolo, 1979. Explicit calculation of the relaxation of functionals in shape design can be found in for example Kohn and Strang, 1986a, 1986b, Buttazzo and Dal Maso, 1991, Buttazzo, 1992, Buttazzo et al, 1994. Consult also the books mentioned above.

[23] Relaxation, effective media and optimal design. The close connection between generalized optimal shape design, relaxation and effective media characteristics is discussed in for example Lurie, 1980, 1992, 1993b, 1993c, Lurie, Cherkaev and Fedorov, 1982, Murat and Tartar, 1985a, 1885b, Kohn and Strang, 1982, 1986a, 1986b, Lurie and Cherkaev, 1986, 1993c, Kohn, 1991, 1992. (see also [34], below)

[24] The homogenization method for topology design using optimal energies. The explicit derivation of extremal energies and associated lamination parameters for minimum compliance design can be found in Kohn, 1992, Allaire and Kohn, 1993c, 1993d, Jog, Haber and Bendsøe, 1993a, 1994a, for the 2-D case, in Cherkaev and Palais, 1994, for the axisymmetric 3-D case and in Allaire, 1994, for the full 3-D case. The use of these expressions for numerical optimal design calculation is also treated in these papers, as well as in Allaire and Francfort, 1993, Allaire, 1994, and the interactive steering of the associated algorithms in a distributed computational environment is described in Haber, Bliss, Jablonowski and Jog, 1992, Jablonowski, Bliss, Bruner and Haber, 1993. The saddle point and duality principle associated with these calculations are discussed in Lipton, 1993a, 1994b, and the relation between the topology design using the homogenization modelling and the design of Michell frames is discussed in Allaire and Kohn, 1993d, Bendsøe and Haber, 1993. Finally, the problem of unstable microstructures is discussed in Cherkaev, 1993a, with a proposal for achieving stability by finite sub-structuring in Cherkaev, 1993d.

[25] Optimal design of topology, shape and material. The use of a free parametrization of material for design has been studied intensively over the recent period, with studies in Bendsøe, Haber, Guedes, Pedersen and Taylor, 1993, Bendsøe, Díaz, Lipton and Taylor, 1994, Bendsøe, Guedes, Plaxton and Taylor, 1994, Bendsøe and Díaz, 1993, 1994, Bendsøe and Guedes, 1994, Ringertz, 1993. The design of materials with prescribed properties is discussed in Autio, Laitinen, Pramila, 1992, for laminates, in Dvorak, 1993b, for conduction problems and in Milton and Cherkaev, 1993, Sigmund, 1994a, 1994b, for arbitrary continua. This latter work uses homogenization for thin structures as treated in e.g., Nayfeh and Hefzy, 1981, Cioranescu and Saint Jean Paulin, 1986, Bakhvalov and Panasenko, 1989, Griso, 1993.

[26] Classical truss topology design by computational methods. The classical formulations as LP problems can be found in for example Dorn, Gomory and Greenberg, 1964, Fleron, 1964, Pedersen, 1970, 1972, Reinschmidt and Russell, 1974, Hörnlein, 1979. The use of optimality criteria methods are described in Taylor and Rossow, 1977, Prager, 1985b. In Ringertz, 1985, 1988, LP solutions are used to produce moderate sized initial designs for more complicated design formulations. More recent studies can be found in for example Kirsch, 1989b, 1990, 1993a, 1993b, Zhou and Xia, 1990, Cheng and Jiang, 1992, Kirsch and Rozvany, 1993, Pedersen 1993c, 1993d, Smith, 1994. Recent applications of optimality criteria algorithms can be found in Rozvany, Lewinski, Sigmund, Gerdes and Birker, 1993, Zhou and Rozvany, 1991. The use of a simultaneous analysis and design formulation in the numerical implementation of truss topology design has been studied in Saka, 1980, Ringertz, 1988, Bendsøe, Ben-Tal and Haftka, 1991, Sankaranaryanan, Haftka and Kapania, 1993.

[27] Reformulations of truss topology design. Displacements only formulations of truss topology problems and other reformulations in terms of stresses only have been considered in Achtziger, Bendsøe, Ben-Tal and Zowe, 1992, Ben-Tal and Bendsøe, 1993, Bendsøe and Ben-Tal, 1993, Bendsøe, Ben-Tal and Zowe, 1994, with numerical aspect discussed in detail in Kocvara and Zowe, 1991. Extension to contact problems can be found in Klarbring, Petersson and Rönnqvist, 1994, Petersson and Klarbring, 1994. The multiple load case in its min-max formulation has been considered in Achtziger, 1992, 1993a, 1993b. The use of interior point methods for truss topology problems in its various reformulations has been treated in Ringertz, 1988, and is discussed in detail in Ben-Tal and Nemirovskii, 1993, 1994, Ben-Tal and Zibulevsky, 1993, Ben-Tal, Yuzefovich and Zibulevsky, 1992, Zibulevsky and Ben-Tal, 1993. Finally the use of convex linearization methods is reported in Beckers and Fleury, 1994. The application of reformulated truss topology problems for the design of aircraft structures can be found in Balabanov and Haftka, 1994.

[28] Discrete valued optimal topology design problems. For continuum structures Anagnostou, Rønquist and and Patera, 1992, discussed the use of a pixel-based discrete optimization procedure for part design and the use of simulated annealing for solving such problems is discussed in for example Szykman and Cagan, 1994. For trusses and discrete structures a few example references are Ringertz, 1986, where truss topology problems are solved by branch and bound, Fleury, 1993, where material selection and element selection problems are treated as discrete optimization problems, Koumousis, 1993, where design according to engineering codes is discussed. The use of genetic algorithms for selection and topology problems are discussed in Grierson and Pak, 1993a, 1993b, Hajela, Lee and Lin, 1993, Chapman and Jakiela, 1994, and similar techniques are used for design of active structures and associated controls in Padula and Sandridge, 1993, Ponslet, Haftka and Cudney, 1993.

[29] Topology and shape design for vibration problems. Topology design for improved vibration response of continuum structures using the homogenization method is described in Díaz and Kikuchi, 1992, Ma, Kikuchi and Hagiwara 1992a, 1992b, Ma, Kikuchi, Cheng and Hagiwara, 1993, Soto and Díaz, 1993d, Kawabe and Yosida, 1994. For grillages, see for example Olhoff and Rozvany, 1982. For trusses such problems are treated in Nakamura, Ohsaki, 1992. Homogenization for eigenvalue problems is treated in for example Kesavan, 1979. Design for improved vibration response by variational analysis is described in for example Olhoff, 1970, 1974, 1976, Bendsøe, Olhoff and Taylor, 1983, with a survey in Olhoff, 1980, 1987. The relationship to design of controlled structures is illustrated in Bendsøe, Olhoff and Taylor, 1987. The main problem of these types of optimization problems is the non-smoothness of the eigenvalues (see also [33]). Special optimization algorithms to cater for this are described in for example Wardi and Polak 1982, Overton, 1988, 1992, and recent detailed accounts of the non-smoothness problem is addressed by Seyranian, 1993, Cox and Overton, 1992, Seyranian, Lund and Olhoff, 1994.

[30] Topology and shape design for elasto-plastic problems. Sizing design of discrete elasto-plastic structures is covered in for examples Dems and Mroz, 1978, Cinquini and Sacchi,. 1980, Kaneko and Maier, 1981, Cyras, 1983, Cinquini and Contro, 1985, Selyugin, 1992, with sensitivity analysis in Bendsøe and Sokolowski, 1988. The design for power-law type models is discussed in Pedersen and Taylor, 1993. Shape design of elasto-plastic structures is discussed in for example Hlavacek, 1986, 1987, 1991, Haslinger and Mäkinen, 1992, Haslinger and Dimitrovova, 1993. The design of structures within a unified formulation of elasto-plastic problems and limit analysis has been studied recently in Bendsøe, Olhoff and Taylor, 1993, Taylor, 1993c, Taylor and Logo, 1993, Taylor and Washabaugh, 1994, for discrete structures and as a free material design problem in Bendsøe, Guedes, Plaxton and Taylor, 1994. This work is based on the modelling described in Ben-Tal and Taylor, 1992, Plaxton and Taylor, 1993, Taylor, 1989, 1993a, 1993b. For a description of related models, see for example Maier, 1970, Sayegh and Rubenstein, 1972, Necas and Hlavacek, 1981, as well as the references of Taylor, 1993a. The homogenization modelling method for topology design has yet to be implemented for these problems, but could be based on studies of the homogenization for elasto-plastic problems as described in, e.g., Bouchitte and Suquet, 1991, Lin, Yang, Mura and Iwakuma, 1992, Michel and Suquet, 1993.

[31] The plate problem. This is one of the classical problems in structural optimization. Kirchhoff plate design using the thickness only was treated for example by Kozlowski and Mroz, 1969, Olhoff, 1970, 1974, Banichuk, 1975, 1981. A survey of such studies can be found in Haftka and Prasad, 1981. Armand and Lodier, 1978, found by numerical means certain numerical instabilities and this was investigated in detail by Cheng and Olhoff, 1981, leading to the use of rib-stiffened plates in design of Kirchhoff plates. Such applications for elastic plates were described in Cheng and 1981, Olhoff and Lurie, Cherkaev and Fedorov, 1981, Cheng and Olhoff, 1982, Armand, Lurie and Cherkaev, 1982, Bonnetier and Vogelius, 1987, with one field of stiffeners, and in Bendsøe, 1986, for two fields of stiffeners. Design of plastic plates and the relation to lay-out theory was discussed in Rozvany, Olhoff, Cheng and Taylor, 1982. The optimality of a rank-2 stiffened plate was shown in Gibiansky and Cherkaev, 1984, with a sub-problem discussed in Lurie and Cherkaev, 1984b. Analytical studies of rank-2 perforated plates was carried out in Rozvany, Ong, Szeto, Olhoff and Bendsøe, 1987, Ong, Rozvany and Szeto, 1988, and the problem of placing a discrete number of stiffeners on a plate by Samsonov, 1980, 1983. Multiple load problems and random load problems are studied in Lipton, 1993d, 1994a, 1994d, Lurie, 1993a, 1994, while the use of the homogenization method for topology design for

Mindlin plates is discussed in Soto and Díaz, 1993a-c, Díaz, Lipton and Soto, 1994. Existence of solutions to the plate problem by bounding the variation of the thickness has been discussed in Litvinov, 1980, Litvinov and Panteleev, 1980, Niordson, 1983, Sokolowski, 1981b, Bendsøe, 1983, 1984. Homogenization of the plate equations has been dealt with in Duvaut and Metellus, 1976, Artola and Duvaut, 1977, Duvaut, 1977, Kolpakov, 1983, while various models of ribbed plates derived from 3D elasticity are derived and discussed in Caillerie, 1982, 1984, Kohn and Vogelius, 1984, 1985, 1986, Lewinski, 1991a, 1991b, 1991c, 1993. The latter studies relate directly to design problems, as does the detailed study of various stiffened plate models by Soto and Díaz, 1993a. These works relate directly to formal justifications of plate models from 3-D elasticity theory as described in, e.g., Ciarlet, 1979, 1980, Ciarlet and Rabier, 1980, Destuynder, 1981, 1986. A recent discussion of the problem of finding a 'good' or 'correct' plate model can be found in Babuska, 1992.

[32] Topology and shape design for thermo-elastic and damage problems. Topology design of thermo-elastic structures has been described in Rodrigues and Fernandes, 1993a, 1993b, based on the homogenization results presented in, e.g., Francfort, 1983, Brahlm-Otsmane, Francfort and Murat, 1989. The relation between damage models, homogenization and generalized 'shape' design is discussed in Suquet, 1985, Francfort and Marigo, 1991, 1993.

[33] Topology design for stability problems. Structural design under stability constraints is a vast subject as can be seen by consulting Zyczkowski and Gajewski, 1988, Zyczkowski (ed.), 1989. However, topology design is less well studied, with recent contributions in Pedersen 1993c, 1993d, for trusses and in Neves, Guedes and Rodrigues, 1993, 1994, Neves, 1994, for continuum structures. The related problem of homogenization of buckling problems is treated in Mignot, Puel and Suquet, 1980, Suquet 1981a, and the relation between microscopic and macroscopic buckling is discussed in Bendsøe and Triantafyllidis, 1990, Geymonat, Müller and Triantafyllidis, 1993, Triantafyllidis and Schnaidt, 1993. As for vibration problems, a major obstacle in computations is the non-smoothness of the eigenvalues (see [29]) in the stability problems at multi-modal solutions (such solutions were first discovered by Olhoff and Rasmussen, 1977, for columns).

[34] Other areas of application. The basic developments of relaxation, optimal bounds and optimal lay-out for elasticity have had a parallel (actually slightly preceding) history for problems in conduction, see for example Lurie and Cherkaev, 1982a, 1982b, 1984a, Goodman, Kohn and Reyna, 1986, Kawohl, Stara and Wittum, 1991, Lurie and Lipton, 1992. Similar design problem arise also in impedance computed tomography as described in, e.g., Kohn and Vogelius, 1987. Of another design problem which has been solved by analogous ideas and techniques as described in these notes we can mention the optimal topology design of a photocell using a variable thickness type approach, see Achdou, 1993.

References

The list of references is ordered alphabetically according to author and sub-ordered according to year of publication. Reference to an entry in the main text and the bibliographical notes is of the form Smith and Wesson, 1887.

Aboudi J (1991): Mechanics of Composite Materials. Elsevier Science Publ., Amsterdam.

Achdou Y (1993): Numerical Optimization of a Photocell. Comp. Meth. Appl. Mech. Engng., 102, 89-106.

Achtziger W (1992): Truss Topology Design under Multiple Loadings. DFG-Report (FSP 'Applied Optimization and Control'), no. 367, Universität Bayreuth, FRG.

Achtziger W (1993a): Minimax Compliance Truss Topology Subject to Multiple Loadings. loc. cit. Bendsøe and Mota Soares, 1993, 43-54

Achtziger W (1993b): Optimierung von einfach und mehrfach belasteten Stabwerken. Bayreuther Mathematische Schriften, Heft 46.

Achtziger W (1994): Multiple Load Truss Topology and Sizing Optimization: Some Properties of Minimax Vompliance. MAT-report no. 1994-41, Math. Inst., Techn. Univ. of Denmark, DK-2800 Lyngby, Denmark.

Achtziger W; Bendsøe MP; Ben-Tal A; Zowe J (1992): Equivalent Displacement Based Formulations for Maximum Strength Truss Topology Design. IMPACT of Computing in Science and Engineering, 4, 315-345.

Allaire G (1992): Homogenization and Two-Scale Convergence. SIAM J. Math. Anal., 23, 1482-1518.

Allaire G (1994a): Explicit Lamination Parameters for Three-Dimensional Shape Optimization. Control and Cybernetics, 23, 309-326.

Allaire G (1994b): Relaxation of Structural Optimization Problems by Homogenization. Preprint, Commissariat a l'Energie Atomique, Gif sur Yvette, France.

Allaire G; Francfort GA (1993): A Numerical Algorithm for Topology and Shape Optimization. loc. cit. Bendsøe and Mota Soares, 1993, 239-248

Allaire G; Kohn RV (1993a): Explicit Bounds on the Elastic Energy of a Two-Phase Composite in Two Space Dimensions. Q. Appl. Math., 51, 675-699.

Allaire G; Kohn RV (1993b): Optimal Bounds on the Effective Behaviour of a Mixture of Two Well-Ordered Elastic Materials. Q. Appl. Math., 51, 643-674.

Allaire G; Kohn RV (1993c): Topology Optimization and Optimal Shape Design using Homogenization. loc. cit. Bendsøe and Mota Soares, 207-218

Allaire G; Kohn RV (1993d): Optimal Design for Minimum Weight and Compliance in Plane Stress using Extremal Microstructures. European J. Mech. A, 12, 839-878.

Ambrosio L; Buttazzo G (1993): An Optimal Design Problem with Perimeter Penalization. Calc. Var., 1, 55-69.

Anagnostou G; Rønquist EM; Patera AT (1992): A Computational Procedure for Part Design. Comp. Meth. Appl. Mech. Engng., 97, 33-48.

Armand JL; Lodier B (1978): Optimal Design of Bending Elements. Int. J. Num. Meth. Engng., 13, 373-384.

Armand JL; Lurie KA; Cherkaev AV (1982): Optimal Control Theory and Structural Design. In Gallagher RH; Atrek E; Ragsdell K; Zienkiewicz OC (eds.), Optimum Structural Design, Vol. 2., John Wiley and Sons, New York.

Artola M; Duvaut G (1977): Homogeneisation d'une plaque renforcee. C. R. Acad. Sc. Paris, Serie A, t. 284, 707-710.

Ashby MF (1991): Materials and Shape. Acta Metall. Mater., 39, 1025-1039.

Atrek E (1989): SHAPE: A Program for Shape Optimization of Continuum Structures. In: Brebbia, C.; Hernandez, S. (eds.), Computer Aided Design of Structures: Applications. Springer Verlag, 135-144.

Atrek E (1993): SHAPE: A Structural Shape Optimization Program. loc. cit. Hörnlein, and Schittkowski, 1993, 229-250.

Attouch H (1984): Variational Convergence for Functions and Operators. Pitman, London, United Kingdom.

Autio M; Laitinen M; Pramila A (1992): Systematic Creation of Composite Structures with Prescribed Thermomechanical Properties. Comp. Eng., 3, 249-259.

Avellaneda M (1987): Optimal Bounds and Microgeometries for Elastic Two-Phase Composites. SIAM J. Appl. Math., 47, 1216-1228.

Avellaneda M (1989): Bounds on the Effective Elastic Constants of Two-Plane Composite Materials. Proc. Sem. College de France, X, (Brezis V; Lions J-L, eds.), Pitman, London.

Avellaneda M; Milton GW (1989): Bounds on the Effective Elasticity Tensor Composites based on Two-point Correlation. In Hui D; Kozik TJ (eds.), Composite Material Technology, ASME, 89-93.

Babuska I (1992): The Problem of Plate Modelling: Theoretical and Computational Results. Comp. Meth. Appl. Mech. Engng., 100, 249-273.

Bakhvalov N; Panasenko G (1989): Homogenization: Averaging Processes in Periodic Media. Kluwer Academic Publishers, Dordrecht, The Netherlands.

Balabanov V; Haftka RT (1994): Topology Optimization of Transport Wing Internal Structure. In Proc. 5th AIAA/USAF/NASA/ISSMO Symposium on Multidisciplinary Analysis and Optimization, Panama City, Fl., September 7-9, 1994, Vol. 2, 1395-1406.

Banichuk NV (1975): Optimal Elastic Plate Shapes in Bending Problems, Mekh. Tverd. Tela, 10, 151-158

Banichuk NV (1981): Design of Plates for Minimum Deflection and Stress. loc. cit. Haug; and Cea, 1981, 283-308.

Banichuk NV (1982): Current Problems in the Optimization of Structures. Mechanics of Solids, 17, 95-105.

Banichuk NV (1983): Problems and Methods of Optimal Structural Design. Plenum Press, New-York, USA.

Banichuk NV (1990): Introduction to Optimization of Structures. Springer Verlag, New-York, USA.

Beckers M; Fleury C (1994): A Primal-Dual Approach in Truss Optimization. In Topping BHV; Papadrakakis M (eds.), Advances in Structural Optimization, CIVIL-COMP Press, Edinburgh, Scotland, 91-101.

Begis D; Duvaut G; Hassim A (1981): Homogeneisation par Element Finis des Modules de Comportements Elastiques de Materiaux Composites. Rapports de Recherche No. 101, INRIA, Rocquencourt, Le Chesnay, France.

Ben-Tal A; Bendsøe MP (1993) A New Method for Optimal Truss Topology Design. SIAM J. Optimization, 3, 322-358.

Ben-Tal A; Kocvara M; Zowe J (1993): Two Non-Smooth Methods for Simultaneous Geometry and Topology Design of Trusses. loc. cit. Bendsøe and Mota Soares, 1993, 31-42.

Ben-Tal A; Nemirovskii A (1993): An Interior Point Algorithm for Truss Topology Design. loc. cit. Bendsøe and Mota Soares, 1993, 55-70

Ben-Tal A; Nemirovskii A (1994): Potential Reduction Polynomial Time Method for Truss Topology Design. SIAM J. Optimization, 4, 596-612.

Ben-Tal A; Taylor JE (1992): A Unified Model for Elastoplastic Structural Analysis Via Dual Variational Principles. In Field DA; Komkov V (eds.), Theoretical Aspects of Industrial Design, SIAM, Philadelphia, 12-31.

Ben-Tal A; Yuzefovich I; Zibulevsky M (1992): Penalty/Barrier Multiplier Methods for Minmax and Constrained Smooth Convex Problems. Research Report 9/92, Optimization Lab., Technion, (Israel Inst. of Technology).

Ben-Tal A; Zibulevsky M (1993): Penalty/Barrier Multiplier Methods: A New Class of Augmented Lagrangian Algorithms for Large Scale Convex Programming Problems. Research Report 6/93, Optimization Lab., Technion, (Israel Inst. of Technology).

Bendsøe MP (1983): On Obtaining a Solution to Optimization Problems for Solid, Elastic Plates by Restriction of the Design Space. J. Struct. Mech., 11, 501-521.

Bendsøe MP (1984): Existence Proofs for a Class of Plate Optimization Problems. Lecture Notes in Control and Information Sciences, Vol. 59, Springer Verlag, Berlin, 773-779

Bendsøe MP (1986): Generalized Plate Models and Optimal Design. loc. cit. Eriksen et al, 1986, 1-26.

Bendsøe MP (1989): Optimal Shape Design as a Material Distribution Problem. Struct. Optim., 1, 193-202.

Bendsøe MP; Ben-Tal A (1993): Truss Topology Optimization by a Displacements Based Optimality Criterion Approach. loc. cit. Rozvany, 1993a, 139-155.

Bendsøe MP; Ben-Tal A; Haftka RT (1991): New Displacement - Based Methods for Optimal Truss Topology Design. Proc. AIAA/ASME/ASCE/ AHS/ASC 32nd. Structures, Structural Dynamics and Materials Conference, Baltimore, MD, USA, April 8-10.

Bendsøe MP; Ben-Tal A; Zowe J (1994): Optimization Methods for Truss Geometry and Topology Design. Struct. Optim., 7, 141-159.

Bendsøe MP; Díaz AR (1993): Optimization of Material Properties for Mindlin Plate Design. Struct. Optim., 6, 268-270.

Bendsøe MP; Díaz AR (1994): Optimization of Material Properties for Improved Frequency Responce. Struct. Optim., 7, 138-140.

Bendsøe MP; Díaz AR; Kikuchi N (1993): Topology and Generalized Layout Optimization of Elastic Structures. loc. cit. Bendsøe and Mota Soares, 159-206

Bendsøe MP; Díaz AR; Lipton R; Taylor JE (1994): Optimal Design of Material Properties and Material Distribution for Multiple Loading Conditions. Int. J. Num. Meth. Engng., 38.

Bendsøe MP; Guedes JM (1994): Some Computational Aspects of Using Extremal Material Properties in the Optimal Design of Shape, Topology and Material. Control and Cybernetics, 23, 327-349.

Bendsøe MP; Guedes JM; Haber RB; Pedersen P; Taylor JE (1993): An Analytical Model to Predict Optimal Material Properties in the Context of Optimal Structural Design. J. Applied Mech. (to appear).

Bendsøe MP; Guedes JM; Plaxton S; Taylor JE (1994): Optimization of Structure and Material Properties for Solids Composed of Softening Material. Proc. 5th AIAA/USAF/NASA/ISSMO Symposium on Multidisciplinary Analysis and Optimization, Panama City, Fl., Sept. 7-9, 1994, Vol. 2, pp. 1057- 1065.

Bendsøe MP; Haber RB (1993): The Michell Layout Problem as a Low Volume Fraction Limit of the Perforated Plate Optimization Problem: An Asymptotic Study. Struct. Optim., 6, 263-267.

Bendsøe MP; Kikuchi N (1988): Generating Optimal Topologies in Structural Design Using a Homogenization Method. Comp. Meth. Appl. Mechs. Engrg., 71, 197-224.

Bendsøe MP; Kikuchi N (1993): Topology and Layout Optimization of Discrete and Continuum Structures. loc. cit. Kamat, 1993, 517-547.

Bendsøe MP; Mota Soares CA (eds.) (1993): Topology Optimization of Structures. Kluwer Academic Press, Dordrecht, The Netherlands.

Bendsøe MP; Olhoff N; Sokolowski J (1985): Sensitivity Analysis of Problems of Elasticity with Unilateral Constraints. J. Struct. Mech., 13, 201-222.

Bendsøe MP; Olhoff N; Taylor JE (1983): A Variational Formulation for Multicriteria Structural Optimization. J. Struct. Mech., 11, 523-544.

Bendsøe MP; Olhoff N; Taylor JE (1987): On the Design of Structure and Controls for Optimal Performance of Actively Controlled Flexible Structures. Mech. Struct. Mach., 15, 265-295.

Bendsøe MP; Olhoff N; Taylor JE (1993): A Unified Approach to the Analysis and Design of Elasto-Plastic Structures with Mechanical Contact. loc. cit. Rozvany, 1993a, 697-706.

Bendsøe MP; Rodrigues HC (1989): OPTI-2D-TOPOLOGY-SHAPE, Users guide. Version 0.5, June 1989. Mathematical Institute, Technical Umiversity of Denmark, DK-2800 Lyngby.

Bendsøe MP; Rodrigues HC (1991): Integrated Topology and Boundary Shape Optimization of 2-D solids. Comp. Meth. Appl. Mech. Engng., 87, 15-34.

Bendsøe MP; Sokolowski J (1987): Sensitivity Analysis and Optimal Design of Elastic Plates with Unilateral Point Supports. Mech. Struct. Mach., 15, 383-393.

Bendsøe MP; Sokolowski J (1988): Design Sensitivity Analysis of Elastic-Plastic Analysis Problems. Mech. Struct. Mach., 16, 81-102.

Bendsøe MP; Sokolowski J (1995): Shape Sensitivity Analysis of Optimal Compliance Functionals. Mech. Struct. Mach., 23, 35-58.

Bendsøe MP; Triantafyllidis N (1990): Scale Effects in the Optimal Design of a Microstructured Medium against Buckling. Int. J. Solids Struct., 26, 725-741.

Bennett JA; Botkin M (eds.) (1986): The Optimum Shape: Automated Structural Design. Plenum Press, New York, USA.

Bennett JA (1980): Topological Structural Synthesis. Computers and Structures, 12, 273-280.

Bensoussan A; Lions J-L; Papanicolaou G (1978): Asymptotic Analysis for Periodic Structures. North-Holland, Amsterdam.

Bonnetier E; Vogelius M (1987): Relaxation of a Compliance Functional for a Plate Optimization Problem. In Ciarlet PG; Sanchez-Palencia E (eds.), Applications of Multiple Scaling in Mechanics, Masson, Paris, France, 31-53.

Bouchitte G; Suquet P (1991): Homogenization, Plasticity, and Yield Design. loc. cit. Dal Maso and Dell'Antonio, 1991, 107-134.

Bourgat JF (1977): Numerical Experiments of the Homogenization Method for Operators with Periodic Coefficients. Lecture Notes in Mathematics, 704, Springer Verlag, Berlin, 330-356.

Brahlm-Otsmane S; Francfort GA; Murat F (1989): Homogenization in Thermoelasticity Report no. R89011, Publications du Laboratoire d'Analyse Numérique, Universite Pierre et Marie Curie, Centre National de la Recherche Scientifique, Paris, France.

Braibant V; Fleury C (1984): Shape Optimal Design using B-Splines. Comp. Meth. Appl. Mech. Engng., 44, 247-267.

Bremicker M; Chirehdast M; Kikuchi N; Papalambros P (1992): Integrated Topology and Shape Optimization in Structural Design. Mech. Struct. Mach., 19, 551-587.

Brezzi F; Fortin M (1991): Mixed and Hybrid Finite Element Methods. Springer Verlag, New York.

Buttazzo G (1989): Semicontinuity, Relaxation and Integral Representation in the Calculus of Variations. Research Notes in Math., Vol. 207, Pitman, Boston.

Buttazzo G (1992): Existence Via Relaxation for Some Domain Optimization Problems. loc. cit. Bendsøe and Mota Soares, 1993, 337-344

Buttazzo G; Dal Maso G (1991): Shape Optimization for Dirichlet Problems: Relaxed Solutions and Optimality Conditions. Appl Math. Optim. , 23, 17-49.

Buttazzo G; Dal Maso G; Garroni A; Malusa A (1994): On The Relaxed Formulation of some Shape Optimization Problems. Preprint, SISSA-ISAS, Trieste, Italy.

Cabib E; Dal Maso G (1988): On a Class of Optimum Problems in Structural Design. J. Optim. Th. Appl., 56, 39-65.

Caillerie D (1982): Plaques elastiques minces structure periodique et d'epaisseur comparables. C.R. Acad. Sc. Paris, t. 298, Serie II, 159-162.

Caillerie D (1984): Thin Elastic and Periodic Plates. Math. Meth. Appl. Sci., 6, 159-191.

Cea J; Gioan A; Michel J (1973): Quelques resultat sur l'identification de domaines. Calcolo III / IV.

Cea J; Malanowski K (1970): An Example of a Max-Min Problem in Partial Differential Equations. SIAM J. Control, 8, 305-316.

Chapman CD; Jakiela MJ (1994): Genetic Algorithm-Based Structural Topology Design with Compliance and Manufacturability Considerations. In Proc. 20th ASME Design Automation Conference, Minneapolis, Mn, September 11-14, 1994, ASME publication DE-Vol. 69-2.

Chenais D (1975): On the Existence of a Solution in a Domain Identification Problem. J. Math. Anal. Appl., 52, 189-289.

Chenais D (1993): Why Does It Seem Difficult to Avoid Homogenization Type Methods in Order to Change Topology in Shape Optimization. loc. cit. Bendsøe and Mota Soares, 1993, 331-336

Cheng G (1981): On Non-Smoothness in Optimal Design of Solid, Elastic Plates. Int. J. Solids Struct., 17, 795-810.

Cheng G; Jiang Z (1992): Study on Topology Optimization with Stress Constraints. Eng. Opt., 20, 129-148.

Cheng G; Olhoff N (1981): An Investigation Concerning Optimal Design of Solid Elastic Plates. Int. J. Solids Struct., 16, 305-323.

Cheng G; Olhoff N (1982): Regularized Formulation for Optimal Design of Axisymmetric Plates. Int. J. Solids Struct., 18, 153-170.

Cherkaev AV (1993a): Stability of Optimal Structures of Elastic Composites. loc. cit. Bendsøe and Mota Soares, 1993, 547-558

Cherkaev AV (1993b): Conducting and Elastic Composites of Optimal Structures. loc. cit. Herskovits, 1993a, 377-385.

Cherkaev AV (1993c): Relaxation of Problems of Optimal Structural Design. Preprint, Department of Mathematics, University of Utah, Salt Lake City, UT, USA.

Cherkaev AV (1993d): Optimization of the Energy by Composites with Piecewise Constant Structures. Preprint, Department of Mathematics, University of Utah, Salt Lake City, UT, USA.

Cherkaev AV; Palais R (1994): Optimal Design of Three-Dimensional Axisymmetric Elastic Structures Preprint, Department of Mathematics, University of Utah, Salt Lake City, UT, USA.

Chirehdast M; Sankaranarayanan S; Ambo S; Johnson R (1994): Validation of Topology Optimization for Component Design. In Proc. 5th AIAA/USAF/NASA/ISSMO Symposium on Multidisciplinary Analysis and Optimization, Panama City, Fl., September 7-9, 1994, Vol. 1, 132-137.

Christensen RM (1991): Mechanics of Composite Materials. Krieger, Amsterdam.

Ciarlet PG (1979): A Justification of the Two-Dimensional Linear Plate Model. Journal de Mécanique, 18, 315-344.

Ciarlet PG (1980): A Justification of the Von Karman Equations. Arch. Rat. Mech. Anal., 73, 349-389.

Ciarlet PG; Rabier P (1980): Les Equations de von Karman. Lecture Notes in Mathematics, Vol. 826, Springer, Berlin.

Cinquini C; Contro R (1985): Optimal Design of Beams Discretized by Elastic Plastic Finite Element. Comp. Struct., 20, 475-485.

Cinquini C; Rovati M (1993): Optimal Orientation of Orthotropic Properties for Continuum Bodies and Structural Elements. loc. cit. Rozvany, 1993a, 707-730.

Cinquini C; Sacchi G (1980): Problems of Optimal Design for Elastic and Plastic Structures. Journal de Mecanique appl., 4, 31-59.

Cioranescu D; Saint Jean Paulin J (1979): Homogenization in Open Sets with Holes. J. Math. Anal. Appl., 71, 590-607.

Cioranescu D; Saint Jean Paulin J (1986): Reinforced and Honey-comb Structures. J. Math. Pure et Appl., 65, 403-422.

Cowin SC (1990): Structural Adaptation of Bones. Appl. Mech. Rev., 43, S127-S133.

Cox SJ; Overton ML (1992): On the Optimal Design of Columns Against Buckling. SIAM J. Math. Anal., 23, 287-325.

Cyras AA (1983): Mathematical Models for the Analysis and Optimization of Elastoplastic Structures. Ellis Horwood Ltd., Chichester, UK.

Dacorogna B (1989): Direct Methods in the Calculus of Variations. Springer Verlag, Berlin

Dal Maso G (1993): An Introduction to Γ-Convergence. Birkhäuser, Boston, USA.

Dal Maso G; Dell'Antonio GF (eds.) (1991): Composite Media and Homogenization Theory. Birkhäuser, Boston, USA.

De Giorgi E; Spagnolo S (1973): Sulla convergenza degli integrali dell'energia per operatori ellittici del secondo ordine. Boll. U. M. I., 8, 391-411.

Dems K; Mroz Z (1978): Multiparameter Structural Shape Optimization by the Finite Element Method. Int J. Num. Meth. Engng., 13, 247-263.

Demyanov VF; Malozemov VN (1974): Introduction to Minimax., John Wiley and Sons, New York.

Destuynder Ph (1981): Comparaison entre les mod les tridimensionnels et bidimensionnels de plaques en elasticite. R.A.I.R.O. Analyse Numerique, 15, 331-369.

Destuynder Ph (1986): Une theorie asymptotique des plaques minces en elasticite lineaire. Masson, Paris, France.

Díaz AR; Belding B (1993): On Optimum Truss Layout by a Homogenization Method. ASME Transactions of Mechanical Design.

Díaz AR; Bendsøe MP (1992): Shape Optimization of Structures for Multiple Loading Conditions using a Homogenization Method, Struct. Optim., 4, 17-22.

Díaz AR; Kikuchi N (1992): Solutions to Shape and Topology Eigenvalue Optimization Problems using a Homogenization Method. Int. J. Num. Meth. Engng., 35, 1487-1502.

Díaz AR; Lipton R; Soto CA (1994): A New Formulation of the Problem of Optimum Reinforcement of Reissner-Mindlin Plates. Comp. Meth. Appl. Mechs. Engrg. (to appear).

Díaz AR; Sigmund O (1994): Checkerboard Patterns in Layout Optimization. Preprint, Department of Mechanical Engineering, Michigan State University, East Lansing, MI, USA.

Didenko NI (1981): Optimal Distribution of Bending Stiffness of an Elastic Freely Supported Plate. Mech. Solids (MTT), 16, 133-143.

Ding Y (1986): Shape Optimization of Structures: A Literature Survey. Computers and Structures, 24, 985-1004.

Dorn W; Gomory R; Greenberg M (1964): Automatic Design of Optimal Structures, J. de Mecanique, 3, 25-52.

Duvaut G (1976): Analyse fonctionnelle et mecanique des milieux continus. Application l'etude des materiaux composites elastiques a structure periodique - homogeneisation. In: Proc. 14the IUTAM Congress, Delft, The Netherlands (1976), North- Holland Publ., Amsterdam, 119-132.

Duvaut G (1977): Comportement macroscopique d'une plaque perforeée périodiquement. Lecture Notes in Mathematics, 594, Springer, Berlin, 131-145.

Duvaut G; Metellus A-M (1976): Homogénéisation d'une plaque mince en flexion de structure périodique et symétrique. C.R. Acad. Sc. Paris, t. 283, Serie A, 947-950.

Dvorak J (1993a): A Reliable Method of Computing Homogenized Coefficients. In Haslinger J (ed.), Mathematical Models in Computer Aided Optimal Design, Lecture Notes, Advanced TEMPUS course, July 12-16, Faculty of Mathematics and Physics, Charles University, Prague, Czech Republic.

Dvorak J (1993b): Optimization of Composite Materials. Master's Thesis, Faculty of Mathematics and Physics, Charles University, Prague, Czech Republic.

Eriksen JL; Kinderlehrer D; Kohn RV; Lions J-L (eds.) (1986): Homogenization and Effective Moduli of Materials and Media. The IMA Volumes in Mathematics and Its Applications, Springer, Berlin.

Escauriaza L; Seo JK (1993): Regularity Properties of Solutions to Transmission Problems. Trans. AMS, 338, 405-430.

Eschenauer HA; Kobelev V; Schumacher A (1994): Bubble Method of Topology and Shape Optimization of Structures. Struct. Optim., 8, 42-51.

Eschenauer HA; Schumacher A; Vietor T (1993): Decision Makings for Initial Designs Made of Advanced Materials. loc. cit. Bendsøe and Mota Soares, 1993, 469-478.

Fedorov AV; Cherkaev AV (1983): Choice of Optimal Orientation of Axes of Elastic Symmetry for an Orthotropic Plate. MTT, 18, 135-142.

Fishman L; McCoy JJ (1980): Homogenization and Smoothing: A Unified View of Two Derivations of Effective Property Theories and Extensions. J. Appl. Mech., 47, 679-682.

Fleron P (1964): The Minimum Weight of Trusses. Bygnings statiske Meddelelser, 35, 81-96.

Fleury C (1993): Discrete Valued Optimal Design Problems. loc. cit. Bendsøe and Mota Soares, 1993, 81-88

Francfort GA (1983): Homogenization and Linear Thermoelasticity. SIAM J. Math. Anal., 14, 696-708.

Francfort GA; Marigo J-J (1991): Mathematical Analysis of the Damage Evolution in a Brittle Damaging Continuous Medium. In Blanc RH; Roous M; Suquet P (eds.), Mecanique, Modelisation Numerique et Dynamique des Materiaux, Publ. du Lab. de Mecanique at d'Acoustique de Marseilles, CNRS, France, no. 124, 245-276.

Francfort GA; Marigo J-J (1993): Stable Damage Evolution in a Brittle Continuous Medium. Eur. J. Mech. A/Solids, 12, 149-189.

Francfort GA; Murat F (1986): Homogenization and Optimal Bounds in Linear Elasticity. Arch. Rat. Mech. Anal., 94, 307-334.

Francu J (1982): Homogenization of Linear Elasticity Equations. Aplikace Matematiky, 27, 96-117.

Fukanaga H; Vanderplaats GN (1991): Stiffness Optimization of Orthotropic Laminated Composites Using Lamination Parameters. AIAA J., 29, 641-646.

Fukishima J; Suzuki K; Kikuchi N (1993): Applications to Car Bodies: Generalized Layout Design of Three-Dimensional Shells. loc. cit. Rozvany, 1993a, 177-191.

Geymonat G; Müller S; Triantafyllidis N (1993): Homogenization of Nonlinear Elastic Materials, Microscopic Bifurcation and Macroscopic Loss of Rank-One Convexity. Arch. Rat. Mech. Anal., 122, 231-290.

Gibiansky LV; Cherkaev AV (1984): Design of Composite Plates of Optimal Rigidity. Rept. No. 914, A.F. Ioffe Physical Technical Institute, Academy of Sciences of the USSR, Leningrad (in Russian).

Gibiansky LV; Cherkaev AV (1987): Microstructures of Composites of Extremal Rigidity and Exact Estimates of the Associated Energy Density. Ioffe Physicotechnical Institute preprint 1115, Leningrad (in Russian); Also in Kohn RV (ed.), Topics in the Mathematical Modelling of Composite Materials, Birkhauser, New York, USA, 1994.

Goebel M (1981): Optimal Control of Coefficients in Linear Elliptic Equations I. Existence of Optimal Control. Math. Operationsforsh. Statist. Ser. Optim., 12, 525-533.

Goodman J; Kohn RV; Reyna L (1986): Numerical Study of a Relaxed Variational Problem from Optimal Design. Comp. Meth. Appl. Mech. Engrg., 57, 107-127.

Grabovsky Y (1994): Bounds and Extremal Microstructures for Two-Component Composites: A Unified Treatment Based on the Translation Method. Preprint, Courant Institute, NYU, New York, NY, USA.

Grabovsky Y; Kohn RV (1994a): Microstructures minimizing the Energy of a Two Phase Elastic Composite in Two Space Dimensions. I: The Confocal Ellipse Construction. Preprint, Courant Institute, NYU, New York, NY, USA.

Grabovsky Y; Kohn RV (1994b): Microstructures minimizing the Energy of a Two Phase Elastic Composite in Two Space Dimensions. II: The Vigdergauz Microstructure. Preprint, Courant Institute, NYU, New York, NY, USA.

Grenestedt JL; Gudmundson P (1993): Layup Optimization of Composite Material Structures loc. cit. Pedersen, 1993c, 311-336.

Grierson DE; Pak WH (1993a): Discrete Optimal Design Using a Genetic Algorithm. loc. cit. Bendsøe and Mota Soares, 1993, 89-102

Grierson DE; Pak WH (1993b): Optimal Sizing, Geometrical and Topological Design Using a Genetic Algorithm. Struct. Optim., 6, 151-159.

Griso G (1993): Etude d'un probleme elliptique avec conditions de Neuman dans un domaine reticule. Preprint, Lab. Analyse Numerique, Universite Paris VI, 4 place Jussieu, F-75252 Paris, France.

Guedes JM (1992): Effective Properties for Non-Linear Composite Materials: Computational Aspects loc. cit. Bendsøe and Mota Soares, 1993, 375-394

Guedes JM; Kikuchi N (1990): Pre- and Postprocessing for Materials based on the Homogenization Method with Adaptive Finite Element Methods. Comp. Meth. Appl. Mech. Engng., 83, 143-198.

Haber RB; Bliss B; Jablonnowski DJ; Jog C (1992): A Distributed Environment for Run-time Visualization and Application Steering in Computational Mechanics. Comp. Systems Engng., 3, 501-515.

Haftka RT; Gandhi RV (1986): Structural Shape Optimization - A Survey. Comp. Meth. Appl. Mech. Engrg. 57 91-106.

Haftka RT; Gürdal Z; Kamat MP (1990): Elements of Structural Optimization. 2nd edition, Kluwer Academic Publishers, Dordrecht, The Netherlands.

Haftka RT; Prasad B (1981): Optimum Structural Design with Plate Bending Elements - A Survey. AIAA Journal, 19, 517-522.

Hajela P; Lee E; Lin CY (1993): Genetic Algorithms in Structural Topology Optimization. loc. cit. Bendsøe and Mota Soares, 1993, 117-134

Haslinger J (1992): Imbedding / Control Approach for Solving Optimal Shape Design Problems. loc. cit. Bendsøe and Mota Soares, 1993, 303-306

Haslinger J; Dimitrovova Z (1993): Shape Optimization of Elasto-Plastic Bodies: Mathematical Theory. Aplikace Matematiky (to appear).

Haslinger J; Hoffmann KH; Kocvara M (1992): Control/Fictitious Domain Method for Solving Optimal Shape Problems. Preprint, Charles University, Prague, Czech Republic.

Haslinger J; Mäkinen R (1992): Shape Optimization of Elasto-Plastic Bodies: Sensitivity Analysis and Numerical Realization. Struct. Optim., 4, 133-141.

Haslinger J; Neittaanmäki P (1988): Finite Element Approximation for Optimal Shape Design: Theory and Applications. John Wiley & Sons, Chichester, GB.

Haug EJ; Cea, J. (1981): Optimization of Distributed Parameter Structures Vols. I and II. Sijthoff and Noordhoff, Alphen aan den Rijn, The Netherlands.

Haug EJ; Choi KK; Komkov V: Design Sensitivity Analysis of Structural Systems. Academic Press, New York, USA.

Haug EJ; Rousselet B (1980a): Design Sensitivity Analysis in Structural Mechanics. I. Static Responce Variations. J. Struct. Mech., 8, 17-41.

Haug EJ; Rousselet B (1980b): Design Sensitivity Analysis in Structural Mechanics. II. Eigenvalue Variations. J. Struct. Mech., 8, 161-186.

Hemp WS (1973): Optimum Structures, Clarendon Press, Oxford, UK.

Herskovits J (ed.) (1993a): Structural Optimization 1993, The World Congress on Optimal Design of Structural Systems. Proceedings VOL. 1., Mech. Engng. Program, COPPE/Federal University of Rio de Janeiro, Rio de Janeiro, Brazil.

Herskovits J (ed.) (1993b): Structural Optimization 1993, The World Congress on Optimal Design of Structural Systems. Proceedings VOL. 2., Mech. Engng. Program, COPPE/Federal University of Rio de Janeiro, Rio de Janeiro, Brazil.

Hlavacek I (1986): Shape Optimization of Elasto-Plastic Bodies Obeyings Hencky's Law. Apl. Mat., 31, 486-499.

Hlavacek I (1987): Shape Optimization of an Elasto-Perfectly Plastic Body. Apl. Mat., 32, 381-400.

Hlavacek I (1991): Shape Optimization of Elasto-Plastic Axisymmetric Bodies. Apl. Mat., 36, 469-491.

Holnicki-Szulc J (1989): Optimal Structural Remodelling - Simulation by Virtual Distortions. Comm. Appl. Num. Meth., 5, 289-298.

Hörnlein HREM (1979): Ein Algorithmus zur Strukturoptimierung von Fachwerkkonstruktionen. Diplomarbeit, Ludwig-Maximillians-Universität München.

Hörnlein HREM; Schittkowski K (eds.) (1993): Software Systems for Structural Optimization. Birkhäuser, Boston, USA.

Hughes TJR (1987): The Finite Element Method. Prentice-Hall, Englewood Cliffs, New Jersey.

Jablonowski DJ; Bliss B; Bruner JD; Haber RB (1993): VASE: The Visualization and Application Steering Environment. Proceedings of Supercomputing 1993, Portland Oregon, pp 560-569.

Jog C; Haber RB (1994): Stability of Finite Element Models for Distributed-Parameter Optimization and Topology Design. TAM Report No. 758, Dept. of Theoretical and Applied Mechanics, Univ. of Illinois at Urbana-Champaign, Urbana, Illinois, USA.

Jog C; Haber RB; Bendsøe MP (1993a): A Displacement-Based Topology Design Method with Self-Adaptive Layered Materials. loc. cit. Bendsøe and Mota Soares, 219-238

Jog C; Haber RB; Bendsøe MP (1993b): Computational Aspects of Topology Design by the Homogenization Method. Abstracts of Second U.S. National Congress on Compuataional Mechanics, Wahington D.C., USA, August 16-18, 1993.

Jog C; Haber RB; Bendsøe MP (1994a): Topology Design with Optimized, Self-Adaptive Materials. Int. J. Num. Meth. Engng., 37, 1323-1350.

Jog C; Haber RB; Bendsøe MP (1994b): Variable-Topology Shape Optimization with a Constraint on the Perimeter. Proc. 20th ASME Design Automation Conference, Minneapolis, Mn, September 11-14, 1994, ASME publication DE-Vol. 69-2, 261-272.

Johnson C; Pitkränta J (1982): Analysis of Some Mixed Finite Element Methods Related to Reduced Integration. Math. of Computations, 38 (158), 375-400.

Kamat MP (1993): Structural Optimization -Status and Promise. AIAA Progress in Aeronautics and Astronautics Series, Vol. 150, American Institute of Aeronautics and Astronautics, Washington D.C, USA.

Kaneko I; Maier G (1981): Optimum Design of Plastic Structures under Displacement Constraints. Comp. Meth. Appl. Mech. Engng., 27, 369-391.

Kawabe Y; Yoshida S (1994): An Approach to the Problem of Vibration: Structural Modification by Optimizing Density Distribution. In Proc. 20th ASME Design Automation Conference, Minneapolis, Mn, September 11-14, 1994, ASME publication DE-Vol. 69-2.

Kawohl B; Stara J; Wittum G (1991): Analysis and Numerical Studies of a Problem of Shape Design. Arch. Rat. Mech. Anal., 114, 349-363.

Kesavan S (1979): Homogenization of Elliptic Eigenvalue Problems. Appl. Math. Optim., 5, 153-167 (part I) and 197-216 (part II).

Kikuchi N (1986): Adaptive Grid Design Methods for Finite Element Analysis. Comp. Meth. Appl. Mechs. Engrg. 55, 129-160.

Kikuchi N; Chung KY; Torigaki T; Taylor JE (1986): Adaptive Finite Element Methods for Shape Optimization of Linearly Elastic Structures. Comp. Meth. Appl. Mech. Engng., 57, 67-91.

Kikuchi N; Oden JT; Song YJ (1984): Convergence of Modified Penalty Methods and Smoothing Schemes of Pressure for Stoke's Flow Problems. In Gallagher R et al (eds.), Finite Elements in Fluids, Vol. 5, John Wiley & Sons, Ltd., 107-126.

Kikuchi N; Suzuki K (1991): Structural Optimization of a Linearly Elastic Structure using the Homogenization Method. loc. cit. Dal Maso and Dell'Antonio, 1991, 183-204.

Kikuchi N; Suzuki K (1992): Structural Optimization of a Linearly Elastic Structure using the Homogenization Method loc. cit. Rozvany, 1992, 199-242.

Kikuchi N; Suzuki K; Fukushima, I. (1991): Layout Optimization Using the Homogenization Method: Generalized Layout Design of Three-Dimensional Shells for Car Bodies. In.: Rozvany GIN (ed.), Optimization of Large Structural Systems, Lecture Notes, NATO-ASI, Berchtesgaden, FRG, Vol 3., 110-126.

Kirsch U (1989a): Optimal Topologies of Structures. Appl. Mech. Rev., 42, 223-239.

Kirsch U (1989b): Optimal Topologies of Truss Structures. Comp. Meth. Engrg., 72, 15-28.

Kirsch U (1990): On the Relationship Between Optimum Structural Topologies and Geometries. Struct. Optim., 2, 39-45.

Kirsch U (1993a): Fundamental Properties of Optimal Topologies. loc. cit. Bendsøe and Mota Soares, 1993, 3-18

Kirsch U (1993b): Efficient Reanalysis for Topological Optimization. Struct. Optim., 6, 143-150.

Kirsh U; Rozvany GIN (1993): Design Considerations in the Optimization of Structural Topologies. loc. cit. Rozvany, 1993a, 103-120.

Klarbring A; (1992): On the Problem of Optimizing Contact Force Distributions. JOTA, 74 , 131-150.

Klarbring A; Petersson J; Rönnqvist M (1993): Truss Topology Optimization Involving Unilateral Contact. Preprint, Department of Mechanical Engineering, Linköping Institute of Technology, S-58183 Linköping, Sweden.

Kocvara M; Zowe J (1991); Codes for Truss Topology Design: A Numerical Comparison. Preprint, Universität Bayreuth.

Kohn RV (1988): Recent Progress in the Mathematical Modelling of Composite Materials. In Sih G et al (eds.), Composite Material Response: Constitutive Relations and Damage Mechanisms, Elsevier, Amsterdam, The Netherlands, 155-177.

Kohn RV (1991): Composite Materials and Structural Optimization. Proc. Workshop on Smart/Intelligent Materials, Honolulu, Hawaii, March 19-23, 1990. Technomic Press, Lancaster, Pa., USA.

Kohn RV (1992): Numerical Structural Optimization via a Relaxed Formulation. In Delfour MC (ed.), Shape Optimization and Free Boundaries, Kluwer Academic Publishers, Dordrecht, The Netherlands, 173-211.

Kohn RV; Lipton R (1988): Optimal Bounds for the Effective Energy of a Mixture of Isotropic, Incompressible, Elastic Materials. Arch. Rat. Mech. Anal., 102, 331-350.

Kohn RV; Strang G (1982): Structural Design Optimization, Homogenization and Relaxation of Variational Problems. Lecture Notes in Physics, Vol. 154, Springer, Berlin, 131-147.

Kohn RV; Strang G (1986a): Optimal Design and Relaxation of Variational Problems. Comm. Pure Appl. Math., 39, 1-25 (Part I), 139-182 (Part II) and 353-377 (Part III).

Kohn RV; Strang G (1986b): Optimal Design in Elasticity and Plasticity. Int. J. Num. Meth. Engrg., 22, 183-188.

Kohn RV; Vogelius M (1984): A New Model for Thin Plates with Rapidly Varying Thickness. I Int. J. Solids Struct., 29, 333-350.

Kohn RV; Vogelius M (1985): A New Model for Thin Plates with Rapidly Varying Thickness. II: A Convergence Proof. Quart. Appl. Math., 43, 1-21.

Kohn RV; Vogelius M (1986): A New Model for Thin Plates with Rapidly Varying Thickness. III: Comparison of Different Scalings. Quart. Appl. Math., 44, 35-48.

Kohn RV; Vogelius M (1987): Relaxation of a Variational Method for Impedance Computed Tomography. Comm. Pure Appl. Math., 40, 745-777.

Kolpakov A G (1983): Effective Rigidities of Composite Plates. J. Appl. Math. Mech. (PMM), 46, 529-535.

Koumousis VK (1993): Lay-out and Sizing Design of Civil Engineering Structures in Accordance with the Eurocodes. loc. cit. Bendsøe and Mota Soares, 1993, 103-116

Kozlowski W; Mroz Z (1969): Optimal Design of Solid Plates. Int. J. Solids Struct., 5, 781-794.

Krein MG; Nudelman AA (1977): The Markov Moment Problem and Extremal Problems. Translations of Math. Monographs, 50, American Mathematical Society, Providence, USA.

Lagache J-M (1981): Treillis de volume minimal dans une region donnée. J. de Mécanique, 20, 415-448.

Lakes R (1993): Materials with Structural Hierarchy. Nature, 361, 511-515.

Lene F; Duvaut G (1981): Resultats d'isotropie pour des milieux homogeneises. C.R. Acad. Sc. Paris, 7 293, Serie II, 477-480.

Levy R (1991): Fixed Point Theory and Structural Optimization. Eng. Opt., 17, 251-261.

Lewinski T (1991a): Effective Models of Composite Periodic Plates - I. Asymptotic Solution. Int. J. Solids Struct., 27, 1155-1172.

Lewinski T (1991b): Effective Models of Composite Periodic Plates - II. Simplifications Due to Symmetries. Int. J. Solids Struct., 27, 1173-1184.

Lewinski T (1991c): Effective Models of Composite Periodic Plates - III. Two-Dimensional Approaches. Int. J. Solids Struct., 27, 1185-1203.

Lewinski T (1993): On Recent Developments in the Homogenization Theory of Elastic Plates and Their Application to the Optimal Design. Struct. Optim., 6, 59-64.

Lewinski T; Zhou M; Rozvany GIN (1993): Exact Least-Weight Truss Layouts for Rectangular Domains with Various Support Conditions. Preprint, FB 10, Universität Essen, D-4300 Essen 1, Germany.

Lin SC; Yang CC; Mura T; Iwakuma T (1992): Average Elastic-Plastic Behaviour of Composite Materials. Int. J. Solids Struct., 29, 1859-1872.

Lions J-L (1972): Some Aspects of the Optimal Control of Distributed Parameter Systems. SIAM, Philadelphia, PA.

Lions J-L (1978): Asymptotic Methods in the Optimal Control of Distributed Systems. Automatica, 14, 199-211.

Lions J-L (1981): Some Methods in the Mathematical Analysis of Systems and Their Control. Gordon and Breach Science Publishers, Inc., New York 1981.

Lipton R (1988): On the Effective Elasticity of a Two-Dimensional Homogenised Incompressible Elastic Composite. Proc. Royal Soc. Edinburgh, 110A, 45-61.

Lipton R (1990): Saturation of the Even-Order Bounds on Effective Elastic Moduli by Finite-Rank Laminates. J. Appl. Phys., 67, 7300-7306.

Lipton R (1991): On the Behavior of Elastic Composites with Transverse Isotropic Symmetry. J. Mech. Phys. Solids, 39, 663-681.

Lipton R (1993a): On Implementation of Partial Relaxation for Optimal Structural Compliance Problems loc. cit. Pedersen, 1993c, 451-468

Lipton R (1993b): Identification of Microstructures that Extremize Sums of Energies. Preprint, Worcester Polytecnic, Worcester, MA, USA.

Lipton R (1993c): Composites with Symmetry and Their Extremal Properties. Preprint, Worcester Polytecnic, Worcester, MA, USA.

Lipton R (1993d): Optimal Reliability Design of Plates. loc. cit. Bendsøe and Mota Soares, 1993, 421-437

Lipton R (1994a): Optimal Design and Relaxation for Reinforced Plates Subject to Random Transverse Loads. J. Prob. Engng. Mech., 9, 167-177.

Lipton R (1994b): On the Relaxation for Optimal Structural Compliance. JOTA, 81, 549-568.

Lipton R (1994c): Optimal Bounds on Effective Elastic Tensors for Orthotropic Composites. Proc. Royal Society (London), 443, 399-410.

Lipton R (1994d): On Optimal Reinforcement of Plates and Choice of Design Parameters. Control and Cybernetics, 23, 481- 493.

Litvinov VG (1980): Optimal Control of the Natural Frequency of a Plate of Variable Thickness. U.S.S.R. Comp. Maths. Math. Phys., 19, 70-86.

Litvinov VG; Panteleev AD (1980): Optimization Problem for Plates of Variable Thickness. Mech. of Solids (MTT), 15, No. 2, 140-146.

Lurie KA (1980): Optimal Design of Elastic Bodies and the Problem of Regularization. Wissenschaftliche Zeitschrift, Techn. Hochschule Leipzig, 4, 339-347.

Lurie KA (1992): Direct Solution of an Optimal Layout Problem for Isotropic and Anisotropic Heat Conductors on a Plane. JOTA, 72, 553-575.

Lurie KA (1993a): Direct Relaxation of Optimal Layout Problems for Plates. loc. cit. Pedersen, 1993c, 425-445.

Lurie KA (1993b): Direct Relaxation of Structural Design Problems. loc. cit. Herskovits, 1993a, 387-391.

Lurie KA (1993c): Direct Relaxation of Nonselfadjoint Problems of Optimal Layout. Notes, Second Workshop on Composite Media and Homogenization, ICTP, Tieste, Italy, September 20 to October 1.

Lurie KA (1993d): Applied Optimal Control Theory of Distributed Systems. Plenum Press, New York, USA.

Lurie KA (1994): Direct Relaxation of Optimal Layout Problems for Plates. JOTA, 80, 93-116.

Lurie KA; Cherkaev AV (1982a): Accurate Estimates of the Conductivity of Mixtures Formed of Two Materials in a Given Proportion (Two-Dimensional Problem). Sov. Phys. Dokl., 27(6), 461-462.

Lurie KA; Cherkaev AV (1982b): Exact Estimates of Conductivity of Composites Formed by Two Isotropically Conducting Media Taken in Prescribed Proportion. Preprint, A.F. Ioffe Physical Technical Institute, Leningrad.

Lurie KA; Cherkaev AV (1984a): G-closure of a Set of Anisotropically Conducting Media in the Two-Dimensional Case. JOTA, 42, 283-304.

Lurie KA; Cherkaev AV (1984b): G-closure of some Particular Sets of Admissible Material Characteristics for the Problem of Bending of Thin Plates. JOTA, 42, 305-316.

Lurie KA; Cherkaev AV (1986): The Effective Properties of Composites and Problems of Optimal Design of Constructions. Uspekhi Mekhaniki, 9, 1-81 (in Russian). Also as Effective Characteristics of Composite Materials and the Optimal Design of Structural Elements. In Kohn RV (ed.), Topics in the Mathematical Modelling of Composite Materials, Birkhauser, New York, USA, 1994.

Lurie KA; Cherkaev AV; Fedorov AV (1982): Regularization of Optimal Design Problems for Bars and Plates. JOTA, 37, 499-522 (Part I), 37, 523-543 (Part II) and 42, 247-282 (Part III).

Lurie KA; Lipton R (1992): Direct Solution of an Optimal Layout Problem for Isotropic Heat Conductors in Three Dimensions. In Field DA; Komkov V (eds.), Theoretical Aspects of Industrial Design, SIAM, Philadelphia, 1-11.

Ma Z D; Kikuchi N; Hagiwara I (1992a): Structural Topology/Shape Optimization for a Frequence Response Problem, Int. J. Num. Meth. Engrg. (to appear).

Ma Z-D; Kikuchi N; Hagiwara I (1992b): Structural Topology/Shape optimization for a Structural Dynamics Problem, ASME Winter Annual Meeting.

Ma Z-D; Kikuchi N; Cheng H-C; Hagiwara I (1993): Topology and Shape Optimization Methods for Structural Dynamic Problems loc. cit. Pedersen, 1993c, 247-261.

Maier G (1970): A Matrix Structural Theory of Piecewise Linear Elastoplasticity with Inteacting Yield Planes. Meccanica, 5, 54-66.

Masur EF (1970): Optimum Stiffness and Strenght of Elastic Structures. J. Engng. Mech. Div., ASCE, 96, 621-640.

Maute K; Ramm E (1994): Adaptive Techniques in Topology Optimization. In Proc. 5th AIAA/USAF/NASA/ISSMO Symposium on Multidisciplinary Analysis and Optimization, Panama City, Fl., September 7-9, 1994, Vol. 1, 121- 131.

Michel JM; Suquet PM (1993): On the Strength of Composite Materials: Variational Bounds and Computational Aspects. loc. cit. Bendsøe and Mota Soares, 1993, 355-374

Michell AGM (1904): The Limits of Economy of Material in Frame Structures, Philosophical Magazine, Series 6, 8, 589-597.

Mignot F; Puel J-P; Suquet P-M (1980): Homogenization and Bifurcation of Perforated Plates. Int. J. Engng. Sci., 18, 409-414.

Miki M; Sugiyama Y (1993): Optimum Design of Laminated Composite Plates Using Lamination Parameters. AIAA J., 31, 921-922.

Milton GW (1990): On Characterizing the Set of Possible Effective Tensors of Composites: The Variational Method and the Translation Method. Comm. Pure Appl. Math., 43, 63-125.

Milton GW; Kohn RV (1988): Variational Bounds on the Effective Moduli of Anisotopic Composites. J. Mech. Phys. Solids, 36, 597-629.

Milton GW, Cherkaev AV (1993): Materials with Elastic Tensors that Range Over the Entire Set Compatible with Thermodynamics, In Herakovich CT; Duva JM (eds.), Abstracts of the Joint ASCE-ASME-SES Meet'N', June 6-9, University of Virginia, Charlottesville, Virginia, USA, p. 342.

Mirsky L (1959): On the trace of matrix products, Math. Nach., 20 , 171-174.

Mlejnek HP (1992): Some Explorations in the Genesis of Structures. loc. cit. Bendsøe and Mota Soares, 1993, 287-300

Mlejnik HP; Jehle U; Schirrmacher R (1991): Some Approaches for Shape Finding in Optimal Structural Design. In Eschenauer HA; Mattheck C; Olhoff N (eds.), Proc. Int. Conf. Engrg. Optimization in Design Processes, Karlsruhe; Lecture Notes in Engineering, vol 63, Springer Verlag, 59-70.

Mlejnik HP; Schirrmacher R (1993): An Engineering Approach to Optimal Material Distribution and Shape Finding. Comp. Meth. Appl. Mech. Engng., 106, 1-26.

Morris AJ (ed.) (1982): Foundations of Structural Optimization: A Unified Approach. John Wiley & Sons, Chichester.

Mota Soares CA (ed.) (1987): Computer Aided Optimal Design: Structural and Mechanical Systems. Springer-Verlag, Berlin.

Murat F (1977): Contre-exemples pour divers problémes ou le contrôle intervient dans les coefficients. Ann. Mat. Pura ed Appl., Serie 4, 112, 49-68.

Murat F (1985): Control in Coefficients. In Systems and Control Encyclopedia: Theory, Technology, Applications, Pergamon Press.

Murat F; Simon J (1976): Studies on Optimal Shape Design Problems. Lectures Notes in Computer Science, 41, Springer Verlag, Berlin.

Murat F; Tartar L (1985a): Calcul des variations et homogeneisation. In Les Methodes de l'Homogeneisation: Theorie et Applications en Physique, Coll. de la Dir. des Etudes et Recherches de Electricite de France, Eyrolles, Paris, 319-370.

Murat F; Tartar L (1985b): Optimality Conditions and Homogenization. In Marino A et al (eds.), Nonlinear Variational Problems, Pitman Advanced Publishing Program, Boston, 1-8.

Myslinski A, Sokolowski J (1985): Nondifferentiable Optimization Problems for Elliptic Systems. SIAM J. Control Opt., 23, 632-648.

Nakamura T; Ohsaki M (1992): A Natural Generator of Optimum Topology of Plane Trusses for Specified Fundamental Frequency. Comp. Meth. App. Mech. Engrg. 94, 113-129.

Nayfeh AH; Hefzy MS (1981): Continuum Modelling of the Mechanical and Thermal Behaviour of Discrete Large Structures. AIAA J., 19, 766-773.

Necas J; Hlavacek I (1981): Mathematical Theory of Elastic and Elatico-Plastic Bodies: An Introduction. Elsevier, Amsterdam, The Netherlands.

Neittaanmäki P; Tiba D (1992): An Embedding of Domains Approach in Free Boundary Problems and Optimal Shape Design. Preprint No. 145, Department of Mathematics, University of Jyväskylä, Finland.

Neves MM (1994): Topology Optimization of Structures with Critical Load Constraints. (in Portuguese) M.Sc. Thesis, Mech. Engng. Dept., Instituto Superior Tecnico, Lisboa, Portugal, 1994.

Neves MM; Guedes JM; Rodrigues HC (1993): Topology Optimization of Elastic 2D Structures with Critical Load Constraints. loc. cit. Herskovits, 1993a, 119-128.

Neves MM; Guedes JM; Rodrigues HC (1994): Generalized Topology Design of Structures with a Buckling Load Criterion. Preprint, IDMEC-Instituto Superior Tecnico, 1096 Lisboa, Portugal.

Niordson FI (1983): Optimal Design of Plates with a Constraint on the Slope of the Thickness Function. Int. J. Solids Struct., 19, 141-151.

Nishino F; Duggal R (1990): Shape Optimum Design of Trusses under Multiple Loading. Int. J. Solids Struct., 26, 17-27.

Olhoff N (1970): Optimal Design of Vibrating Circular Plates. Int. J. Solids Struct., 6, 139-156.

Olhoff N (1974): Optimal Design of Vibrating Rectangular Plates. Int. J. Solids Struct., 10 1974, 93-109.

Olhoff N (1976): Optimization of Vibrating Beams with Respect to Higher Order Natural Frequencies. J. Struct. Mech., 4, 87-122.

Olhoff N (1980): Optimal Design with Respect to Structural Eigenvalues. In Proc. XV ICTAM (Rimrott and Tabarrok, Eds.), North-holland, Amsterdam, 1980, 133-149.

Olhoff N (1987): Structural Optimization by Variational Method. loc. cit. Mota Soares, 1987, 87-179.

Olhoff N (1989): Multicriterion Structural Optimization via Bound Formulation and Mathematical Programming. Struct. Optim., 1, 11-17.

Olhoff N; Bendsøe MP; Rasmussen J (1992): On CAD-Integrated Structural Topology and Design Optimization. Comp. Meth. Appl. Mechs. Engng., 89, 259-279.

Olhoff N; Krog L; Thomsen J (1993): Bi-material Topology Optimization. loc. cit. Herskovits, 1993a, 327-334.

Olhoff N; Lund E; Rasmussen J (1993): Concurrent Engineering Design Optimization in CAD Environment. In Haug EJ (ed.), Concurrent Engineering Tools and Technologies for Mechanical Systems Design, Springer Verlag, New York, USA, 523-586.

Olhoff N; Lurie KA; Cherkaev AV; Fedorov A (1981): Sliding Regimes and Anisotropy in Optimal Design of Vibrating Axisymmetric Plates. Int. J. Solids Struct., 17, 931-948.

Olhoff N; Rasmussen SH (1977): On Single and Bimodal Optimum Buckling Loads of Clamped Columns. Int. J. Solids Struct., 13, 605-614.

Olhoff N; Rozvany, GIN (1982): Optimal Grillage Lay-out for Given Natural Frequency. ASCE J. Engng. Mech. Div., 108, 971-957.

Olhoff N; Taylor JE (1979): On Optimal Structural Remodeling. JOTA, 27, 571-582.

Olhoff N; Taylor JE (1983): On Structural Optimization. J. Appl. Mech., 50, 1134-1151.

Olhoff N; Thomsen J; Rasmussen J (1993): Topology Optimization of Bi-material Structures. loc. cit. Pedersen, 1993c, 191-206.

Ong T; Rozvany GIN; Szeto W (1988): Least-Weight Design of Perforated Elastic Plates for Given Compliance: Non-Zero Poisson's Ratio. Comp. Meth. Appl. Mech. Engrg., 66, 301-322.

Overton ML (1988): On Minimizing the Maximum Eigenvalue of a Symmetric Matrix. SIAM J. Matrix Anal. Appl., 9, 256-268.

Overton ML (1992): Large-Scale Optimization of Eigenvalues. SIAM J. Optimization, 2, 88-120.

Padula S; Sandridge CA (1993): Passive/Active Strut Placement by Integer Programming. loc. cit. Bendsøe and Mota Soares, 1993, 145-156

Papalambros PY; Chirehdast M (1990): An Integrated Environment for Structural Configuration Design. J. Engrg. Design, 1, 73-96.

Papalambros PY; Chirehdast M (1993): Integrated Structural Optimization System. loc. cit. Bendsøe and Mota Soares, 1993, 501-514

Pedersen P (1970): On the Minimum Mass Layout of Trusses. AGARD Conf. Proc. No. 36, Symposium on Structural Optimization, AGARD-CP-36-70.

Pedersen P (1972): On the Optimal Layout of Multi-Purpose Trusses. Computers and Structures, 2, 695-712.

Pedersen P (1973): Optimal Joint Positions for Space Trusses. ASCE Journal, 99, 2459-2476.

Pedersen P (1989): On Optimal Orientation of Orthotropic Materials. Struct. Optim., 1, 101-106.

Pedersen P (1990): Bounds on Elastic Energy in Solids of Orthotropic Materials. Struct. Optim., 2, 55-63.

Pedersen P (1991): On Thickness and Orientational Design with Orthotropic Materials. Struct. Optim., 3, 69-78.

Pedersen P (1993a): Concurrent Engineering Design with and of Advanced Materials. In Haug EJ (ed.), Concurrent Engineering Tools and Technologies for Mechanical Systems Design, Springer Verlag, New York, USA, 627-670.

Pedersen P (1993b): Optimal Orientation of Anisotropic Materials. Optimal Distibution of Anisotropic Materials. Optimal Shape Design with Anisotropic Materials. Optimal Design for a Class of Non-Linear Elasticity. loc. cit. Rozvany GIN, 1993a, 649-682.

Pedersen P (ed.) (1993c): Optimal Design with Advanced Materials. Elsevier, Amsterdam, The Netherlands.

Pedersen P; Taylor JE (1993): Optimal Design Based on Power-Law Non-Linear Elasticity loc. cit. Pedersen, 1993c, 51-66.

Pedersen P (1993c): Topology Optimization of Three Dimensional Trusses. loc. cit. Bendsøe and Mota Soares, 1993, 19-30

Pedersen P (1993d): Topology Optimization of Three Dimensional Trusses with Cost of Supports. loc. cit. Herskovits, 1993a, 11-20.

Petersson J; Klarbring A; (1994): Saddle Point Approach to Stiffness Optimization of Discrete Structures Including Unilateral Contact. Control and Cybernetics, 23, 461-479.

Pironneau O (1984): Optimal Shape Design for Elliptic Systems. Springer Verlag , Berlin, FRG.

Plaxton S, Taylor JE (1993): Applications of a Generalized Complementary Energy Principle for the Equilibrium Analysis of Softening Material. Comp. Meth. Appl. Mech. Engng. (to appear).

Ponslet E; Haftka RT; Cudney HH (1993): Optimal Placements of Actuators and other Peripherals for Large Truss Structures. loc. cit. Bendsøe and Mota Soares, 1993, 135-144

Prager W (1963): Optimization in Structural Design, in Bellman, R. (ed.), Mathematical Optimization Techniques RAND Corp. Report P-396-PR, April 1963, 279-289.

Prager W (1974): Introduction to Structural Optimization. CISM Lecture Notes, Vol. 212, Springer Verlag, Wien.

Prager W (1985a): Optimal Design of Grillages. loc. cit. Save and Prager (eds.), 1985, 153-200.

Prager, W. (1985b): Optimal Design of Trusses. loc. cit. Save and Prager (eds.), 1985, 121-152.

Prager W; Rozvany GIN (1977): Optimization of Structural Geometry. In Bednarek A; Cesari L (eds.), Dynamical Systems, Academic Press, New York, USA, 265-294.

Prager W; Taylor JE (1968): Problems of Optimal Structural Design. J. Applied Mechs., 35, 102-106.

Raitum U (1978): The Extension of Extremal Problems Connected with a Linear Elliptic Equation. Soviet Math., 19, 1342-1345.

Raitum U (1979): On Optimal Control Problems for Linear Elliptic Equations. Soviet Math. Dokl. 20, 129-132.

Rajan SD; Belegundu AD; Budiman J (1988): An Integrated System for Shape Optimal Design. Computers and Structures, 30, 337-346.

Ramm E; Bletzinger K-U; Reitinger R; Maute K (1994): The Challenge of Structural Optimization. In Topping BHV; Papadrakakis M (eds.), Advances in Structural Optimization, CIVIL-COMP Press, Edingburgh, Scotland, 103-112.

Rasmussen J (1988): Interactive Shape Optimization with Design Elements. In Eschenauer, HA (ed.), Proc. GAMM Seminar on Discretization Methods and Structural Optimization Precedures and Applications, Siegen, FRG, Oct. 1988, Lecture Notes in Engng., Vol. 48, Springer Verlag, 284-290.

Rasmussen J (1990): The Structural Optimization System CAOS. Struct. Optim., 2, 109-115.

Rasmussen J (1991): Structural Optimization and CAD. Int. J. Systems Automation: Research and Appl., 1, 33-45.

Rasmussen J; Lund E; Birker T (1992): Collection of Examples, CAOS Optimization System, 3rd edition. Special Report no. 1c, Inst. of Mech. Engng., Universtiy of Aalborg, Denmark.

Rasmussen J; Lund E; Birker T; Olhoff N (1993): The CAOS System. loc. cit. Hörnlein and Schittkowski, 1993, 75-96.

Rasmussen J; Lund E; Olhoff N (1993a): Parametric Modelling Techniques in Structural Optimization Systems. In Haslinger J (ed.), Mathematical Models in Computer Aided Optimal Design, Lecture Notes, Advanced TEMPUS course, July 12-16, Faculty of Mathematics and Physics, Charles University, Prague, Czech Republic.

Rasmussen J; Lund E; Olhoff N (1993b): Integration of Parametric Modelling and Structural Analysis for Optimum Design. In Gilmore et al (eds.), Advances in Design Automation, Proceedings, ASME, Albuquerque, New Mexico, USA.

Rasmussen J; Thomsen J; Olhoff N (1993): Integrating Topology and Boundary Variations Design Methods in a CAD system. loc. cit. Bendsøe and Mota Soares, 1993, 483-500

Rasmussen SH (1979): Optimization of Fiber-Reinforced Structures (in Danish). DCAMM Report No. S12, The Danish Center for Applied Mathematics and Mechanics, The Technical University of Denmark, DK-2800 Lyngby, January 1979.

Reinschmidt KF; Russell AD (1974): Applications of Linear Programming in Structural Layout and Optimization. Computers and Structures, 4, 855-869.

Reiter TJ; Rammerstorfer FG (1993): Simulation of Natural Adaptation of Bone Material and Application in Optimum Composite Design. loc. cit. Pedersen, 1993c, 25-36.

Reiter TJ; Rammerstorfer FG; Böhm HJ (1993): Structural Design Improvement by Functional Adaptation. loc. cit. Herskovits, 1993a, 361-368.

Ringertz U (1985): On Topology Optimization of Trusses, Engrg. Optim., 9, 21-36.

Ringertz U (1986): A Branch and Bound Algorithm for Topology Optimization of Truss Structures. Engrg. Optim., 10, 111-124.

Ringertz U (1988): Newton Methods for Structural Optimization. Research Report No. 88-19, Department of Leightweight Structures, The Royal Institute of Technology, Stockholm, S-100 44 Sweden.

Ringertz U (1993): On Finding the Optimal Distribution of Material Properties. Struct. Optim., 5, 265-267.

Rodrigues HC (1988): Shape Optimal Design of Elastic Bodies using a Mixed Variational Formulation. Comp. Meth. Appl. Mech. Engng., 69, 29-44.

Rodrigues HC; Fernandes P (1993a): Topology Optimization of Linear Elastic Structures Subjected to Thermal Loads. loc. cit. Bendsøe and Mota Soares, 1993, 437-450

Rodrigues HC; Fernandes P (1993b): A Material Based Model for Topology Optimization of Thermoelastic Structures. loc. cit. Herskovits, 1993a, 129-138. Extended version to appear in Int. J. Num. Meth. Engng., 1994.

Rossow MP; Taylor JE (1973): A Finite Element Method for the Optimal Design of Variable Thickness Sheets. AIAA J. , 11, 1566-1569.

Rosyid DM; Caldwell JB (1991): Design Approach and Dimensional Similarity in Lay-Out Optimization of Structural Systems. Computers and Structures, 40, 1125-1137.

Rousselet B; Haug EJ (1983): Design Sensitivity Analysis in Structural Mechanics, III. Effects of Shape Variation. J. Struct. Mech., 10, 273-310.

Rovati M; Taliercio A (1991): Optimal Orientation of the Symmetry Axes of Orthotropic 3-D Materials. In Eschenauer HA; Mattheck C; Olhoff N (eds.), Proc. Int. Conf. Engng. Optimization in Design Processes , Karlsruhe; Lecture Notes in Engineering, 63, Springer Verlag, Berlin, FRG, 127-134.

Rozvany GIN (1976): Optimal Design of Flexural Systems. Pergamon Press, Oxford, UK

Rozvany GIN (1984): Structural Layout Theory - the Present State of Knowledge. In Atrek E; Gallagher RH; Ragsdell KM; Zienkiewicz OC (eds.), Directions in Optimum Structural Design, Wiley, Chichester, U.K. 1984, Ch. 7.

Rozvany GIN (1989). Structural Design via Optimality Criteria. Kluwer Academic Publishers, Dordrecht, The Netherlands.

Rozvany GIN (ed.) (1992): Shape and Lay-Out Optimization of Structural Systems and Optimality Criteria Methods. CISM Lecture Notes No. 325, Springer Verlag, Wien.

Rozvany GIN (ed.) (1993a): Optimization of Large Structural Systems. Kluwer Academic Publishers, Dordrecht, The Netherlands.

Rozvany GIN (1993b): Lay-out Theory for Grid-type Structures. loc. cit. Bendsøe and Mota Soares, 1993, 251-272

Rozvany GIN; Bendsøe MP; Kirsch U (1994): Layout Optimization of Structures. Appl. Mech. Rev. (to appear).

Rozvany GIN; Lewinski T; Sigmund O; Gerdes D; Birker T (1993): Optimal Topology of Trusses or Perforated Deep Beams with Rotational Restraints at Both Ends. Struct. Optim., 5, 268-270.

Rozvany GIN; Olhoff N; Cheng K-T; Taylor JE (1982): On the Solid Plate Paradox in Structural Optimization. J. Struct. Mech., 10, 1-32.

Rozvany GIN; Ong TG; Szeto WT; Olhoff N; Bendsøe MP (1987): Least-weight design of perforated plates. Internat. J. Solids and Structures, 23, 521-536 (Part I), 537-550 (Part II).

Rozvany GIN; Sigmund O; Birker T (1993): Optimal Design of Composite and Fibre-reinforced Plates. loc. cit. Pedersen, 1993c, 293-309.

Rozvany GIN; Sigmund O; Lewinski T; Gerdes D; Birker T (1993): Exact Optimal Structural Layouts for Non-Self-Adjoint Problems. Struct. Optim., 5, 204-206.

Rozvany GIN; Sigmund O; Zhou M; Birker T (1993): Iterative Discretized Methods for Layout Optimization and Generalized Shape Optimization. loc. cit. Herskovits, 1993a, 139-151.

Rozvany GIN; Zhou M (1991a): Applications of the COC Algorithm in Layout Optimization. In Eschenauer HA; Mattheck C; Olhoff N (eds.), Proc. Int. Conf. Engng. Optimization in Design Processes , Karlsruhe; Lecture Notes in Engineering, 63, Springer Verlag, Berlin, FRG, 59-70.

Rozvany GIN; Zhou M (1991b): The COC Algorithm, Part I: Cross-section Optimization or Sizing. Comp. Meth. Appl. Mechs. Engng., 89, 281-308.

Rozvany GIN; Zhou M (1993a): Layout and Generalized Shape Optimization by Iterative COC Methods. loc. cit. Rozvany GIN, 1993a, 121-138.

Rozvany GIN; Zhou M (1993b): Optimality Criteria Methods for Large Structural Systems. Forschungsbericht Fachbereich Bauwesen No. 58, Universität-Gesamthochschule-Essen, Essen, FRG.

Rozvany GIN; Zhou M; Birker T; Sigmund O (1993): Topology Optimization using Iterative Continuum-Type Optimality Criteria (COC) Methods for Discretized Systems. loc. cit. Bendsøe and Mota Soares, 1993, 273-286

Rozvany GIN; Zhou M; Lewinski T; Sigmund O (1993): Optimal Layout Theory: New Classes of Exact Solutions for Trusses Including Several Load Conditions and Non-Self-Adjoint Problems. loc. cit. Herskovits, 1993a, 37-46.

Rozvany GIN; Zhou M; Sigmund O (1994): Topology Optimization in Structural Design. In Adeli H (ed.), Advances in Design Optimization, Chapman and Hall, London, UK, 340-399.

Saka MP (1980): Shape Optimization of Trusses. ACSE J. Struct. Engrg., 106, 1155-1174.

Samsonov AM (1980): Necessary Optimality Conditions for Stiffness Distribution of a Rib on a Elastic Plate. Mech. of Solids (MTT), 15, 122-129.

Samsonov AM (1983): Optimal Design of Ribreinforced Plates. In Eschenauer HA; Olhoff N (eds.), Optimization Methods in Structural Design, Bibliographisches Institut, Zürich, 387-393.

Sanchez-Palencia E (1980): Non-Homogeneous Media and Vibration Theory. Lecture Notes in Physics, 127, Springer Verlag, Berlin.

Sankaranaryanan S; Haftka RT; Kapania RK (1993): Truss Topology Optimization with Stress and Displacement Constraints. loc. cit. Bendsøe and Mota Soares, 1993, 71-78

Save M; Prager W (eds.) (1985): Structural Optimization. Volume 1, Optimality Criteria. Plenum Press, New York, USA.

Save M; Prager W (eds.) (1990): Structural Optimization. Volume 2, Mathematical Optimization. Plenum Press, New York, USA.

Sayegh AF; Rubenstein MF (1972): Elatic-Plastic Analysis by Quadratic Programming. J. Engng. Mech. Div., ASCE, 98, 1547-1572.

Schittkowski K (1985): NLPQL: A FORTRAN Subroutine Solving Constrained Nonlinear Programming Problems. Annals Oper. Res., 5, 485-500.

Schramm H; Zowe J (1992): A Version of the Bundle Idea for Minimizing a Nonsmooth Function: Conceptual Idea, Convergence Analysis, Numerical Results. SIAM J. Optimization, 1, 121-152.

Selyugin SV (1992): Optimization Criteria and Algorithms for Bar Structures Made of Work-Hardening Elasto-Plastic Materials. Struct. Optim., 4, 218-223.

Senger W (1993): Mechanik des Knochenumbaus um Implantate. Fortschritt-Berichte VDI Reihe 17 Nr. 99, VDI-Verlag, Düsseldorf.

Seregin GA; Troitskii VA (1982): On the Best Position of Elastic Symmetry Planes in an Orthotropic Body. PMM USSR, 45, 139-142.

Seyranian AP (1993): Sensitivity Analysis of Multiple Eigenvalues. Mech. Struct. Mach., 21, 261-284.

Seyranian AP; Lund E; Olhoff N (1994): Multiple Eigenvalues in Structural Optimization Problems. Struct. Optim., 8 (to appear).

Sigmund O (1994a): Materials with Prescribed Constitutive Parameters: An Inverse Homogenization Problem. Int. J. Solids Struct., 31, 2313-2329.

Sigmund O (1994b): Tayloring Materials with Prescribed Elastic Properties. Mech. Mat. (to appear).

Sigmund O; Zhou M; Rozvany GIN (1993): Layout Optimization of Large FE systems by New Optimality Criteria Methods: Applications to Beam Systems. In Haug EJ (ed.), Concurrent Engineering Tools and Technologies for Mechanical Systems Design, Springer Verlag, New York,

Simon J (1980): Differentiation with Respect to the Domain in Boundary Value Problems. Num. Funct. Anal. Opt., 2, 649-687.

Simon L (1979): On G-Convergence of Elliptic Operators. Indiana Univ. Math. J., 28, 587-594.

Sion M (1958): On General Minimax Theorems. Pacific J. Math., 8, 171-176.

Smith O (1994): An interactive system for truss topology design with automatic generation of the ground structure In Topping BHV; Papadrakakis M (eds.), Advances in Structural Optimization, CIVIL-COMP Press, Edinburgh, Scotland, 103-112.

Sokolowski J (1981a): Control in Coefficients for PDE. Abhandlungen. Akad. der Wiss. der DDR; Abt. Math., 287-295.

Sokolowski J (1981b): Optimal Control in Coefficients for Weak Variational Problems in Hilbert Space. Appl. Math. Optim., 7, 283-293.

Sokolowski J (1993): Applications of Material Derivative Method. loc. cit. Bendsøe and Mota Soares, 1993, 307-312

Sokolowski J, Zolesio JP (1992): Introduction to Shape Optimization. Shape Sensitivity Analysis. Springer Series in Computational Mathematics, 16, Springer Verlag, New York, USA.

Soto CA; Díaz AR. (1993a): On the Modeling of Ribbed Plates for Shape Optimization. Struct. Optim., 6, 175-188.

Soto CA; Díaz AR. (1993b): Optimum Layout and Shape of Plate Structures using Homogenization. loc. cit. Bendsøe and Mota Soares, 1993, 407-420

Soto CA; Díaz AR. (1993c): A Model for Layout Optimization of Plate Structures. loc. cit. Pedersen, 1993c, 337-350.

Soto CA; Díaz AR. (1993d): Layout of Plate Structures for Improved Dynamic Response using a Homogenization Method In Gilmore et al (eds.), Advances in Design Automation, Proceedings, ASME, Albuquerque, New Mexico, USA.

Spagnolo S (1976): Convergence in Energy for Elliptic Operators. In Hubbard B (ed.), Numerical Solution of Partial Differential Equations, Vol. III, Academic Press, New York, 469-498.

Spagnolo S (1979): Quelques remarques sur la G-convergence. In Berestycki H; Brezis H (eds.), Recent Contributions to Nonlinear Partial Differential Equations, Pitman, London, 217-226.

Stadler W (1986): Non-Existence of Solutions in Optimal Structural Design. Opt. Control Appl. Meth., 7, 243-258.

Stavroulakis GE; Tzaferopoulos MA (1994): A Variational Inequality Approach to Optimal Plastic Design of Structures via the Prager-Rozvany Theory. Struct. Optim., 7, 160-169.

Strang G; Kohn RV (1981): Hencky-Prandtl Nets and Constrained Michell Trusses. In Proc. Int. Symposium on Optimum Structural Design, Tucson, Arizona, Oct. 1981. Pineridge Press Ltd., Swansea, 4-17 to 4-22.

Suquet P (1981a): Prevision par homogneisation du flambement de plaques lastiques renforcees. Rech. Aerosp., 99-107.

Suquet P (1981b): Une methode duale en homogeneisation. Application aux milieux élastiques periodiques. C.R. Acad. Sc. Paris, t. 291, Serie A, 181-184.

Suquet P (1982): Une methode duale en homogeneisation: Application aux milieux élastiques. J. Mecanique theorique et appl., Mumero special, 1982, pp. 79-98.

Suquet P (1985): Approach by Homogenization of Some Linear and Nonlinear Problems in Solid Mechanics. In Boehler JP (ed.), Plastic Behavior of Anisotropic Solids, Proc. CNRS Int. Coll. 319, CNRS, Paris, 1985.

Suzuki K and Kikuchi N (1990): Generalized Layout Optimization of Shape and Topology in Three-Dimensional Shell Structures. Rept. No. 90-05, Dept. Mech. Engrg. and Appl. Mech., Comp. Mech. Lab., University of Michigan, USA.

Suzuki K; Kikuchi N (1991a): Shape and Topology Optimization for Generalized Layout Problems Using the Homogenization Method. Comp. Meth. Appl. Mechs. Engng., 93, 291-318.

Suzuki K; Kikuchi N (1991b): Shape and Topology Optimization of Three-Dimensional Solid-Structures. Report No. 91-7, Department of Mechanical Engineering and Applied Mechanics, The University of Michigan, USA.

Suzuki K; Kikuchi N (1991c): Layout Optimization Using the Homogenization Method: Generalized Layout Design of Three-Dimensional Shells for Car Bodies. In.: Rozvany GIN (ed.) Optimization of Large Structural Systems, Lecture Notes, NATO-ASI, Berchtesgaden, FRG, Vol 3., 110-126.

Suzuki K; Kikuchi N (1992): Generalized Layout Optimization of Three-Dimensional Shell Structures. In Field DA; Komkov V (eds.), Geometric Aspects of Industrial Design, SIAM, Philadelphia, 62-88.

Suzuki K; Kikuchi N (1993): Layout Optimization Using the Homogenization Method. loc. cit. Rozvany, 1993a, 157-176.

Suzuki K; Kikuchi N; Bendsøe MP (1988): OPTISHAPE-2D User's Manual The University of Michigan, MI, USA.

Svanberg K (1984): On Local And Global Minima in Structural Optimization. In Atrek A; Gallagher RH; Ragsdell KM; Zienkiewicz OC (eds.), New Directions in Optimum Structural Design, Wiley, New York, 327-341.

Svanberg K (1992): On the Global Convergence of a Modified Optimality Criteria Method for Compliance-Constrained Truss Sizing and Topology Optimization. Preprint, Dept. of Optimization and Systems Theory, The Royal Institute of Technology, Stockholm, S-10044, Sweden.

Svanberg K (1994a): On the Convexity and Concavity of Compliances. Struct. Optim., 7, 42-46.

Svanberg K (1994b): Global Convergence of the Stress Ratio Method for Truss Sizing. Struct. Optim., 8, 60-68.

Szykman S; Cagan J (1994): Three Dimensional Component Layout Using Simulated Annealing. In Proc. 20th ASME Design Automation Conference, Minneapolis, Mn, September 11-14, 1994, ASME publication DE-Vol. 69-2.

Tartar L (1977): Estimation de Coefficients Homogeneises. Lecture Notes in Mathematics, 704, Springer Verlag, Berlin , 364-373.

Taylor JE (1969): Maximum Strength Elastic Structural Design, Proc. ASCE, 95, 653-663.

Taylor JE (1987): Distributed Parameter Optimal Structural Design: Some Basic Problem Formulations and Their Applications. loc. cit. Mota Soares, 1987, 3-85.

Taylor JE (1989): Towards a Unified Model for Elastoplastic Structural Analysis. Mech. Res. Comm., 16, 125-131.

Taylor JE (1993a): A Global Extremum Principle for the Analysis of Solids Composed of Softening Material. Int. J. Solids Struct., 30, 2057-2069.

Taylor JE (1993b): A Global Extremum Principle in Mixed Form for Equilibrium Analysis with Elastic/Stiffening Materials (A Generalized Minimum Potential Energy Principle). J. Appl. Mech. (to appear).

Taylor JE (1993c): Truss Topology Design for Elatic/Softening Materials. loc. cit. Bendsøe and Mota Soares, 1993, 451-467.

Taylor JE; Bendsøe MP (1984): An Interpretation for Min-Max Structural Design Problems Including a Method for Relaxing Constraints. Int. J. Solids Struct., 20, 301-314.

Taylor JE; Logo J (1993): Analysis and Design of Elastic/Softening Truss Structures Based on a Mixed-Form Extremum Principle. loc. cit. Rozvany, 1993a, 683-696.

Taylor JE; Rossow MP (1977): Optimal Truss Design Based on an Algorithm using Optimality Criteria Int. J. Solids Struct., 13, 913-923.

Taylor JE; Washabaugh PD (1994): Analysis and Design of Trussed Structures Made of Elastic/Stiffening Materials. Struct. Optim., 8, 1-8.

Thompson TF; Warsi ZUA; Mastin CW (1985): Numerical Grid Generation, Foundations and Applications. North Holland, New York.

Thomsen J (1991): Optimization of Composite Discs. Struct. Optim., 3, 89-98.

Thomsen J (1992): Topology Optimization of Structures Composed of One or Two Materials. Struct. Optim., 5, 108-115.

Tiba D (1991): Controllability Properties for Elliptic Systems, the Fictitious Domain Method and Optimal Shape Design Problems. Rapports de Recherche No. 1500, INRIA, Rocquencourt, Le Chesnay, France.

Tiba D; Neittaanmäki P; Mäkinen R (1990): A Fixed domain Approach in an Optimal Shape Design Problem. Preprint No. 121, Department of Mathematics, University of Jyväskylä, Finland.

Topping BMV (1983): Shape Optimization of Skeletal Structures: A Review. ACSE J. Struct. Engrg. 109-1951.

Topping BMV (1992): Mathematical Programming Techniques for Shape Optimization of Skeletal Structures. loc. cit. Rozvany, 1992, 349-276.

Topping BMV (1993): Topology Design of Discrete Structures. loc. cit. Bendsøe and Mota Soares, 1993, 517-534

Triantafyllidis N; Schnaidt W (1993): Comparison of Microscopic and Macroscopic Instabilities in a Class of Two Dimensional Periodic Composites. Preprint, Dept. Aerospace Engng., University of Michigan, Ann Arbor, MI, USA.

Turbe N (1982): Applications of Bloch Expansions to Periodic Elastic and Viscoelastic Media. Math. Meth. Appl. Sci., 4, 433-449.

Vanderplaats GN (1984): Numerical Methods for Shape Optimization: An Assessment of the State of the Art. In Atrek E et al. (eds.), New Directions in Optimum Structural Design, Wiley, Chichester, UK.

Velte W; Villaggio P (1982): Are the Optimum Problems in Structural Design Well Posed?. Arch. Rat. Mech. Anal., 78, 199-211.

Vigdergauz S (1986): Effective Elastic Parameters of a Plate with a Regular System of Equal-Strength Holes. Mechanics of Solids (transl. of Mekh. Tver. Tela.), 21, 162-166.

Walther F; Mattheck C (1993): Local stiffening and Sustaining of Shell- and Plate Structures by SKO and CAO. loc. cit. Herskovits, 1993a, 181-188.

Wardi YY; Polak E (1982): A Nondifferentiable Optimization Algorithm for Structural Problems with Eigenvalue Inequality Constraints. J. Struct. Mech., 11, 561-577.

Washizu K (1983): Variational Methods in Elasticity and Plasticity. Pergamon, Oxford, Great Britain.

Wasiutynski Z (1960): On the Congruency of the Forming According to the Minimum Potential Energy with that According to Equal Strength. Bull. de L'Academie Polonaise des Sciences, Serie des Sciences Techniques, VIII, 259-268.

Weinans H; Huiskes R; Grootenboer HJ (1992): The Behavior of Adaptive Bone-Remodeling Simulation Models. J. Biomechanics, 25, 1425-1441.

Zhikov V; Kozlov S; Oleinik O; Ngoan K (1979): Averaging and G-Convergence of Differential Operator. Russian Math. Surveys, 34, 69-147.

Zhou M; Rozvany GIN (1991): The COC Algorithm, Part II: Topological, Geometrical and Generalized Shape Optimization. Comp. Meth. Appl. Mechs. Engng., 89, 309-336.

Zhou M; Xia R (1990): An Efficient Method of Truss Design for Optimum Geometry. Computers and Structures, 35, 115-119.

Zibulevsky M; Ben-Tal A (1993): On a New Class of Augmented Lagrangian Methods for Large Scale Convex Programming Problems. Research Report 2/93, Optimization Lab. , Technion, (Israel Inst. of Technology).

Zochowski A (1988): The Design of a Two-Dimensional Domain. J. Struc. Mech., 16, 17-34.

Zolesio JP (1981): Material Derivative (or Speed) Method for Shape Optimization. loc. cit. Haug and Cea, 1981, 1089-1151.

Zyczkowski M (ed.) (1989): Structural Optimization under Stability and Vibration Constraints. CISM Lecture Notes No. 308, Springer Verlag, Wien.

Zyczkowski M; Gajewski A (1988): Optimal Structural Design under Stability Constraints. Kluwer Academic Press, Dordrecht.

Author index

Subject index

Springer-Verlag and the Environment

We at Springer-Verlag firmly believe that an international science publisher has a special obligation to the environment, and our corporate policies consistently reflect this conviction.

We also expect our business partners – paper mills, printers, packaging manufacturers, etc. – to commit themselves to using environmentally friendly materials and production processes.

The paper in this book is made from low- or no-chlorine pulp and is acid free, in conformance with international standards for paper permanency.